AD_____

Award Number: DAMD17-98-1-8569

TITLE: Transgenic Models for Prostate Cancer

PRINCIPAL INVESTIGATOR: Charles L. Sawyers, M.D.

CONTRACTING ORGANIZATION: UCLA-Medicine, Hemotology/Onocology
Los Angeles, CA 90095-1678

REPORT DATE: February 2003

TYPE OF REPORT: Annual Summary

PREPARED FOR: U.S. Army Medical Research and Materiel Command
Fort Detrick, Maryland 21702-5012

DISTRIBUTION STATEMENT: Approved for Public Release;
Distribution Unlimited

The views, opinions and/or findings contained in this report are those of the author(s) and should not be construed as an official Department of the Army position, policy or decision unless so designated by other documentation.

REPORT DOCUMENTATION PAGE

Form Approved
OMB No. 074-0188

1. AGENCY USE ONLY (Leave blank)	2. REPORT DATE	3. REPORT TYPE AND DATES COVERED
	February 2003	Annual Summary (1 Aug 1998 - 28 Jan 2003)

4. TITLE AND SUBTITLE
Transgenic Models for Prostate Cancer

5. FUNDING NUMBERS
DAMD17-98-1-8569

6. AUTHOR(S)
Charles L. Sawyers, M.D.

7. PERFORMING ORGANIZATION NAME(S) AND ADDRESS(ES)
UCLA-Medicine, Hematology/Oncology
Los Angeles, CA 90095-1678

E-Mail: Sawyersl@mednet.ucla.edu

8. PERFORMING ORGANIZATION REPORT NUMBER

9. SPONSORING / MONITORING AGENCY NAME(S) AND ADDRESS(ES)
U.S. Army Medical Research and Materiel Command
Fort Detrick, Maryland 21702-5012

10. SPONSORING / MONITORING AGENCY REPORT NUMBER

11. SUPPLEMENTARY NOTES
Original contains color plates; All DTIC reproductions will be in black and white.

12a. DISTRIBUTION / AVAILABILITY STATEMENT
Approved for Public Release; Distribution Unlimited

12b. DISTRIBUTION CODE

13. ABSTRACT (Maximum 200 Words)

During phase II of this IDEA Award, our goal was to study genes/pathways implicated in prostate cancer progression using transgenic mouse models. Our efforts focused on creating transgenic models that express 1 of 4 different genes in the mouse prostate. All 4 genes were selected based on studies from our lab and others implicating these genes in human prostate cancer. These include Her-2/neu, cathepsin D, Akt, and Myc. We were successful in generating each of the transgenic mice, and the phenotypes of 3 of them (Cathepsin D, Akt, and Myc) have been fully characterized. Cathepsin D and Akt mice develop prostatic intraepithelial neoplasia (PIN) only, whereas Myc mice develop PIN that progresses to invasive prostatic adenocarcinoma. In addition, we created transgenic mice expressing the avian retrovirus receptor TVA to permit introduction of multiple transgenes into the prostate in a stepwise manner and to manipulate androgen levels without affecting transgene expression. We documented successful infection with avian retroviruses expressing marker genes (GFP) and are optimizing conditions for transfer of oncogenes. We also generated luciferase transgenic mice, which allow us to visualize the mouse prostatet using optimal imaging tools.

14. SUBJECT TERMS
Her-2/neu, cathepsin, Akt, Myc, TVA, luciferase

15. NUMBER OF PAGES
113

16. PRICE CODE

17. SECURITY CLASSIFICATION OF REPORT	18. SECURITY CLASSIFICATION OF THIS PAGE	19. SECURITY CLASSIFICATION OF ABSTRACT	20. LIMITATION OF ABSTRACT
Unclassified	Unclassified	Unclassified	Unlimited

Table of Contents

Introduction

Overview

The goal of this Prostate Cancer Center Initiation Award is to examine signal transduction pathways involved in prostate cancer progression, with an eye toward translational research applications. The current funded program has two Projects and a Core Animal Facility. The first project, directed by Dr. Carey, focused on crosstalk between receptor tyrosine kinases and the androgen receptor (AR), using the Her2/neu kinase as a model system. The second project, directed by Dr. Cohen, examined the role of IGF binding protein 3 (IGFBP-3) in the context of crosstalk with the retinoic acid co-receptor RXRα. The Core facility, directed by Dr. Sawyers, provided xenograft tissue and mouse models for preclinical therapeutic studies for both projects. Dr. Sawyers was also a collaborator for both projects.

Project 1 (Carey)

In the early phases of androgen-independence, genes traditionally regulated by androgen receptor are activated. The thesis underlying this project is that receptor tyrosine kinase (RTK) signaling pathways lead to modifications of AR or its co-activators, which in turn permit AR to function in a ligand-deprived environment. We and others have previously shown that tyrosine kinases such as Her-2/neu/Erb-B2 (Craft et al., 1999a). This project examined the hypothesis that there is a common theme in ligand-independent activation of AR using the receptor tyrosine kinases Her-2 and IGF-1R as models to pursue the mechanism. The study is a multidisciplinary collaboration with Dr. Charles Sawyers (Her-2) and Dr. Pinchas Cohen (IGF-I/IGF-1R). Our proposal articulated a plan to systematically test predictions of the RTK signaling hypothesis. First, the signaling should be blocked by interfering directly with RTK function and this should in principle revert tumors to ligand-dependence. During year 2 of the project Dr. Sawyers' group successfully tested this hypothesis using an EGFR/Her-2 kinase inhibitor (Mellinghoff et al., 2002). One outcome of the study is the recognition that Erk kinase activation (also called MAP kinase) is associated with evolution to androgen independence. Therefore, new efforts have been undertaken to development imaging technologies that will allow the transition to androgen independence to be visualized in mouse models. The first paper describing this two-step transcriptional activation system was published in year 2 (Zhang et al., 2002). Second, because AR is the proposed endpoint of the pathway, its biochemical alteration represents an important step in cancer progression. A direct effect of this pathway on association of co-activators with AR was proposed. Intensive efforts to address this question using a proteomics approach were made in year 2, but the results were disappointing, largely for technical reasons. Recognizing the shortcomings of this strategy, we modified our approach and have successfully used chromatin immunoprecipitation of AR bound to the promoter of AR response genes.

Project 2 (Cohen)

The goals of this project were to identify and characterize the role of IGFBP-3 in androgen receptor-signaling in androgen-dependent and -independent prostate cancer models. We examined if IGFBP-3 is essential for apoptosis in response to androgen withdrawal. We tested the effects of androgen deprivation on IGFBP-3 induction, IGF/IGF-R suppression, and prostatic apoptosis, in the AI and AD LAPC-4 and -9 cell lines and xenograft models of prostate cancer and in genetically altered mouse models. We also treated these mice with systemic IGFBP-3.

Body

Project 1 (Carey)

Changes in the IGF pathway during progression to androgen independence

In the year 1 progress report, we reported our initial findings on the expression of insulin-like growth factors (IGFs), IGF binding proteins and the IGF receptor during the progression of prostate cancer xenografts to androgen independence (AI). We used three *in vivo* models of androgen-dependent human prostate cancer to study this issue, in collaboration with Dr. Michael Pollack's lab in Canada. Progression to AI growth was associated with a 60-fold increase in expression of IGF-I mRNA in LAPC-9 xenografts and a 28-fold increase in IGF-I expression in LNCAP xenografts, relative to the initial AD neoplasms. *IGF-IR* mRNA levels were ~2.5-fold and ~5-fold higher respectively in AI LAPC-9 and LNCaP tumors compared to the original AD neoplasms. AI growth of these xenografts was also associated with significant reductions in IGFBP-3 expression. LAPC-4 xenografts, which previously have been shown to exhibit molecular pathology related to HER2-neu expression with progression to AI, showed relatively minor changes in expression of the genes investigated, but we nevertheless found evidence of increased IGF-IR phosphorylation with progression to AI in this model. Taken together with prior observations, our results suggest that deregulation of expression of genes related to any one of several critical receptor tyrosine kinase regulatory systems, including cellular IGF signaling, may confer androgen independence (Nickerson et al., 2001).

Evidence for selective requirement of the EGFR/Her2 pathway in androgen-independent prostate cancer

We previously showed that signaling through the epidermal growth factor (EGF) receptor family can affect androgen receptor activity and growth in human prostate cancer (Craft et al., 1999a). Here we asked whether interruption of ErbB-1 receptor signaling by an ErbB-1 receptor kinase specific inhibitor affects growth of human prostate cancer xenografts in our *scid* mice model (Klein et al., 1997). PKI-166 (Novartis) is an orally administered, ATP-site specific, reversible inhibitor of the ErbB-1 receptor kinase domain. In year 2 we completed a comprehensive series of preclinical studies of PKI-166 using our prostate cancer models that were published in **Cancer Research** (see attached reprint for details). The major findings were:

(i) PKI-166 blocks ErbB1/ErbB2 activity in prostate cancer cells
(ii) PKI-166 blocks ErbB1/ErbB2 signal transduction in tumors in mice
(iii) PKI-166 blocks the growth of prostate cancers in mice in an androgen-dependent fashion
(iv) Sensitivity to growth inhibition by PKI-166 is correlated with ERK activation

In summary, our preclinical findings with PKI-166 support the hypothesis that EGFR/Her2 pathway signaling plays a functional role in androgen-independent prostate cancer growth and suggests some molecular correlates of response.

Developing novel systems to monitor androgen independent progression

Based on the success of the preclinical studies with the EGFR/Her-2 kinase inhibitor and the potential importance of Erk kinase activation as a biomarker, we developed an imaging system in which the transition to the hormone refractory stage can be visualized in a living mouse. This will serve as a tool for further evaluation of the transition to hormone independence and for evaluation of novel therapeutics. First, we developed enhancers from the prostate specific antigen gene (PSA) that express the highly active chimeric transcription factor GAL4-VP16. Within the same construct we engineered expression of the reporter gene firefly luciferase from 5 GAL4 sites (which respond specifically to the GAL4-VP16 fusion protein). We have recently shown that this approach, known as the two-step transcriptional activation system (TSTA), works extremely well in mouse prostate cancer models (Zhang et al, Molecular Therapy, manuscript appended). We built this system (AdTSTALuc) into adenovirus vectors and showed that it detects tumors in LAPC9 AD and AI mice using charge coupled device imaging (Fig. 1). The figure demonstrates that the system demonstrates tight specificity for prostate tumors in contrast to Ad based CMV vectors, which express in the liver. Based on our data showing that Erk kinase activation is tightly correlated with evolution to androgen independence in the LAPC models, we adapted the system to express GAL4-Elk1, a chimeric transcription factor that will respond to the Erk kinase. We have demonstrated a robust response of the PSA-GAL4-Elk-1 system to activators of Erk kinase in LNCaP cells. In year 3 we generated viral vectors and transgenic animals that express this TSTA-MAPK sensing system for examining levels of Erk activity in androgen independent prostate cancer. These mice are currently being characterized for their imaging potential.

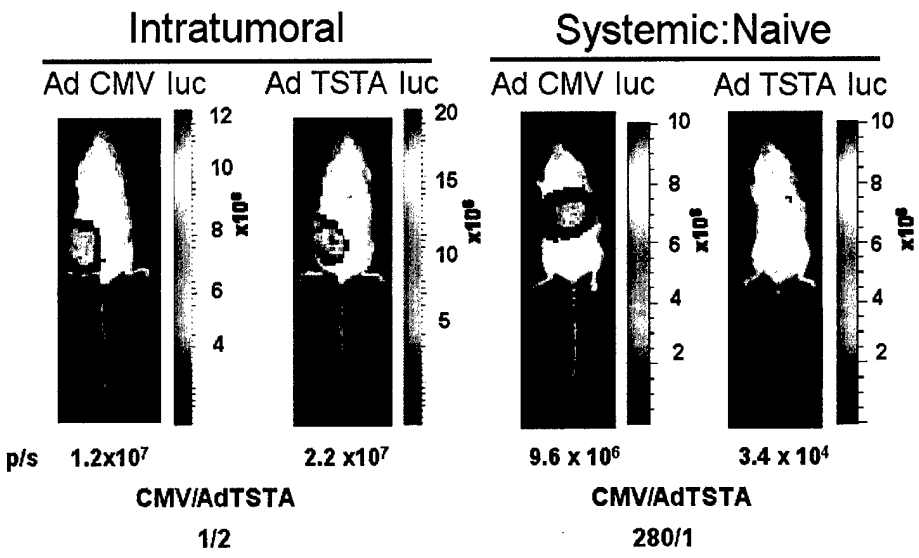

Figure 1. Intratumoral injection of 10^7 AdCMV-luc and AdTSTA-luc into LAPC9 (left set of panels) and naïve mice (right panels). After injection mice were injected with D-luciferin and imaged using a CCD optical imaging system. The TSTA system exhibited twice the activity of CMV in the tumor but was hundreds of fold more specific when analyzing the background signals in liver.

Identification of androgen receptor alterations that occur during progression to androgen independence

The focus of this part of the project was to probe the molecular alterations of AR when androgen signaling is replaced by RTKs. The ability to complete this aim is predicated on the development of techniques for efficiently analyzing AR, its modifications and its associated factors from cell lines and tumors. Our hypothesis is that signal transduction pathways regulate association of AR and its co-factors during the AD-AI transition. The initial approach was to identify AR-associated proteins participating in this transition using mass spectroscopy. Unfortunately, we were stymied by technical issues that limited our ability to make rapid progress toward these goals, as detailed in prior progress reports. Last year we have shifted our emphasis to the use of chromatin immunoprecipitation technology to analyze the AR complexes present on genes like PSA in androgen-dependent versus androgen-independent disease. This technology has already been shown to work for AR by others (Shang et al., 2002) and is working very well in our hands (figure 2). This technique measures transcription complexes bound to endogenous chromatin templates. We immunoprecipitate AR from formaldehyde treated cells under varying

conditions of androgen stimulation and determine if AR is bound to the endogenous PSA promoter using specific PCR primers. The presence or absence of coactivators and corepressors present in the complex can be discerned using appropriate antibodies. We have been able to demonstrate AR binding to the PSA enhancer in LNCaP cells and in AI and AD tumors. We do not fully understand this phenomenon since PSA levels returned to baseline after castration. The goal for year 3 is to determine if differences exist between AI and AD cells with respect to known AR co-activators like SRC-1, -2 and -3 and p300.

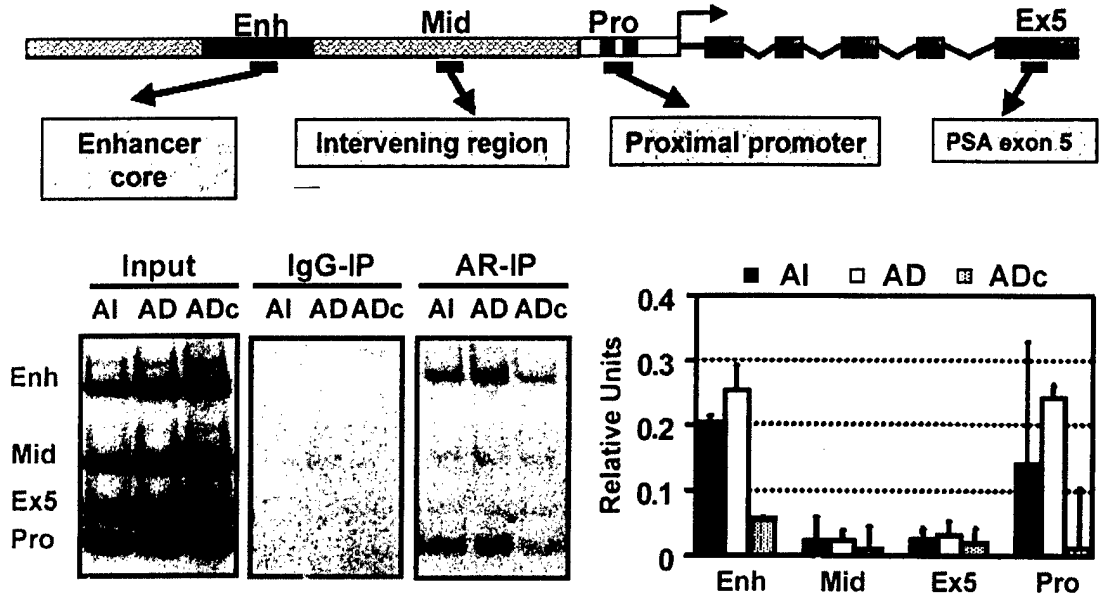

Fig. 2. Chromatin immunoprecipitation assays in LAPC9 tumors. The diagram describes the PSA regulatory region. Short black line underneath indicates the positions targeted by PCR. Enh: enhancer core; Mid: intermediate region; Pro: proximal promoter; Ex5: PSA exon 5 (for sequence coordinates see Methods). Tumors were isolated from mice sacrificed at day 10 (6 days post castration for ADc), minced, crosslinked with formaldehyde and immunoprecipitated with anti-AR. An autoradiograph of the multiplex PCR reactions is shown for AD, AI and ADc tumors. Graph of Multiple Tumor ChIP Analyses. The band intensities were analyzed using ImageQuant. Background values from a mock (IgG) ChIP were subtracted from each band and normalized to the signal from onput DNA. Error bars shown are standard deviation of three values obtained in independent experiments.

Summary

Project 1 established the role of RTKs such as EGFR/Her2 in modulating AR function and provide insight into potential clinical applications of EGFR pathway inhibitors. We also developed in vivo imaging technologies to measure gene expression in mouse models to study progression to androgen independence by making Erk-responsive luciferase reporter constructs. We have also used chromatin immunoprecipitation to eludicate the mechanism of crosstalk between EGFR/Her2 and AR, as this assay is likely to be important in evaluating the clinical use of signaling pathway inhibitors.

Project 2 (Cohen)

The goal of this project was to identify and characterize the role of IGFBP-3 in androgen receptor-signaling in androgen-dependent and -independent prostate cancer models. We asked if IGFBP-3 is essential for apoptosis in response to androgen withdrawal and tested the effects of androgen deprivation on IGFBP-3 induction, IGF/IGF-R suppression, and prostatic apoptosis, in the AI and AD LAPC-4 and -9 cell lines and xenograft models of prostate cancer and in genetically altered mouse models. We also induced prostate cell death by treating these mice with systemic IGFBP-3. We also examined the role of RXR-α in IGFBP-3 actions in the prostate. We initiated studies to generate prostatic RXR-α conditional (cre-lox) knockout models in order to evaluate the prostates of these mice before and after castration or IGFBP-3 treatment. These experiments will determine if RXR is required for apoptosis in response to androgen deprivation. We are also studying IGFBP-3 synergism with ligands of RXR-alpha and related receptors both *in vivo* in the AD and AI LAPC models and *in vitro* in prostate cancer cell line models.

IGFBP-3 and RXR synergism *in vitro*

We also showed (Fig. 3) that IGFBP-3 and a specific rexinoid (from Allergan Inc.) had additive effects in inhibiting LAPC-4 cells. This is an important observation as it suggests that IGFBP-3 and RXR ligands co-operate on inducing gene transcription that leads to apoptosis. Furthermore, these data suggest that these agents will have a synergistic effect on CaP tumors *in vivo* and thus may be useful as co-adjuvant therapy in prostate cancer.

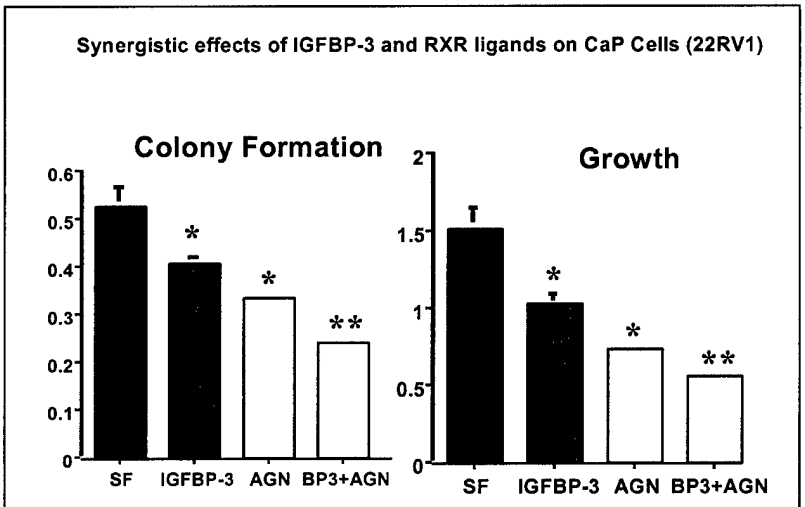

Figure 3. Synergistic effects of IGFBP-3 and RXR agonists on the growth of LAPC-4 prostate cancer cells. This experiments illustrates the potential utility of IGFBP-3 as a adjuvant therapy for prostate cancer.

IGFBP-3 and RXR synergism *in vivo*

We also evaluated the effect of infusing IGFBP-3 alone or in combination with RXR ligands on the growth of LAPC-4 and LAPC-9 xenografts in SCID mice. Preliminary data shows combination therapy with IGFBP-3 and an RXR ligand from Allergan results in suppression of tumor growth (data presented in the 2002 AACR meetings and shown below).

Creation of prostatic RXR knockout mice

In year 3 we began generating these mice by crossing Flox RXR mice with transgenic mice expressing Cre under the control of the probasin promoter to achieve prostate-specific excision of RXR. We will examine homozygous mice histologically before and after castration and will treat mice with IGFBP-3 and rexinoids and study prostates looking for apoptotic effects. These studies, begun in year 3, will be completed using additional funds.

Mechanism of action of IGFBP-3

We have enhanced our understanding of the mechanism of interaction between RXR and IGFBP-3 in terms of mediating apoptosis in CaP cells. This appears to involve IGFBP-3 induced dissociation of the RXR-TR3 complex and translocation of TR3/Nur77 to the mitochondria. Our xenograft studies are allowing us to refine the in vivo dosing strategy for IGFBP-3 and RXR-ligands. Protigen and Allergan are companies that supply us with appropriate reagents for this development. IGFBP-3 as well as several nuclear receptor systems are critical regulators of CaP death/survival signaling pathways, and RXR-α is an IGFBP-3 association protein which is critical to IGFBP-3 signal transduction (and vice versa). Our investigation into the interactions between IGFBP-3/RXR/TR3, has confirmed that IGFBP-3 does translocate the nuclear receptor TR3 leading to cellular apoptosis in vitro. We are currently testing if this phenomenon also occurs in vivo. Our preliminary studies also indicate that co-overexpression of IGFBP-3 and TR3 are synergistic in their apoptotic effects on prostate cancer cells (Figure 7).

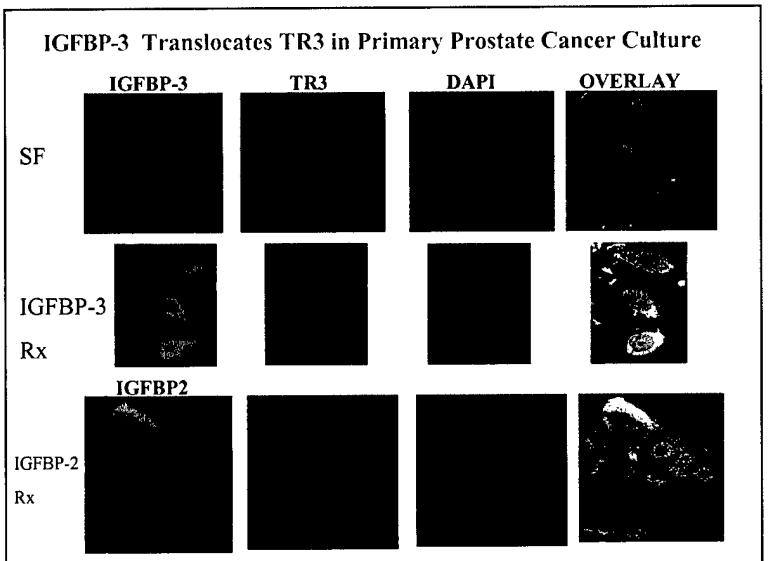

Figure 4. IGFBP-3 Translocates TR3 in Primary Prostate Cancer Culture Row Headings are treatments, column headings are staining. Note absence of nuclear TR3 after IGFBP-3 treatment.

TR3 translocation by IGFBP-3 is specific to cancerous cells

In preliminary work with Dr. Donna Peehl at Stanford University, we obtained prostate cancer primary cultures with matched adjacent normal prostate epithelium at the time of surgery. These primary cells were cultured and treated with IGFBP-3 and then immunostained for TR3 using confocal microscopy. Treatment with IGFBP-3 completes leaves the nucleus devoid of TR3. This is a specific action of IGFBP-3 as IGFBP-2 does not translocate TR3 (Figure 5). Treatment of matched primary non-malignant epithelial cells from the same donor fails to show translocation (data not shown). This TR3 translocation specificity to malignant cells by IGFBP-3 mirrors effects on apoptosis that we observe in cell lines.

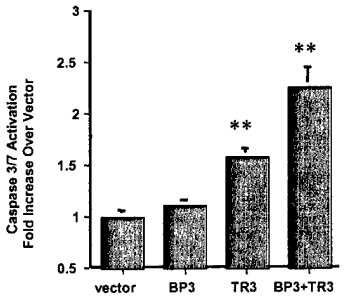

Figure 7 IGFBP-3 and TR3 synergize in killing prostate cancer cells Note that co-transfection of IGFBP-3 and TR3 has additive effects.

The present work clearly demonstrates that IGFBP-3 is *a unique* signal molecule in its ability to both a) modulate traditional nuclear receptor roles as DNA transcription factors and b) modulate novel nuclear receptor roles as extra-nuclear mediators of cellular biologic processes. The specificity of IGFBP-

3 induced TR3 translocation to cancerous cells makes it an attractive target in the therapy of prostatic malignancy. Thus, IGFBP-3 protein therapy, a molecule downstream of the AR, is of potential value in the treatment of AI CaP. By using a SCID mouse LAPC-4 xenograft model, we have very early data that these observations are confirmed *in vivo*. We utilized LAPC-4 xenografts in SCID mice that were treated with daily IP injections of either saline, IGFBP-3, an RXR ligand produced by Allergan, or IGFBP-3/RXR ligand combination. The individual treatments showed little or no effect in terms of tumor size, but the combination showed a dramatic reduction in growth. The PSA levels demonstrated a similar trend and a gene array analysis in response to these treatments also demonstrated a coordinated pattern of gene induction (data not shown).

Summary:

Collectively, our recently obtained data indicate, that IGFBP-3 as well as IGF-I are critical regulators of androgen-dependent as well as androgen-independent CaP death/survival signalling pathways, and that RXR-α and TR3 are IGFBP-3 association protein which are critical to IGFBP-3 signal transduction. We have demonstrated, this year, that androgen withdrawal induces IGFBP-3 in a variety of systems. Our experiments show that both exogenous addition of IGFBP-3 protein or transfection of IGFBP-3 kills CaP cells and enhances the effects of other chemo-therapeutic agents such as Taxol and RXR-ligands. Most importantly, we can reproduce these effects in the absence of androgens, indicating that IGFBP-3 can kill androgen-independent CaP cells.

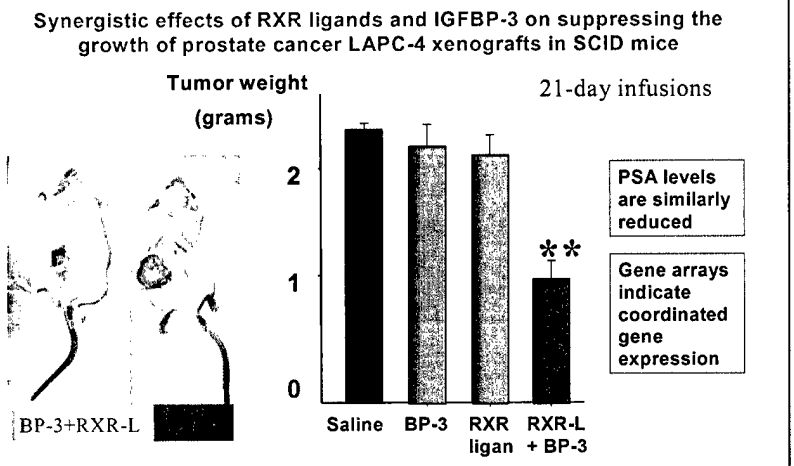

Figure 8 IGFBP-3 and RXR ligands synergize in killing prostate cancer cells *in vivo* Note that a 21-day infusion of either agent alone has minimal effects, but a combination arm resulted in a dramatic suppression of tumor growth.

Conclusions

Project 2 used innovative approaches to characterize prostate cancer pathophysiology as it relates to nuclear receptors and their interactions with IGFBP-3. We showed that IGFBP-3 is an important regulator of apoptosis in prostate cells, particularly in conjunction with RXR agonists. The novel observation linking TR3 to IGFBP-3 actions opens new avenues of addressing prostate cancer. Since pharmacological modulation of this pathway is clinically feasible, we anticipate that this project will also lead to clinical trials.

Core Facility (Sawyers)

Under Dr. Sawyers' direction, the core facility has provided human prostate cancer xenograft material for study of signaling pathways in Projects 1 and 2. In addition the core facility set up the tumor models for preclinical studies and assisted investigators in the conduct of these studies by measuring tumor volume and serum PSA levels. The core facility also assisted in genotype analysis RXRα knockout mice for Project 2 and in crossing the mice to probasin-Cre strains. Finally, the core handled tissue fixation, H&E staining and immunohistochemical analysis of xenograft and mouse tissues (Dr. Said, Pathology).

Key Research Accomplishments

Project 1

1. We showed that IGF-I and IGF-IR expression and activity are altered in some xenografts during the transition to androgen independence and published the findings.
2. We showed specific activity of the EGFR/Her-2 tyrosine kinase inhibitor PKI-166 against androgen independent prostate cancer xenografts and published the findings.
3. We identified the phosphorylation status of Erk kinase as the best determinant of sensitivity to EGFR/Her-2 inhibition in prostate cancer and published the findings.
4. We constructed a 2-step luciferace reporter gene imaging system to measure Erk kinase activation in mouse prostate cancer models.
5. We defined the promoter region of the prostate stem cell antigen gene.
6. We developed chromatin immunoprecipitation as a tool to monitor AR transcriptional function in living cells on endogenous gene templates.

Project 2

7. We showed that IGFBP-3 can induce prostate cell apoptosis by interaction with RXR
8. We have identified a synergistic effect of IGFBP-3 and RXR ligands on the killing of prostate cancer cells.
9. We discovered a novel mechanism for the actions of IGFBP-3 involving TR3 translocation from the nucleus.

Reportable Outcomes

Publications

Project 1

Mellinghoff, I. K., Tran, C., and Sawyers, C. L. (2002). Growth inhibitory effects of the dual ErbB1/ErbB2 tyrosine kinase inhibitor PKI-166 on human prostate cancer xenografts. Cancer Research 62:5254-5259.

Nickerson, T., Chang, F., Lorimer, D., Smeekens, S. P., Sawyers, C. L., and Pollak, M. (2001). In vivo progression of LAPC-9 and LNCaP prostate cancer models to androgen independence is associated with

increased expression of insulin-like growth factor I (IGF-I) and IGF-I receptor (IGF-IR). Cancer Res *61*, 6276-6280.

Zhang, L., Adams, J. Y., Billick, E., Ilagan, R., Iyer, M., Le, K., Smallwood, A., Gambhir, S. S., Carey, M., and Wu, L. (2002). Molecular engineering of a two-step transcription amplification (TSTA) system for transgene delivery in prostate cancer. Mol Ther *5*, 223-232.

Jain, A., Lam, A., Carey, M., and Reiter, R. (2002). Identification of an Androgen-Dependent Enhancer Within the Prostate Stem Cell Antigen Gene. Molecular Endocrinology 16:2323-2337.

Wu, L., Matherly, J., Smallwood, A., Adams, J. Y., Billick, E., Belldegrun, A., and Carey, M. (2001). Chimeric PSA enhancers exhibit augmented activity in prostate cancer gene therapy vectors. Gene Ther *8*, 1416-1426.

Adams, J. A., Johnson, M., Sato, M., Berger, F., Gambhir, S. S., Carey, M., Iruela-Arispe, L., and Wu, L. (2002). Visualization of Advanced Human Prostate Cancer Lesions in Living Mice by a Targeted Gene Transfer Vector and Optical Imaging. Nature Medicine 8:891-897.

Zhang L, Johnson M, Le KH, Sato M, Ilagan R, Iyer M, Gambhir SS, Wu L, Carey M. (2003) Interrogating Androgen Receptor Function in Recurrent Prostate Cancer. Submitted.

Project 2

Boyle, B. J., Zhao, X. Y., Cohen, P., and Feldman, D. (2001). Insulin-like growth factor binding protein-3 mediates 1 alpha,25-dihydroxyvitamin d(3) growth inhibition in the LNCaP prostate cancer cell line through p21/WAF1. J Urol *165*, 1319-1324.

Weinzimer, S. A., Gibson, T. B., Collett-Solberg, P. F., Khare, A., Liu, B., and Cohen, P. (2001). Transferrin is an insulin-like growth factor-binding protein-3 binding protein. J Clin Endocrinol Metab *86*, 1806-1813.

Cohen, P. (2001). Clinical implications of the IGF-cancer connection. Growth Horm IGF Res *11*, 336-338.

Rajah, R., Lee, K. W., and Cohen, P. (2002). Insulin-like Growth Factor Binding Protein-3 Mediates Tumor Necrosis Factor-alpha-induced Apoptosis: Role of Bcl-2 Phosphorylation. Cell Growth Differ *13*, 163-171.

Grimberg, A., Liu, B., Bannerman, P., El-Deiry, W. S., and Cohen, P. (2002). IGFBP-3 mediates p53-induced apoptosis during serum starvation. Int J Oncol *21*, 327-335.

Lee, H. Y., Chun, K. H., Liu, B., Wiehle, S. A., Cristiano, R. J., Hong, W. K., Cohen, P., and Kurie, J. M. (2002). Insulin-like growth factor binding protein-3 inhibits the growth of non-small cell lung cancer. Cancer Res *62*, 3530-3537.

Lee KW, Cohen P. Nuclear effects: unexpected intracellular actions of insulin-like growth factor binding protein-3. *J Endocrinol* 2002; 175:33-40.

Monzavi R, Cohen P. IGFs and IGFBPs: role in health and disease. Best Pract Res Clin Endocrinol Metab. 2002; 16:433-47.

Ngo TH, Barnard RJ, Tymchuk CN, Cohen P, Aronson WJ. Effect of diet and exercise on serum insulin, IGF-I, and IGFBP-1 levels and growth of LNCaP cells in vitro. Cancer Causes and Control 2002; 13:929–935.

Weinzimer S, Cohen P. Biological significance of the IGFBPs. *Growth and Lactogenic Hormones*. R Rappaport Ed. Elsvier Science B.V. 2002.

Franklin SL, Ferry RJ Jr, Cohen P. Rapid Insulin-Like Growth Factor (IGF)-Independent Effects of IGF Binding Protein-3 on Endothelial Cell Survival. *J Clin Endocrinol Metab* 2003; 88:900-7.

Moore MG, Wetterau LA, Francis MJ, Peehl DM, Cohen P. Novel stimulatory role for insulin-like growth factor binding protein-2 in prostate cancer cells. *Int J Cancer* 2003; 105:14-9.

Special Editorial: Growth Hormone Treatment and Neoplasia—Coincidence or Consequence? Lawson Wilkins Pediatric Endocrine Society (LWPES). J.Clin Endocrinol Metab. 2002: 87 (12):5351-5352.

Major Presentations:

Project 1

Mar	2001	American Association of Cancer Research Education Session, New Orleans, Louisiana. Lecture: "Signal Transduction by P13K/PTEN/Akt"
Sept	2001	CaP CURE Annual Retreat, Lake Tahoe, Nevada. Lecture: "Interrogating AR Signaling In Vitro and In Vivo"
Nov	2001	Society for Basic Urologic Research, Tucson, Arizona. Lecture: "Kinase Signaling in Prostate Tumorigenesis"
Feb	2002	UCSF Urology Department in San Francisco, CA Lecture: "Interrogating AR Signaling In Vitro and In Vivo"
Apr	2002	American Association for Cancer Research (AACR) Annual Meeting, Symposium on Targeted Therapy, San Francisco, California. Lecture: "PTEN Pathway in Prostate Cancer"
Apr	2002	CaP CURE, Los Angeles, California. Lecture: "Signal Transduction Inhibitor Therapy in Prostate Cancer"

Project 2

Aug	2001	Annual Japanese Growth Study meeting, Tokyo, Japan. Lecture: "IGFBP-3 and its biological functions"
Jan	2002	Cal Tech Research Symposium, Pasadena CA. "Nuclear interactions of IGFBPs".
Feb	2002	International Aging Male Symposium, Berlin, Germany. "The IGFs axis in prostate cancer".

Apr	2002	International Growth Hormone Symposium, Budapest, Hungary. "IGFBPs, what do they do and why should we monitor them".
May	2002	ACVIM Annual meeting, Dallas TX. "Interactions between the IGF axis and retinoid receptors".
Aug	2002	MD Anderson Oncology Grand Rounds, Houston, Texas. "IGFBPs and cancer: roles in pathogenesis and treatment".
Oct	2002	Endocrinology of Aging Symposium, Munich, Germany "Should we be concerned about malignancy in GH recipients?"
Nov	2002	Functional Roles of IGFBPs Symposium, Tubingen, Germany. "Clinical potential of IGFBP-3".
Dec	2002	NCI Prostate SPORE Annual meeting, San Francisco. "IGFBP-3 and its role in prostate cancer".
Feb	2003	Stanford University Endocrine Grand Rounds. " The IGF system and cancer".
Mar	2003	Annual German Endocrine Society Meeting, Munich, Germany. Lecture: "GH-IGF and cancer risk"
Apr	2003	NIH apoptosis and aging workshop, Bethesda MD. Lecture: "intra-nuclear roles of IGFBP-3 in apoptosis"

Translational research:

Both projects formed the basis for two projects that are now funded within the UCLA Prostate Cancer SPORE grant. Project 1 laid the groundwork for a translational clinical trial with monoclonal antibody therapy directed against Her2/neu using the antibody 2C4 (Genentech, David Agus, PI) and a separate study of the small molecule EGFR kinase inhibitor Iressa (AstraZeneca). Project 2 had led to further translational studies to define the mechanism of IGFBP3/ RXR syngergy using expression profiling technlogy, which is expected to lead to a clinical trial within 3 years.

Personnel receiving pay from the research effort:

Charles Sawyers, M.D.	Professor
Pinchas Cohen, M.D.	Professor
Michael Carey, Ph.D	Professor
Robert E. Reiter, M.D.	Associate Professor in Residence
Hong Wu, M.D., Ph.D	Ass't Investigator/Ass't Professor
Kuk-Wha Lee	Clinical Instructor
Charlie (Degui) Chen	Visiting Ass't Researcher
Romyla Ilagan	Postdoc
Liqun Joann Zhang	Postdoc
Andrea Smallwood	Staff Research Associate II / Postdoc
Brian James Skaggs	Postgrad Researcher
Dorian Gui	Postgrad Researcher
Liqun Ma	Postgrad Researcher
Igor Vivanco	Grad Student
Neshat S. Mehran	Grad Student
Orlando Gutierrez	Staff Research Associate
Kim Hoang Le	Staff Research Associate I

Paul Tarr	Staff Research Associate I
Susan Salas	Lab Ass't I
Lisa Rosenfelt	Lab Helper
Adam Sasson	Lab Helper

Conclusions

This Prostate Cancer Center Initiation Award examined signal transduction pathways involved in prostate cancer progression, with an eye toward translational research applications. Project 1 showed the potential role of the EGFR/Her-2 pathway in androgen independence, with a clear path toward testing kinase inhibitors of this pathway in patients. Importantly, this work identified a candidate biomarker for signaling prostate cancer progression to androgen independence, which will also be useful for molecular imaging studies. Project 2 used innovative approaches to characterize prostate cancer pathophysiology as it relates to nuclear receptors and their interactions with IGFBP-3. The data showed that IGFBP-3 is an important regulator of apoptosis in prostate cells, particularly in conjunction with RXR agonists. Since pharmacological modulation of this pathway is clinically feasible, this project will also lead to clinical trials in the context of the UCLA Prostate Cancer SPORE.

References

Brandt, R., Wong, A. M., and Hynes, N. E. (2001). Mammary glands reconstituted with Neu/ErbB2 transformed HC11 cells provide a novel orthotopic tumor model for testing anti-cancer agents. Oncogene *20*, 5459-5465.

Bruns, C. J., Solorzano, C. C., Harbison, M. T., Ozawa, S., Tsan, R., Fan, D., Abbruzzese, J., Traxler, P., Buchdunger, E., Radinsky, R., and Fidler, I. J. (2000). Blockade of the epidermal growth factor receptor signaling by a novel tyrosine kinase inhibitor leads to apoptosis of endothelial cells and therapy of human pancreatic carcinoma. Cancer Res *60*, 2926-2935.

Chen, W. S., Lazar, C. S., Poenie, M., Tsien, R. Y., Gill, G. N., and Rosenfeld, M. G. (1987). Requirement for intrinsic protein tyrosine kinase in the immediate and late actions of the EGF receptor. Nature *328*, 820-823.

Craft, N., Chhor, C., Tran, C., Belldegrun, A., DeKernion, J., Witte, O. N., Said, J., Reiter, R. E., and Sawyers, C. L. (1999a). Evidence for clonal outgrowth of androgen-independent prostate cancer cells from androgen-dependent tumors through a two-step process. Cancer Res *59*, 5030-5036.

Craft, N., Shostak, Y., Carey, M., and Sawyers, C. L. (1999b). A mechanism for hormone-independent prostate cancer through modulation of androgen receptor signaling by the HER-2/neu tyrosine kinase. Nat Med *5*, 280-285.

Donaldson, R. W., and Cohen, S. (1992). Epidermal growth factor stimulates tyrosine phosphorylation in the neonatal mouse: association of a M(r) 55,000 substrate with the receptor. Proc Natl Acad Sci U S A *89*, 8477-8481.

Gioeli, D., Mandell, J. W., Petroni, G. R., Frierson, H. F., Jr., and Weber, M. J. (1999). Activation of mitogen-activated protein kinase associated with prostate cancer progression. Cancer Res *59*, 279-284.

Gioeli, D., Zecevic, M., and Weber, M. J. (2001). Immunostaining for activated extracellular signal-regulated kinases in cells and tissues. Methods Enzymol *332*, 343-353.

Honegger, A. M., Dull, T. J., Felder, S., Van Obberghen, E., Bellot, F., Szapary, D., Schmidt, A., Ullrich, A., and Schlessinger, J. (1987). Point mutation at the ATP binding site of EGF receptor abolishes protein-tyrosine kinase activity and alters cellular routing. Cell *51*, 199-209.

Klein, K. A., Reiter, R. E., Redula, J., Moradi, H., Zhu, X. L., Brothman, A. R., Lamb, D. J., Marcelli, M., Belldegrun, A., Witte, O. N., and Sawyers, C. L. (1997). Progression of metastatic human prostate cancer to androgen independence in immunodeficient SCID mice. Nat Med *3*, 402-408.

Lane, H. A., Beuvink, I., Motoyama, A. B., Daly, J. M., Neve, R. M., and Hynes, N. E. (2000). ErbB2 potentiates breast tumor proliferation through modulation of p27(Kip1)-Cdk2 complex formation: receptor overexpression does not determine growth dependency. Mol Cell Biol *20*, 3210-3223.

Malik, S. N., Brattain, M., Ghosh, P. M., Troyer, D. A., Prihoda, T., Bedolla, R., and Kreisberg, J. I. (2002). Immunohistochemical demonstration of phospho-akt in high Gleason grade prostate cancer. Clin Cancer Res *8*, 1168-1171.

Mellinghoff, I. K., Tran, C., and Sawyers, C. L. (2002). Growth inhibitory effects of the dual ErbB1/ErbB2 tyrosine kinase inhibitor PKI-166 on human prostate cancer xenografts. Cancer Research *In press*.

Moasser, M. M., Basso, A., Averbuch, S. D., and Rosen, N. (2001). The tyrosine kinase inhibitor ZD1839 ("Iressa") inhibits HER2-driven signaling and suppresses the growth of HER2-overexpressing tumor cells. Cancer Res *61*, 7184-7188.

Nickerson, T., Chang, F., Lorimer, D., Smeekens, S. P., Sawyers, C. L., and Pollak, M. (2001). In vivo progression of LAPC-9 and LNCaP prostate cancer models to androgen independence is associated with increased expression of insulin-like growth factor I (IGF-I) and IGF-I receptor (IGF-IR). Cancer Res *61*, 6276-6280.

Scher, H. I., Sarkis, A., Reuter, V., Cohen, D., Netto, G., Petrylak, D., Lianes, P., Fuks, Z., Mendelsohn, J., and Cordon-Cardo, C. (1995). Changing pattern of expression of the epidermal growth factor receptor and transforming growth factor alpha in the progression of prostatic neoplasms. Clin Cancer Res *1*, 545-550.

Scheving, L. A., Stevenson, M. C., Taylormoore, J. M., Traxler, P., and Russell, W. E. (2002). Integral role of the EGF receptor in HGF-mediated hepatocyte proliferation. Biochem Biophys Res Commun *290*, 197-203.

Shang, Y., Myers, M., and Brown, M. (2002). Formation of the androgen receptor transcription complex. Mol Cell *9*, 601-610.

Stoscheck, C. M., and Carpenter, G. (1984). Down regulation of epidermal growth factor receptors: direct demonstration of receptor degradation in human fibroblasts. J Cell Biol *98*, 1048-1053.

Wen, Y., Hu, M. C., Makino, K., Spohn, B., Bartholomeusz, G., Yan, D. H., and Hung, M. C. (2000). HER-2/neu promotes androgen-independent survival and growth of prostate cancer cells through the Akt pathway. Cancer Res *60*, 6841-6845.

Yarden, Y., and Sliwkowski, M. X. (2001). Untangling the ErbB signalling network. Nat Rev Mol Cell Biol *2*, 127-137.

Yeh, S., Lin, H. K., Kang, H. Y., Thin, T. H., Lin, M. F., and Chang, C. (1999). From HER2/Neu signal cascade to androgen receptor and its coactivators: a novel pathway by induction of androgen target genes through MAP kinase in prostate cancer cells. Proc Natl Acad Sci U S A *96*, 5458-5463.

Zhang, L., Adams, J. Y., Billick, E., Ilagan, R., Iyer, M., Le, K., Smallwood, A., Gambhir, S. S., Carey, M., and Wu, L. (2002). Molecular engineering of a two-step transcription amplification (TSTA) system for transgene delivery in prostate cancer. Mol Ther *5*, 223-232.

Appendix

(Please note we are only sending articles published since last progress report)

[CANCER RESEARCH 62, 5254–5259, September 15, 2002]

Growth Inhibitory Effects of the Dual ErbB1/ErbB2 Tyrosine Kinase Inhibitor PKI-166 on Human Prostate Cancer Xenografts[1]

Ingo K. Mellinghoff, Chris Tran, and Charles L. Sawyers[2]

Departments of Medicine [I. K. M., C. T., C. L. S.] and Molecular Biology Institute [C. L. S.], University of California Los Angeles, School of Medicine, Los Angeles, California, 90095

ABSTRACT

Experiments with human prostate cancer cell lines have shown that forced overexpression of the ErbB2-receptor tyrosine kinase (RTK) promotes androgen-independent growth and increases androgen receptor-transcriptional activity in a ligand-independent fashion. To investigate the relationship between ErbB-RTK signaling and androgen in genetically unmanipulated human prostate cancer, we performed biochemical and biological studies with the dual ErbB1/ErbB2 RTK inhibitor PKI-166 using human prostate cancer xenograft models with isogenic sublines reflecting the transition from androgen-dependent to androgen-independent growth. In the presence of low androgen concentrations, PKI-166 showed profound growth-inhibitory effects on tumor growth, which could be partially reversed by androgen add-back. At physiological androgen concentrations, androgen withdrawal greatly enhanced the ability of PKI-166 to retard tumor growth. The level of extracellular signal-regulated kinase activation correlated with the response to PKI-166 treatment, whereas the expression levels of ErbB1 and ErbB2 did not. These results suggest that ErbB1/ErbB2 RTKs play an important role in the biology of androgen-independent prostate cancer and provide a rationale for clinical evaluation of inhibitors targeted to this pathway.

INTRODUCTION

Carcinoma of the prostate is the most common malignancy affecting males and causes enormous morbidity and mortality in the United States and Western Europe. About one-third of men relapse after radical prostatectomy surgery because of previously undetected metastatic disease. Metastatic prostate cancer responds for a variable period of time to androgen-deprivation therapy but eventually resumes growth despite castrate levels of androgen. This state of disease, termed "androgen-independent" prostate cancer, is characterized by expression of the *AR*[3] and AR-regulated genes, suggesting that the AR pathway is reactivated in a "ligand-independent" fashion. Several mechanisms have been proposed to explain the phenomenon of AR reactivation in the setting of castrate levels of ligand. These include mutations in *AR* that alter its ligand-binding affinity, overexpression of AR because of gene amplification, and/or increased recruitment of intracellular signal transduction pathways, which activate AR through ligand-independent mechanisms (1).

ErbB RTKs have been implicated as one such pathway that may play a role in androgen-independent prostate cancer progression. Experimental support for this concept comes from the observation that: (*a*) activation of ErbB1 and/or ErbB2 RTKs by EGF or forced overexpression of ErbB2, respectively, results in androgen-independent activation of AR transcriptional activity in prostate cancer cell lines (2–4); (*b*) forced overexpression of ErbB2 promotes androgen-independent growth of prostate cancer cells (2, 3); and (*c*) androgen-independent prostate cancers express increased levels of ErbB2 receptor protein (2, 5–7). However, it is still uncertain whether ErbB1- and ErbB2-mediated signals contribute to the progression of human prostate cancer, which, unlike breast cancer (8), rarely shows amplification of *ErbB*-gene loci. Using xenograft models of human prostate cancer, we show here a striking interplay of AR and ErbB signaling pathways. Growth inhibition by the ATP site-specific ErbB1/ErbB2 RTK inhibitor PKI-166 was greatest in androgen-independent tumors, significantly augmented by simultaneous AW, and partially rescued by androgen supplementation. Growth inhibition by PKI-166 was positively correlated with the basal activation state of the ERKs ERK1/2. Our findings suggest that ErbB1/ErbB2 RTKs play an important role in the biology of human prostate cancer and may be a viable therapeutic target for novel kinase inhibitors (9).

MATERIALS AND METHODS

Reagents. The LAPC4 cell line was established from the LAPC4 human prostate cancer xenograft (10), A431 cells were kindly provided by Dr. Harvey Hershman (UCLA), and LNCaP cells were purchased from American Type Culture Collection. PKI-166 was obtained from Novartis Pharma AG, Basel, Switzerland. EGF and standard chemical reagents were obtained from Sigma. Antibodies against ErbB1 (*sc-101* and *sc-03*), ERK1/2 (*sc-94*), TGF-α (*sc-9043*), and prostate-specific antigen (*sc-7638*) were obtained from Santa Cruz Biotechnology, against ErbB2 from Oncogene Sciences (*OP-15*), against phosphotyrosine from Upstate (*4G10*), against activated ErbB1 from Chemicon (*MAb3052*), against phospho-ERK (Thr183/Tyr185) from Promega (*V8031*), and against phospho-Akt (Ser473) from Cell Signaling Technology (*Ab9271*).

Pulse-Chase Experiments and Immunoblotting. A431 cells were labeled for 12 h in methionine-free DMEM with 0.2 mCi [^{35}S]methionine/cysteine (Translabel; ICN Biomedicals) per 10-cm plate. Cells were subsequently washed three times in serum-free DMEM. Serum-free DMEM with 15 mg/liter unlabeled methionine ("chase-medium") was added to each plate in the presence or absence of 5 μM PKI-166. Ten min later 100 ng/ml EGF was added where indicated in Fig. 1*B*. Cells were lysed immediately after the third wash in serum-free DMEM (baseline sample) and at various intervals after the addition of chase-medium. Cell lysis, immunoprecipitation, SDS-PAGE-electrophoresis, autoradiography, and immunoblotting was performed following standard protocols (11). Protein concentration was determined in all of the lysates by Bio-Rad, and equal amounts of protein were loaded per lane. Quantification of immunoblot bands was performed using ImageQuant software.

Animal Experiments. SCID (C.B.-17 *Scid/Scid*) mice were bred and maintained in a laminar flow tower in a defined flora colony as described previously (12). All of the manipulations with the animals were performed in a laminar flow hood with sterile techniques following the guidelines of the UCLA Animal Research Committee. For preparation of single cell suspensions, LAPC4 (10) and LAPC9 (13) tumors continuously passaged in SCID mice were minced in serum-free Iscove's medium (Life Technologies, Inc. Grand Island, NY), washed, digested with 0.1% Pronase E (EM Science, Gibbstown, NJ), washed again, and filtered through a 200 μm nylon mesh (BioDesign Inc. of New York, Carmel, NY). The cells were plated overnight, resuspended in PrEGM, and injected with Matrigel into the right flank of SCID mice. Tumor size was determined with calipers, and mice were randomized to

Received 5/16/02; accepted 7/12/02.

The costs of publication of this article were defrayed in part by the payment of page charges. This article must therefore be hereby marked *advertisement* in accordance with 18 U.S.C. Section 1734 solely to indicate this fact.

[1] Supported by grants from the National Cancer Institute, Department of Defense, and CaPCure. C. L. S. is a Doris Duke Distinguished Clinical Scientist.

[2] To whom requests for reprints should be addressed, at 11-934 Factor Building, University of California Los Angeles-Hematology-Oncology; 10833 Le Conte Avenue, Los Angeles, CA 90095-1678. Phone: (310) 206-5585; Fax: (310) 206-8502; E-mail: csawyers@mednet.ucla.edu.

[3] The abbreviations used are: AR, androgen receptor; RTK, receptor tyrosine kinase; EGF, epidermal growth factor; ERK, extracellular signal-regulated kinase; UCLA, University of California Los Angeles; TGF, transforming growth factor; SCID, severe combined immunodeficient; AW, androgen withdrawal; MAPK, mitogen-activated protein kinase.

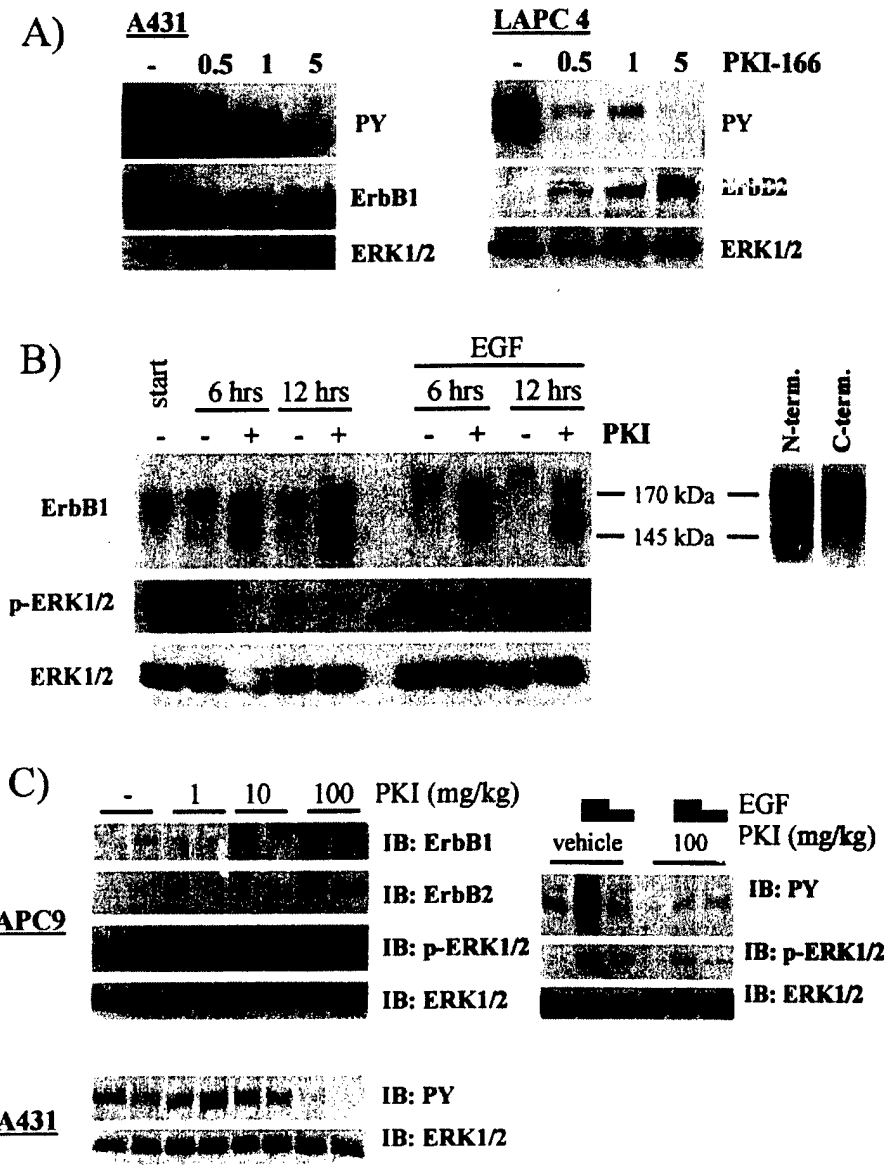

Fig. 1. PKI-166 inhibits ErbB1 and ErbB2 receptor signaling and degradation. *A*, immunoblots of A431 (*left panel*) and LAPC4 (*right panel*) cells treated for 12 h with various concentrations of PKI-166 (in μM) before stimulation with EGF (100 ng/ml) for 10 min. *B, left panel*, autoradiograph of immunoprecipitated ErbB1 (*top row*) and immunoblots (*middle and bottom row*) of lysates from A431 cells metabolically labeled for 12 h with [^{35}S]methionine and chased in the presence of PKI-166 (5 μM) and/or EGF (100 ng/ml). PKI-166 was added 10 min before EGF where indicated. *Right panel*, immunoblot of A431 cells treated with PKI-166 for 12 h using a ErbB1 antibodies directed against NH_2-terminal and COOH-terminal epitopes. *C*, immunoblots of lysates from LAPC9 (*left top panel* and *right panel*) or A431 (*left bottom panel*) xenograft tumors harvested 1 h after the fifth daily dose of PKI-166 (2 tumors per condition). The *right panel* shows lysates of LAPC9 tumors from mice injected i.p. with PBS, 0.1 mg EGF, or 0.01 mg EGF 1 h after the fifth daily dose of PKI-166. Tumors were harvested 5 min after EGF injection.

treatment groups when tumor size reached ~100 mm^3. Mean tumor volumes (in mm^3) at treatment begin was equal between groups. PKI-166 was administered daily by gavage with an 18-gauge animal feeding needle (VWR, San Dimas, CA). Testosterone pellets (Innovative Research of America) were implanted s.c. Tumor growth data are expressed as fold tumor volume compared with day 1 (Fig. 2, *A* and *C*) or as ratio between the fold increases in tumor volume for PKI-166 and vehicle treated mice ("T/C"; Figs. 2*B* and 3*B*). Statistical analyses comparing fold increases between groups were performed on the natural logarithms of the tumor volumes corrected for baseline volumes. Student's *t* test was used for comparison of two groups. ANOVA using the Tukey Studentized range method was used for multigroup comparisons.

RESULTS

PKI-166 Blocks ErbB1/ErbB2 Activity in Prostate Cancer Cells. We first examined the effects of PKI-166 on EGF-induced signal transduction through ErbB1 and ErbB2 RTKs in the human prostate cancer cell lines LAPC4 and LNCaP, both of which express the AR. The human vulvar carcinoma cell line A431, which expresses high levels of *ErbB1* because of amplification of the erbB1 locus, was used as a positive control. In A431 cells treated with EGF, immunoblotting with a phosphotyrosine antibody showed a dominant band of M_r ~170,000 representing the phosphorylated ErbB1 receptor (Fig. 1*A*). In EGF-treated LAPC-4 cells, which express considerably less ErbB1 than A431 cells but more ErbB2 (data not shown), tyrosine phosphorylation of a M_r 170,000 and a M_r 185,000 band was observed representing phosphorylated ErbB1 and ErbB2, respectively. Dose-dependent inhibition of receptor autophosphorylation was noted after pretreatment with PKI-166, with estimated IC_{50} values of 0.5 μM for ErbB1 and 5 μM for ErbB2. Similar doses of PKI-166 have been reported to inhibit phosphorylation of ErbB1 and ErbB2 RTKs but not other tyrosine or serine/threonine kinases in nonprostatic human cancer cell lines (14–16). We also noted that PKI-166 treatment resulted in a dose-dependent increase in the level of ErbB1 protein in A431 cells and ErbB2 protein in LAPC4 cells. The increase in ErbB2 expression in LAPC4 cells was apparent at 0.5 μM PKI-166, a concentration that predominantly inhibits phosphorylation of ErbB1.

Previous work has indicated that ErbB1 protein is degraded after receptor activation by ligand, raising the possibility that the increased levels of ErbB1 and ErbB2 in PKI-166-treated cells are a reflection of

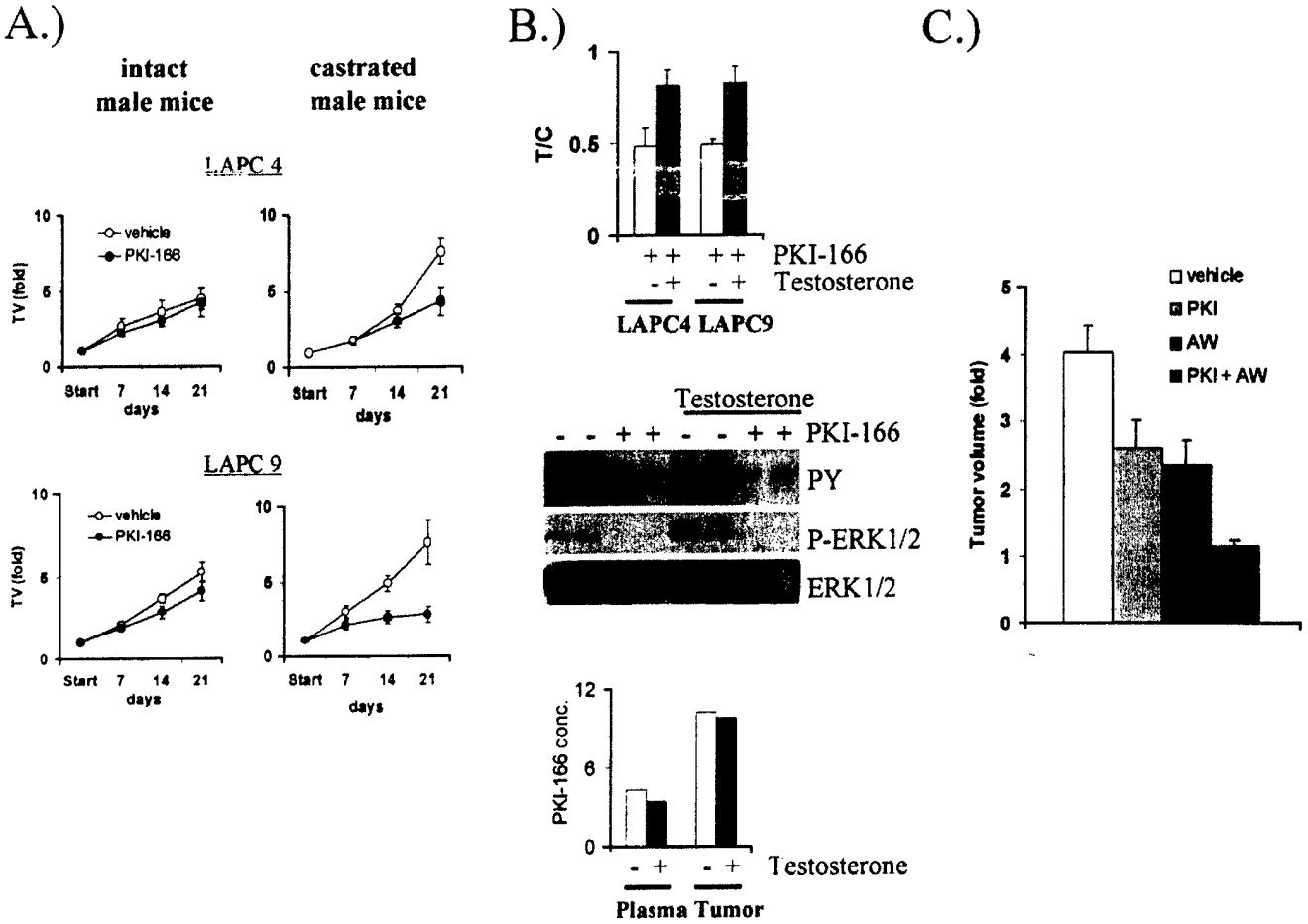

Fig. 2. Androgen modifies the growth response to PKI-166. *A*, PKI-166 inhibits the growth of human prostate cancer xenografts growing in castrated mice. Mice bearing LAPC4 or LAPC9 xenograft tumors were treated daily for 3 weeks with 100 mg/kg PKI-166 *versus* vehicle (n = 6–9 per group). Data are expressed as fold tumor volume compared with day 1; *bars*, ± SE. *B, top panel*, testosterone rescues growth inhibition by PKI-166 in castrated animals. Castrated male mice bearing androgen-independent xenografts were randomized to four treatment groups (vehicle, PKI-166, vehicle plus testosterone, and PKI plus testosterone). Data are expressed as ratio between the fold increase in tumor volume for PKI-166 treated mice and the fold increase in tumor volume for vehicle treated mice (*T/C*). Each treatment group consisted of 8–9 mice. *Middle panel*, testosterone does not impair the ability of PKI-166 to inhibit ErbB1/ErbB2 signaling. Castrated male mice bearing LAPC9 xenograft tumors were treated with PKI-166 +/− testosterone for 21 days, and EGF (0.1 mg) was administered i.p. 1 h after the last PKI-166 dose. Tumors (n = 2 per treatment condition) were harvested 5 min later. Displayed are immunoblots for PY, ERK1/2, and total ERK1/2. *Bottom panel*, testosterone does not affect PKI-166 bioavailability in mice. PKI-166 levels in plasma (μM) and LAPC9 tumors (nmol/g) were determined by reversed-phase high-performance liquid chromatography in castrated mice after 21 days of treatment with PKI-166 (100 mg/kg) +/− testosterone. Blood and tumors were collected 1 h after the last dose of PKI-166 and displayed as mean values (n = 3 per group). *C*, AW augments inhibitory effect of PKI-166 on LAPC4 xenografts in intact male mice. Surgical castration was performed on the same day as PKI-166 treatment was started. Data are expressed as fold tumor volume compared with day 1. Six mice were treated per group; *bars*, ± SE.

kinase inhibition. To determine whether pharmacologic inhibition of RTK activity delays receptor degradation, we measured the effect of PKI-166 on immunoprecipitated, [^{35}S]methionine/cysteine radiolabeled ErbB1 receptors in A431 cells (Fig. 1*B, left panel*). In the absence of PKI-166 and EGF, the receptor half-life of ErbB1 was between 6 and 12 h, consistent with the half-life of ~9 h published previously (17). Stimulation of A431 cells with EGF resulted in phosphorylation of ErbB1, as evidenced by retarded electrophoretic mobility compared with the unphosphorylated receptor, and shortening of the receptor half-life to <6 h. PKI-166 impaired the degradation of ErbB-1 receptor protein in both the presence and absence of EGF. These data support the concept that kinase activity is required for receptor degradation, consistent with prior work showing increased receptor half-life in ErbB1 alleles containing point mutations within the ErbB1 ATP-binding site (18, 19). We also noted accumulation of a lower molecular weight protein in the ErbB1 immunoprecipitates from PKI-166-treated cells. This M_r 145,000 protein was immunoprecipitated by an ErbB1 antibody directed against a cell-surface epitope but not by an antibody directed against a COOH-terminal epitope (Fig. 1*B, right panel*), indicating that it is likely to be a COOH-terminal truncation of the receptor. Similarly sized bands have been observed previously after treatment of A431 cells with the lysosomal inhibitor methylamine (17) and presumably represent an intermediate step in receptor degradation.

Because many growth factor signals are transmitted to the nucleus through ERKs (20), we also measured the effect of PKI-166 on ERK1/2 activation. At a dose that inhibits ErbB1 phosphorylation, PKI-166 completely blocked basal and EGF-induced ERK1/2 activation in A431 cells (Fig. 1*B*). Similar results were obtained in LAPC4 and LNCaP prostate cancer cells (data not shown). These data establish the biochemical activity of PKI-166 against ErbB1/ErbB2 RTKs *in vitro*, including effects on receptor autophosphorylation, receptor degradation, and additional signal transduction.

PKI-166 Blocks ErbB1/ErbB2 Signal Transduction in Tumors in Mice. We next examined the effects of PKI-166 treatment on ErbB1/ErbB2-mediated signaling *in vivo*. SCID mice bearing tumors from the human prostate cancer xenografts LAPC4 (10) and LAPC9 (13) or from the A431 cell line were treated for 5 days with 0, 1, 10, and 100 mg/kg of PKI-166, and tumor tissue was harvested 1 h after the last dose was administered. Lysates from A431 tumors displayed

constitutive phosphorylation of ErbB-1 that was inhibited by treatment of mice with 100 mg/kg PKI-166. Similar analysis of ErbB phosphorylation in prostate cancer xenografts was not informative because of low basal levels of phosphotyrosine (data not shown). However, we did observe decreased ERK1/2 activation and increased levels of total ErbB1 and ErbB2 protein in the prostate cancer xenografts from mice treated with 100 mg/kg of PKI-166, providing indirect evidence for ErbB1/ErbB2 RTK inhibition at this dose (Fig. 1*C, left panel*). To obtain direct evidence of ErbB1/ErbB2 blockade in PKI-166-treated mice, we induced receptor activation by systemic administration of EGF (21). Two different doses of EGF were injected i.p. and resulted in dose-dependent receptor phosphorylation and ERK1/2 activation in LAPC9 tumors (Fig. 1*C, right panel*). PKI-166 given p.o. at a dose of 100 mg/kg markedly blunted this activation (Fig. 1*C, right panel*). Similar results were obtained in mice bearing LAPC4 or A431 xenografts (data not shown).

PKI-166 Blocks the Growth of Prostate Cancers in Mice in an Androgen-dependent Fashion. Having defined the dose of PKI-166 required to inhibit ErbB1/ErbB2 RTKs *in vivo*, we were now able to examine the role of these RTKs in the growth of human prostate cancer. We chose the LAPC xenograft model to address this question because of its similarity to clinical prostate cancer (10) and the convenience of monitoring drug effects on s.c. tumor volumes. Tumors derived from the A431 cell line were used as a positive control and were completely growth arrested by PKI-166 (data not shown). Androgen-independent sublines of the prostate cancer xenografts grown in castrated host mice were consistently more sensitive to growth inhibition by PKI-166 than androgen-dependent sublines of the same xenograft growing in intact male ($P < 0.005$). This observation was confirmed in multiple experiments and noted in both LAPC4 and LAPC9 xenografts (Fig. 2*A*).

The trend toward enhanced activity of PKI-166 in the absence of androgen was reminiscent of our previous data showing more dramatic effects of forced ErbB2 overexpression on prostate cancer growth in castrated *versus* intact male mice (2). At that time we postulated that the major effects of ErbB1/ErbB2 pathway activation might be mediated through AR but that these effects were most relevant in the setting of low (castrate) levels of androgen. To examine this hypothesis, we asked if the suppression of growth by PKI-166 in castrated male mice could be rescued by androgen supplementation, which was administered by s.c. implantation of slow release testosterone pellets. In both LAPC4 and LAPC9 xenografts (Fig. 2*B, top panel*), androgen add-back partially rescued the growth inhibitory effects of PKI-166 ($P < 0.05$). One potential explanation for this result is that androgen impairs the ability of PKI-166 to inhibit ErbB1/ErbB2 RTKs. To examine this possibility, we treated eight castrated male mice bearing LAPC tumors with PKI-166 in the presence or absence of supplemental testosterone, and measured ErbB receptor and ERK1 activation in tumor lysates after systemic administration of EGF. Androgen supplementation did not impair the ability of PKI-166 to inhibit EGF-induced signal transduction (Fig. 2*B, middle panel*) nor did androgen affect the bioavailability of PKI-166 as shown by similar mean plasma and tumor drug levels in castrated and androgen-supplemented mice (Fig. 2*B, bottom panel*). These data indicate that the rescue of PKI-166-induced growth suppression by androgen supplementation cannot be explained by a failure of PKI-166 to inhibit its target. Rather, our findings suggest that ErbB1/ErbB2 signaling is not required for prostate cancer growth when androgen is present at high levels.

If a threshold level of circulating androgen exists below which ErbB1/ErbB2 RTKs are required for prostate cancer growth, acute AW by surgical castration should increase the growth-inhibitory effects of PKI-166. To test this hypothesis, we randomized intact male SCID mice bearing the LAPC4 xenograft to four treatment groups. Compared with vehicle-treated mice, AW by surgical castration slowed the growth of LAPC4 tumors ($P < 0.05$), as expected (10). Growth inhibition by PKI-166 given at 100 mg/kg daily did not reach statistical significance. However, the combination of PKI-166 with AW resulted in nearly complete growth suppression (Fig. 2*C*). The difference between the combined treatment group and any of the other three treatment groups was highly statistically significant ($P < 0.001$).

Sensitivity to Growth Inhibition by PKI-166 Is Correlated with ERK Activation. The LAPC-4 and LAPC-9 xenografts have been passaged in mice over multiple generations, and various androgen-dependent and androgen-independent subclones derived from the original parental lines have been maintained independently. In the course of these studies we noted that subclones derived from the same parental line occasionally displayed differences in their sensitivity to PKI-166. These sublines provide an opportunity, within an isogenic system, to examine variables in the ErbB1/ErbB2 signaling pathway that might determine response to ErbB1/ErbB2 inhibition. To address this question, we performed biochemical analysis on six LAPC xenograft clones, of which four were grown in intact male mice (clones 1 and 2 for both LAPC 4 and LAPC 9) and two in castrated male mice (clones 3 for both LAPC 4 and LAPC 9). We examined not only the expression levels of the direct PKI-166 targets ErbB1 and ErbB2, but also the activation state of the Ras/MAPK and phosphatidylinositol 3′-kinase/Akt-pathways. Both pathways are considered central effectors of the ErbB signaling network (20) and have been implicated in the progression of human prostate cancer (3, 22–24). Expression of the ErbB-1 ligand TGF-α was included in the analysis because of its suggested role as an autocrine growth factor in androgen-independent prostate cancer (25). To be able to correlate for each subline the expression of these biochemical parameters with the growth response to PKI-166, we quantified the relevant immunoblot bands (Fig. 3*A*) by densitometry. Despite differences in the magnitude of ERK1/2-activation between the LAPC4 and LAPC9 xenograft models, we found within each model a positive correlation between the degree of growth-inhibition by PKI-166 and the level of ERK1/2-activation (Fig. 3*B*). No such correlation was found for expression levels of ErbB1, ErbB2, TGF-α, or activation level of Akt. Whereas the number of available sublines for each xenograft was not sufficient to perform a multivariate analysis, our results in an isogenic system suggest that expression levels of ErbB-1 or ErbB-2 are not sufficient to determine sensitivity to PKI-166 and are consistent with studies using the ErbB-1 inhibitor ZD1839 (26) or the anti-ErbB-2 monoclonal antibody Mab 4D5 (27).

We also noted that androgen-independent tumors (clones 3) showed increased activation of ERK1/2 when compared with tumors grown in intact male mice (Fig. 3*A*). This observation was confirmed by serial analysis of androgen-dependent LAPC4 xenografts at various times postcastration during the evolution to androgen independence (Fig. 3*B*). This data are consistent with results of immunohistochemical analyses of human prostate cancer specimens using phosphospecific antibodies to ERK1/2 (28).

DISCUSSION

In conclusion, our study shows that ErbB1/ErbB2 RTKs contribute to the growth of human prostate cancer and that this contribution is greatest when levels of androgen are limiting. The nature of the interaction between AR pathway and ErbB1/ErbB2 RTKs remains to be defined. It is conceivable that ErbB-RTKs provide growth and survival signals for prostate cancer cells, which are completely independent of AR and only biologically relevant under the selective pressure of androgen deprivation. Alternatively, ErbB-RTKs might

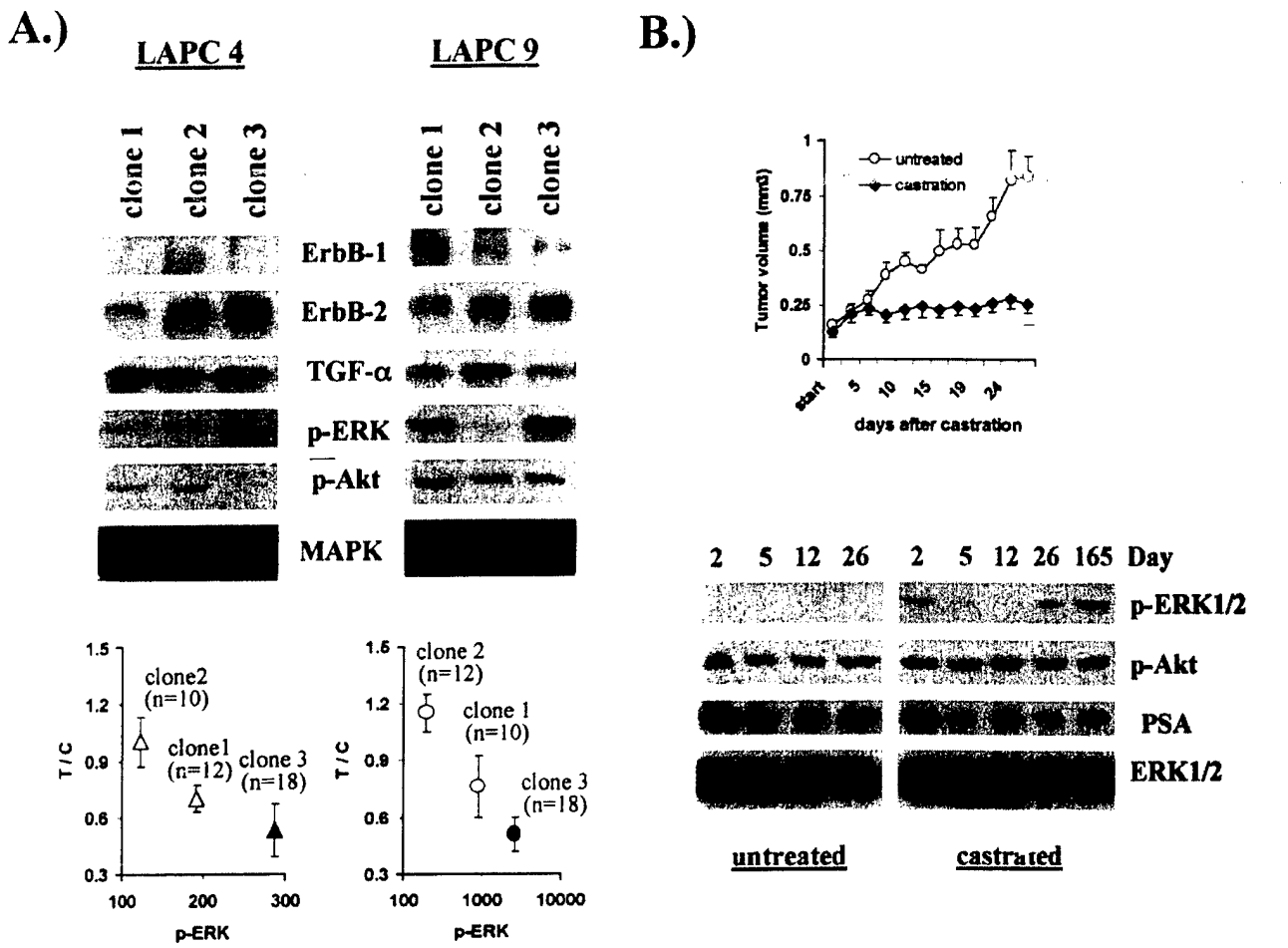

Fig. 3. Activity of p-ERK correlates with growth-inhibition by PKI-166 *in vivo* and is increased in androgen-independent tumors. *A, top panel,* immunoblot of tumor lysates from six different LAPC sublines; *bottom panel,* correlation between growth inhibition by PKI-166 and levels of activated ERK for six LAPC clones. Immunoblot bands were quantified by densitometry, and the absolute value under the peak was plotted on the X-axis. The Y-axis shows the ratio between the fold increase in tumor volume for PKI-166 treated mice and the fold increase in tumor volume for vehicle treated mice (*T/C*). *Open symbols* represent xenograft clones grown in intact mice; *closed symbols* represent xenograft clones growing in castrated animals. *B,* effect of castration on p-ERK levels in LAPC4 xenograft tumors harvested at various time points after castration; *bars,* ±SE.

promote prostate cancer growth through ligand-independent activation of AR (2, 3). MAPKs, the primary effectors of the ErbB/Ras/Raf signaling pathway, have been suggested to link growth factor receptors and steroid hormone receptors, possibly by direct phosphorylation of the latter (29). In that context, our observation that increased ERK1/2 activation is positively correlated with response to ErbB1/ErbB2 pathway inhibition is particularly intriguing and warrants additional investigation.

A growing number of small molecule inhibitors of ErbB1 and/or ErbB2 are making their way into clinical trials and show slightly different potencies in relative inhibition of ErbB1 *versus* ErbB2 RTKs (9). Because these compounds appear to have therapeutic effects in subsets of patients, the question of which kinase is important for targeting, ErbB1 or ErbB2, is frequently raised. The dose of PKI-166 (100 mg/kg) used in most of our experiments inhibited both ErbB1 and ErbB2 RTKs, as evidenced by biochemical studies on tumor lysates, comparison of drug levels in mice with *in vitro* drug concentrations, and recent data from other mouse models of cancer treated with PKI-166 (15). Interestingly, the ErbB-2 RTK monoclonal antibody Herceptin failed to inhibit the growth of androgen-independent sublines of the CWR22 human prostate cancer xenograft model (30). Whereas this difference may reflect the use of different cell lines, it raises the possibility that inhibition of the ErbB-1 RTK is required to halt androgen-independent growth.

Despite the difficulty in dissecting the relative contribution of individual ErbB-receptor family members in naturally arising tumors, our data provide rationale for testing ErbB1/2-RTK inhibitors in clinical trials of human prostate cancer. It may also offer some guidance for the design of such studies. Whereas most current trials study the effects of ErbB-inhibitors in patients who failed hormonal therapy, our data suggest a role for combining ErbB-RTK inhibition with AW for patients with early-stage disease. Our findings also raise the possibility that the activation state of the Ras/MAPK pathway in clinical specimens might serve as a biomarker to identify tumors that "depend" on this pathway and may be more likely to respond to treatment with ErbB1/ErbB2 inhibitors.

ACKNOWLEDGMENTS

We thank Drs. Elisabeth Buchdunger and Peter Traxler (Novartis Pharma AG) for providing PKI-166, Drs. Josef Brueggen and Robert Cozens (Novartis Pharma AG) for determination of PKI-166 concentrations, Dr. Elliot Landaw (UCLA) for statistical analyses, Randy Chen for technical assistance, and Phuong Huynh for assistance in preparation of the manuscript.

REFERENCES

1. Grossmann, M. E., Huang, H., and Tindall, D. J. Androgen receptor signaling in androgen-refractory prostate cancer. J. Natl. Cancer Inst., *93:* 1687–1697, 2001.

2. Craft, N., Shostak, Y., Carey, M., and Sawyers, C. L. A mechanism for hormone-independent prostate cancer through modulation of androgen receptor signaling by the HER-2/neu tyrosine kinase. Nat. Med., *5:* 280–285, 1999.
3. Yeh, S., Lin, H. K., Kang, H. Y., Thin, T. H., Lin, M. F., and Chang, C. From HER2/Neu signal cascade to androgen receptor and its coactivators: a novel pathway by induction of androgen target genes through MAP kinase in prostate cancer cells. Proc. Natl. Acad. Sci. USA, *96:* 5458–5463, 1999.
4. Culig, Z., Hobisch, A., Cronauer, M. V., Radmayr, C., Trapman, J., Hittmair, A., Bartsch, G., and Klocker, H. Androgen receptor activation in prostatic tumor cell lines by insulin- like growth factor-I, keratinocyte growth factor, and epidermal growth factor. Cancer Res., *54:* 5474–5478, 1994.
5. Signoretti, S., Montironi, R., Manola, J., Altimari, A., Tam, C., Bubley, G., Balk, S., Thomas, G., Kaplan, I., Hlatky, L., Hahnfeldt, P., Kantoff, P., and Loda, M. Her-2-neu expression and progression toward androgen independence in human prostate cancer. J. Natl. Cancer Inst., *92:* 1918–1925, 2000.
6. Osman, I., Scher, H. I., Drobnjak, M., Verbel, D., Morris, M., Agus, D., Ross, J. S., and Cordon-Cardo, C. HER-2/neu (p185neu) protein expression in the natural or treated history of prostate cancer. Clin. Cancer Res., *7:* 2643–2647, 2001.
7. Shi, Y., Brands, F. H., Chatterjee, S., Feng, A. C., Groshen, S., Schewe, J., Lieskovsky, G., and Cote, R. J. Her-2/neu expression in prostate cancer: high level of expression associated with exposure to hormone therapy and androgen independent disease. J. Urol., *166:* 1514–1519, 2001.
8. Slamon, D. J., Clark, G. M., Wong, S. G., Levin, W. J., Ullrich, A., and McGuire, W. L. Human breast cancer: correlation of relapse and survival with amplification of the HER-2/neu oncogene. Science (Wash. DC), *235:* 177–182, 1987.
9. Mendelsohn, J. The epidermal growth factor receptor as a target for cancer therapy. Endocr. Relat. Cancer, *8:* 3–9, 2001.
10. Klein, K. A., Reiter, R. E., Redula, J., Moradi, H., Zhu, X. L., Brothman, A. R., Lamb, D. J., Marcelli, M., Belldegrun, A., Witte, O. N., and Sawyers, C. L. Progression of metastatic human prostate cancer to androgen independence in immunodeficient SCID mice. Nat. Med., *3:* 402–408, 1997.
11. Daub, H., Wallasch, C., Lankenau, A., Herrlich, A., and Ullrich, A. Signal characteristics of G protein-transactivated EGF receptor. EMBO J., *16:* 7032–7044, 1997.
12. Chackal-Roy, M., Niemeyer, C., Moore, M., and Zetter, B. R. Stimulation of human prostatic carcinoma cell growth by factors present in human bone marrow. J. Clin. Investig., *84:* 43–50. 1989.
13. Craft, N., Chhor, C., Tran, C., Belldegrun, A., DeKernion, J., Witte, O. N., Said, J., Reiter, R. E., and Sawyers, C. L. Evidence for clonal outgrowth of androgen-independent prostate cancer cells from androgen-dependent tumors through a two-step process. Cancer Res., *59:* 5030–5036, 1999.
14. Bruns, C. J., Solorzano, C. C., Harbison, M. T., Ozawa, S., Tsan, R., Fan, D., Abbruzzese, J., Traxler, P., Buchdunger, E., Radinsky, R., and Fidler, I. J. Blockade of the epidermal growth factor receptor signaling by a novel tyrosine kinase inhibitor leads to apoptosis of endothelial cells and therapy of human pancreatic carcinoma. Cancer Res., *60:* 2926–2935, 2000.
15. Brandt, R., Wong, A. M., and Hynes, N. E. Mammary glands reconstituted with Neu/ErbB2 transformed HC11 cells provide a novel orthotopic tumor model for testing anti-cancer agents. Oncogene, *20:* 5459–5465, 2001.
16. Scheving, L. A., Stevenson, M. C., Taylormoore, J. M., Traxler, P., and Russell, W. E. Integral role of the EGF receptor in HGF-mediated hepatocyte proliferation. Biochem. Biophys. Res. Commun., *290:* 197–203, 2002.
17. Stoscheck, C. M., and Carpenter, G. Down regulation of epidermal growth factor receptors: direct demonstration of receptor degradation in human fibroblasts. J. Cell Biol., *98:* 1048–1053, 1984.
18. Honegger, A. M., Dull, T. J., Felder, S., Van Obberghen, E., Bellot, F., Szapary, D., Schmidt, A., Ullrich, A., and Schlessinger, J. Point mutation at the ATP binding site of EGF receptor abolishes protein-tyrosine kinase activity and alters cellular routing. Cell. *51:* 199–209, 1987.
19. Chen, W. S., Lazar, C. S., Poenie, M., Tsien, R. Y., Gill, G. N., and Rosenfeld, M. G. Requirement for intrinsic protein tyrosine kinase in the immediate and late actions of the EGF receptor. Nature (Lond.), *328:* 820–823, 1987.
20. Yarden, Y., and Sliwkowski, M. X. Untangling the ErbB signalling network. Nat. Rev. Mol. Cell. Biol., *2:* 127–137, 2001.
21. Donaldson, R. W., and Cohen, S. Epidermal growth factor stimulates tyrosine phosphorylation in the neonatal mouse: association of a M(r) 55, 000 substrate with the receptor. Proc. Natl. Acad. Sci. USA, *89:* 8477–8481, 1992.
22. Gioeli, D., Zecevic, M., and Weber, M. J. Immunostaining for activated extracellular signal-regulated kinases in cells and tissues. Methods Enzymol., *332:* 343–353, 2001.
23. Wen, Y., Hu, M. C., Makino, K., Spohn, B., Bartholomeusz, G., Yan, D. H., and Hung, M. C. HER-2/neu promotes androgen-independent survival and growth of prostate cancer cells through the Akt pathway. Cancer Res., *60:* 6841–6845, 2000.
24. Malik, S. N., Brattain, M., Ghosh, P. M., Troyer, D. A., Prihoda, T., Bedolla, R., and Kreisberg, J. I. Immunohistochemical demonstration of phospho-akt in high Gleason grade prostate cancer. Clin. Cancer Res., *8:* 1168–1171, 2002.
25. Scher, H. I., Sarkis, A., Reuter, V., Cohen, D., Netto, G., Petrylak, D., Lianes, P., Fuks, Z., Mendelsohn, J., and Cordon-Cardo, C. Changing pattern of expression of the epidermal growth factor receptor and transforming growth factor α in the progression of prostatic neoplasms. Clin. Cancer Res., *1:* 545–550, 1995.
26. Moasser, M. M., Basso, A., Averbuch, S. D., and Rosen, N. The tyrosine kinase inhibitor ZD1839 ("Iressa") inhibits HER2-driven signaling and suppresses the growth of HER2-overexpressing tumor cells. Cancer Res., *61:* 7184–7188, 2001.
27. Lane, H. A., Beuvink, I., Motoyama, A. B., Daly, J. M., Neve, R. M., and Hynes, N. E. ErbB2 potentiates breast tumor proliferation through modulation of p27(Kip1)-Cdk2 complex formation: receptor overexpression does not determine growth dependency. Mol. Cell. Biol., *20:* 3210–3223, 2000.
28. Gioeli, D., Mandell, J. W., Petroni, G. R., Frierson, H. F., Jr., and Weber, M. J. Activation of mitogen-activated protein kinase associated with prostate cancer progression. Cancer Res., *59:* 279–284, 1999.
29. Kato, S., Endoh, H., Masuhiro, Y., Kitamoto, T., Uchiyama, S., Sasaki, H., Masushige, S., Gotoh, Y., Nishida, E., Kawashima, H., and *et al.* Activation of the estrogen receptor through phosphorylation by mitogen-activated protein kinase. Science (Wash. DC), *270:* 1491–1494, 1995.
30. Agus, D. B., Scher, H. I., Higgins, B., Fox, W. D., Heller, G., Fazzari, M., Cordon-Cardo, C., and Golde, D. W. Response of prostate cancer to anti-Her-2/neu antibody in androgen-dependent and -independent human xenograft models. Cancer Res., *59:* 4761–4764, 1999.

0888-8809/02/$15.00/0
Printed in U.S.A.

Molecular Endocrinology 16(10):2323–2337

doi: 10.1210/me.2002-0004

Identification of an Androgen-Dependent Enhancer within the Prostate Stem Cell Antigen Gene

ANJALI JAIN, AMANDA LAM, IGOR VIVANCO, MICHAEL F. CAREY AND ROBERT E. REITER

Departments of Urology (A.J., R.E.R.), Biological Chemistry (A.L., M.F.C.), and Medicine (I.V.), and Molecular Biology Institute (M.F.C., R.E.R.), UCLA School of Medicine, Los Angeles, California 90095

Prostate stem cell antigen (PSCA) is emerging as an important diagnostic marker and therapeutic target in prostate cancer. Previous studies indicated that PSCA was directly regulated by androgens, but the mechanism has not been elucidated. Here we describe the identification of a compact cell-specific and androgen-responsive enhancer between 2.7 and 3 kb upstream of the transcription start site. The enhancer functions autonomously when positioned immediately adjacent to a minimal promoter. Deoxyribonuclease I footprinting analysis with recombinant androgen receptor (AR) reveals that the enhancer contains two AR binding sites at one end. Mutational analysis of the AR binding sites revealed the importance of the higher affinity one. The dissociation constant of the high affinity binding site (androgen response element I) was determined to be approximately 87 nM. The remainder of the enhancer contains elements that function synergistically with the AR. We discuss the structural organization of the PSCA enhancer and compare it with that found in other AR-regulated genes. (*Molecular Endocrinology* 16: 2323–2337, 2002)

PROSTATE CANCER BEGINS as an androgen-dependent (AD) tumor but progresses to an an drogen-independent (AI) phenotype upon androgen deprivation (1–3). Serum levels of the prostate-specific antigen (PSA) are used clinically as a marker for diagnosis and management of prostate cancer. Analysis of PSA gene regulation has provided considerable insight into the mechanisms of prostate cancer progression and the role that the androgen receptor (AR) plays in this transition (4–10). However, PSA is not an ideal marker for prostate cancer progression (11–13), and considerable effort has been expended to identify new markers and understand their regulation.

One such marker is prostate stem cell antigen (PSCA) (14), a cell surface protein related to the Ly-6/Thy-1 family of glycosylphosphatidyl-inositol (GPI)-anchored antigens. PSCA is expressed in normal prostate and bladder and is up-regulated in a large proportion of localized and metastatic prostate cancers (15). Overexpression of PSCA correlates with increasing tumor stage, grade, and metastasis to bone. A murine homolog of PSCA (mPSCA has been isolated and has a similar tissue distribution to human PSCA (16, 17). Like human PSCA, expression of mPSCA is up-regulated in multiple mouse models of prostate cancer, such as TRAMP (transgenic adenocarcinoma of the mouse prostate) and PTEN (phosphatase and tensin homolog) heterozygous mice. PSCA is also overexpressed in a large percentage of bladder and pancreatic cancers (18, 19). Although the precise role of PSCA in cancer progression is not known, its homologs (Thy-1 and Ly-6) have defined roles in cell signaling (20, 21) and have been implicated in cancer progression. A role for PSCA in cancer progression is suggested by studies showing that monoclonal antibodies targeting PSCA can block prostate cancer growth and metastasis in xenograft models of human prostate cancer (22). Together, these studies suggest that PSCA expression is both linked to and may play a biological role in carcinogenesis.

The mechanism(s) by which PSCA expression is regulated in normal tissue and cancer is not known. To study PSCA gene regulation, we recently isolated a 9-kb genomic fragment containing the human PSCA promoter/enhancer region (23). Consistent with the normal tissue distribution of PSCA, the 9-kb promoter/enhancer region was active in cell lines derived from normal and malignant prostate and bladder cells. This region was also androgen responsive in the LNCaP prostate cancer cell line, consistent with *in vivo* studies of mPSCA showing down-regulation of PSCA after castration (16). These initial studies suggest that the PSCA promoter is tissue specific and may be regulated by both AD (LNCaP) and AI (normal AR-negative prostate epithelial cells and bladder cells) pathways.

Abbreviations: AD, Androgen dependent; AI, androgen independent; AR, androgen receptor; ARDBD, AR DNA binding domain; ARE (AREI, AREII, AREIII), androgen response element (I, II, or III); ARR, androgen-responsive region; CMV, cytomegalovirus; DNase, deoxyribonuclease; FACS, fluorescence-activated cell sorting; FLAG, epitope DYKDDDDK; GFP, green fluorescent protein; GPI, glycosylphosphatidyl-inositol; GR, glucocorticoid receptor; GRDBD, glucocorticoid receptor DNA binding domain; high-mut, high affinity site mutant; HRE, hormone response element; K_d, dissociation constant; low-mut, low affinity site mutant; mPSCA, murine prostate stem cell antigen; PrEC, prostate epithelial cell; PrSC, prostate stromal cell; PSA, prostate-specific antigen; PSCA, prostate stem cell antigen; PTEN, phosphatase and tensin homolog; RACE, rapid amplification of cDNA ends; RLU, relative light units; RPMI, Roswell Park Memorial Institute; Slp, sex-limited protein; TRAMP, transgenic adenocarcinoma of the mouse prostate.

Transgenic mice bearing the human PSCA promoter region fused to green fluorescent protein (GFP) express GFP in mid-gestation after the appearance of prostatic buds from the urogenital sinus (23). In adult mice, GFP expression was restricted to a subset of cells located in the distal tips of the glands, which are hypothesized to be progenitors for the terminally differentiated secretory cells. GFP expression increased and expanded during periods of active ductal growth, such as puberty and after administration of testosterone to castrate mice, but was barely detectable after castration-induced prostate regression. Prostate carcinogenesis driven by T antigen in the TRAMP model resulted in an increased percentage and intensity level for PSCA promoter-driven GFP-positive cells. These results indicate that PSCA expression *in vivo* is related to growth, regeneration, and tumorigenesis of the prostate and that PSCA is regulated at the transcriptional level.

A critical observation is that PSCA and its regulatory regions are androgen regulated. It is not known whether androgen regulates the PSCA promoter directly or indirectly. It is possible, for example, that androgen induction of the PSCA promoter is related to the positive proliferative effect of androgen on LNCaP or to the expansion of GFP-positive progenitor cells during prostatic growth. To address this specific question, we have now carried out a detailed analysis of the PSCA regulatory region. Our major findings are 1) that androgen regulates PSCA directly and 2) that the bulk of PSCA androgen responsiveness can be mapped to one of two AR binding sites within a 300-bp enhancer region located 2.7 kb upstream of its transcription start site. Mutation of the high affinity binding site results in loss of binding to an AR DNA binding domain (ARDBD) *in vitro* and to a significant loss of androgen responsiveness *in vivo* These studies demonstrate that the PSCA promoter/enhancer has an androgen-responsive region with structure and function reminiscent of other prostate-specific and AD genes. The relationship of this region to PSCA overexpression in cancer remains to be determined.

RESULTS

Transcription Start Site Mapping

As a preliminary step in characterizing the DNA elements involved in androgen regulation of PSCA it was necessary to identify the transcriptional start site. Total RNA from the LAPC9-AD and AI prostate cancer xenografts (24) was subjected to Cap-dependent RACE (rapid amplification of cDNA ends), which accurately identifies transcription initiation sites because it is dependent upon the presence of a 7 meGTP Cap at the 5′end of the mRNA. Of 19 clones sequenced, 10 indicated that the major transcription start site was an adenine, 18 bp upstream from the initiating AUG (GenBank accession no. AF176678; this sequence represents the antisense strand of the genomic clone where nucleotide no. 65248 represents the initiating ATG) and 23 bp downstream of the putative TATA box. A minor start site was located 2 bp downstream of the adenine.

Promoter Activity in Cell Line Transfections Correlates with Endogenous PSCA Expression

To determine whether the cell specificity of the PSCA promoter constructs match that of the endogenous gene, a PSCA promoter-luciferase construct bearing 6 kb of upstream sequence was transfected into a panel of prostate and nonprostate cell lines and normalized to cytomegalovirus (CMV) luciferase activity (Fig. 1). Previous studies had shown that the 6-kb construct elicited a transcriptional activity similar to that of the 9-kb construct employed in the transgenic study (23). Transfections were performed in the presence and absence of the synthetic androgen R1881.

The promoter was found to be active and androgen-inducible in the AR-positive prostate cancer LNCaP cell line (25) and in a cell line derived from the LAPC4 xenograft. It was also active but not inducible in the bladder carcinoma cell line HT1376 (26), which lacks AR but still expresses PSCA, and in the LAPC9 xenograft, which contains AR and expresses PSCA. The transfected gene was active but not androgen inducible in AR-negative, PrEC populations, which express PSCA. In contrast, the promoter was relatively inactive

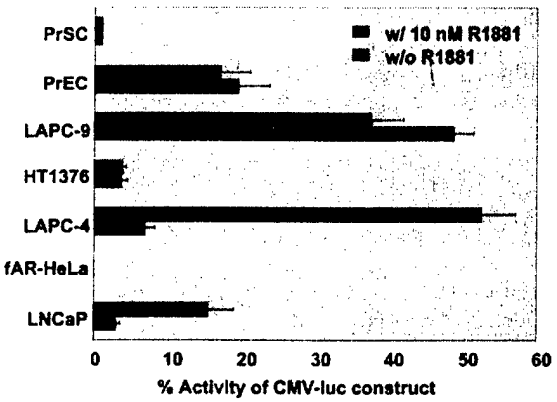

Fig. 1. Activity of the PSCA Promoter in Cell Lines

The 6-kb PSCA promoter, PSCA-6.0, was analyzed by transient transfection into various cell lines in the presence or absence of 10 nM R1881. For each cell line tested, the data are represented as a percentage of the CMV-luciferase activity. The PSCA promoter is active in human prostate (LNCaP, LAPC4, and LAPC9) and bladder (HT1376) cell lines but is relatively inactive in FLAG-tagged AR containing cervical carcinoma cells (fAR-HeLa). The promoter is also active in primary prostate epithelial cell culture (PrEC) but not in primary prostate stromal cell culture (PrSC). The promoter is androgen-inducible in LNCaP and LAPC4 cells. PSCA expression has been observed in LAPC4, LAPC9, PrEC, and HT1376 cells, whereas it is absent in fAR-HeLa and PrSC cells.

in a panel of cell lines derived from tissues that do not express PSCA, such as primary PrSCs (Fig. 1), HeLa cells expressing FLAG-AR (AR with N-terminal FLAG epitope tag DYKDDDDK) (cervical carcinoma) (27), 293T (human kidney) (not shown), baby hamster kidney cells (not shown), MCF7 (breast carcinoma), and NIH3T3 fibroblasts (23). The data indicate a selectivity of PSCA expression in cell culture that parallels the *in vivo* pattern.

Authentic Regulation Is Achieved with Stably Integrated Reporter Constructs in LNCaP Cells

LNCaP cells were employed as an experimental system for promoter mapping because these cells support a robust androgen response analogous to that observed in the transgenic models (23). To validate the system for detailed expression studies, a 6-kb PSCA-GFP fusion was stably integrated into LNCaP cells, and androgen-inducible GFP expression was assessed by fluorescence microscopy and fluorescence-activated cell sorting (FACS). In the absence of androgen, the PSCA 6-kb GFP cells displayed low but measurable levels of expression *vs.* the GFP control by both microscopy and FACS analysis (Fig. 2, panel C *vs.* A). However, with the addition of androgen a 2-fold increase in the number of cells expressing GFP (panel C *vs.* D) was observed along with a 10-fold increase in the fluorescence intensity (Fig. 2, panel C *vs.* D). These data demonstrated that authentic PSCA gene regulation could be recreated in the LNCaP cell line and that it maintained its binary mode of regulation in the context of a chromatin environment. This is an important observation because it has been established that appropriate assessment of endogenous transcriptional responses to hormones requires a chromatin environment (28, 29).

Identification of the PSCA Enhancer and Promoter

LNCaP cells were employed to systematically map the promoter using a collection of 5′ promoter deletions between −38 bp and −6 kb (Fig. 3A). We performed the analysis in a stepwise fashion by gradually homing in on the androgen-responsive enhancer using two sets of deletions. The first set comprised 500-bp to 1-kb deletions (Fig. 3B) and the second set comprised 200- to 300-bp deletions (Fig. 3C). Each set provided data that allowed us to assign functional borders to the regions conferring AI and AD promoter activity. The PSA basic promoter-enhancer construct (PSA-2.4; Ref. 30), a classic AR-responsive regulatory region, and two other constructs, ARE4 (30) and EnhE4 (27), were used as positive controls for androgen induction. All three positive controls lacked AI activity but displayed a robust androgen response in the presence of 10 nM R1881 (Fig. 3B).

The PSCA-0.038 construct or $PSCA_T$, bearing the putative TATA box, does not contribute significantly to the reporter activity in either the presence or absence of R1881 (Fig. 3B). The AI promoter activity is first detected in PSCA-0.5 and continues to increase grad-

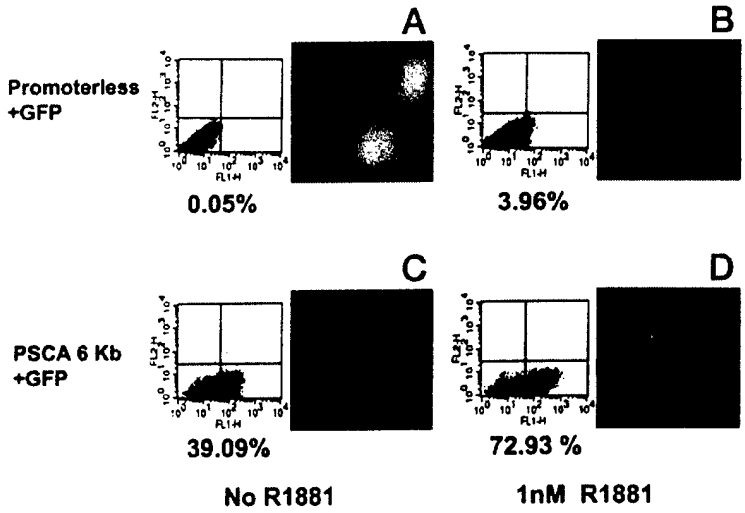

Fig. 2. PSCA Promoter Is Androgen Responsive in a Genomic Context

The androgen responsiveness of the PSCA promoter was assessed in the human prostate cancer cell line, LNCaP. Stable LNCaP cell lines expressing the GFP reporter were generated using either the PSCA 6-kb promoter (PSCA 6 kb+GFP) or a promoterless construct (Promoterless + GFP) as a negative control. These lines were grown in steroid-depleted medium for 1 wk and androgen (10 nM R1881) was added for 48 h. The GFP expression was assessed by FACS (*left figure in every panel*) and by fluorescence microscopy (*right figure in every set*) in the presence (B and D) and absence (A and C) of 10 nM R1881. The x-axis on the FACS graph represents the FL1 channel which measures light in the *green* range of the spectrum (515–545 nm) and the y-axis represents the FL2 channel that measures the *orange-red* light (564–606 nm). The PSCA promoter was clearly induced in the presence of androgen as is demonstrated by the increase in the number (39–73%) and intensity (~10-fold induction) of cells expressing GFP.

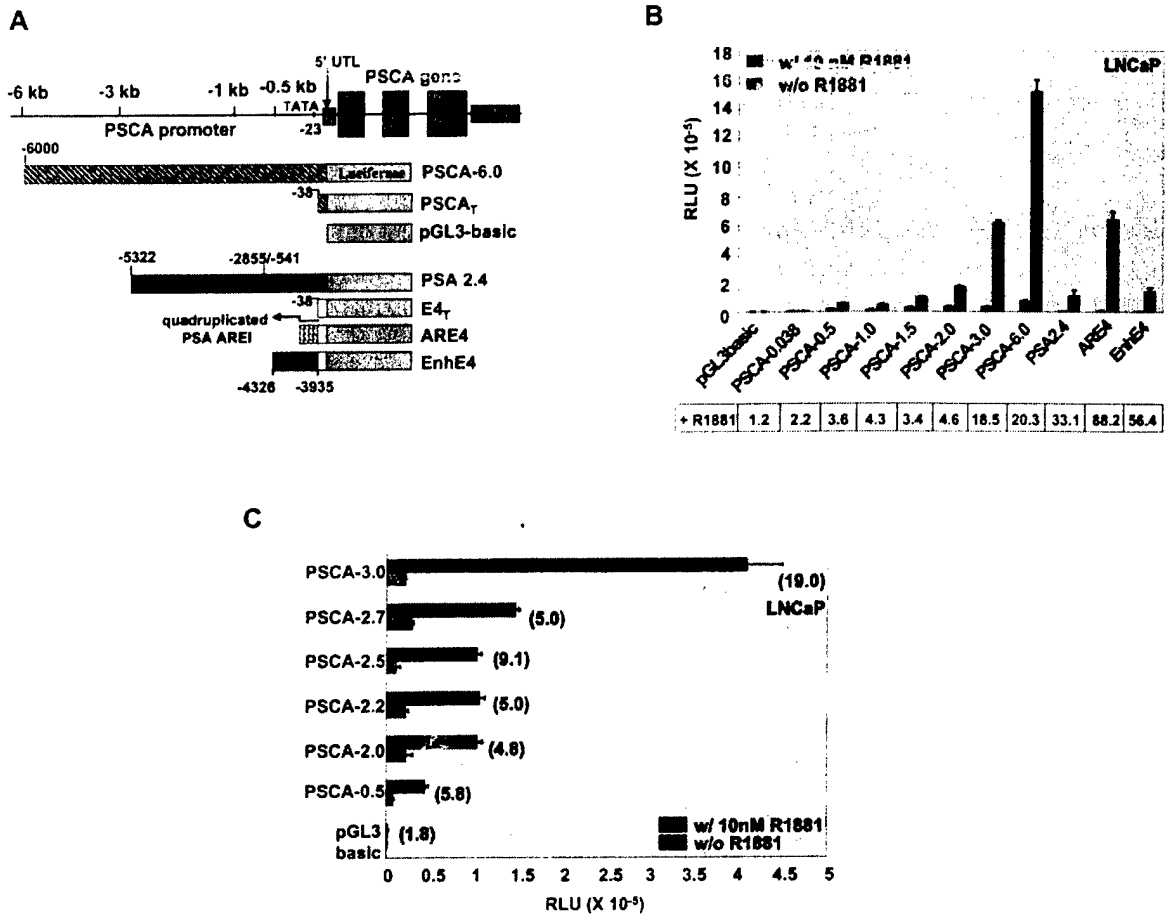

Fig. 3. Delineating the PSCA Enhancer

A, Schematic of PSCA promoter deletion constructs. Progressive 5′ deletions of the PSCA promoter between −6 kb and the TATA box at −0.038 (PSCA$_T$) were linked to the luciferase reporter gene and analyzed in transient transfection assays. The *shaded boxes 1–3* represent exons I–III of the PSCA gene. 5′ UTL and 3′ UTR refer to the 5′ untranslated leader and 3′ untranslated regions respectively. The PSA promoter-enhancer construct (PSA 2.4), quadruplicated PSA ARE1 construct (ARE4) and PSA enhancer core construct (EnhE4) were used as a positive controls (30). ARE4 and EnhE4 were cloned upstream to the E4 TATA box in the E4$_T$ construct. B, The PSCA promoter exhibits distinct AD and AI modes of regulation. The PSCA promoter deletion series (PSCA$_T$, PSCA-0.5, PSCA-1.0, PSCA-1.5, PSCA-2.0, PSCA-3.0, and PSCA-6.0) was analyzed by transient transfection into LNCaP cells in the presence or absence of 10 nM R1881. The pGL3basic (promoterless vector alone) construct was used as a negative control. PSA2.4, ARE4, and EnhE4 were used as positive controls to assess androgen responsiveness. The results are average ± SD of triplicate samples and are expressed in relative light units (RLU). Luciferase values were normalized to the protein content. The table below the graph indicates the fold activation of a construct in the presence (+R1881) of androgen. Fold activation in the presence of androgen was calculated by dividing the average luciferase value obtained in the presence of androgen by that obtained in the absence of androgen. C, The PSCA androgen-responsive enhancer lies within a 300-bp sequence between −2.7 kb and −3.0 kb. The PSCA androgen-responsive element was narrowed down to a 300-bp region by transfection of finer deletions between −2.0 kb and −3.0 kb (PSCA-2.2, PSCA-2.5 and PSCA-2.7). The deletion series was analyzed in the presence or absence of 10 nM synthetic androgen analog, R1881. The luciferase activity is the average of an experiment performed in triplicate and is represented as RLU. The *numbers in parentheses* represent the fold induction in the presence of R1881.

ually (~67-fold) up to PSCA-6.0. The androgen-inducible transcription is first measurable in PSCA-0.5. The most dramatic increase occurs between PSCA-2.0 and PSCA-3.0 (Fig. 3B). No additional fold increases in androgen responsiveness are observed between PSCA-3.0 and PSCA-6.0. To delineate the DNA region conferring the steep increase in androgen responsiveness further, we analyzed a second set of deletions between PSCA-2.0 and PSCA-3.0 (Fig. 3C). The R1881-induced luciferase activity of PSCA-3.0 is significantly higher than that of PSCA-2.7. The androgen responsiveness of PSCA-3.0 is 19-fold, as compared with 5-fold for PSCA-2.7. The results indicated the sharp increase in androgen responsiveness was conferred by DNA elements located within a 300-bp region between 2.7 and 3 kb.

Sufficiency of the PSCA Enhancer

The deletion data suggested the possibility that the 300-bp region contained an enhancer. One definition of an enhancer is its ability to function autonomously when tethered to a heterologous promoter (*i.e.* a sufficiency clone). The enhancer was positioned upstream of both the heterologous adenovirus E4 minimal promoter from −38 to +40, and its own minimal promoter from −38 to +12, each bearing the natural TATA box, start site and 5′ untranslated region. The two sufficiency constructs, $E4_T$+2.7–3 and $PSCA_T$+2.7–3, were transfected into LNCaP cells (Fig. 4A) to measure androgen inducibility and into HT1376 (Fig. 4B), 293T, and fAR-Hela (data not shown) to determine whether the enhancer maintained the proper cell specificity (see Fig. 1). In LNCaP, both constructs exhibited increased basal expression above the minimal promoter controls and responded to androgen 12.4- and 18.0-fold, respectively. The constructs were active in HT1376 but not induced by androgen (Fig. 4B), indicating that the enhancer maintains a level of AI activity. Finally, the constructs were inactive in 293T cells and fAR-HeLa cells, indicating that the enhancer maintains tissue selectivity (data not shown). Remarkably, the constructs were as active and specific as PSCA-3.0, indicating that they retained the stimulatory activity and specificity of the parental construct. The strong androgen responsiveness of the constructs indicated that the 0.3-kb PSCA enhancer might plausibly contain AREs (androgen response elements), the binding sites for AR.

Identification of AREs within the PSCA Enhancer

To determine if AR was acting directly, we mapped binding sites for AR within the 300-bp androgen-responsive PSCA enhancer by deoxyribonuclease (DNase) I footprinting using recombinant ARDBD (27). The PSA enhancer was included as a positive control because it contains AREs that have been validated by footprinting and detailed mutational analysis (27). Two DNase I footprints, each encompassing a region of 23-bp and separated from each other by a distance of 25-bp, were detected on the PSCA enhancer (Fig. 5, *right panel*). Both of these sites were present between −2.7 kb and −2.8 kb. We term these sites high affinity and low affinity. The high affinity site appeared at approximately 14.8 nM of recombinant ARDBD (active protein), whereas the low affinity site did not appear until approximately 133.3 nM of ARDBD. As shown in the *left panel* of Fig. 5, AREIII of the PSA enhancer (31) and PSCA high affinity site seem to display comparable affinities for ARDBD. The sequence of the high affinity site is GGAACTttcCGTCCT, and the sequence of the low affinity site is CGCACAagaCGTTTT. Both sites display approximately 67% homology to the ARE consensus sequence (GGTACAnnnTGTTCT) (32).

Determination of the Relative Affinity of ARDBD to PSCA AR Binding Sites

To evaluate the binding affinities of the two AR binding sites within the PSCA enhancer, their dissociation constants or K_d values were determined and compared with several known naturally occurring ARE sequences (summarized in Table 1). The active protein concentration of ARDBD was first shown to be approximately 4×10^{-7} M. This preparation was used to determine the dissociation constants in EMSAs (see *Materials and Methods* and Fig. 6A). The PSCA low affinity site sequence did not display a detectable DNA-protein complex in a gel shift assay. The apparent dissociation constant of the PSCA high affinity binding site was determined to be approximately 87 nM, which was about twice that for PSA AREIII sequence (~46 nM). The affinity of PSA AREIII was almost half of that reported for the PSA AREI sequence

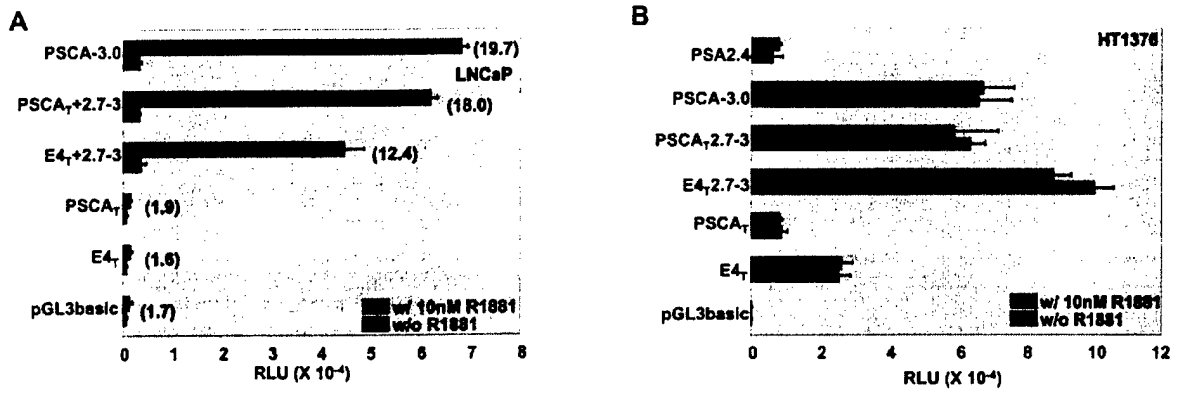

Fig. 4. The 300-bp PSCA Enhancer Can Function Autonomously

Constructs bearing the 300-bp enhancer (−2.7-kb to −3.0-kb) linked to the PSCA TATA box ($PSCA_T$+2.7–3) or to the E4 TATA box ($E4_T$+2.7–3) were generated. These were tested in transient transfection assays in A, LNCaP cells or B, HT1376 cells in the presence or absence of 10 nM R1881. The *numbers in parentheses* indicate the fold induction in the presence of the androgen analog, R1881.

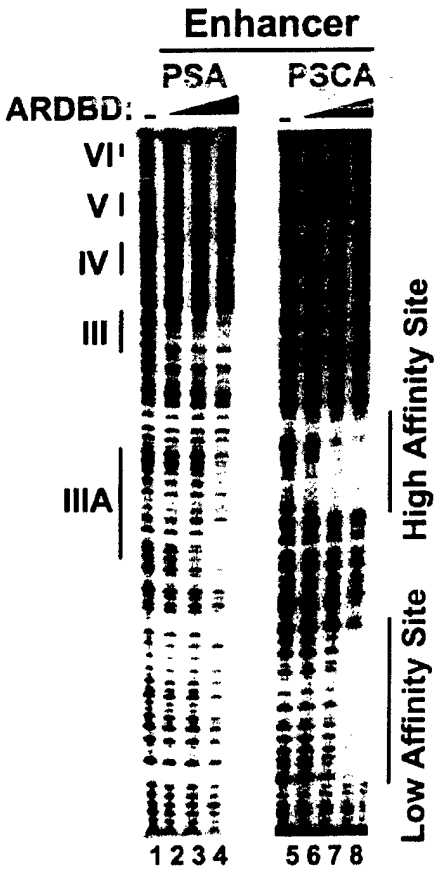

Fig. 5. The PSCA Enhancer Binds Recombinant ARDBD

In vitro DNase I footprinting of the PSA enhancer region with increasing amounts of recombinant ARDBD was used as a positive control (lanes 1–4). The positions of ARE III, IIIA, IV, V, and VI are shown. DNase I footprinting of the 300-bp PSCA promoter region with recombinant ARDBD revealed two distinct protected sites (lanes 6–8; lane 5 is a DNA alone control): a high affinity site and a low affinity site. Similar amounts of active ARDBD [0 (lanes 1 and 5), 14.8 nM (lanes 2 and 6), 44.4 nM (lanes 3 and 7), and 133.3 nM (lanes 4 and 8); ARDBD active concentration: 4×10^{-7} M] were used for both PSA and PSCA enhancers.

(~26 nM), which agrees with the PSA ARE affinity order as determined by Huang *et al.* (27).

Both PSCA AR Binding Site Mutants Abolish ARDBD Binding, whereas Only the High Affinity Site Mutation Abolishes Function

To determine whether PSCA AR binding site sequences are functional, we mutated the sites at positions important for AR binding (33–35). The mutations (Table 2) were tested in an EMSA (Fig. 6A) and a DNase I footprinting assay (Fig. 6B). They were also introduced in the context of the PSCA-6.0 construct or the $PSCA_T$+2.7–3 construct and subjected to transfection analyses (Fig. 7).

Table 1. K_d Values of Androgen Response Elements

ARE	ARDBD K_d (nM)
Consensus ARE	9.6 ± 1
PSA AREIII	46.3 ± 2
PSCA AREI or high affinity site	87.5 ± 5
Values from literature:	
PB ARE1 (35)	45 ± 6
PB ARE2 (35)	23 ± 5
C3 (1) ARE (35)	5 ± 1
PSA AREI (35)	26 ± 4
SC ARE1.2 (59)	251
TAT HRE II (64)	152
Slp HRE3 (64)	460
Slp HRE2 (59)	166
C3 IVS (64)	43

The dissociation constants of consensus ARE, PSA AREIII, and PSCA AREI are compared with some of the known androgen response elements. The dissociation constants were determined in triplicate sets of experiments in an EMSA (see *Materials and Methods*) and an average of those values ± SD is presented. PB, Probasin; TAT, tyrosine aminotransferase; C3 IVS, C3 intron sequence.

The gel shift assay indicated that the ARDBD binding was abolished in the high affinity site mutant (compare PSCA-high to PSCA high-mut; Fig. 6A). As stated earlier, we could not detect a stable DNA-protein complex using the PSCA low affinity binding site in this assay. The consensus ARE sequence, its mutant, and the PSA AREIII sequence were used for comparisons (Fig. 6A). The footprinting analysis indicated that ARDBD binding was also abrogated in both the high affinity (high-mut) and low affinity (low-mut) site mutants compared with the wild-type probe (Fig. 6B).

The transfection analyses into LNCaP and LAPC4 cells revealed that mutations in the high affinity site (PSCA-6.0 high-mut) cause a significant reduction in androgen-responsive activity (Fig. 7, A and B). In contrast, mutations in the low affinity site (PSCA-6.0 low-mut) had only a marginal effect (Fig. 7A). Note that in some cases the basal activity is reduced with the mutation. We have found via casodex inhibition with the PSA enhancer that there are still residual androgens in our depleted medium. Based on these results, it was clear that the high affinity binding site was an authentic androgen response element and we termed it PSCA AREI. The low affinity site did not seem to play an essential role in the androgen responsiveness of the PSCA enhancer. The effect of the AREI mutant was restricted to LNCaP and LAPC4 cells because the mutations failed to affect the AI activity of PSCA-6.0 in HT1376 cells (not shown).

To solidify our conclusion that the reduction in androgen responsiveness was due to mutation of the high affinity AREI, the same mutations were tested in the context of the minimal construct, $PSCA_T$+2.7–3. As expected, the AREI mutant ($PSCA_T$+2.7–3.0 AREImut) caused a decrease in androgen inducibility (Fig. 7C).

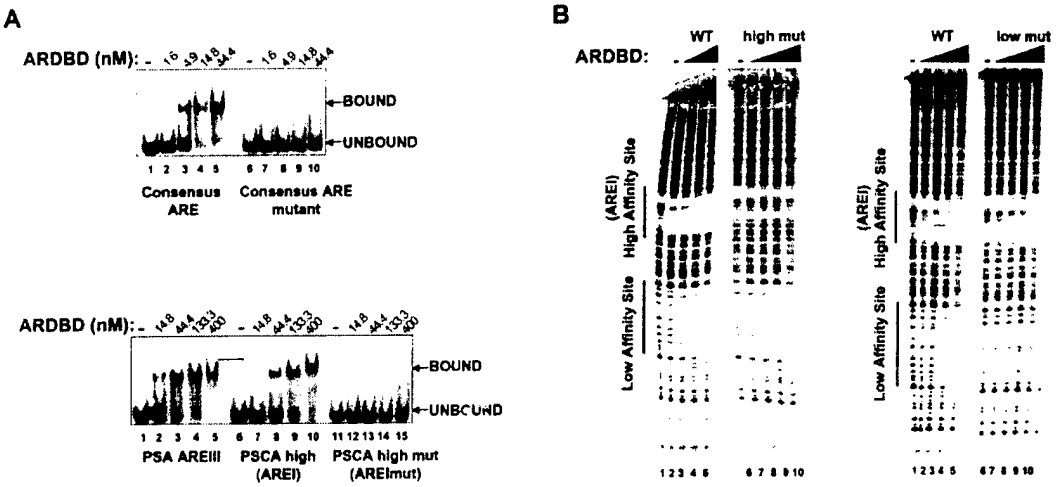

Fig. 6. PSCA Binding Site Mutations Abrogate ARDBD Binding

A, An EMSA demonstrating the ARDBD dose-response curve on consensus ARE, consensus ARE mutant (*top panel*), PSA AREIII, PSCA high and PSCA high-mut (*bottom panel*) oligonucleotides is shown. See Table 2 for a description of the PSCA ARE mutations. The ARDBD complex (bound) and the free probe (unbound) are marked with arrows. These dose curves were used to calculate the K_d of ARDBD on various ARE sequences (*see Materials and Methods* and Table 1). The molar active concentrations of ARDBD used are as follows—*Top panel,* 0 (lanes 1 and 6), 1.6 nM (lanes 2 and 7), 4.9 nM (lanes 3 and 8), 14.8 nM (lanes 4 and 9) and 44.4 nM (lanes 5 and 10). *Bottom panel,* 0 (lanes 1, 6, and 11), 14.8 nM (lanes 2, 7 and 12), 44.4 nM (lanes 3, 8, and 13), 133.3 nM (lanes 4, 9, and 14) and 400 nM (lanes 5, 10 and 15). B, DNaseI footprinting analysis was carried out with the PSCA binding sites and their mutants in presence of recombinant ARDBD. Mutation of either the high affinity binding site (high-mut; lanes 6–10 in the *left panels*) or the low affinity binding site (low-mut; lanes 6–10 in the *right panels*) abolished ARDBD binding when compared with the unmutated (WT) control (lanes 1–5 *in both left and right panels*). ARDBD active concentrations used are as follows: 0 (lanes 1 and 6), 20 nM (lanes 2 and 7), 40 nM (lanes 3 and 8), 80 nM (lanes 4 and 9) and 160 nM (lanes 5 and 10).

Table 2. Sequences of PSCA AR Binding Site Mutations

Consensus ARE	GGTACAnnnTGTTCT
PSCA low affinity site (antisense)	ccCGCACAagaCGTTTTct
PSCA low-mut	ccCCGGGAagaCGTTTTct
PSCA high affinity site (antisense)	ctGGAACTttcCGTCCTca
PSCA high-mut	ctGCGGGTttcCGTCCTca

The table shows the consensus ARE sequence with the critical guanosines in *bold.* PSCA high affinity site and PSCA low affinity site are compared with the consensus ARE sequence (AR binding sequence shown in *uppercase*). The critical guanosines conserved in these sequences are shown in *bold.* In each half-site of the AR binding sequence, the crucial contacts are between the first lysine of the ARDBD recognition helix (CGSCKVFFKRAAE), which binds to the second guanine GGTACA of the consensus half-site and the arginine, which binds to a conserved G base paired to cytosine GGTACA. We mutated the PSCA AR binding sequences based on this knowledge. Four bases in one half-site of each PSCA AR binding site were mutated (the mutation is *underlined*).

PSCA AREI Sequence Has a Low Affinity in Isolation But Can Nevertheless Function as a Genuine ARE

A bona fide ARE should be able to function by itself and from a heterologous gene promoter, *i.e.* respond to androgens *in vivo*. To test these definitions for PSCA AREI, we multimerized the AREI sequence and cloned it next to a TATA box from the adenovirus E4 gene. The constructs were subjected to transient transfection analyses in the presence of the androgen analog R1881 in LNCaP cells. Although a duplicated version of the ARE displayed a low level of androgen responsiveness (data not shown), a robust response (~18-fold induction) was observed with a quadruplicated version of the ARE ($E4_T$+PSCA ARE4; Fig. 8). This androgen response was lowered to 3.6-fold when the quadruplicated sequence contained the AREI mutation ($E4_T$+PSCA ARE4mut). As a control, we compared the PSCA ARE4 construct to the PSA ARE4 construct (quadruplicated PSA AREI sequence upstream of an E4 TATA box). The androgen induction of the PSA ARE4 construct was approximately 137-fold. The higher responsiveness of this construct is in agreement with the higher affinity of PSA AREI (Table 1). These data demonstrate that the PSCA AREI sequence, albeit of a lower affinity, has the ability to direct androgen response from a heterologous promoter.

Sequences Flanking AREI Are Required for the AD Activity of the PSCA Enhancer

The functional AREI sequence is located between 2.7 and 2.8 kb upstream of the gene and constitutes the downstream end of the enhancer. To determine if the

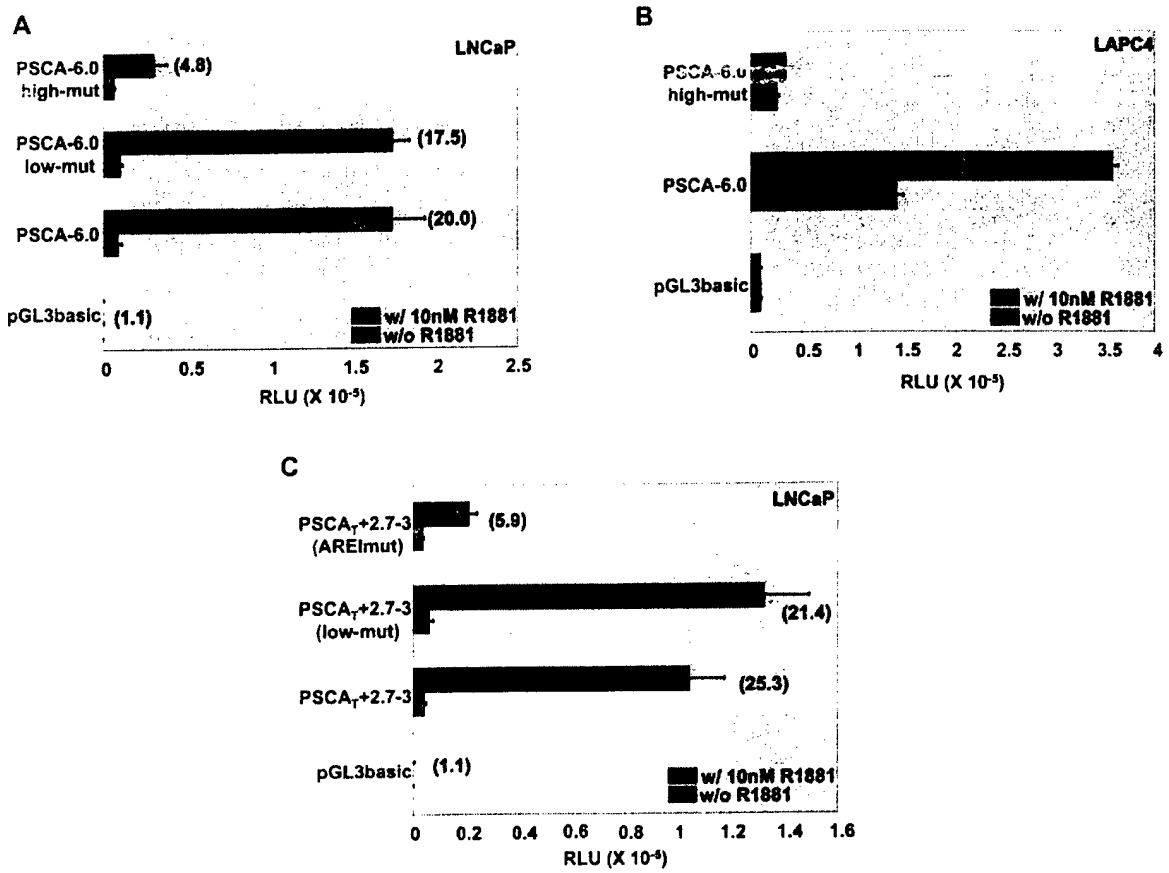

Fig. 7. PSCA AREI Responds to Androgen *in Vivo*

The contribution of PSCA ARDBD binding sites to androgen responsiveness was demonstrated by analyzing the binding site mutations in the context of PSCA-6.0 (PSCA-6.0 AREImut, PSCA-6.0 low-mut; see *Materials and Methods* and Table 2 for mutant details) in transient transfection assays in the presence and absence of R1881. The mutations were tested in AR-responsive prostate cancer cell lines: A, LNCaP cells; and B, LAPC4 cells. C, The mutations were also tested in the context of the sufficiency clones ($PSCA_T$+2.7–3 AREImut and $PSCA_T$+2.7–3 low-mut). RLU normalized to total protein amount is presented. The *values in parentheses* indicate the fold enhancement in luciferase activity in the presence of R1881.

enhancer could be further delineated, we analyzed it in greater detail by creating additional 100-bp deletions within the 300-bp region (Fig. 9, PSCA-2.8 and PSCA-2.9). Surprisingly, deletions outside of the ARE between 2.8 and 3.0 kb severely reduced enhancer activity. To rule out the possibility of additional AR binding sites between 2.8 and 3.0 kb, we carried out DNase I footprinting assays and gel shift assays (data not shown) with the 300-bp enhancer region. The major binding site was that of AREI, which was abolished upon mutation. We saw very low affinity nonspecific complexes of varying mobilities within the 2.8–3.0 region, but only at very high concentrations of ARDBD. We also analyzed two additional clones, $PSCA_T$+2.8–3.0 and $PSCA_T$+2.7–2.8 in transient transfection assays (data not shown). Neither of the two clones displayed any androgen responsiveness above that of the $PSCA_T$ construct; however, they interacted synergistically to provide robust levels of androgen responsiveness in $PSCA_T$+2.7–3.0. The data suggest that the PSCA enhancer comprises an androgen responsive component in combination with other elements important for synergizing with the ARE and possibly for conferring the cell specificity of the enhancer.

DISCUSSION

We have focused our efforts on the identification and characterization of androgen-responsive enhancers that function during prostate cancer progression from the AD to the AI state (27, 30, 36). PSCA is an ideal gene to pursue this problem because of its natural expression patterns and response to androgens only in certain epithelial cells of the prostate and in prostate cancer. Our study indicates that PSCA contains a proximal promoter located within the 500-bp region upstream from the TATA box and an enhancer located between −2.7 and −3.0 kb. The promoter is weakly responsive to androgens and contains a putative sequence that binds to ARDBD in *in vitro* DNA binding

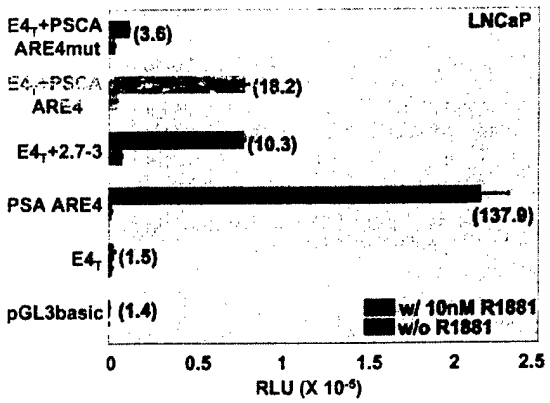

Fig. 8. PSCA AREI Is a Bona Fide ARE

PSCA AREI oligonucleotide sequence and the mutated version were quadruplicated ($E4_T$+PSCA ARE4 and $E4_T$+PSCA ARE4mut) and cloned next to a heterologous E4 TATA box. The multimerized clones were analyzed in a transient transfection assay in LNCaP cells with or without 10 nM R1881. pGL3basic (vector alone), $E4_T$, $E4_T$+2.7–3 (300-bp PSCA enhancer cloned next to the $E4_T$) and PSA ARE4 (same as ARE4 *i.e.* quadruplicated PSA AREI sequence cloned next to the $E4_T$) were used as controls. The data are presented normalized to the total protein content, and the *numbers in parentheses* indicate the fold induction achieved in the presence of R1881.

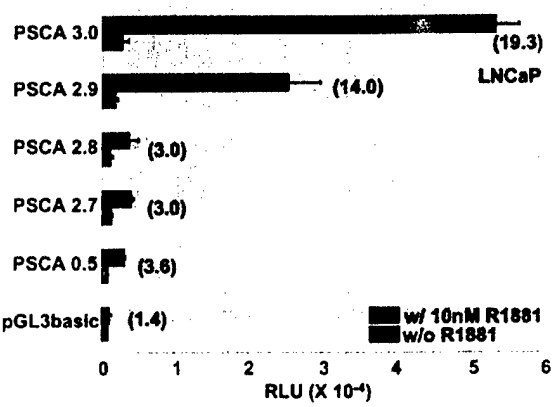

Fig. 9. The 300-bp PSCA Enhancer Consists of Multiple Components that Are Necessary for Androgen Responsiveness

The 300-bp PSCA enhancer was characterized further by generating additional 5′ deletions within the enhancer sequence (PSCA-2.8 and PSCA-2.9). These were analyzed by transient transfection into LNCaP cells in the presence and absence of 10 nM R1881. The data are presented as RLU normalized to protein content, and the *numbers in parentheses* indicate the fold androgen responsiveness.

assays. However, this sequence element is not responsible for the androgen responsiveness as determined by mutagenesis (data not shown). A deletion analysis of the promoter narrowed the androgen-responsive region to another sequence element that does not bind ARDBD. The androgen-responsive mechanism of the promoter region is not fully understood, but it is possible that this may be an indirect effect, *i.e.* another AD protein may bind to and regulate this region. Analysis of PSCA upstream sequences (−3.0 to −6.0 kb) failed to identify any additional androgen-responsive activity in transient transfection assays (data not shown). The enhancer, however, is localized to a 300-bp region and confers strong androgen responsiveness.

The enhancer functions autonomously in the context of a heterologous promoter and contains cell-type specific elements that allow PSCA to be expressed in both AI cell lines such as the bladder cancer line HT1376, and in the AD prostate cancer lines such as LNCaP and LAPC4. It does not function in human kidney (293T) or cervical carcinoma (HeLa) cells that do not support the expression of PSCA. The absolute promoter activity and androgen responsiveness of this mini-enhancer is equal to that of the entire 3-kb PSCA regulatory sequence. The data imply that the tissue-specific and AI elements overlap at the PSCA enhancer, making it an important target for detailed genetic analysis. Intriguingly, the enhancer also responds to dexamethasone (data not shown) but only at much higher concentrations than its K_d for a wild-type GR (glucocorticoid receptor) (37). It would be interesting to analyze the effect of GR on the endogenous PSCA gene. We have identified the key enhancer ARE through DNA binding and transfection studies and have validated its relevance by mutagenesis and multimerization studies. The K_d of PSCA AREI is higher than that of PSA AREI, which is also reflected on multimerizing the two ARE sequences.

It is remarkable that PSCA promoter is not androgen responsive in the LAPC9 cells, which express AR and PSA. LAPC9 cells express the highest levels of PSCA that we have detected. It is plausible that expression in these cells has plateaued, muting the effect of added androgens. It is also plausible that PSCA expression in this cell population has evolved to become independent of androgen as in PrEC cells and bladder carcinomas. The physiological role of androgens in expression of PSCA is not known and the other signaling pathways that influence PSCA expression *in vivo* need to be examined.

The promoter-enhancer of PSCA conforms to the general organizational principles observed in other androgen-regulated, prostate-specific genes like PSA, Slp (sex limited protein), probasin and hK2 (31, 38–40). The PSA regulatory region comprises a 541-bp core promoter bearing two AREs with an enhancer element at −4.2 kb. The enhancer contains multiple AREs that function with nearby cell-specific elements to activate transcription (27, 31, 41–43). Slp and probasin regulatory regions have identified androgen-responsive regions (ARR) where single or multiple AR binding sequences function in conjunction with neighboring sequences (44–46). The principle of coupling an ARR to a strong ARE was initially elucidated for the enhancer within the first intron of the C3 (1) gene (47–49).

The PSCA enhancer follows a similar scheme of an ARR in that the adjoining sequences in combination with AREI are necessary for providing androgen responsiveness. DNA-binding studies failed to identify additional AR binding sites within −2.8 to −3.0 kb (data not shown); however, this region was necessary to provide androgen responsiveness from the enhancer. The sequence between −2.8 and −3.0 kb was also scanned for potential transcription factor binding sites. We did not find sites for any prostate-specific transcription factors, such as the Ets family member prostate-derived Ets factor (50). However, some interesting observations were: acute myeloid leukemia transcription factor (AML)-1a (85% homology), Arnt (aryl hydrocarbon receptor nuclear receptor; 86% homology), GATA-1 (89% homology), and activator protein-1 (87% homology). An AML family member has been shown to be functionally required for hormonal induction of the Slp enhancer (51). Likewise, six GATA sites have been shown flanking an androgen-response element located in the far-upstream enhancer of the PSA gene, and the study suggested the involvement of prostatic GATA factors in androgen regulation of the gene (52).

A key issue that we and others have faced is what DNA sequences constitute an authentic ARE. It is becoming apparent that the answer to this question involves several complexities. Subtle amino acid differences in the ARDBD coupled with subtle differences in the steroid receptor-responsive elements play a role in simple recognition by AR and allow it to be used in place of related steroid receptors (33–35, 53). However, cooperativity of AR both with itself and nearby proteins also probably contributes to the stringency of the receptor response (27, 43).

The optimized ARE is an imperfect palindrome, GGTACAnnnTGTTCT (32, 33) comprising four highly conserved guanines on the sense and antisense strands (Table 3). Modeling of the crystal structure of the related GR (54, 55) suggests that these guanines directly contact the recognition helix (CGSCKVFFKRAAE) of the protein. Functional AREs apparently display a minimal requirement for three out of the four guanine contacts. PSCA AREI (AGGACGgaaAGTTCC) and PSCA low affinity site (AAAACGtctTGTGCG) maintain this requirement. However, PSCA low affinity site displays a poor match with other bases in the optimal site (32, 56). This observation is reinforced by comparison to the ARE consensus determined in a competitive amplification and binding assay, where AR was forced to select a binding site in the presence of a competing steroid receptor. Based on this assay, Nelson *et al.* (33) determined the AR-specific ARE sequence as: (G/A)G(T/A)AC(A/G) (C/t)(g/a)(G/c) TGTTCT. This site contains a bias away from the optimized steroid response element at positions −2, −5, and −7 (Table 3). The middle base of the 3-bp spacer is considered as position 0 for nomenclature purposes. The authors noticed a bias against cytosines except at position −3 in the left half-site (Table 3). Both PSCA AR binding sequences adhere to this restriction. The weaker binding of AR at the low affinity binding site may inhibit association with specific coactivators making the site nonfunctional (57, 58).

Although binding site selection studies have assumed that AR typically recognizes an imperfect inverted repeat (32), an argument has been made that structural determinants in AR may allow it to bind direct repeats of the consensus half site. It was proposed that this is one mechanism for conferring AR specificity (35, 56). The PSCA ARE sequences match to a certain extent both the putative inverted repeat and the direct repeat. More work will have to be done to resolve this issue.

Claessens and colleagues (59, 60) have defined an HRE (hormone response element) as a sequence

Table 3. Comparison of Human PSCA AR Binding Sites to Naturally Occurring AREs

Consensus ARE	GGTACA	nnn	TGTTCT
Highest affinity ARE (33)	G/AGTACA/g	tNG/t	TGTTCT
Receptor specific ARE (33)	G/AGT/AACA/G	C/tg/aG/c	TGTTCT
Consensus class I ARE (62)	RGAACA	ngn	TGTNCT
Consensus class II ARE (62)	RGGACA	nna	AGCCAA
Human PSCA low affinity binding site (sense)	AAAACG	tct	TGTGCG
Human PSCA AREI (sense)	AGGACG	gaa	AGTTCC
AR-specific ARE (59)	KGNTCW	nnn	AGTWCT
Probasin ARE2 (65)	GGTTCT	tgg	AGTACT
SC ARE1.2 (59)	GGCTCT	ttc	AGTTCT
Slp HRE2 (59)	TGGTCA	gcc	AGTTCT
Probasin ARE1 (65)	ATAGCA	tct	TGTTCT
PSA AREIII (31)	AATACA	ata	TGTTGG
PSA ARR (62)	GAGACT	ccc	TGATCC
PSA ARE (62)	AGCACT	tgc	TGTTCT
Slp3 (44)	GAAACA	gcc	TGTTCT

The human PSCA AR binding sequences are compared on the antisense strands with the high affinity ARE consensus, and receptor-specific ARE determined on the basis of the CAAB assay (33). The class I and class II ARE sequences (62) are also shown. The two binding sequences are also compared to a few naturally occurring AREs in prostate-specific genes. The critical guanosines are shown in *bold.*

which responds to multiple steroid receptors. Various sequence changes in these HREs cause them to favor one steroid receptor over another. An AR-specific consensus HRE sequence (called AR-specific ARE; see Table 3) was determined by mutagenesis of AR-specific AREs from the secretory component and Slp enhancers and the probasin promoter. An A at position +2 (relative to the central nucleotide in the three nucleotide spacer) and a T at position −4 are critical to these AR-specific AREs and are never found in sequences recognized by GRDBD (glucocorticoid receptor DNA binding domain) (59). In contrast, a C at position −3 and an A at position −4 will favor binding of GR (glucocorticoid receptor) and response to dexamethasone (61). PSCA AREI has an A at position +2, suggesting that this ARE may be AR-selective (Table 3). However, it has a C and an A at positions −3 and −4, respectively. Not surprisingly, the 300-bp PSCA enhancer responds to dexamethasone but only at very high concentrations (data not shown). In conclusion, it seems that PSCA AREI is largely AR selective but less than the AR-specific AREs. Further experiments would be needed to address this issue in detail.

AREs have been further classified as class I and class II elements (62) determined by the nucleotide sequences that function to mediate cooperative binding, hormone sensitivity and transcriptional activity. It has been suggested that the two classes function cooperatively to achieve a robust hormone response. PSCA AREI seems to conform as a class I element in terms of its guanine contacts and androgen sensitivity (Table 3). This is also apparent by comparing the sequence to other class I elements identified in naturally occurring ARE sequences (see Table 3). PSCA low affinity site matches well with the class I sequences only in one half-site. It does not match very well with the suggested class II consensus sequence and the ARDBD binding at the two sites is not cooperative.

The PSCA promoter sequence is well conserved across species. DNA sequencing analysis of the first 3-kb of the mouse PSCA promoter revealed a 49.3% identity with the human sequence. The mouse promoter sequence has several gaps in it as 2930 bp of the mouse sequence aligns up with 3513 bp of the human sequence. More importantly, however, comparison of the 300-bp human PSCA enhancer with the corresponding mouse sequence revealed a high homology (~60%) (Fig. 10). Interestingly, the sequence corresponding to the PSCA AREI displayed a higher identity than the low affinity binding site sequence and contained base pair changes that would still maintain the site as an AR binding site. Further, the 5′ sequence flanking the AREI was identical (~80% identity within the first 50 bp 5′ to AREI) to the human sequence. This sequence was shown to be important for androgen responsiveness from the human PSCA enhancer.

With the identification of a dual regulatory pathway within the PSCA promoter, we have demonstrated that the nature of the PSCA-expressing cells is mirrored within the promoter itself. The natural AI and AD response patterns of the promoter will provide an important tool to generate models that can be used to address basic questions in prostate cancer progression and the role of PSCA in that process.

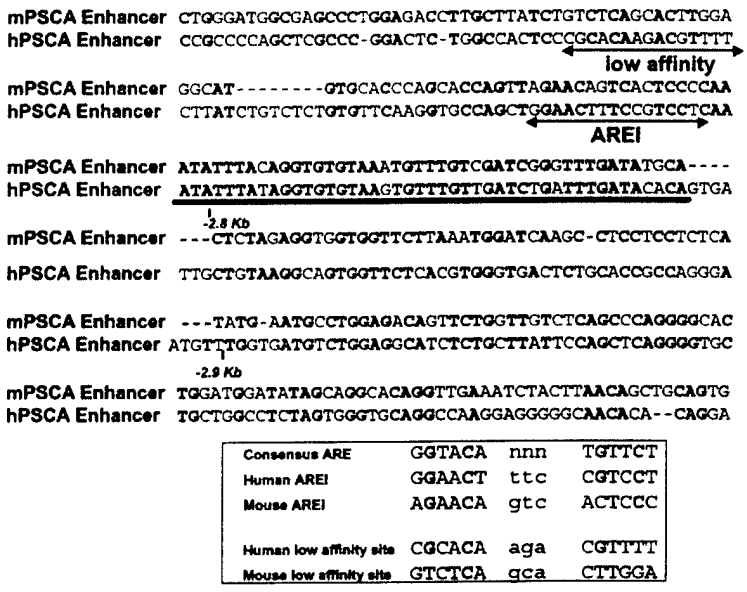

Fig. 10. Sequence Comparison of the PSCA Enhancer

The 300-bp human PSCA enhancer sequence was aligned to that of the mouse PSCA sequence (mPSCA enhancer). The bases in *bold* represent the identical bases between the two sequences. The position of AREI and the low affinity binding site (low affinity) in the human enhancer sequence is *underlined* with *arrows*. The −2.8-kb and −2.9-kb positions on the human PSCA enhancer are shown. The *bold line* represents the region of high homology between the two sequences. The *box* shows the sequence comparisons between the human PSCA ARDBD binding sites and the putative mouse sequences.

MATERIALS AND METHODS

Transcription Start Site Mapping

The PSCA transcription start site was mapped using the GeneRacer Kit (Invitrogen, Carlsbad, CA), which employs the Cap-dependent RACE method to detect transcripts containing authentic 5′ends. Five micrograms of total RNA from LAPC9 AD and AI tumors were decapped and ligated to an RNA oligonucleotide. PCR was performed using a 3′ PSCA-specific primer with the 5′ GeneRacer primer complementary to the RNA oligonucleotide. The sequence and the T_m of the primer were 5′ CTGGCTGCAGGGCCAAGCCT 3′ and 76 C, respectively. The PCR product, a slightly diffuse single band of approximately 100 bp, was cloned into the pCR4Blunt-TOPO vector using the Zero Blunt TOPO PCR cloning kit (Invitrogen). Plasmid DNA was extracted from 19 colonies and sequenced (Laragen, Inc., Santa Monica, CA) using the flanking T7 promoter primer. The DNA sequences were aligned to the human PSCA genomic sequence to determine the transcription start site.

PSCA Deletions

The PSCA promoter-luciferase reporter constructs (PSCA-1.0, PSCA-3.0 and PSCA-6.0) are as described (23). Briefly, PSCA-1.0, PSCA-3.0 and PSCA-6.0 contain 1 kb, 3 kb, and 6 kb of sequence upstream of the PSCA transcription start site. The ATG of the PSCA coding sequence was changed to CTG so that the ATG of luciferase gene could be used in the transient transfection experiments. All the subsequent promoter deletion constructs were constructed from the PSCA-6.0 clone. The promoter deletion constructs PSCA-0.038 or $PSCA_T$ (10-bp upstream to the TATA box) and PSCA-0.5 were constructed by subcloning the appropriate PCR promoter fragments into *KpnI/Hind*III cleaved pGL3basic vector (Promega Corp., Madison, WI). Likewise, PSCA-2.0 was generated by subcloning the appropriate PCR promoter fragment into *Bgl*II/*Hind*III sites of the pGL3basic vector (Promega Corp.). The constructs PSCA-1.5, PSCA-2.2, PSCA-2.5, PSCA-2.7, PSCA-2.8, and PSCA-2.9 were generated by subcloning the appropriate PCR promoter fragments into the *Kpn*I site of the PSCA-1.0 construct. The integrity of all the constructs was confirmed by automated sequencing reactions (Laragen Inc., Santa Monica, CA).

PSCA Sufficiency Clones

The $E4_T$ construct contains the adenovirus E4 TATA, start site and 5′untranslated sequences (−38 to +40) cloned into pGL3basic vector (Promega Corp.) at the *Sac*I and *Xho*I restriction enzyme sites. $PSCA_T$+2.7–3.0 and $E4_T$+2.7–3.0 were constructed by PCR-amplifying the 300-bp enhancer and subcloning it into the *Kpn*I site of the $PSCA_T$ and $E4_T$ constructs. Multimerized PSCA AREI clones were constructed by phosphorylation followed by self-ligation of the following oligonucleotides: For $E4_T$+PSCA ARE4 (5′ CGGAACTTTCCGTCCTCCTTGAACACGGAACTTTCCGTCCTGGTAC 3′) and for $E4_T$+PSCA ARE4mut (5′ CGCGGGTTTCCGTCCTCCTTGAACACGCGGGTTTCCGTCCTCCTAC 3′). The *underlined* sequences represent the PSCA AREI sequence. The ligated oligonucleotides were cloned into *Kpn*I site of $E4_T$ construct. All constructs were confirmed by automated sequencing (Laragen Inc.).

PSCA ARE Mutations

PSCA ARE mutations were generated using a site-directed mutagenesis technique based on the QuikChange procedure described by Stratagene (La Jolla, CA). Briefly, complementary oligonucleotides containing the desired high affinity AR binding site mutation (5′-CAAGGTGCCAGCCTGCGGGTTTCCGTCCTCAAATATTTATA-3′) and the low affinity AR binding site mutation (5′-ACTCTGGCCACTCCCCGGGAAGACGTTTTCTTATCTGTCTC-3′) (the mutant bases are *underlined*) were synthesized and used as primers with wild-type PSCA-6.0 or the sufficiency clone $PSCA_T$+2.7–3.0 as template in a standard amplification reaction. The resulting product was cleaved with *Dpn*I to remove the wild-type template and the products were transformed into competent DH5α *Escherichia coli*. The clones were sequenced by automated sequencing (Laragen Inc.) to confirm the position of the mutation and integrity of the clone.

Cell Culture and Transfections

LNCaP cells were grown in Roswell Park Memorial Institute (RPMI) 1640 medium (Life Technologies, Inc., Gaithersburg, MD) supplemented with 10% FBS, L-glutamine, and antibiotics (penicillin/streptomycin). Twenty-four hours before transfections, 2.5×10^5 cells per well were seeded into 6-well plates in phenol red-free RPMI 1640 (Mediatech, Herndon, VA) supplemented with 10% charcoal/dextran-treated FBS (Omega Scientific, Tarzana, CA), L-glutamine, and antibiotics (penicillin/streptomycin). LNCaP cells were transfected with 1.5 μg of plasmid DNA containing 400 ng of reporter plasmid using Tfx-50 reagent (Promega Corp.). Androgen-responsive expression was induced with 10 nM R1881. After 48 h, reporter gene expression was measured using a luciferase assay kit (Promega Corp.). Each experiment was repeated three times or more and in each experiment the transfection assays were carried out in triplicate to determine the standard deviations. Relative luciferase activity is maintained in different experiments but due to cell density and other experimental variations, absolute luciferase units vary.

fAR-HeLa cells stably express FLAG-tagged AR. These were maintained as described previously (27). HT1376, human bladder carcinoma cells, were maintained in DMEM (Life Technologies, Inc.) supplemented with 10% FBS, 1% non-essential amino acids (Life Technologies, Inc.), 1% sodium pyruvate (Life Technologies, Inc.) and antibiotics (penicillin/streptomycin). LAPC4 (cell line derived from a human prostate xenograft) were cultured in Iscove's modified DMEM (Life Technologies, Inc.) with 10% FBS and antibiotics. fAR-HeLa, HT1376 and LAPC4 were transfected with 1.5 μg of plasmid DNA containing 400 ng of reporter plasmid using Tfx-20 reagent (Promega Corp.). Prostate epithelial cells (PrECs) were maintained in serum-free Prostate Epithelial Cell Growth Medium BulletKit (PrEGM~BulletKit, Clonetics, BioWhittaker, Belgium) according to manufacturer's instructions. Prostate stromal cells (PrSC) were maintained in RPMI 1640 medium with 10% FBS. Both the primary cell populations were transfected with similar amounts of plasmid DNA as described above using Tfx50 reagent (Promega Corp.). LAPC9 tumor explants were maintained as a disaggregated single-cell suspension in short-term culture in PrEGM and were transfected with Tfx50 reagent. The disaggregated single-cell suspensions were prepared from approximately 1 g of LAPC9-AD tumor (~1.3–1.5 cm^3) using a standard protocol (63). Briefly, under sterile conditions, the tumor was washed and cut into small pieces of approximately 1–2 mm^3. These pieces were resuspended in Iscove's modified DMEM (Life Technologies, Inc.), and the tissue was disintegrated with 1% pronase for 20 min at room temperature. The cells were washed with Iscove's medium and then resuspended in 25 ml of PrEGM media with 1× fungizone and 10 nM R1881 and seeded in 10-cm cell culture dishes. On the next day, the cells were filtered through a sterile 40-μm mesh to get rid of the cellular aggregates and they were plated back again in 10-cm Petri dishes. Approximately 3×10^7 cells were obtained from 1 g tumor.

DNase I Footprinting

The binding reactions for DNase I footprinting were as described previously (27). Radiolabeled probes were prepared by PCR, where the PSCA-6.0 plasmid (or the respective binding site mutant plasmids) was employed as a template. Two primers, 3 kb-fp1 (5′-GTGTGTTGCCCCCTCCTTGGCC-3′) and 2.7 kb-fp1 (5′-CCGCCCCAGCTCGCCCGGACTC-3′), flanking the 300-bp enhancer region were used for the PCR amplification of the probe. One of the primers, 2.7 kb-fp1 was ^{32}P-end-labeled with polynucleotide kinase and [γ^{32}P]ATP. The probes were purified on a 4% polyacrylamide gel before they were used in DNase I footprinting reactions. The amounts of recombinant ARDBD (27) used were as indicated in the figure legends.

EMSA

Ten picomoles of ARE containing double-stranded oligonucleotides were ^{32}P-end-labeled with polynucleotide kinase and [γ^{32}P]ATP. The oligonucleotides used were as follows: consensus ARE (5′ CCCCCCCGGTACATGATGTTCTCCCCC 3′), consensus ARE mutant (5′ CCCCCCCGGTACATGAACAAGACCCCC 3′), PSA AREIII (5′ CTCTGGAGGAACATATTGTATTGATTG 3′), PSCA high (5′ CCTGGAACTTTCCGTCCTCAAATA 3′), and PSCA high-mut (5′ CCTGTAATTTTCCGTCCTCAAATA 3′). Indicated amounts of recombinant ARDBD was incubated in a 10-μl reaction volume containing 5 fmol of the radiolabeled probe; 20 mM HEPES, pH 7.9; 25% glycerol; 1.5 mM $MgCl_2$; 0.2 mM EDTA; 100 mM KCl; 0.5 mg/ml BSA; 0.01% Nonidet P-40; and 400 ng of poly(deoxyinosine-deoxycytidine). When carrying out a cold competition assay, the required amount of the cold competitor was added to the reaction mixture along with the labeled oligonucleotide. After 20 min at room temperature, the complexes were separated at 4 C on a 4% polyacrylamide gel containing 1% glycerol and 0.5× TBE.

Calculation of the Dissociation Constant

To determine the K_d of ARDBD, we first calculated the active protein concentration. This was determined by an oligonucleotide competition assay in an EMSA. The ARDBD concentration was raised 50- to 100-fold above the concentration required to generate 50% occupancy of the probe or the K_d. At this stage, the amount of cold competitor was gradually raised. As the competitor oligonucleotide is raised, it begins to compete with the bound ^{32}P-labeled oligonucleotide for ARDBD and the unbound radiolabeled DNA is observed by EMSA. When 50% of the labeled oligonucleotide is competed to the unbound form, the oligonucleotide competitor has exceeded the amount of active protein (ARDBD) by 2-fold. The ARDBD active protein concentration was then calculated to be equivalent to half of the molar concentration of the oligonucleotide or approximately 4×10^{-7} M. The active protein concentration was independently calculated with consensus ARE, PSA AREIII, and PSCA-high oligonucleotides, and similar results were obtained.

Having calculated the active protein concentration, ARDBD dose response reactions at low concentrations of ARDBD were carried out in EMSAs over consensus ARE, PSA AREIII, and PSCA-high oligonucleotides. The gels were scanned by a PhosphorImager (Molecular Dynamics, Amersham Biosciences, Sunnyvale, CA) to calculate the intensity of the bound and unbound complexes and the amount of active protein required for 50% complex formation was determined. This value was equivalent to the K_d.

Generation of Stable Cell Lines

GFP-expressing stable cell lines were generated in LNCaP cells. pEGFP-promoterless was generated from pEGFP-N1 (CLONTECH Laboratories, Inc., Palo Alto, CA) by removing the CMV promoter (*AseI-Eco*47III). pEGFP-N1 contains a neomycin-resistance cassette (neo′), which allows stably transfected eukaryotic cells to be selected using G418. PSCA-6.0 GFP clone was constructed by cloning the 6-kb PSCA promoter as a *Hin*dIII/*Bgl*II fragment into pEGFP-promoterless clone. pEGFP-promoterless and PSCA-6.0 GFP clones were transfected into LNCaP cells using Tfx-50 reagent (Promega Corp.), and stable clones were selected over a 3-wk period using 500 μg/ml of G418. To avoid a bias for an integration site, G418-resistant positive populations were employed for the analyses without separating the high expressing populations from the low expressing ones.

Flow Cytometry and Fluorescence Microscopy

Flow cytometric and fluorescent microscopic analyses were performed after the stable cell lines were starved in steroid-depleted RPMI media for 1 wk followed by a 48-h induction with 10 nM R1881 or ethanol as a negative control. In brief, cells were resuspended in RPMI at approximately 10^5 cells/ml and analyzed for GFP fluorescence. In each analysis, 10,000 cells were counted. Analysis was performed on a FACScan (Becton Dickinson and Co., Franklin Lakes, NJ) using Cellquest software. GFP-fluorescence microscopy on live LNCaP cells 48 h post R1881 treatment was performed using the Leica Corp. DM IRBE microscope attached to the Hamamatsu Digital Camera (both instruments were obtained from McBain Instruments, Chatsworth, CA). GFP-fluorescence was captured using Openlab version 3.0 software (Improvision, Coventry, UK).

Acknowledgments

We thank Dr. Owen Witte for the mouse genomic clone containing the mouse PSCA regulatory sequences; Drs. Charles Sawyers, Owen Witte, and Purnima Dubey for helpful discussions; Dr. Joann Zhang for careful reading of the manuscript; and Kim Le for help with the digital artwork.

Received January 4, 2002. Accepted July 5, 2002.

Address all correspondence and requests for reprints to: Dr. Michael F. Carey, Department of Biological Chemistry, UCLA School of Medicine, Box 951737, Los Angeles, California 90095. E-mail: mcarey@mednet.ucla.edu.

This work was supported in part by the CaP CURE (Association for Cure of Cancer of the Prostate) grant (to M.C.); Department of Defense Project Grant DAMD17-00-1-0077 (to C. Sawyers, M. Carey, and P. Cohen); and Grants (to R.E.R.) NCI-K08-CA-74169, NCI-RFA-CA-98-013, and Department of Defense Award No. PC-001588. A.J. was supported by the California Cancer Research Program (2PD0109).

REFERENCES

1. Isaacs JT 1999 The biology of hormone refractory prostate cancer. Why does it develop? Urol Clin North Am 26:263–273
2. Abate-Shen C, Shen MM 2000 Molecular genetics of prostate cancer. Genes Dev 14:2410–2434
3. Elo JP, Visakorpi T 2001 Molecular genetics of prostate cancer. Ann Med 33:130–141
4. Weigel NL, Zhang Y 1998 Ligand-independent activation of steroid hormone receptors. J Mol Med 76:469–479
5. Craft N, Sawyers CL 1998 Mechanistic concepts in androgen-dependence of prostate cancer. Cancer Metastasis Rev 17:421–427

6. Jenster G 1999 The role of the androgen receptor in the development and progression of prostate cancer. Semin Oncol 26:407–421
7. Lamb DJ, Weigel NL, Marcelli M 2001 Androgen receptors and their biology. Vitam Horm 62:199–230
8. Brinkmann AO 2001 Molecular basis of androgen insensitivity. Mol Cell Endocrinol 179:105–109
9. Avila DM, Zoppi S, McPhaul MJ 2001 The androgen receptor (AR) in syndromes of androgen insensitivity and in prostate cancer. J Steroid Biochem Mol Biol 76: 135–142
10. Cinar B, Koeneman KS, Edlund M, Prins GS, Zhau HE, Chung LW 2001 Androgen receptor mediates the reduced tumor growth, enhanced androgen responsiveness, and selected target gene transactivation in a human prostate cancer cell line. Cancer Res 61:7310–7317
11. Stamey TA 2001 Preoperative serum prostate-specific antigen (PSA) below 10 microg/l predicts neither the presence of prostate cancer nor the rate of postoperative PSA failure. Clin Chem 47:631–634
12. Pannek J, Partin AW 1997 Prostate-specific antigen: what's new in 1997. Oncology (Huntingt) 11:1273–8; discussion 1279–1282
13. Lee CT, Oesterling JE 1995 Diagnostic markers of prostate cancer: utility of prostate-specific antigen in diagnosis and staging. Semin Surg Oncol 11:23–35
14. Reiter RE, Gu Z, Watabe T, Thomas G, Szigeti K, Davis E, Wahl M, Nisitani S, Yamashiro J, Le Beau MM, Loda M, Witte ON 1998 Prostate stem cell antigen: a cell surface marker overexpressed in prostate cancer. Proc Natl Acad Sci USA 95:1735–1740
15. Gu Z, Thomas G, Yamashiro J, Shintaku IP, Dorey F, Raitano A, Witte ON, Said JW, Loda M, Reiter RE 2000 Prostate stem cell antigen (PSCA) expression increases with high gleason score, advanced stage and bone metastasis in prostate cancer. Oncogene 19:1288–1296
16. Dubey P, Wu H, Reiter RE, Witte ON 2001 Alternative pathways to prostate carcinoma activate prostate stem cell antigen expression. Cancer Res 61:3256–3261
17. Ross S, Spencer SD, Lasky LA, Koeppen H 2001 Selective expression of murine prostate stem cell antigen in fetal and adult tissues and the transgenic adenocarcinoma of the mouse prostate model of prostate carcinogenesis. Am J Pathol 158:809–816
18. Amara N, Palapattu GS, Schrage M, Gu Z, Thomas GV, Dorey F, Said J, Reiter RE 2001 Prostate stem cell antigen is overexpressed in human transitional cell carcinoma. Cancer Res 61:4660–4665
19. Argani P, Rosty C, Reiter RE, Wilentz RE, Murugesan SR, Leach SD, Ryu B, Skinner HG, Goggins M, Jaffee EM, Yeo CJ, Cameron JL, Kern SE, Hruban RH 2001 Discovery of new markers of cancer through serial analysis of gene expression: prostate stem cell antigen is overexpressed in pancreatic adenocarcinoma. Cancer Res 61: 4320–4324
20. Beissert S, He HT, Hueber AO, Lellouch AC, Metze D, Mehling A, Luger TA, Schwarz T, Grabbe S 1998 Impaired cutaneous immune responses in Thy-1-deficient mice. J Immunol 161:5296–5302
21. Killeen N 1997 T-cell regulation: Thy-1—hiding in full view. Curr Biol 7:R774–R777
22. Saffran DC, Raitano AB, Hubert RS, Witte ON, Reiter RE, Jakobovits A 2001 Anti-PSCA mAbs inhibit tumor growth and metastasis formation and prolong the survival of mice bearing human prostate cancer xenografts. Proc Natl Acad Sci USA 98:2658–2663
23. Watabe T, Lin M, Ide H, Donjacour AA, Cunha GR, Witte ON, Reiter RE 2002 Growth, regeneration, and tumorigenesis of the prostate activates the PSCA promoter. Proc Natl Acad Sci USA 99:401–406
24. Klein KA, Reiter RE, Redula J, Moradi H, Zhu XL, Brothman AR, Lamb DJ, Marcelli M, Belldegrun A, Witte ON, Sawyers CL 1997 Progression of metastatic human prostate cancer to androgen independence in immunodeficient SCID mice. Nat Med 3:402–408
25. Horoszewicz JS, Leong SS, Kawinski E, Karr JP, Rosenthal H, Chu TM, Mirand EA, Murphy GP 1983 LNCaP model of human prostatic carcinoma. Cancer Res 43:1809–1818
26. Rasheed S, Gardner MB, Rongey RW, Nelson-Rees WA, Arnstein P 1977 Human bladder carcinoma: characterization of two new tumor cell lines and search for tumor viruses. J Natl Cancer Inst 58:881–890
27. Huang W, Shostak Y, Tarr P, Sawyers C, Carey M 1999 Cooperative assembly of androgen receptor into a nucleoprotein complex that regulates the prostate-specific antigen enhancer. J Biol Chem 274:25756–25768
28. Cordingley MG, Riegel AT, Hager GL 1987 Steroid-dependent interaction of transcription factors with the inducible promoter of mouse mammary tumor virus *in vivo* Cell 48:261–270
29. Archer TK, Lefebvre P, Wolford RG, Hager GL 1992 Transcription factor loading on the MMTV promoter: a bimodal mechanism for promoter activation. Science 255:1573–1576
30. Wu L, Matherly J, Smallwood A, Adams JY, Billick E, Belldegrun A, Carey M 2001 Chimeric PSA enhancers exhibit augmented activity in prostate cancer gene therapy vectors. Gene Ther 8:1416–1426
31. Cleutjens KB, van der Korput HA, van Eekelen CC, van Rooij HC, Faber PW, Trapman J 1997 An androgen response element in a far upstream enhancer region is essential for high, androgen-regulated activity of the prostate-specific antigen promoter. Mol Endocrinol 11: 148–161
32. Roche PJ, Hoare SA, Parker MG 1992 A consensus DNA-binding site for the androgen receptor. Mol Endocrinol 6:2229–2235
33. Nelson CC, Hendy SC, Shukin RJ, Cheng H, Bruchovsky N, Koop BF, Rennie PS 1999 Determinants of DNA sequence specificity of the androgen, progesterone, and glucocorticoid receptors: evidence for differential steroid receptor response elements. Mol Endocrinol 13: 2090–2107
34. Massaad C, Garlatti M, Wilson EM, Cadepond F, Barouki R 2000 A natural sequence consisting of overlapping glucocorticoid-responsive elements mediates glucocorticoid, but not androgen, regulation of gene expression. Biochem J 350(Part 1):123–129
35. Claessens F, Verrijdt G, Schoenmakers E, Haelens A, Peeters B, Verhoeven G, Rombauts W 2001 Selective DNA binding by the androgen receptor as a mechanism for hormone-specific gene regulation. J Steroid Biochem Mol Biol 76:23–30
36. Craft N, Shostak Y, Carey M, Sawyers CL 1999 A mechanism for hormone-independent prostate cancer through modulation of androgen receptor signaling by the HER-2/neu tyrosine kinase. Nat Med 5:280–285
37. Ray DW, Suen CS, Brass A, Soden J, White A 1999 Structure/function of the human glucocorticoid receptor: tyrosine 735 is important for transactivation. Mol Endocrinol 13:1855–1863
38. Mitchell SH, Murtha PE, Zhang S, Zhu W, Young CY 2000 An androgen response element mediates LNCaP cell dependent androgen induction of the hK2 gene. Mol Cell Endocrinol 168:89–99
39. Yu DC, Sakamoto GT, Henderson DR 1999 Identification of the transcriptional regulatory sequences of human kallikrein 2 and their use in the construction of calydon virus 764, an attenuated replication competent adenovirus for prostate cancer therapy. Cancer Res 59: 1498–1504
40. Xie X, Zhao X, Liu Y, Young CY, Tindall DJ, Slawin KM, Spencer DM 2001 Robust prostate-specific expression for targeted gene therapy based on the human kallikrein 2 promoter. Hum Gene Ther 12:549–561

41. Schuur ER, Henderson GA, Kmetec LA, Miller JD, Lamparski HG, Henderson DR 1996 Prostate-specific antigen expression is regulated by an upstream enhancer. J Biol Chem 271:7043–7051
42. Pang S, Dannull J, Kaboo R, Xie Y, Tso CL, Michel K, deKernion JB, Belldegrun AS 1997 Identification of a positive regulatory element responsible for tissue-specific expression of prostate-specific antigen. Cancer Res 57:495–499
43. Farmer G, Connolly Jr ES, Mocco J, Freedman LP 2001 Molecular analysis of the prostate-specific antigen upstream gene enhancer. Prostate 46:76–85
44. Adler AJ, Scheller A, Robins DM 1993 The stringency and magnitude of androgen-specific gene activation are combinatorial functions of receptor and nonreceptor binding site sequences. Mol Cell Biol 13:6326–6335
45. Adler AJ, Danielsen M, Robins DM 1992 Androgen-specific gene activation via a consensus glucocorticoid response element is determined by interaction with nonreceptor factors. Proc Natl Acad Sci USA 89: 11660–11663
46. Kasper S, Rennie PS, Bruchovsky N, Sheppard PC, Cheng H, Lin L, Shiu RP, Snoek R, Matusik RJ 1994 Cooperative binding of androgen receptors to two DNA sequences is required for androgen induction of the probasin gene. J Biol Chem 269:31763–31769
47. Devos A, Claessens F, Alen P, Winderickx J, Heyns W, Rombauts W, Peeters B 1997 Identification of a functional androgen-response element in the exon 1-coding sequence of the cystatin-related protein gene crp2. Mol Endocrinol 11:1033–1043
48. Claessens F, Celis L, De Vos P, Peeters B, Heyns W, Verhoeven G, Rombauts W 1993 Intronic androgen response elements of prostatic binding protein genes. Biochem Biophys Res Commun 191:688–694
49. Celis L, Claessens F, Peeters B, Heyns W, Verhoeven G, Rombauts W 1993 Proteins interacting with an androgen-responsive unit in the C3(1) gene intron. Mol Cell Endocrinol 94:165–172
50. Oettgen P, Finger E, Sun Z, Akbarali Y, Thamrongsak U, Boltax J, Grall F, Dube A, Weiss A, Brown L, Quinn G, Kas K, Endress G, Kunsch C, Libermann TA 2000 PDEF, a novel prostate epithelium-specific ets transcription factor, interacts with the androgen receptor and activates prostate-specific antigen gene expression. J Biol Chem 275:1216–1225
51. Ning YM, Robins DM 1999 AML3/CBFα1 is required for androgen-specific activation of the enhancer of the mouse sex-limited protein (Slp) gene. J Biol Chem 274: 30624–30630
52. Perez-Stable CM, Pozas A, Roos BA 2000 A role for GATA transcription factors in the androgen regulation of the prostate-specific antigen gene enhancer. Mol Cell Endocrinol 167:43–53
53. Scheller A, Hughes E, Golden KL, Robins DM 1998 Multiple receptor domains interact to permit, or restrict, androgen-specific gene activation. J Biol Chem 273: 24216–24222
54. Luisi BF, Xu WX, Otwinowski Z, Freedman LP, Yamamoto KR, Sigler PB 1991 Crystallographic analysis of the interaction of the glucocorticoid receptor with DNA. Nature 352:497–505
55. Gewirth DT, Sigler PB 1995 The basis for half-site specificity explored through a non-cognate steroid receptor-DNA complex. Nat Struct Biol 2:386–394
56. Zhou Z, Corden JL, Brown TR 1997 Identification and characterization of a novel androgen response element composed of a direct repeat. J Biol Chem 272: 8227–8235
57. Saatcioglu F, Lopez G, West BL, Zandi E, Feng W, Lu H, Esmaili A, Apriletti JW, Kushner PJ, Baxter JD, Karin M 1997 Mutations in the conserved C-terminal sequence in thyroid hormone receptor dissociate hormone-dependent activation from interference with AP-1 activity. Mol Cell Biol 17:4687–4695
58. Brinkmann AO, Blok LJ, de Ruiter PE, Doesburg P, Steketee K, Berrevoets CA, Trapman J 1999 Mechanisms of androgen receptor activation and function. J Steroid Biochem Mol Biol 69:307–313
59. Verrijdt G, Schoenmakers E, Haelens A, Peeters B, Verhoeven G, Rombauts W, Claessens F 2000 Change of specificity mutations in androgen-selective enhancers. Evidence for a role of differential DNA binding by the androgen receptor. J Biol Chem 275:12298–12305
60. Schoenmakers E, Verrijdt G, Peeters B, Verhoeven G, Rombauts W, Claessens F 2000 Differences in DNA binding characteristics of the androgen and glucocorticoid receptors can determine hormone-specific responses. J Biol Chem 275:12290–12297
61. Nordeen SK, Suh BJ, Kuhnel B, Hutchison CD 1990 Structural determinants of a glucocorticoid receptor recognition element. Mol Endocrinol 4:1866–1873
62. Reid KJ, Hendy SC, Saito J, Sorensen P, Nelson CC 2001 Two classes of androgen receptor elements mediate cooperativity through allosteric interactions. J Biol Chem 276:2943–2952
63. Craft N, Chhor C, Tran C, Belldegrun A, DeKernion J, Witte ON, Said J, Reiter RE, Sawyers CL 1999 Evidence for clonal outgrowth of androgen-independent prostate cancer cells from androgen-dependent tumors through a two-step process. Cancer Res 59:5030–5036
64. Rundlett SE, Miesfeld RL 1995 Quantitative differences in androgen and glucocorticoid receptor DNA binding properties contribute to receptor-selective transcriptional regulation. Mol Cell Endocrinol 109:1–10
65. Rennie PS, Bruchovsky N, Leco KJ, Sheppard PC, McQueen SA, Cheng H, Snoek R, Hamel A, Bock ME, MacDonald BS, Nickel BE, Chang C, Liao S, Cattini PA, Matusik RJ 1993 Characterization of two cis-acting DNA elements involved in the androgen regulation of the probasin gene. Mol Endocrinol 7:23–36

Visualization of advanced human prostate cancer lesions in living mice by a targeted gene transfer vector and optical imaging

JASON Y. ADAMS,[1] MAI JOHNSON,[1] MAKOTO SATO,[1] FRANK BERGER,[2] SANJIV S. GAMBHIR,[2] MICHAEL CAREY[3], M. LUISA IRUELA-ARISPE[4] & LILY WU[1]

Departments of [1]Urology and [2]Crump Institute for Molecular Imaging & Department of Molecular & Medical Pharmacology, [3]Biological Chemistry, David Geffen School of Medicine at UCLA, and [4]Department of Molecular Cell and Developmental Biology, College of Letters & Science, UCLA, Los Angeles California 90095, USA

Correspondence should be addressed to L.W.; email: lwu@mednet.ucla.edu

Published online: 22 July 2002, doi:10.1038/nm743

Non-invasive imaging and transcriptional targeting can improve the safety of therapeutic approaches in cancer. Here we demonstrate the ability to identify metastases in a human-prostate cancer model, employing a prostate-specific adenovirus vector (AdPSE-BC-luc) and a charge-coupled device-imaging system. AdPSE-BC-luc, which expresses firefly luciferase from an enhanced prostate-specific antigen promoter, restricted expression in the liver but produced robust signals in prostate tumors. In fact, expression was higher in advanced, androgen-independent tumors than in androgen-dependent lesions. Repetitive imaging over a three-week period after AdPSE-BC-luc injection into tumor-bearing mice revealed that the virus could locate and illuminate metastases in the lung and spine. Systemic injection of low doses of AdPSE-BC-luc illuminated lung metastasis. These results demonstrate the potential use of a non-invasive imaging modality in therapeutic and diagnostic strategies to manage prostate cancer.

Improvements in screening and treatment of localized disease have led to a steady decline in prostate cancer mortality over the past 10 years[1]. Despite these advancements, prostate cancer is the second leading cause of cancer deaths in American men. Endocrine therapy, using androgen ablation, is the current treatment for advanced, metastatic disease[2]. However, the disease invariably relapses within 18–36 months[3], after which it is considered androgen independent (AI) with no effective treatment. Vector-based gene therapy represents a potential alternative or adjuvant to existing therapies for the treatment of AI disease[4]. Strong constitutive viral promoters, such as cytomegalovirus (CMV), enable high transgene expression, but these are not specific. To improve the activity and specificity of prostate-targeted gene expression, we developed enhanced promoters by multimerizing key regulatory elements in the prostate-specific antigen (PSA) enhancer and promoter[5]. The PSE-BC construct was 20-fold more active than the native PSA enhancer/promoter. Furthermore, when incorporated into an adenovirus vector (AdPSE-BC-luc), the promoter exhibited enhanced prostate specificity and restricted expression[5].

To advance the concept of prostate-targeted expression, we tested our approaches in several human prostate cancer (CaP) xenograft models (LAPC series), in severe combined immunedeficient (SCID) mice. The models retain characteristics of clinical disease, including androgen receptor (AR) and PSA expression, androgen requirement, and metastatic potential[6,7]. Demonstration of the utility of our approaches in relevant models suggests that they may be applicable in clinical settings.

The cooled charged-coupled device (CCD) camera is a sensitive optical imaging system for detecting bioluminescence emitted from D-luciferin reacting with firefly luciferase in living animals[8,9]. The advantages of a targeted gene transfer approach coupled with non-invasive imaging include the ability to localize diseased tissue, and importantly, to accurately monitor the kinetics and levels of transgene expression *in vivo*. Here we employed CCD imaging to achieve those ends in mouse models of human CaP.

Calibration of optical CCD signals

Optical CCD imaging has been applied to study animal models of cancer marked with a luciferase gene[8]. The imaging signals generated by a tissue-specific, vector-based approach are not well documented. The CCD signals, which are specifically dependent on the administration of D-luciferin substrate, were quantified as maximum relative light units per minute of acquisition time (RLU/min). To estimate the sensitivity, 1×10^4 to 1×10^6 LNCaP prostate cancer cells, infected with AdCMV-luc or AdPSE-BC-luc, were implanted into the peritoneum. Light signals emitted by 1×10^4, 1×10^5 and 1×10^6 AdCMV-luc-infected cells were 1.4×10^3, 2.3×10^4 and 2.0×10^5 RLU/min, respectively. In comparison, 1×10^5 and 1×10^6 AdPSE-BC-luc-infected cells produced 170 and 1,800 RLU/min, respectively.

Discriminatory expression capability of AdPSE-BC-luc

We assessed the *in vivo* transcriptional targeting capability of AdPSE-BC-luc in comparison to AdCMV-luc[9]. After tail-vein injection of the virus, firefly luciferase expression was monitored by CCD imaging. Despite comparable gene delivery in both groups (Fig. 1*b*), AdPSE-BC-luc-mediated expression in the liver was less than 1×10^{-5} that of AdCMV-luc (Fig. 1*a*). The direct prostate-specific transcriptional activity of AdPSE-BC-luc was evaluated by injection into human CaP tumors. The results from androgen-dependent (AD) LAPC-4 models are shown in Fig. 2*b*. Similar results were observed in LAPC-9 tumors (data not shown). At 11 days post-injection, the average signal in the AdPSE-BC-luc cohort ($n = 5$, 1.3×10^3) displayed a 32-fold lower activity than the AdCMV-luc cohort ($n = 3$, 4.2×10^4). By comparing the ratio of activity in LAPC-4 tumors with that in liver,

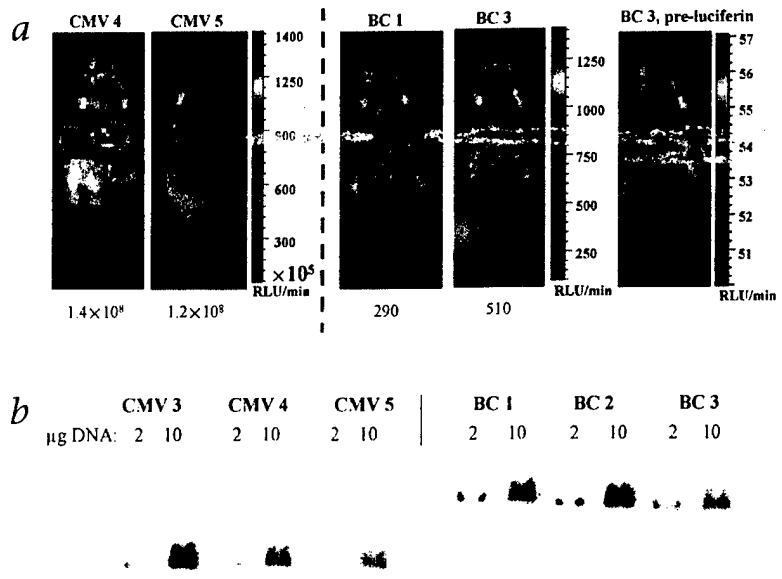

Fig. 1 Adenoviral vector-mediated luciferase gene delivery and expression in the liver after systemic administration. ***a***, CCD images of mice injected with either AdCMV-luc or the prostate-specific AdPSE-BC-luc via tail vein. The images represent the results from 2 animals of each cohort at 4 d post-injection. The animal designation is indicated above the images. BC1 and BC3 represent mice #1 and #3, respectively, in the AdPSE-BC-luc group, and CMV4 and CMV5 indicate the AdCMV-luc-injected animals. The relative light intensity (RLU/min) emitted from the animal was quantified by image analysis software and represented by the color scale, shown next to the images. The maximal signal intensity (maximum RLU/min) is shown below each image. The acquisition times were reduced to offset saturated liver signal intensities in AdCMV-luc cohort. ***b***, Adenoviral gene transfer in livers of two cohorts injected either with AdCMV-luc or AdPSE-BC-luc. Southern-blot analysis of total cellular DNA was shown. *Not*I restriction liberated a 2.8-kb CMV-luc and a 4.6-kb PSE-BC-luc expression cassette. DNA (2 μg and 10 μg) of each sample was analyzed.

AdPSE-BC-luc exhibited ~3,000-fold higher specific expression in CaP tumors than AdCMV-luc (Figs. 1 and 2). Systemic administration of AdPSE-BC-luc resulted in the highest luciferase expression in mouse prostates and LAPC-9 tumors[5]. These results suggest that AdPSE-BC-luc exhibits exquisite prostate-specificity and is able to restrict expression in non-prostate organs (such as liver).

Kinetics of transgene expression in living mice

One major advantage of the CCD non-invasive imaging system is the ability for repetitive monitoring of luciferase gene expression in the same animal over time. Over a 3-week period, the AdCMV-luc-injected mouse (CMV1) displayed high intratumoral signals 2–4 days post-injection (Fig. 2*a*). Leakage of AdCMV-luc into the circulation after intratumoral injections was indicated by the signals appearing in the liver (Fig. 2*a*). In fact, after 4 days, the liver signals exceeded those in the tumor, and remained at ~1.5×10^6 RLU/min (Fig. 2*a*). The intratumoral signals gradually decrease to below 4×10^4 RLU/min, the minimum scale set for this experiment.

The time-course of intratumoral AdPSE-BC-luc expression was delayed (Fig. 2), which may be attributed to its lower intrinsic activity relative to Ad-CMV-luc. AdPSE-BC-luc-injected tumors expressed negligible luciferase at two days post-injection (3 of 5 mice) (data not shown). Signals were apparent at 4 days, and peaked 8–11 days post-injection (Fig. 2*b*). In the AdPSE-BC-luc-injected cohort, only signals emitted from the tumors were detected on or before 11 days post-injection (Fig. 2*b*). However, at 21 days post-injection, low-magnitude extratumoral signals were visible (~200 RLU/min) (Fig. 2*b*) emanating from the lower back and chest. These signals were above the background luminescence of less than 70 RLU/min.

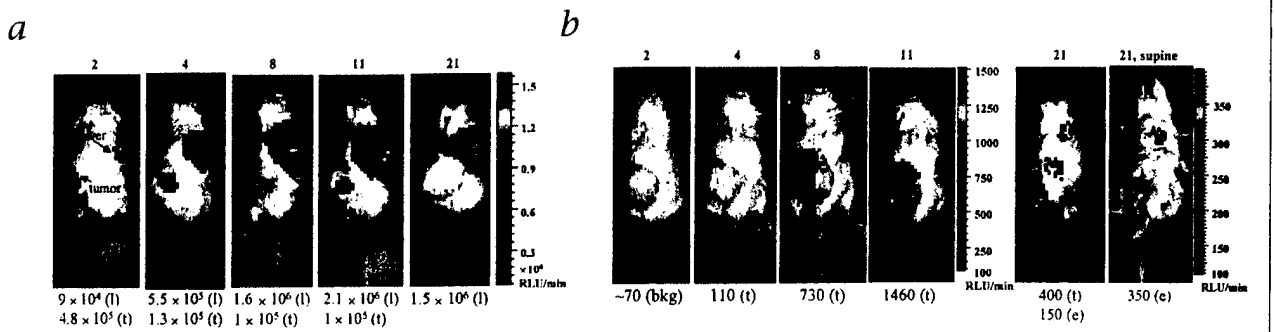

Fig. 2 Kinetics of transgene expression in living mice after intratumoral injection. ***a***, Location and magnitude of luciferase expression in an AdCMV-luc-injected mouse (CMV1). Images from sequential d after injection (indicated at the top of each image) displayed two sites of optical signal, that is, in the liver (l) and in the tumor (t). Tumor signal at 21 d post-injection was below 4×10^4. 1.8×10^9 infectious units of Ad were injected into ~7-mm diameter tumors in six divided doses in two consecutive d. In the AdCMV-luc-injected cohort of 3 mice, the average signal (RLU/min) in the tumor was 7.2×10^4, 4.3×10^4, 4.2×10^4, respectively, on day 4, 8, 11. The liver signal on the same time points was 3.3×10^5, 1.1×10^6, 1.0×10^6, respectively. ***b***, Luciferase-expression profile of an AdPSE-BC-luc-injected animal (BC4). The signals in the tumor (t) and extratumoral lesions (e) are specified below the images. The background luminescence signal at 2 d post-infection was ≤ 70 RLU/min. In the AdPSE-BC-luc-injected cohort of 5 mice, the average signal in the tumor was 900, 1,800 and 1,300, respectively, on days 4, 8 and 11. Low-magnitude extratumoral signals (~200 RLU/min) were visible in the chest and or back (3 of 5 mice).

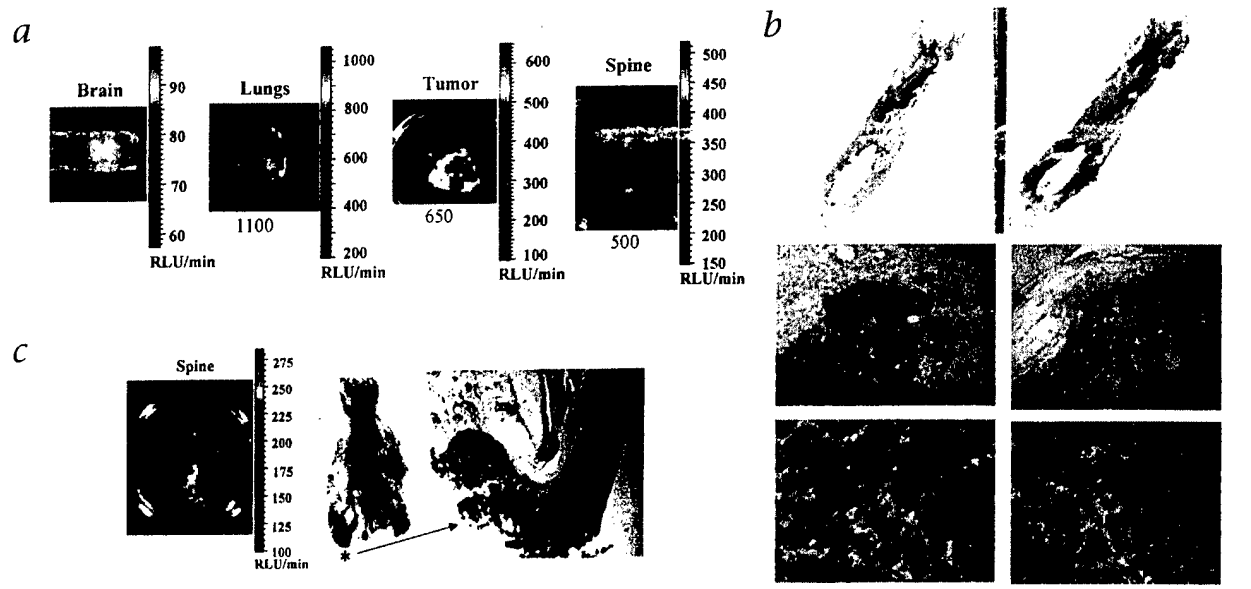

Fig. 3 Detailed histological analysis of spinal metastatic lesions. ***a***, The isolated organs from mouse BC4 (Fig. 2*b*) were imaged. Due to light signal attenuation contributed by the covering tissues, the isolated organs displayed higher signal intensities than in the intact living animal[9]. ***b***, Histological analysis of the spine lesion of mouse BC4. 5-μm sections of spine were stained with H&E (right) and with human-specific antibody against cytokeratin (left). Unmagnified sections (top) show an elongated lesion in the mid-segment of the spine. Higher magnifications (×200, middle and ×400, bottom) of the lesion are shown. Anti-human cytokeratin specifically stained the lesion with a characteristic intense ring of cytoplasmic staining. ***c***, Correspondence of CCD signal and location of a spinal lesion. In another mouse, BC2, with spinal signal, anti-human cytokeratin stain localized the lesion to the caudal end of the spine. Magnification, ×40 in right panel.

Detection and localization of metastases

To localize the origin of the extratumoral luminescence, we isolated organs from the (BC4) mouse and re-imaged them (Fig. 3*a*). The signals in the chest and lower back were found to originate from the lung and spine, respectively (Figs. 2*b* and 3). Histological analysis of the spinal column revealed a lesion localized to the mid-segment (Fig. 3*a* and *b*). Higher magnifications revealed an elongated lesion embedded in spinal musculature, characterized by large pleomorphic nuclei and a high mitotic rate consistent with neoplasia (Fig. 3*b*). Human cytokeratin staining confirmed the lesion was of human origin (Fig. 3*b*). The spinal lesion from another animal (BC2) had the same histological characteristics and a clear correspondence of CCD signal to the lesion located at the caudal end of the spine (Fig. 3*c*).

Immunofluorescent confocal microscopy was used to identify metastatic lung lesions. The lungs of non-tumor-bearing mice stained negative for human cytokeratin (data not shown). Microscopic evaluation of lung sections from tumor-bearing mice revealed the characteristic cytoplasmic cytokeratin staining (Fig. 4*a*). Tumor cells were detected as micrometastatic nodules of 9–74 cells in several independent locations that occupied 377 μm^3 of the right lung and 46 μm^3 of the left lung. The predominant localization of micrometastasis in the right lung corresponded well with the CCD imaging (Fig. 4*a*).

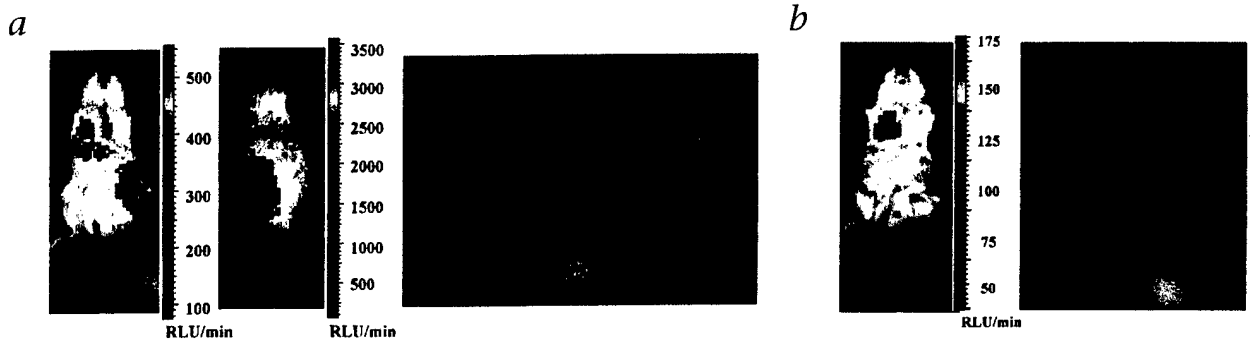

Fig. 4 Optical CCD detection and histological analysis of lung metastases. ***a***, Detection of lung metastasis by CCD imaging and confocal microscopy. In the mouse images, upper chest signals were greater in right image, and were detected in a LAPC-4 AI tumor-bearing mouse (BC1) 21 d after intratumoral injection of 1.8×10^9 infectious units of AdPSE-BC-luc. The right panel is a representative confocal microscopic image of metastatic cells in the lung. On the far right, the cluster of cells exhibits the positive staining of anti-cytokeratin. Magnification, ×400. ***b***, Detection of lung metastases after systemic injection of AdPSE-BC-luc. 3.6×10^7 infectious units were injected via the tail vein in a LAPC-4 AD tumor-bearing mouse. Left panel shows the image at 12 d after injection. Right panel shows a lung section stained positive using anti-cytokeratin (red/orange) visualized in confocal microscopy. Magnification, ×400. Vessels were visualized by lectin (green).

To our knowledge, detection of metastases by a vector-based imaging approach in living animals has not yet been reported. Thus, we investigated whether systemic vector delivery could visualize metastasis. Two expected challenges of systemic delivery are, first, that most of the adenovirus will likely be sequestered in the liver[10], resulting in greatly reduced delivery to organs in the arterial circulation[5]; and second, that systemic delivery of high doses of adenovirus can result in liver toxicity and immune activation[11]. Due to these issues, we focused on determining the lowest viral dose that would allow us to detect metastases. We administered 1.8×10^7 and 3.6×10^7 infectious units of AdPSE-BC-luc (50- to 100-fold lower than the intratumoral injection dose). No specific signals were detected using the lowest dose (data not shown). However, lung metastasis was visualized 12 days after tail-vein injection of the 3.6×10^7 plaque-forming units (p.f.u.) (Fig. 4*b*). Confocal microscopy confirmed the presence of metastatic cancer cells (Fig. 4*b*).

Elevated PSA-based expression in AI tumors

One of the challenges facing the prostate cancer field is localization of recurrent AI disease. We first compared endogenous AR and PSA expression in AD and AI tumors. PSA and AR protein expression increased in the AI subline (Fig. 5*a*). AdPSE-BC-luc-mediated luciferase expression paralleled the endogenous PSA increase (Fig. 5*b*). The CCD images of two mice from AD and AI LAPC-4 tumor-bearing cohorts are shown (Fig. 5*b*). The averaged signal in AI was 10-fold higher than that in the AD cohort 11 days post-injection ($n = 4$). Uneven vector distribution and gene transfer are limitations of intratumoral injections. To rule out these possibilities, we performed *ex vivo* infection of single-cell suspensions derived from the AD and AI xenografts. Both tumor cells were equally infected (data not shown). Luciferase expression 3 days after AdPSE-BC infection was $5.80 \pm 0.87 \times 10^4$ RLU/μg protein in AI LAPC-4 as compared with $2.37 \pm 0.79 \times 10^4$ RLU/μg protein in AD tumor cells ($P = 0.007$, two-tailed *t*-test).

Luciferase expression regulated by the PSA-derived PSE-BC promoter seemed to correlate to the endogenous PSA level, but not to tumor volume (Fig. 5*a* and *b*). To investigate this issue further, we infected LNCaP cells, an androgen-responsive prostate cancer line, with AdPSE-BC-luc. We determined the luciferase activity (Fig. 5*c*) and endogenous PSA and AR expression (Fig. 5*c*) with varying concentrations of synthetic androgen, R1881, added to culture media. Luciferase expression in LNCaP cells mediated by AdPSE-BC-luc exhibited strong androgen inducibility and correlation to endogenous PSA and AR but not to ubiquitous cellular proteins (that is, actin).

Discussion

Hormone therapy for prostate cancer has changed little since its introduction 30 years ago. As a result, gene-based therapeutic strategies, covering a broad spectrum of approaches including replacement of defective tumor suppressors, cytotoxic enzyme-prodrug therapy, suppression of tumor angiogenesis, and up-regulation of immune-mediated tumor surveillance[4], have emerged as promising alternatives or adjuvants to existing modalities. However, the design and application of vector-based cancer gene therapies must address both efficacy and safety.

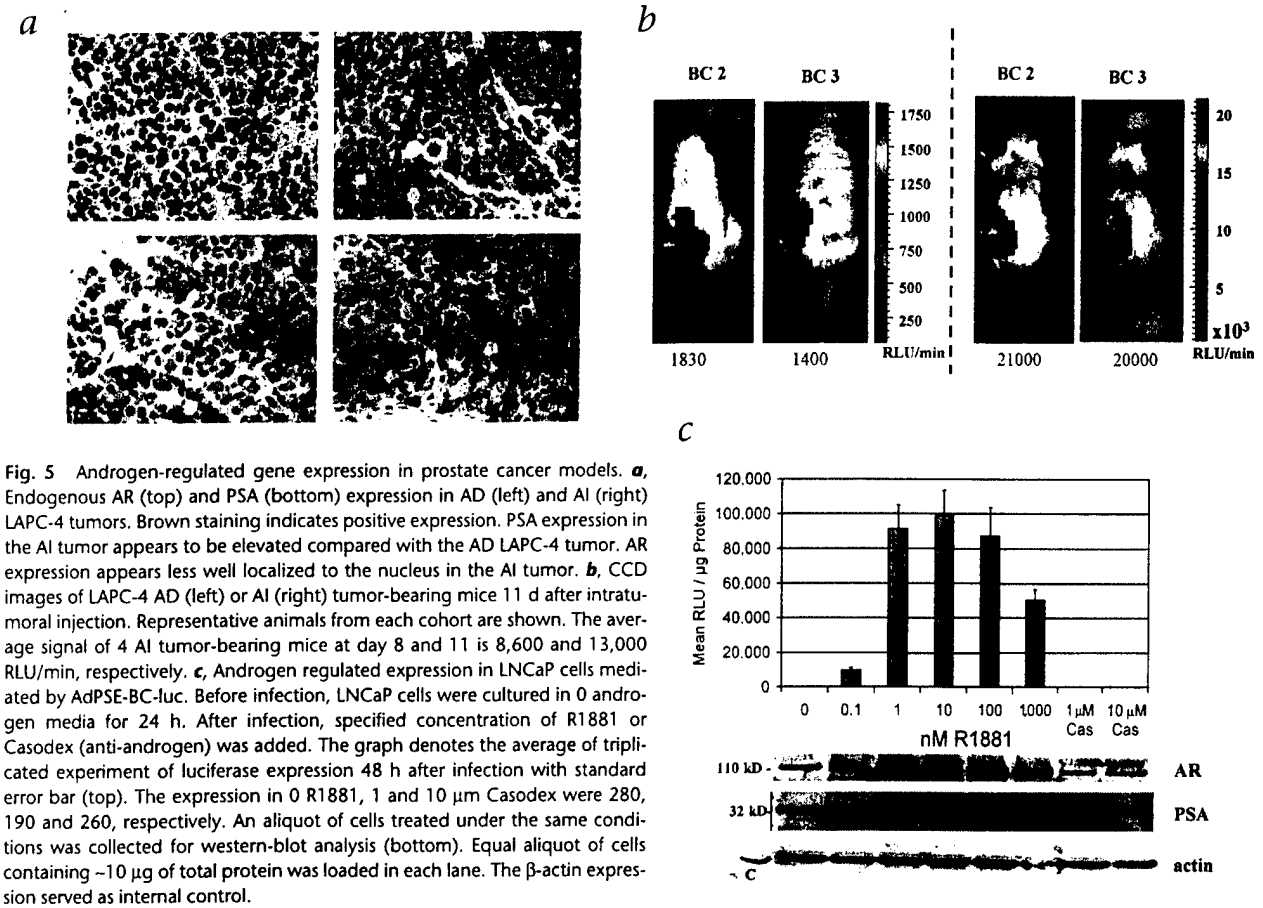

Fig. 5 Androgen-regulated gene expression in prostate cancer models. ***a***, Endogenous AR (top) and PSA (bottom) expression in AD (left) and AI (right) LAPC-4 tumors. Brown staining indicates positive expression. PSA expression in the AI tumor appears to be elevated compared with the AD LAPC-4 tumor. AR expression appears less well localized to the nucleus in the AI tumor. ***b***, CCD images of LAPC-4 AD (left) or AI (right) tumor-bearing mice 11 d after intratumoral injection. Representative animals from each cohort are shown. The average signal of 4 AI tumor-bearing mice at day 8 and 11 is 8,600 and 13,000 RLU/min, respectively. ***c***, Androgen regulated expression in LNCaP cells mediated by AdPSE-BC-luc. Before infection, LNCaP cells were cultured in 0 androgen media for 24 h. After infection, specified concentration of R1881 or Casodex (anti-androgen) was added. The graph denotes the average of triplicated experiment of luciferase expression 48 h after infection with standard error bar (top). The expression in 0 R1881, 1 and 10 μm Casodex were 280, 190 and 260, respectively. An aliquot of cells treated under the same conditions was collected for western-blot analysis (bottom). Equal aliquot of cells containing ~10 μg of total protein was loaded in each lane. The β-actin expression served as internal control.

Methods

Mice and LAPC xenograft propagation and cell cultures. Approximately 1 × 10^6 LAPC-4 seed tumor cells generously provided by C. Sawyers[6,7] were mixed 1:1 with Matrigel (Collaborative Research, Bedford, Massachusetts) and implanted subcutaneously in male SCID (*scid/scid*) mice. The AI sublines were passaged several rounds in castrated male mice[6]. Single-cell suspension cultures of xenografts[7] were maintained on PreBM/GM media (Clonetics, Walkersville Maryland). LNCaP cells were maintained in RPMI media (Invitrogen, Carlsbad, California) with 10% FBS. In 0 androgen condition, 10% charcoal-treated FBS (ref. 5) was used. Methylenetrienolone (R1881; NEN Life Science Products, Boston, Massachusetts) was added at specified concentration.

Adenoviral vectors, Southern hybridization and immunoblotting. AdCMV-luc and AdPSE-BC-luc[5,9] were titered by plaque assays on 293 monolayer cells (infectious units = plaque-forming units). Total DNA was purified by phenol/chloroform extraction and ethanol precipitation after the liver tissues were homogenized and lysed by proteinase K. Southern hybridization conditions are as previously described[5]. Nonradioactive digoxigenin (Roche Molecular Biochemicals, Mannheim, Germany) labeled luciferase DNA fragment was used as probe[5].

LNCaP cells were infected at 10 infectious units/cell, harvested and lysed using RIPA lysis buffer (10 mM Tris, 150 mM NaCl, 0.1% SDS, 1% DOC, 1 mM EDTA and 1% NP40) and 10 μg of protein per lane were analyzed. Primary antibody to PSA (Dako, Copenhagen, Denmark), AR (Upstate, Lake Placid, New York) and actin (Sigma, St. Louis, Missouri) were used. Specific protein was visualized by ECL (Amersham, Piscataway, New Jersey).

CCD imaging to detect *in vivo* luciferase expression. 1-8 × 10^9 infectious units were injected via tail vein into naive animals or intratumorally. At the specified days, the CCD images were obtained using a cooled IVIS CCD camera (Xenogen, Alameda, California) and images were analyzed[9]. Within the linear range of signal intensity (< saturation limit of 65,000 RLU), we determined that the maximum RLU/min within a region of interest (ROI) to be the most consistent for comparative analysis and that the results correlated closely with luminometry[5,9].

Confocal microscopy and immunohistochemical analysis. Animals were perfused with 2% paraformaldehyde, and lungs were inflated with 3% agarose. In some studies, vessels were visualized by injecting 125 μl of fluorescein-conjugated tomato lectin (Vector Laboratories, Burlingame, California). Specimens were fixed, washed in PBS and embedded on 7% agarose. 500-μm vibrotome sections were stained with a CY-3-conjugated human-specific α-cytokeratin cocktail AM273-5M (BioGenex Laboratories, San Ramon, California). Confocal microscopy (BioRad 1024 confocal microscope; BioRad, Hercules, California) was quantified by ImagePro4.0 software.

Immunohistochemistry was performed on paraffin-embedded tumor sections with antigen retrieval[20]. Tissue sections were incubated at 4° C overnight with respective antibodies, AR-β 5 μg/ml (UpState), or PSA 1:40 (Novocastra, Newcastle upon Tyne, UK). After stringent blocking and washing and incubation with multilink 1:20 (BioGenex) and AP label 1:20 for 20 min at room temperature, sections were washed and developed with DAB (BioGenex).

Effective gene therapy is dependent in part on the ability of a vector to transduce the targeted tissue. We demonstrate that our prostate-specific Ad vector was capable of transducing both the AD LAPC-4 and LAPC-9 (data not shown) xenografts. We also showed that as LAPC-4 tumors progressed from AD to AI, the AI tumor cells continued to express AR and PSA, despite the absence of testicular androgen (Fig. 5). Remarkably, not only was the PSA-based Ad transcriptionally active in AI prostate tumors, it displayed 10-fold higher activity than in AD tumors. As all of the models retain important features of clinical disease[6,7], these data support the possibility that a prostate-targeted vector can be developed to treat patients with advanced disease.

We observed that positive AR staining appeared to be less well localized to the nucleus in the AI than in AD tumor sections (Fig. 4*a* and data not shown). This observation is consistent with the current understanding that nuclear translocation of AR is mediated in part by androgen binding to the receptor[12]. Both the mechanism of AR translocation and the functional role of nuclear localized AR may be key to understanding transcriptional regulation in AI prostate cancer. Evidence suggests that AR function critical in AI disease includes AR mutations that confer expanded ligand specificity[13], AR over-expression[14], cross-talk between other signaling cascades and AR pathways[15] and increased expression of the nuclear-receptor transcriptional coactivator, TIF2 (ref. 16). In light of mounting evidence supporting an activated AR pathway in AI progression and the fact that PSA transcription is dependent on AR function, the magnitude of serum PSA measured in recurrent disease might not be a good indicator of tumor volume but rather a reflection of AR function. Our vector, composed of PSA-based transcriptional regulatory elements, will provide a tool to interrogate the endogenous AR pathway (Fig. 5*c*).

One notable, serendipitous discovery was the detection of metastatic lesions. Although the precise transduction mechanism is unclear, we postulated that intratumoral injection of AdPSE-BC-luc leaked to the systemic circulation similar to AdCMV-luc injection and infected the lesions (Fig. 2*a*). This hypothesis is supported by the fact that lung metastasis can be detected by systemic tail-vein injection of AdPSE-BC-luc (Fig. 4*b*). An alternative explanation for detecting metastasis after intratumoral vector injection could be the dissemination of a tranduced cell(s). This hypothesis is less likely because Ad-mediated expression is transient, and expansion from a single cell to the large lesion would have resulted in loss of expression.

Although several studies have supported the utility of CCD imaging to track the dissemination of luciferase-marked tumor cells in small animals[8], the vector-based approach demonstrated in this study could be developed for future clinical applications. Several areas of refinement are needed. Much higher tissue-specific transcriptional activity, approaching the level of CMV, should increase targeted transduction. We have developed a prostate-specific, two-step transcriptional amplification (TSTA) system that exhibits ~2-fold higher activity than CMV but retains specificity and proper androgen regulation[17]. Approaches

that improve the vectorology (reviewed in ref. 18), such as altering viral transduction to favor specific cell-surface markers, or minimizing viral antigenicity, or use of non-viral vectors could be complementary to the transcriptional targeting approach to further enhance safety and efficacy. The vector-mediated cancer targeting approaches need to be validated in a clinically relevant imaging modality. Positron emission tomography (PET) is a clinical modality that can provide quantitative, three-dimensional localization of imaging signals. In fact, we have demonstrated that micro-positron emission tomography (microPET) can track Ad-mediated herpes simplex virus thymidine kinase gene expression in tumors of living mice[19]. Appropriate resolution of the issues discussed should improve future gene-based prostate cancer diagnostic and therapeutic strategies.

Acknowledgments

We thank A. Berk, U. Banerjee, H. Herschman, L. Rome, C. Sawyers, R. Reiter and J. Said for helpful advice and critical review of manuscript; Joseph Wu, Tina Yu, Joyce Yamashiro, Evelyn Kondo and Chris Tran for technical assistance; and W. Aft and D. Nusinow for assistance in the preparation of this manuscript. This work was initiated with seed funding from the California Cancer Research Coordinating Committee, the Carolan Foundation of UCLA and the California Cancer Research Program. L.W. is a member of the Jonsson Comprehensive Cancer Center and the recipient of a STOP Cancer research career development award. Cost of imaging was supported by NIH P50 CA86306 (S.S.G.), R0-1 CA82214 (S.S.G.), SAIRP R24 CA92865 (S.S.G.), Department of Energy Contract DE-FC03-87ER60615 (S.S.G.) and CaPCURE (S.S.G., M.C.).

1. Nash, A.F. & Melezinek, I. The role of prostate specific antigen measurement in the detection and management of prostate cancer. *Endocr. Relat. Cancer* **7**, 37–51 (2000).
2. Rini, B.I. & Small, E.J. An update on prostate cancer. *Curr. Opin. Oncol.* **13**, 204–211 (2001).
3. Bloomfield, D.J. *et al.* Economic evaluation of chemotherapy with mitoxantrone plus prednisone for symptomatic hormone-resistant prostate cancer: based on a Canadian randomized trial with palliative end points. *J. Clin. Oncol.* **16**, 2272–2279 (1998).
4. Harrington, K.J., Spitzweg, C., Bateman, A.R., Morris, J.C. & Vile, R.G. Gene therapy for prostate cancer: Current status and future prospects. *J. Urol.* **166**, 1220–1233 (2001).
5. Wu, L. *et al.* Chimeric PSA enhancers exhibit augmented activity in prostate cancer gene therapy vectors. *Gene Ther.* **8**, 1416–1425 (2001).
6. Klein, K.A. *et al.* Progression of metastatic human prostate cancer to androgen independence in immunodeficient SCID mice. *Nature Med.* **3**, 402–408 (1997).
7. Craft, N. *et al.* Evidence for clonal outgrowth of androgen-independent prostate cancer cells from androgen-dependent tumors through a two-step process. *Cancer Res.* **59**, 5030–5036 (1999).
8. Rehemtulla, A. *et al.* Rapid and quantitative assessment of cancer treatment response using *in vivo* bioluminescence imaging. *Neoplasia* **2**, 491–495 (2000).
9. Wu, J.C., Sundaresan, G., Iyer, M. & Gambhir, S.S. Noninvasive optical imaging of firefly luciferase reporter gene expression in skeletal muscles of living mice. *Mol. Ther.* **4**, 297–306 (2001).
10. Tao, N. *et al.* Sequestration of adenoviral vector by Kupffer cells leads to a nonlinear dose response of transduction in liver. *Mol. Ther.* **3**, 28–35 (2001).
11. Yang, Y. *et al.* Cellular immunity to viral antigens limits E1-deleted adenoviruses for gene therapy. *Proc. Natl. Acad. Sci. USA* **91**, 4407–4411 (1994).
12. Waller, A.S., Sharrard, R.M., Berthon, P. & Maitland, N.J. Androgen receptor localisation and turnover in human prostate epithelium treated with the antiandrogen, casodex. *J. Mol. Endocrinol.* **24**, 339–351 (2000).
13. Zhao, X.Y. *et al.* Glucocorticoids can promote androgen-independent growth of prostate cancer cells through a mutated androgen receptor. *Nature Med.* **6**, 703–706 (2000).
14. Linja, M.J. *et al.* Amplification and overexpression of androgen receptor gene in hormone-refractory prostate cancer. *Cancer Res.* **61**, 3550–3555 (2001).
15. Craft, N., Shostak, Y., Carey, M. & Sawyers, C.L. A mechanism for hormone-independent prostate cancer through modulation of androgen receptor signaling by the HER-2/neu tyrosine kinase. *Nature Med.* **5**, 280–285 (1999).
16. Gregory, C.W. *et al.* A mechanism for androgen receptor-mediated prostate cancer recurrence after androgen deprivation therapy. *Cancer Res.* **61**, 4315–4319 (2001).
17. Zhang, L. *et al.* Molecular engineering of a two-step transcription amplification (TSTA) system for transgene delivery in prostate cancer. *Mol. Ther.* **5**, 223–232 (2002).
18. *The Development of Human Gene Therapy.* (ed. Freidmann, T.) (Cold Spring Harbor Laboratory Press, Cold Spring Harbor, New York, 1999).
19. Yaghoubi, S.S. *et al.* Direct correlation between positron emission tomographic images of two reporter genes delivered by two distinct adenoviral vectors. *Gene Ther.* **8**, 1072–1080 (2001).
20. Leav, I. *et al.* Comparative studies of the estrogen receptors β and α and the androgen receptor in normal human prostate glands, dysplasia, and in primary and metastatic carcinoma. *Am. J. Pathol.* **159**, 79–92 (2001).

Interrogating Androgen Receptor Function in Recurrent Prostate Cancer[1]

Liqun Zhang, Mai Johnson, Kim H. Le, Makoto Sato, Romyla Ilagan, Meera Iyer, Sanjiv S. Gambhir, Lily Wu and Michael Carey[2]

Departments of Biological Chemistry (LZ, KHL, RI, MC) and Urology (MJ, MS, LW), and Crump Institute of Molecular Imaging (SSJ, LW, MC) and Department of Molecular and Medical Pharmacology (MI, SSJ), University of California, Los Angeles, School of Medicine, Los Angeles CA 90095-1737, USA

Running title: Imaging Androgen Receptor During Oncogenesis

Key words: androgen receptor, molecular imaging, prostate cancer

1. Supported by CaPCURE (to MC, SSG), DOD CDMRP PC000046 (to LW), DOD PC991019 (to Charles Sawyers and MC), DOD PC020177 (to MC), an interdisciplinary seed grant from the JCCC (to MC, LW and SSG), R01 CA82214 (to SSG), SAIRP R24 CA92865 (to SSG), and Department of Energy Contract DE-FC03-87ER60615 (to SSG). LZ is supported by USHHS Institutional National Research Service Award #T32CA09056. MI is supported by a Research Training in Pharmacological Sciences Award #T32JM08652.

2. To whom reprint requests should be addressed at Department of Biological Chemistry, UCLA School of Medicine, Box 1737, Los Angeles, CA 90095-1737.

3. The abbreviations used are: AD, androgen dependent; AI, androgen independent; AR, androgen receptor; CCD, charge coupled device; DHT, dihydroxytestosterone; LAPC, Los Angeles prostate cancer; MAPK, mitogen-activated protein kinase; pol II, RNA polymerase II; PSA, prostate specific antigen; SCID, severe combined immunodeficiency; TSTA, two-step transcriptional activation.

ABSTRACT

The early androgen-dependent (AD) phase of prostate cancer is driven by the androgen receptor (AR). An important issue is to what extent AR participates in recurrent prostate cancer after androgen deprivation and how does it function. We interrogated AR signaling in AD and recurrent human prostate cancer xenografts implanted into SCID mice using molecular imaging, serum PSA levels, chromatin immunoprecipitation (ChIP) and immunohistochemistry. An adenovirus-based, two-step transcriptional activation (TSTA) cassette, which sensitively monitors AR activity, was injected into tumors. A charge coupled device optical imaging system, which measures AR-dependent firefly luciferase activity, detected the loss and resurrection of AR transcriptional function during transition of cancer from AD to recurrent growth. The TSTA imaging signal correlated with but was more sensitive than secreted prostate specific antigen (PSA) levels. Chromatin immunoprecipitation and immunohistochemical localization experiments revealed that AR localized to the nucleus and bound to the endogenous PSA enhancer in AD cancer. After castration, the bulk of AR transiently exited the nucleus and dissociated from the enhancer. AR re-entered the nucleus and rebound the PSA enhancer as the cancer transitioned to the recurrent phase. RNA polymerase II and a general transcription factor TFIIB did not dissociate from the PSA gene after castration suggesting that the transcription complexes remain in a transcriptionally poised state, which may facilitate reactivation by AR at castrate levels of ligand.

INTRODUCTION

Prostate cancer growth is controlled by AR[3] (1), a member of the steroid receptor subfamily of nuclear receptors (2). In the presence of its ligand, DHT[3], the bulk of AR moves from the cytoplasm to the nucleus (3, 4), binds to 15-bp DNA elements (ARE[3]) in enhancers and promoters, and activates expression of genes involved in prostate metabolism including PSA[3].

PSA is a secreted kallikrein protease widely used for evaluating treatment and progression of cancer although it has some drawbacks in prognostic utility (5). The PSA promoter and enhancer have been delineated and contain AREs necessary for transcriptional activity in AD[3] cancer cell lines such as LNCaP (6-12). A 440-bp core segment of the enhancer plays the major role in androgen-responsiveness (10). Multiple dimers of AR bind cooperatively to a cluster of AREs in the core enhancer and synergistically activate transcription (13, 14) via interaction with co-activators that recruit pol II[3] and its associated factors (1). DHT-dependent AR binding to the PSA enhancer has been studied extensively in LNCaP cells using ChIP but has not yet been evaluated in tumors (15-17).

A central role for AR in AD prostate cancer has been inferred from the observation that tumor growth initially ceases with treatments that lower the concentration or effectiveness of DHT. Although secreted PSA levels decrease as AR activity is diminished (18) the cancer eventually transitions from the AD state to a recurrent or AI[3] state upon failure of androgen blockade or withdrawal therapies (19-21). As the cancer transitions the levels of secreted PSA rise again.

In many cancers the AR gene is amplified and/or AR is overexpressed (22, 23). The relevance of AR overexpression in cancer is supported by transgenic animal studies where forced overexpression of murine AR from the probasin promoter leads to development of high-grade prostatic intraepithelial neoplasia, a precursor to prostate cancer (24). It has been hypothesized that in recurrent cancer overexpressed AR can function by utilizing castrate levels of DHT or adrenal androgens (22, 25).

Mutations in the AR ligand binding domain also permit AR to function through the use of alternative ligands (21). Somatic mutations in the Transgenic Adenocarcimona of Mouse Prostate model revealed a correlation between reduced androgen dependence and mutations in AR domains known to interact with co-activators that facilitate its transcriptional activity (26). It is plausible that the mutations facilitate co-activator interactions in the absence of ligand or the presence of alternative ligands. However, only a subset of human tumors express mutated AR.

MAPK[3] has been postulated to upregulate AR activity in the absence of ligand (19-21, 27-29). Elevated MAPK has been observed in advanced prostate cancer specimens from patients and in recurrent xenograft models (30, 31). Several receptor tyrosine kinases or growth factors, which signal through MAPKs, activate AR-responsive reporter genes in an AI manner when overexpressed in cell culture (19-21, 27-29). A receptor tyrosine kinase inhibitor that targets the epidermal growth factor receptor pathway inhibits AR activity and tumor growth in animal models (31).

Further support for a direct role of AR in recurrent cancer growth comes from cell line studies. Lowering AR levels in an AI LNCaP cell line in culture by injection of an AR-targeted hammerhead ribozyme or AR antibodies reduces cell proliferation (32). It has been suggested that AR may function not by binding DNA but through cytoplasmic interaction with signaling molecules that activate the MAPK pathway (33, 34). However, the effect of AR on PSA gene transcription in at least one AI cell line involves direct DNA binding because the PSA enhancer requires some of its natural AREs for activity, although other transcription factors also contribute (35).

Despite these intriguing studies neither direct measures of AR activity nor binding of AR to responsive genes have been demonstrated in recurrent cancer in live animal models of the disease. This is an important issue for developing pharmaceuticals targeted to recurrent cancer, the most deadly form of the disease in men. The goal of our study was to confirm AR function in recurrent prostate cancer in an animal model using direct measurements of AR activity in the context of human xenograft tumors implanted into $SCID^3$ mice. We employed the LAPC9 model, a human prostate cancer derived from a bone metastasis (36). LAPC9 tumors express PSA and wild-type AR, and upon castration of the SCID mice, the tumor transiently halts growth and gradually transitions into the recurrent state. Continued passage of the AI tumors in castrated mice generates a stable AI model, which expresses AR and PSA.

We utilized four tools to study AR function in the LAPC9 tumors: secreted PSA levels, $ChIP^3$, immunohistochemistry and molecular imaging. The PSA

levels permitted us to confirm that the tumor responded to androgen deprivation in castrated animals and rose during transition to recurrent cancer. Immunohistochemistry allowed us to monitor nuclear localization, an important parameter of AR function. ChIP enabled us to directly monitor specific AR DNA binding to the endogenous PSA gene within the tumors of LAPC9 mice harboring AD and recurrent tumors. Gene expression-based molecular imaging is a new technology that permitted us to non-invasively visualize transcriptional activity during cancer progression in the LAPC9 models (37-40).

The molecular imaging technology employs a cooled CCD^3 camera, which detects light emitted from living animals when standard reporter genes such as firefly and renilla luciferase are expressed in the presence of their substrates (41). The short half-life of luciferase in conjunction with highly active reporter genes facilitates dynamic measurement of expression occurring over weeks within tumors implanted into an animal (42). Our imaging system is based on prostate specific antigen (PSA) regulatory region because of its AR-responsiveness and prostate specificity (43).

In a previous study we duplicated the core PSA enhancer and significantly augmented AR-responsive firefly luciferase activity in cell culture (44). An adenovector bearing this "first generation" imaging cassette, AdPBC, detected distal metastatic lesions in SCID mouse xenograft models upon intratumoral or systemic injection via tail veins, and visualization with a CCD optical imaging system (45). The overall activity of the imaging cassette was low making it difficult to dynamically monitor the androgen-response. To further improve the

signal we employed a TSTA^3 strategy. The duplicated PSA regulatory region was employed to express the potent artificial transcription activator GAL4-VP16, which acts on a GAL4-responsive firefly luciferase reporter gene resulting in amplified levels of expression (46). We optimized the system by varying the numbers of GAL4 sites and VP16 activation domains (47).

In this paper we incorporated the optimal TSTA system into a replication deficient adenovirus (48), which has a high infection efficiency and is widely used in gene transfer studies in animals and humans (49). We injected AdTSTA into human AD and recurrent tumors implanted into SCID mice and were able to image activation, inactivation and reactivation of AR activity during cancer progression. Immunohistochemical staining and ChIP of AR on the PSA regulatory region in various stages of cancer progression supported the concept that AR is fully active in recurrent cancer. ChIP data also suggested a model whereby the RNA polymerase II (pol II) transcription complexes on AR-responsive genes do not disappear in the absence of androgen but remain poised to resume activity in recurrent cancer.

MATERIALS AND METHODS

Adenovirus Constructs. AdTSTA was generated from the optimal TSTA plasmid (47). A second NotI site 5' from the PBC enhancer was removed to create unique NotI site in the vector. A SalI-NotI fragment containing the core BCVP2G5-Luc fragment was excised by NotI and partial SalI digestion and inserted into the SalI-NotI site of pShuttle vector (Q-Biogene, Carlsbad, CA), which was then incorporated into the adenovirus vector AdEasy^{TM} through homologous recombination. AdCMV was generated as previous described (45). The viruses were packaged and propagated in 293A cells. The virus was scaled up, purified via a CsCl gradient and titered by plaque assays on 293 monolayers (infectious units = plaque-forming units). Virus was stored at ~10^{11}pfu/ml in 10mM Tris-HCl, 1 mM $MgCl_2$, and 10% glycerol. TSTA plasmid vectors that contain convenient restriction sites for removing PBC and replacing it with any promoter have been constructed and will be provided upon request.

Cell Culture and Xenografts. The human prostate cancer cell line LNCaP was grown in RPMI 1640 supplemented with 10% Fetal Bovine Serum and 1% Penicillin/Streptomycin solution. HeLa, MCF-7, and HepG cells were cultured in DMEM with 10% Fetal Bovine Serum and 1% Penicillin/Streptomycin. Prior to transfection, cells were transferred for 24 hours into medium containing 5% charcoal stripped serum (Omega Sci. Tarzana CA). The synthetic androgen

Methylenetrienolone (R1881; NEN Life Science Products, Boston, MA) was added to "ligand positive" samples where indicated.

Human prostate tumor xenografts were generated on SCID mice as previously described (36). Briefly, approximately $1x10^6$ LAPC-9 tumor cells generously provided by Dr. Charles Sawyers were mixed 1:1 with Matrigel (BD Scientific) and implanted subcutaneously on the left flank of male SCID (C.B. –17 *Scid/Scid*) mice. The AI sublines were passaged several rounds in castrated male mice. Single-cell suspension cultures were maintained on PreBM/GM media (Clonetics, Walkersville MD). Alternatively, tumors were extracted from founder mice, minced into ~0.2 mm cubes, bathed in matrigel, and implanted subcutaneously onto the left flanks of SCID mice.

Virus Activity Assays. For firefly luciferase assays, the cultured cells were infected with AdTSTA or AdCMV at an MOI of 0.1. After 48 hours, the cells were harvested and lysed using the passive lysis buffer provided in the firefly luciferase assay kit (Dual-Reporter Luciferase Assay System, Promega, Madison, WI). Firefly luciferase activities of 5% of the cell lysates supplemented with 100 μl of D-luciferin were measured using a luminometer (Lumat 9507, Berthod Germany) with an integration time of 10 sec.

Immunoblot Analysis of GAL4-VP16 Expression. LNCaP cells were grown in 10-cm dishes and infected with AdTSTA at MOI 10. Forty-eight hours later the cells were harvested and lysed with RIPA buffer (10 mM Tris-HCl, 150 mM NaCl,

0.1% SDS, 1% DOC, 1 mM EDTA and 1% NP40). Protein concentrations of the extracts were normalized (Bio-Rad Dc protein assay Kit), the samples were fractionated on 4-15% gradient acrylamide gels (Bio-Rad, Hercules, CA) and subjected to immunoblot analysis with rabbit polyclonal antibodies generated against intact GAL4-VP16 or loading control proteins.

CCD Imaging of Firefly Luciferase Expression. For the naïve mice, 10^7 pfu of AdTSTA or AdCMV suspended in 100 μl phosphate buffered saline (PBS) was injected via the tail vein. For the LAPC9 xenografts, a total of 10^7 pfu of AdTSTA or AdCMV in 40 μl PBS was injected directly into the 0.5-cm diameter tumor xenografts at multiple locations. To ensure adequate distribution throughout the tumor, the injection was carried out twice on two sequential days. The virus was allowed to express the encoded genes and distribute throughout the tissue for 3-4 days prior to imaging. At the days specified in the figures, the mice were anesthesized and injected with ~150 mg/kg D-Luciferin (approximately 3 mg/mouse). Light signals (CCD images) were obtained using a cooled IVIS CCD camera (Xenogen, Alameda, CA) and images were analyzed with IGOR-PRO Living Image Software, which generates a pseudoimage with an adjustable color scale. We determined the maximum photons/second of acquisition/cm^2 pixel/steridian (sr) within a region of interest to be the most consistent measure for comparative analysis. The imaging results correlated closely with luminometry of tissue extracts. Typically our acquisition times ranged from 1 to 10 seconds.

Tumor Immunohistochemical Analysis. Immunohistochemistry was performed on paraffin-embedded tumor sections with antigen retrieval. Tissue sections were incubated at 4°C overnight with anti-AR 5 μg/ml (UpState, Charlottesville, VA). After stringent blocking, washing and incubation with multi-link (BioGenex, San Ramon, CA) and alkaline phosphatase label for 20 min at room temperature, sections were washed and developed according to the manufacturer's instructions (BioGenex).

Secreted PSA and Serum DHT Measurements. Blood was withdrawn from the mice by retro-orbital bleeding and plasma was collected. PSA levels were measured using a PSA ELISA kit (American Qualex, San Clemente, CA) while the DHT levels were measured using a DHT ELISA kit (Alpha Diagnostic International, San Antonio, TX). All measurements were performed in triplicate.

Tumor Chromatin Immunoprecipitation. Tumors were extracted from the mice and washed with ice cold PBS. The tumors were quickly minced and immersed in 1% formaldehyde solution, where they were further minced and homogenized using a glass dounce. The total incubation in formaldehyde solution was for 30 minutes. Prior to sonication, the cell suspensions were washed 10 minutes each in solution I containing 0.25% Triton, 10 mM EDTA, 1 mM EGTA and 10 mM HEPES, pH 7.5, and in solution II containing 0.2 M NaCl, 1 mM EDTA, 1 mM EGTA and 10 mM HEPES, pH 7.5. Extracts were obtained by 8x15 sec sonication in lysis buffer containing 1% SDS and 10 mM EDTA

reactions. The input sample in the data shown in the ChIP experiments was typically 2% of the DNA added to a ChIP reaction.

The PCR analyses were performed with four sets of ^{32}P-labeled of primers:

Enhancer: 5'GGTGACCAGAGCAGTCTAGGTG3' and 5'TGTTTACTGTCAAGGACAATCGAT3'

Promoter: 5'GTATGAAGAATCGGGGATCGT3' and 5' GCTCATGGAGACTTCATCTAG3'

Middle: 5'TATGCTTGGGGACACCGGAT3' and 5'TTAGAGCTGGAGTGGAAGGATAT3'

Exon 5: 5'TAATGGTGTGCTTCAAGGTATCACG3' and 5'GTGTCCTTGATCCACTTCCGGTAAT3'

The PCR cycling protocol was 40 sec at 94°C, 3 minutes at 75°C, 2 minutes at 65°C, followed by 20 cycles of 40 sec at 94°C, 1 minute at 65°C and 2 minutes at 72°C, followed by a 10 minute extension at 72°C. The PCR products were phenol-extracted, separated on 6% polyacrylamide gels and autoradiographed by exposure to XAR-5 film.

RESULTS

AdTSTA Is AR-responsive in Cell-based Assays. The transcriptional activity of AR is the most relevant measure of its function *in vivo*. Our previous cell culture study employed a plasmid expressing the TSTA system to study AR-mediated gene expression in cell culture (47). To monitor AR in live animal models of prostate cancer it was necessary to insert the TSTA cassette (Fig. 1) into an adenovirus, which could be injected directly into tumors in different stages of cancer progression. A modified PSA regulatory region containing two copies of the AR-responsive core PSA enhancer was placed upstream of the fusion protein GAL4-VP2, bearing two copies of the VP16 activation domain. In the presence of androgen, GAL4-VP2 is synthesized and binds to five GAL4 binding sites positioned upstream of the adenovirus E4 core promoter. GAL4-VP2 activates high levels of firefly luciferase expression. Luciferase was measured in cell culture by luminometry and *in vivo* in D-Luciferin-injected live animals using a Xenogen cooled CCD optical imaging system (42). The two expression cassettes were joined in a divergently-expressed orientation in the genome of Adenovirus serotype 5, with the E1 and E3 coding regions deleted, which renders the packaged virus replication deficient (48).

To validate the androgen responsiveness of the TSTA system in the context of the adenoviral vector cell culture, we infected the model androgen dependent prostate cancer cell line, LNCaP, with AdTSTA (Fig. 1*B*). GAL4-VP2 and firefly luciferase levels were enhanced significantly in the presence of the synthetic

androgen agonist R1881. The largest increase of luciferase activity was observed at the 48-hour time point (Fig. 1*B*, bottom), which correlated with the appearance of GAL4-VP2 by immunoblot analysis (Fig. 1*B*, top).

The AdTSTA system maintained cell selectivity in culture (Fig. 1*C*). An example of these findings is shown for cells derived from prostate cancer (LNCaP), liver (HepG) and cervical cancer (HeLa). LNCaP is an androgen-dependent prostate cancer cell line (50), which contains a mutant form of AR and secretes PSA (51, 52). AR expression is not observed in HeLa and HepG (data not shown). PCR analysis demonstrated that viral infectivity was similar within a two-fold range among the cell lines tested (data not shown). The LNCaP cells displayed significantly higher firefly luciferase activity than HeLa and HepG and responded to the androgen agonist R1881. MCF-7 cells (an AR-expressing breast cancer cell line), PC3 (an AR-negative prostate cancer cell line), and PC3 stably expressing AR were also tested. These lines displayed only a low basal level of TSTA expression and did not respond to R1881 (data not shown). Thus, the AdTSTA system responds to AR specifically expressed in natural AD prostate cells. The residual signal present in LNCaP cells in the absence of ligand could be suppressed by addition of the AR antagonist casodex suggesting that the amplification system is sensitive enough to respond to trace androgen levels present in the charcoal-stripped medium (data not shown).

High levels of luciferase are necessary to observe signals from cell-specific promoters in CCD imaging studies. Previous engineering of the PSA enhancer led to the adenovector, AdPBC, which expressed firefly luciferase in a prostate

specific manner but with only 5% the activity of the highly active viral enhancer from Cytomegalovirus (CMV). The low level of activity was suitable for initial *in vivo* studies but two problems limited its utility in evaluating AR function during tumor progression: The extended time frame necessary to observe firefly luciferase expression in tumors and the long acquisition times on the CCD optical imaging system. Side-by-side comparison demonstrated that AdTSTA displayed a ligand-induced firefly luciferase activity 10-fold greater than AdCMV (Fig. 1*C*) and nearly 200-fold greater than AdPBC (data not shown). The gain of activity obtained by utilizing the TSTA approach reduced the average CCD acquisition times on average from 5 minutes to a few seconds versus AdPBC. This gain in signal permitted us to perform direct measurements of AR function at various stages of cancer growth.

The signal obtained from the studies was tumor specific and robust. Direct intratumoral injection of the viruses into LAPC9 AD xenografts followed by CCD imaging demonstrated that the AdTSTA was routinely twice as active as AdCMV in the tumors but unlike CMV did not generate a signal in liver when injected via the tail vein into non-tumor bearing SCID mice (Supplementary data). Typically, injection of 10^7 pfu of AdTSTA generated a robust signal in tumors and was employed for the experiments described below.

AR Signaling Is Active in AI tumors. To demonstrate the androgen responsiveness of the tumor model we first castrated male mice bearing LAPC9 AD tumors and measured serum PSA levels (Fig. 2). A decrease or plateau of serum PSA is indicative of successful hormone blockade therapy in humans. The

xenograft data revealed that the PSA levels ceased rising and dropped slightly beginning 1 day after castration and remained flat, recapitulating the clinical response to androgen blockade therapy. At later time points the PSA began to rise as tumors transitioned from AD to AI, an issue that is discussed further in a later figure. After castration the serum DHT levels decreased to as low as 85% of the intact animals. The DHT levels remained flat even as PSA levels increased (data not shown).

Analysis of AD and castrated AD (ADc) tumors revealed that the imaging signal responded well to castration (Fig. 3*A*). The AdTSTA-injected tumors typically emitted $>10^7$ photons/sec/cm^2/sr on day 4 after virus injection. Castration on day 4 led to a >10-fold drop in the imaging signal by day 10 (Fig. 3*A*: AD vs. ADc, p=0.01). In contrast, AdTSTA displayed robust activity in established AI mice where over the same time frame the signal increased. The increasing signal in AI versus AD tumors was somewhat perplexing and we do not yet understand the cause. We have noted that AD tumors contain a large necrotic center whereas AI tumors do not. It is plausible that the necrosis leads to some diminution in signal due to death of a subset of infected cells. We conclude from these data that the AR-responsive TSTA system is specifically responding to the loss of AR activity in the ADc tumor but that the activity is regained in established AI tumors.

Localization of AR in Tumors. The distribution of AR is sensitive to androgen depletion. AR is known to localize predominantly to the nucleus in the presence of androgen whereas in the absence of androgen AR localization

becomes diffuse and distributes between the cytoplasm and nucleus (22). Immunohistochemical analyses of tumors from the sacrificed LAPC9 animals used in the imaging studies showed that AR was tightly localized to the nucleus of AD and established AI tumors (Fig 3*B*). The staining in ADc was heterogeneous with a small number of cells showing nuclear staining but most showing a diffuse pattern of nuclear and cytoplasmic staining. Typically 30-35% of the field stained strongly while ~20% stained weakly and the remainder displayed marginal or no staining in both AD and recurrent tumors.

Taken together the imaging and cytology data imply that AR has resumed functioning in AI cancer. However, other proposals have been made to explain how androgen-responsive genes might function in cells lacking physiological levels of androgen. For example, NF-κB has been proposed to bind regulatory regions of androgen-responsive genes and might substitute for AR in AI cancer (53). Nevertheless, the predominant nuclear location of AR in AI tumors implied that AR might be functional. One prediction of this hypothesis is that AR should bind directly to responsive enhancers and promoters in AI cancer.

Transcription Complex Assembly in Tumors To determine if AR was binding to the endogenous PSA regulatory region in AI tumors we employed ChIP (Fig. 4). Previous ChIP experiments performed in LNCaP cells in culture have shown that AR and pol II bind to the enhancer and promoter consistent with *in vitro* DNA binding studies (15, 54). We confirmed these results and then analyzed AR and pol II binding to the PSA gene in the context of LAPC9 AD and AI tumor samples. The tumor ChIP experiments were significantly more difficult

to perform than those in cell culture because the tumor is highly heterogeneous solid tissue. We rapidly minced and crosslinked the tissue during tumor harvest and performed sonication in detergent containing high levels of SDS followed by ChIP in the presence of low SDS and high levels of deoxycholate. This procedure resulted in signals that were detectable although not as strong relative to input DNA as the signals observed in ChIP experiments performed on cells in culture (data not shown).

We analyzed AR binding to four regions of the gene: The enhancer, the promoter, a region located between the enhancer and promoter, and downstream exon 5 (Fig. 4, see schematic). AR binding in both the AD and AI samples was detectable well above background at both the enhancer and promoter. Binding was minimal within the middle intervening region and exon 5. Each experiment was performed on three tumors and specific signals were confirmed by comparing the AR-antibody signal to the background observed in a mock immunoprecipitation with IgG. When normalized to the signal from input DNA and averaged among experiments, the binding to the enhancer in AI tumors was only slightly lower than in AD tumors (see graph). In contrast, upon castration (ADc) AR binding to the enhancer and promoter decreased about 4-fold vs. AD tumors. There is still evidence of specific AR binding in ADc as the signals on the enhancer and promoter are above the IgG background. The residual binding can be explained in part by the cytology data in which some AR remains in the nucleus even in ADc. Additionally, the PSA levels and imaging signals do not decrease to baseline values in ADc but drop transiently as the

tumor begins to transition to AI suggesting that residual AR-dependent transcription occurs even in the presence of castrate levels of ligand.

We initiated a mechanistic study to examine how preinitiation complexes respond to the presence and absence of AR. We began by analyzing pol II, which should be found in both transcription-elongating and promoter-bound positions (Fig. 5). Elongating pol II was analyzed by measuring binding to exon 5. Exon 5 is well into the gene and the ChIP signal is easily discriminated from the promoter. As predicted, pol II binding was observed at both the promoter and downstream exon 5 in the AD and AI tumors. However, the ratio of the signal at exon 5 versus the proximal promoter shows that in AD and AI tumors pol II is primarily localized at exon 5 in the elongating position. The signal is specific because it is found only weakly at the enhancer and not in the intervening region.

Remarkably, in ADc tumors after castration, pol II remained bound to the gene at levels similar to those seen in AD tumors. However, pol II was positioned primarily at the promoter (Fig. 5, top). This variation was in contrast to the general factor TFIIB, which was present at equal levels at the promoter in AD, ADc and AI in all experiments that we performed. One interpretation of these findings is that the transcription complex remains intact after androgen deprivation but a greater fraction of pol II is not actively transcribing in ADc versus AD and AI. A scatter plot summarizing four representative experiments is shown in Supplementary data.

Visualizing the AD-AI Transition. The original goal in developing the TSTA system was to monitor the loss and gain of AR-mediated transcription over time

in a single individual as a tumor transitioned from ADc to AI. In a human, the failure of androgen deprivation therapy occurs gradually over a period of time that can vary from weeks to years. The LAPC9 models were originally adapted to an androgen-rich environment in immunodeficient mice and then trained to grow in castrate or female mice. We have found that the transition time in our animals occurs more rapidly as the tumor grows larger. Typically we begin an experiment when a tumor reaches 0.5 cm but it grows to 1.5 cm within two or three weeks. Usually we have to sacrifice the animals before the transition occurs to adhere to the 1.5-cm tumor size limitation set by our institutional animal care guidelines. However, some individuals transition faster and in these we are able to monitor the transition in real time, as opposed to studying established AI tumors as we described above. The data in Fig. 6 illustrate a typical example of an animal that underwent the transition prior to sacrifice.

In this animal, we injected the AdTSTA virus, imaged the mice four days later, and then castrated the animal when the tumor reached 1 cm. We found that the PSA levels initially dropped 2.4-fold by day 10, six days post-castration, and then began rising again up to day 17, when we had to sacrifice the animal because the tumor had reached the size limit.

Over this same time frame, the imaging signal was high on day 4 reached a minimum by day 10 and then gradually rose again by day 17 (Fig. 6, top). ChIP and immunohistochemical analyses on the tumor from the day 21-sacrificed animal revealed that AR had resumed its predominantly nuclear location and was bound primarily to the PSA enhancer, while pol II was found predominantly in the

elongating state at exon 5 (Fig. 6, bottom). In short, we show an example, where AR has adapted to the androgen-deprived environment and resumed activity in the AI state as measured by imaging, immunohistochemistry and ChIP.

DISCUSSION

AR Function in Recurrent Cancer. The natural response of prostate cancer to DHT withdrawal is transition to the recurrent state. In man localized cancer can be treated surgically but metastasized cancers become refractory to androgen withdrawal and resume growth. The ability to recapitulate the transition to the recurrent state in xenograft models has provided a powerful tool for studying prostate tumor biology. The xenograft animals display the typical loss and then rise again in PSA levels upon castration. While PSA is an AR-regulated gene, there have been proposals that other transcription factors may substitute for AR or that AR may be activating genes by a non-genotropic mechanism.

Three observations argue for a direct restoration of AR function: First, we redesigned the PSA transcriptional regulatory region to dramatically increase its response to AR. The modified PSA regulatory region was then built into a TSTA cassette to amplify its potency for use in live animal imaging. The imaging signals in recurrent tumors strongly suggested that AR was fully active. Further we could monitor the transition of an AD tumor to a recurrent state in a single individual and visualize the loss and gain of AR activity during tumor progression. Second, immunohistochemistry on the xenograft tumors showed that AR localization became diffuse upon androgen withdrawal but became tightly localized to the nucleus in recurrent tumors consistent with its role in DNA binding and transactivation. Finally, AR bound directly to the regulatory region of the PSA gene of AD tumors as measured by ChIP. Although the bulk of AR dissociated

upon castration it rebound again in recurrent tumors. This last observation is particularly significant since direct AR binding to a prostate-expressed gene has not been shown yet in advanced cancers.

Molecular Imaging of Prostate Cancer. The TSTA imaging system is a powerful means to amplify weak cell specific promoters and monitor their activity in live animals. By cloning the PSA-based TSTA cassette into adenovirus we provided a tool to monitor AR function during tumor progression from the AD to recurrent state. The AdTSTA system was designed to be particularly sensitive to AR by manipulating the enhancer region, which binds multiple molecules of AR cooperatively. The system responded dynamically and sensitively to castration of tumor bearing mice. Typically imaging signals decreased more rapidly than PSA levels and the magnitude of the decrease was greater with the imaging system (10- to 20-fold) than PSA (2- to 3-fold). The short half-life of firefly luciferase (about 12 hours in the tumor) and the fact it is an intracellular protein may have contributed to the enhanced sensitivity of the imaging. PSA is a secreted protein that exists both in the cell and serum. PSA half-life and secretion rates are likely to respond variably to the tumor environment and may not provide an immediate measure of AR activity.

The TSTA system is versatile and modular. We have now completed cloning of shuttle vectors where the reporter gene can be replaced by any reporter (e.g., thymidine kinase, GFP or renilla luciferase) or therapeutic gene for imaging or gene therapy. Furthermore, although we chose the modified PSA enhancer in our studies the vector can accommodate any cell-specific or viral

promoter. Finally, the system is titratable. In our previous cell culture study, which used plasmids, we systematically varied both the number of VP16 activation domains attached to GAL4 or the number of GAL4 sites driving the reporter. We were able to achieve a range of activities that varied by 3 orders of magnitude. This variation should allow optimization of signal-to-noise ratios and amplification of weak promoters for any application. Additionally the vector is designed to replace the VP16 activation domain with other domains that may respond to signal transduction cascades. For example, we have successfully replaced VP16 with the activation domain of Elk-1 and shown that the system responds in a binary fashion to AR and signals emanating from the MAPK cascade.

On a technical note, we have some concerns about GAL4-VP16 and firefly luciferase toxicity. However, if toxicity was a significant issue we would predict that infected cells would die rapidly and the imaging signal would decay. However, under the conditions employed in our study we were able to obtain persistent imaging signals in tumors over the course of the experiments, which last up to a month. Also, the virus is not unusually toxic in cell culture studies, where cells appear to divide after virus infection. Our ability to employ low doses of virus in the animal studies may permit a less immunogenic response and enable us to transit the system into non-SCID prostate models as well as transgenic animals.

Mechanism of AR Activation. The mechanism by which AR is reactivated in tumors has been the subject of much research and is commented on in the Introduction. There are several interconnected issues. How does AR

localize to the nucleus in the presence of castrate amounts of ligand, and how does it bind DNA and function in this environment? Is AR modified to utilize at castrate levels of ligand?

AR overexpression, ligand binding domain mutations and MAPK signaling have all been proposed as possible mechanisms to facilitate AR translocation and activity. Overexpression of SRC-1 and –2 co-activators has also been observed in some prostate tumors and may facilitate AR function. We and others have made two observations that bear on this issue. First, the AR levels in our recurrent tumors, when normalized to β-tubulin using a human specific antibody, are not dramatically higher than those in AD tumors. We have also measured SRC-1, -2 and –3 levels and they vary less than a few-fold among LAPC9 cancers. Thus, the localization of AR to the nuclei of recurrent tumors is not due to AR or co-activator overexpression bypassing the normal cell trafficking checkpoints. Second, the AR in our LAPC9 tumors has been sequenced and does not contain mutations in the ligand binding domains, which might permit use of alternative ligands. Furthermore, circulating levels of DHT in the LAPC9 mice drop up to 85% immediately after castration and remain at castrate levels throughout tumor growth. If somehow the tumors were adapting to castration by hyperactivating pathways that convert adrenal androgen to DHT, we would have expected to see gradual increases in serum DHT over time. Finally, it is plausible that MAPK pathways are influencing AR translocation. We note that the particular tumor model we employ, LAPC9, has been shown to display elevated EGFR and MAPK signaling (31).

Transcription Complex Assembly by AR. The binding of AR to the PSA enhancer paralleled PSA levels, the imaging signal, and AR cellular localization. AR-enhancer binding decreased 4-fold in ADc but increased again in AI cancer. As mentioned previously, PSA levels do not disappear completely in ADc but transiently plateau or drop as the tumors adapt. This observation can explain why a subset of tumor cells from castrated animals still display AR nuclear localization and we still observe residual AR binding to the enhancer in the ChIP experiments.

Although our data do not illuminate the precise mechanism of AR reactivation they provide insight into how the AD-AI transition may be facilitated. The most intriguing result is that although castration causes 75% of AR to dissociate from the PSA enhancer the levels of bound TFIIB and pol II remain unchanged. Castration did, however, result in redistribution of pol II from exon 5 to the promoter. These observations suggest that transcription complexes do not disappear but remain poised to facilitate reactivation of AR-mediated transcription.

AR and pol II are known to cycle on and off the promoter during gene activation in LNCaP cells (15, 54). The peaks of AR and subsequent pol II binding after androgen addition do not coincide suggesting that AR can leave while pol II is engaging the promoter. Analysis of genes such as α1-AT have also established that pol II can be bound with the GTFs in a quiescent state, prior to binding of activator (55). These data along with older studies of the heat shock locus in drosophila (56) indicate that a pre-poised pol II may provide a

mechanism for maintaining promoter accessibility during a transcriptionally inactive state. In addition, mutations in forkhead transcription factors in yeast cause redistribution of pol II to the promoter (57). It is plausible that the poised complexes may be sensitive to lower levels of functional AR thereby allowing activation in the absence of physiological levels of DHT. We are currently pursuing the mechanism of this effect.

ACKNOWLEDGEMENTS

We thank Erika Billick for technical assistance during the early stages of the study and Charles Sawyers and his lab for helpful discussions.

REFERENCES

1. Gelmann, E. P. Molecular biology of the androgen receptor. J Clin Oncol, *20:* 3001-3015, 2002.
2. Freedman, L. P. Increasing the complexity of coactivation in nuclear receptor signaling. Cell, *97:* 5-8, 1999.
3. Waller, A. S., Sharrard, R. M., Berthon, P., and Maitland, N. J. Androgen receptor localisation and turnover in human prostate epithelium treated with the antiandrogen, casodex. J Mol Endocrinol, *24:* 339-251, 2000.
4. Tyagi, R. K., Lavrovsky, Y., Ahn, S. C., Song, C. S., Chatterjee, B., and Roy, A. K. Dynamics of intracellular movement and nucleocytoplasmic recycling of the ligand-activated androgen receptor in living cells. Mol Endocrinol, *14:* 1162-1174, 2000.
5. Bok, R. A. and Small, E. J. Bloodborne biomolecular markers in prostate cancer development and progression. Nat Rev Cancer, *2:* 918-926, 2002.
6. Pang, S., Taneja, S., Dardashti, K., Cohan, P., Kaboo, R., Sokoloff, M., Tso, C. L., Dekernion, J. B., and Belldegrun, A. S. Prostate tissue

specificity of the prostate-specific antigen promoter isolated from a patient with prostate cancer. Hum Gene Ther, *6:* 1417-1426, 1995

7. Pang, S., Dannull, J., Kaboo, R., Xie, Y., Tso, C. L., Michel, K., deKernion, J. B., and Belldegrun, A. S. Identification of a positive regulatory element responsible for tissue- specific expression of prostate-specific antigen. Cancer Res, *57:* 495-499, 1997.

8. Schuur, E. R., Henderson, G. A., Kmetec, L. A., Miller, J. D., Lamparski, H. G., and Henderson, D. R. Prostate-specific antigen expression is regulated by an upstream enhancer. J Biol Chem, *271:* 7043-7051, 1996.

9. Cleutjens, K. B., van Eekelen, C. C., van der Korput, H. A., Brinkman, A. O., and Trapman, J. Two androgen response regions cooperate in steroid hormone regulated activity of the prostate-specfic antigen promoter. J Biol Chem, *271:* 6379-6388, 1996.

10. Cleutjens, K. B., van der Korput, H. A., van Eekelen, C. C., van Rooij, H. C., Faber, P. W., and Trapman, J. An androgen response element in a far upstream enhancer region is essential for high, androgen-regulated activity of the prostate-specific antigen promoter. Mol Endocrinol, *11:* 148-161, 1997.

11. Cleutjens, K. B., van der Korput, H. A., Ehren-van Eekelen, C. C., Sikes, R. A., Fasciana, C., Chung, L. W., and Trapman, J. A 6-kb promoter fragment mimics in transgenic mice the prostate-specific and androgen-regulated expression of the endogenous prostate-specific antigen gene in humans. Mol Endocrinol, *11:* 1256-1265, 1997.

12. Zhang, S., Murtha, P. E., and Young, C. Y. Defining a functional androgen responsive element in the 5' far upstream flanking region of the prostate-specific antigen gene. Biochem Biophys Res Commun, *231:* 784-788, 1997.

13. Huang, W., Shostak, Y., Tarr, P., Sawyers, C., and Carey, M. Cooperative assembly of androgen receptor into a nucleoprotein complex that regulates the prostate-specific antigen enhancer. J Biol Chem, *274:* 25756-25768, 1999.

14. Reid, K. J., Hendy, S. C., Saito, J., Sorensen, P., and Nelson, C. C. Two classes of androgen receptor elements mediate cooperativity through allosteric interactions. J Biol Chem, *276:* 2943-2952, 2001.

15. Kang, Z., Pirskanen, A., Janne, O. A., and Palvimo, J. J. Involvement of proteasome in the dynamic assembly of the androgen receptor transcription complex. J Biol Chem, *277:* 48366-48371, 2002.

16. Louie, M. C., Yang, H. Q., Ma, A. H., Xu, W., Zou, J. X., Kung, H. J., and Chen, H. W. Androgen-induced recruitment of RNA polymerase II to a nuclear receptor-p160 coactivator complex. Proc Natl Acad Sci U S A, *100:* 2226-2230, 2003.

17. Shang, Y., Hu, X., DiRenzo, J., Lazar, M. A., and Brown, M. Cofactor dynamics and sufficiency in estrogen receptor-regulated transcription. Cell, *103:* 843-852, 2000.

18. Lee, C. T. and Oesterling, J. E. Diagnostic markers of prostate cancer: utility of prostate-specific antigen in diagnosis and staging. Semin Surg Oncol, *11:* 23-35, 1995.

19. Abate-Shen, C. and Shen, M. M. Molecular genetics of prostate cancer. Genes Dev, *14:* 2410-2434, 2000.

20. Arnold, J. T. and Isaacs, J. T. Mechanisms involved in the progression of androgen-independent prostate cancers: it is not only the cancer cell's fault. Endocr Relat Cancer, *9:* 61-73, 2002.

21. Feldman, B. J. and Feldman, D. The development of androgen-independent prostate cancer. Nat Rev Cancer, *1:* 34-45, 2001.

22. Gregory, C. W., Johnson, R. T., Jr., Mohler, J. L., French, F. S., and Wilson, E. M. Androgen receptor stabilization in recurrent prostate cancer is associated with hypersensitivity to low androgen. Cancer Res, *61:* 2892-2898, 2001.

23. Visakorpi, T., Hyytinen, E., Koivisto, P., Tanner, M., Keinanen, R., Palmberg, C., Palotie, A., Tammela, T., Isola, J., and Kallioniemi, O. P. In vivo amplification of the androgen receptor gene and progression of human prostate cancer. Nat Genet, *9:* 401-406, 1995.

24. Stanbrough, M., Leav, I., Kwan, P. W., Bubley, G. J., and Balk, S. P. Prostatic intraepithelial neoplasia in mice expressing an androgen receptor transgene in prostate epithelium. Proc Natl Acad Sci U S A, *98:* 10823-10828, 2001.

25. Gregory, C. W., He, B., Johnson, R. T., Ford, O. H., Mohler, J. L., French, F. S., and Wilson, E. M. A mechanism for androgen receptor-mediated prostate cancer recurrence after androgen deprivation therapy. Cancer Res, *61:* 4315-4319, 2001.

26. Han, G., Foster, B. A., Mistry, S., Buchanan, G., Harris, J. M., Tilley, W. D., and Greenberg, N. M. Hormone status selects for spontaneous somatic androgen receptor variants that demonstrate specific ligand and cofactor dependent activities in autochthonous prostate cancer. J Biol Chem, *276:* 11204-11213, 2001.

27. Grossmann, M. E., Huang, H., and Tindall, D. J. Androgen receptor signaling in androgen-refractory prostate cancer. J Natl Cancer Inst, *93:* 1687-1697, 2001.

28. Craft, N. and Sawyers, C. L. Mechanistic concepts in androgen-dependence of prostate cancer. Cancer Metastasis Rev, *17:* 421-427, 1998.

29. Elo, J. P. and Visakorpi, T. Molecular genetics of prostate cancer. Ann Med, *33:* 130-141, 2001.

30. Gioeli, D., Mandell, J. W., Petroni, G. R., Frierson, H. F., Jr., and Weber, M. J. Activation of mitogen-activated protein kinase associated with prostate cancer progression. Cancer Res, *59:* 279-284, 1999.

31. Mellinghoff, I. K., Tran, C., and Sawyers, C. L. Growth Inhibitory Effects of the Dual ErbB1/ErbB2 Tyrosine Kinase Inhibitor PKI-166 on Human Prostate Cancer Xenografts. Cancer Res, *62:* 5254-5259, 2002.

32. Zegarra-Moro, O. L., Schmidt, L. J., Huang, H., and Tindall, D. J. Disruption of androgen receptor function inhibits proliferation of androgen-refractory prostate cancer cells. Cancer Res, *62:* 1008-1013, 2002.

33. Kousteni, S., Bellido, T., Plotkin, L. I., O'Brien, C. A., Bodenner, D. L., Han, L., Han, K., DiGregorio, G. B., Katzenellenbogen, J. A., Katzenellenbogen, B. S., Roberson, P. K., Weinstein, R. S., Jilka, R. L., and Manolagas, S. C. Nongenotropic, sex-nonspecific signaling through the estrogen or androgen receptors: dissociation from transcriptional activity. Cell, *104:* 719-730, 2001.

34. Peterziel, H., Mink, S., Schonert, A., Becker, M., Klocker, H., and Cato, A. C. Rapid signalling by androgen receptor in prostate cancer cells. Oncogene, *18:* 6322-6329, 1999.

35. Yeung, F., Li, X., Ellett, J., Trapman, J., Kao, C., and Chung, L. W. Regions of prostate-specific antigen (PSA) promoter confer androgen-independent expression of PSA in prostate cancer cells. J Biol Chem, *275:* 40846-40855, 2000.

36. Klein, K. A., Reiter, R. E., Redula, J., Moradi, H., Zhu, X. L., Brothman, A. R., Lamb, D. J., Marcelli, M., Belldegrun, A., Witte, O. N., and Sawyers, C. L. Progression of metastatic human prostate cancer to androgen independence in immunodeficient SCID mice. Nat Med, *3:* 402-408, 1997.

37. Contag, C. H., Jenkins, D., Contag, P. R., and Negrin, R. S. Use of reporter genes for optical measurements of neoplastic disease in vivo. Neoplasia, *2:* 41-52, 2000.

38. Contag, P. R. Whole-animal cellular and molecular imaging to accelerate drug development Drug Discov Today, *7:* 555-562. 2002.

39. Herschman, H. R., MacLaren, D. C., Iyer, M., Namavari, M., Bobinski, K., Green, L. A., Wu, L., Berk, A. J., Toyokuni, T., Barrio, J. R., Cherry, S. R., Phelps, M. E., Sandgren, E. P., and Gambhir, S. S. Seeing is believing: non-invasive, quantitative and repetitive imaging of reporter gene expression in living animals, using positron emission tomography. J Neurosci Res, *59:* 699-705, 2000.

40. Massoud, T. and Gambhir, S. S. Molecular imaging in living subjects: Seeing fundamental biological processes in a new light. Genes & Development, *in press:* 2003.

41. O'Connell-Rodwell, C. E., Burns, S. M., Bachmann, M. H., and Contag, C. H. Bioluminescent indicators for in vivo measurements of gene expression. Trends Biotechnol, *20:* S19-S23, 2002.

42. Wu, J. C., Sundaresan, G., Iyer, M., and Gambhir, S. S. Noninvasive optical imaging of firefly luciferase reporter gene expression in skeletal muscles of living mice. Mol Ther, *4:* 297-306, 2001.

43. Cleutjens, K. B., van Eekelen, C. C., van der Korput, H. A., Brinkmann, A. O., and Trapman, J. Two androgen response regions cooperate in steroid hormone regulated activity of the prostate-specific antigen promoter. J Biol Chem, *271:* 6379-6388, 1996.

44. Wu, L., Matherly, J., Smallwood, A., Adams, J. Y., Billick, E., Belldegrun, A., and Carey, M. Chimeric PSA enhancers exhibit augmented activity in prostate cancer gene therapy vectors. Gene Ther, *8:* 1416-1426, 2001.

45. Adams, J. Y., Johnson, M., Sato, M., Berger, F., Gambhir, S. S., Carey, M., Iruela-Arispe, M. L., and Wu, L. Visualization of advanced human prostate cancer lesions in living mice by a targeted gene transfer vector and optical imaging. Nat Med, *8:* 891-897, 2002.

46. Iyer, M., Wu, L., Carey, M., Wang, Y., Smallwood, A., and Gambhir, S. S. Two-step transcriptional amplification as a method for imaging reporter gene expression using weak promoters. Proc. Natl. Acad. Sci. U S A, *98:* 14595-14600, 2001.

47. Zhang, L., Adams, J. Y., Billick, E., Ilagan, R., Iyer, M., Le, K., Smallwood, A., Gambhir, S. S., Carey, M., and Wu, L. Molecular engineering of a two-step transcription amplification (TSTA) system for transgene delivery in prostate cancer. Mol Ther, *5:* 223-232, 2002.

48. He, T. C., Zhou, S., da Costa, L. T., Yu, J., Kinzler, K. W., and Vogelstein, B. A simplified system for generating recombinant adenoviruses. Proc Natl Acad Sci U S A, *95:* 2509-2514, 1998.

49. Pfeifer, A. and Verma, I. M. Gene therapy: promises and problems. Annu Rev Genomics Hum Genet, *2:* 177-211, 2001.

50. Horoszewicz, J. S., Leong, S. S., Kawinski, E., Karr, J. P., Rosenthal, H., Chu, T. M., Mirand, E. A., and Murphy, G. P. LNCaP model of human prostatic carcinoma. Cancer Res, *43:* 1809-1818, 1983.

51. Tilley, W. D., Wilson, C. M., Marcelli, M., and McPhaul, M. J. Androgen receptor gene expression in human prostate carcinoma cell lines. Cancer Res, *50:* 5382-5386, 1990.

52. Montgomery, B. T., Young, C. Y., Bilhartz, D. L., Andrews, P. E., Prescott, J. L., Thompson, N. F., and Tindall, D. J. Hormonal regulation of prostate-specific antigen (PSA) glycoprotein in the human prostatic adenocarcinoma cell line, LNCaP. Prostate, *21:* 63-73, 1992.

53. Chen, C. D. and Sawyers, C. L. NF-kappa B activates prostate-specific antigen expression and is upregulated in androgen-independent prostate cancer. Mol Cell Biol, *22:* 2862-2870, 2002.

54. Shang, Y., Myers, M., and Brown, M. Formation of the androgen receptor transcription complex. Mol Cell, *9:* 601-610, 2002.

55. Cosma, M. Ordered recruitment: Gene-specific mechanism of transcription activation. Mol Cell, *10:* 227-236, 2002.

56. Gilmour, D. S. and Lis, J. T. RNA polymerase II interacts with the promoter region of the noninduced hsp70 gene in Drosophila melanogaster cells. Mol Cell Biol, *6:* 3984-3989, 1986.

57. Morillon, A., O'Sullivan, J., Azad, A., Proudfoot, N., and Mellor, J. Regulation of Elongating RNA Polymerase II by Forkhead Transcription Factors in Yeast. Science, *300:* 492-495, 2003.

FIGURE LEGENDS

Fig. 1. Validation of the molecular imaging system in cell culture. In *A,* is a schematic of the adenovirus two-step transcription activation (AdTSTA) imaging system. The upper portion of the diagram shows the TSTA imaging cassette. The PSA enhancer from –4326 to –3935 was duplicated (the chimeric enhancer core) within the upstream regulatory region from -5322 to –3744 and attached to the proximal promoter from -541 to 1. Each enhancer bears a cluster of six AREs and the promoter contains two AREs. The PSA regulatory region is shown expressing GAL4-VP2 bearing two amino-terminal Herpes Simplex Virus 1 VP16 activation domains (amino acids 413-454) fused to the GAL4 DNA binding domain (amino acids 1-147). A GAL4-responsive promoter is fused in the divergent orientation to the PSA regulatory region. The GAL4-responsive promoter contains five 17-bp GAL4 sites upstream of the adenovirus E4 promoter driving firefly luciferase. The entire cassette was cloned into a shuttle vector and introduced into Ad5 deleted (Δ) for E1 and E3 using the AdEasy™ system. The virus was propagated in 293 cells, purified and titered. In *B* is a demonstration of AdTSTA activity in cancer cell lines. LNCaP cells were infected with AdTSTA at an MOI of 10 for 1 hour and treated with 10 nM R1881 (+Ligand) or vehicle (-Ligand). At the indicated time points, the cells were lysed with Reporter Lysis Buffer and firefly luciferase activity was analyzed either by luminometry (*lower panel*, Y-axis: Relative Luciferase Units/μg of total protein

normalized to 100%) or by immunoblotting (*Upper panel*, AR: Anti-Androgen Receptor; Tub: Anti-Tubulin; GAL4: anti-GAL4-VP16). Samples were prepared in triplicate and the average reading with standard error is shown. The triplicate samples were mixed for immunoblot analysis. *C.* LNCaP, HeLa or HepG cells were infected with AdTSTA at an MOI of 0.1 for 1 hour followed by treatment with 10nM R1881. The cells were harvested 48 hours later and luciferase levels were measured. Data are normalized to the ligand-induced signal in LNCaP (100%). The AdCMV (MOI 0.1) signal in LNCaP is shown in hatched bars for comparison of the AdTSTA and AdCMV luciferase activity.

Fig. 2. Serum PSA measurements for AD and castrated mice. Serum Elisa measurements of PSA at various time points during tumor growth. Values are in ng per ml.

Fig. 3. AR signaling in LAPC 9 tumors. In *A* SCID mice implanted with LAPC9 xenografts (>0.5 cm) were injected with 10^7 pfu of AdTSTA and the mice were imaged every 3-4 days until day 14. Representative mice at day 4 and day 10 post virus injection from the AD group, the castrated (on day 4) AD group (ADc), and the stable AI group. The bar graph summarizes a cohort of three or more and summarizes the log of the % change in signal from day 4 (blue bars) to day 10 (purple bars). Day 4 is set at 2 (log 10) in each case. *B* shows representative immunohistochemical localization of AR in the various tumors using anti-AR

antibodies. AR stains brown against the blue-stained nuclei. For both AD and AI tumors, five high power fields (40X) from multiple sample slides were counted, with an average of 100 cells per field. AR nuclear staining was recorded as percentage of cells counted. For AD tumors, cells with high AR nuclear staining are 33% (+/-5%) while cells with no or very faint AR nuclear staining is 19% (+/-6%) with the remainder staining at an intermediate intensity. For AI tumors, 30% (+/-2.7%) of the cells stained intensely while cells with no or very faint AR nuclear staining was 22% (+/- 3%). In conclusion AR nuclear staining does not differ significantly between AD and AI tumors (p=0.3 one tail and 0.7 two tail).

Fig. 4. Chromatin immunoprecipitation assays in LAPC9 tumors. The diagram describes the PSA regulatory region. Short black line underneath indicates the positions targeted by PCR. Enh: enhancer core; Mid: intermediate region; Pro: proximal promoter; Ex5: PSA exon 5 (for sequence coordinates see Methods). Tumors were isolated from mice sacrificed at day 10 (6 days post castration for ADc), minced, crosslinked with formaldehyde and immunoprecipitated with anti-AR. An autoradiograph of the multiplex PCR reactions is shown for AD, AI and ADc tumors. Graph of Multiple Tumor ChIP Analyses. The band intensities were analyzed using ImageQuant. Background values from a mock (IgG) ChIP were subtracted from each band and normalized to the signal from onput DNA. Error bars shown are standard deviation of three values obtained in independent experiments.

Fig. 5. ChIP analysis of RNA Polymerase II and TFIIB from LAPC9 tumors. The bands are described in the Figure 6 legend. Representative experiments from AD, AI and ADc tumors are shown. The *top panels* are pol II and the *bottom panels* are TFIIB.

Fig. 6. Dynamic AR signaling. A SCID mouse bearing an LAPC9 AD tumor was injected with AdTSTA, imaged and castrated. The *upper panel* shows the entire time course with signals adjusted to the same color scale. Imaging measurements and PSA levels determined by Serum ELISA are shown below the images. *Lower left panel*: the tumors were extracted and subjected to immunohistological staining with AR antibodies. *Lower right panel*: a ChIP assay of the extracted tumors with IgG, AR and pol II antibodies.

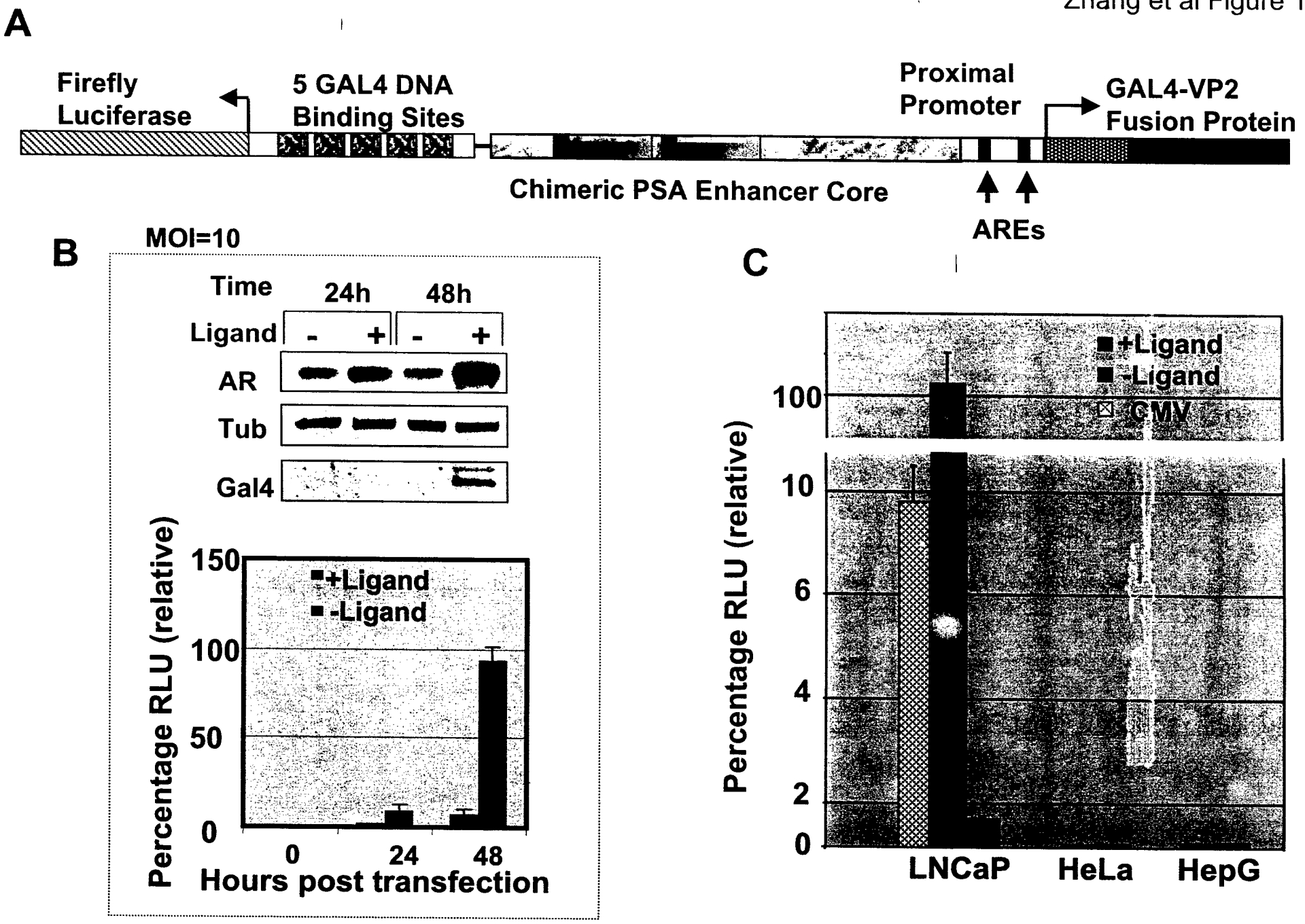
A
Firefly Luciferase
5 GAL4 DNA Binding Sites
Proximal Promoter
GAL4-VP2 Fusion Protein
Chimeric PSA Enhancer Core
AREs
B
MOI=10
Time
24h
48h
Ligand
-
+
-
+
AR
Tub
Gal4
Percentage RLU (relative)
150
100
50
0
+Ligand
-Ligand
0
24
48
Hours post transfection
C
Percentage RLU (relative)
100
10
6
4
2
0
+Ligand
-Ligand
CMV
LNCaP
HeLa
HepG

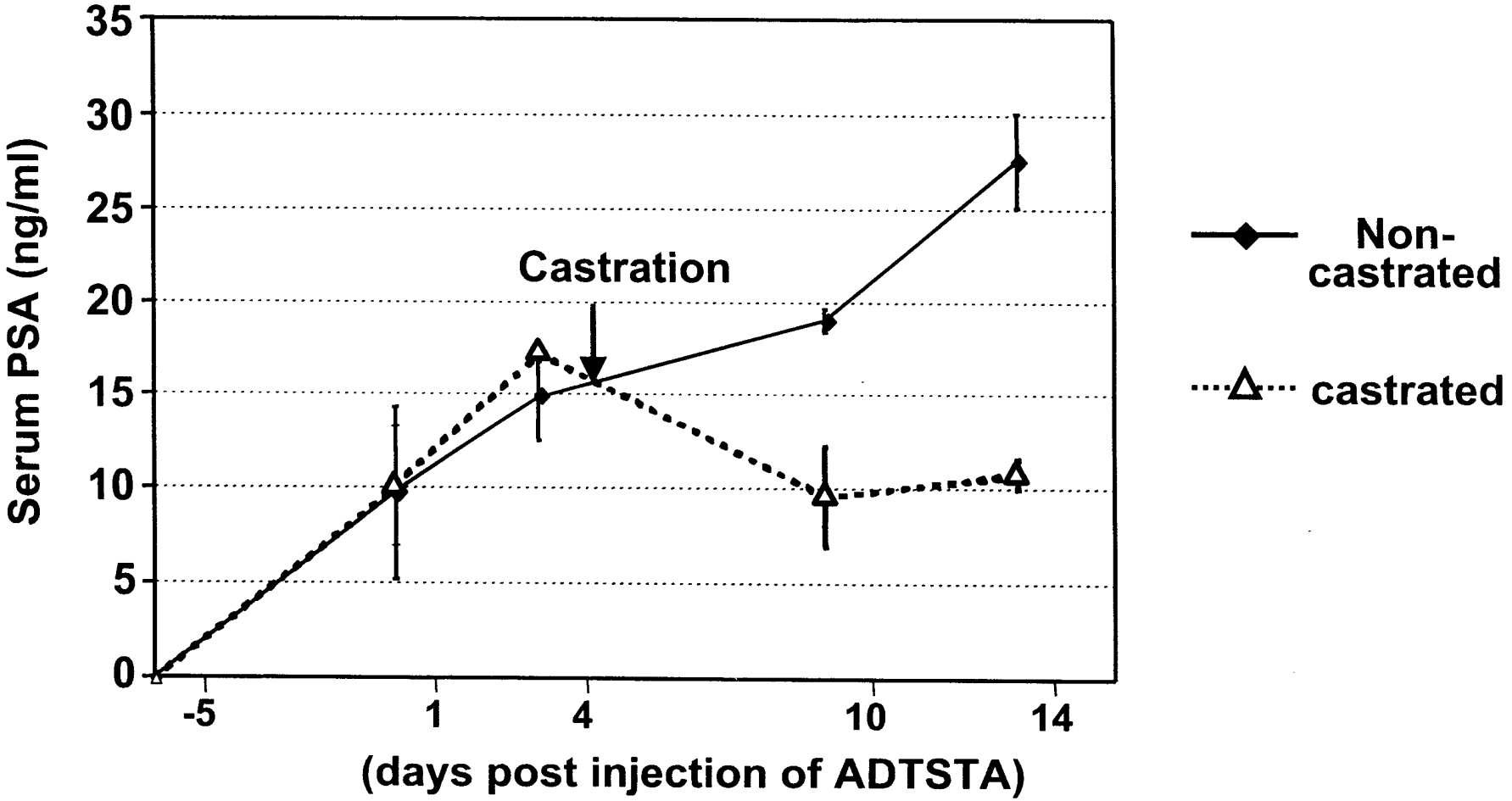
35
30
25
20
15
10
5
0
Serum PSA (ng/ml)
Castration
-5
1
4
10
14
(days post injection of ADTSTA)
Non-castrated
castrated

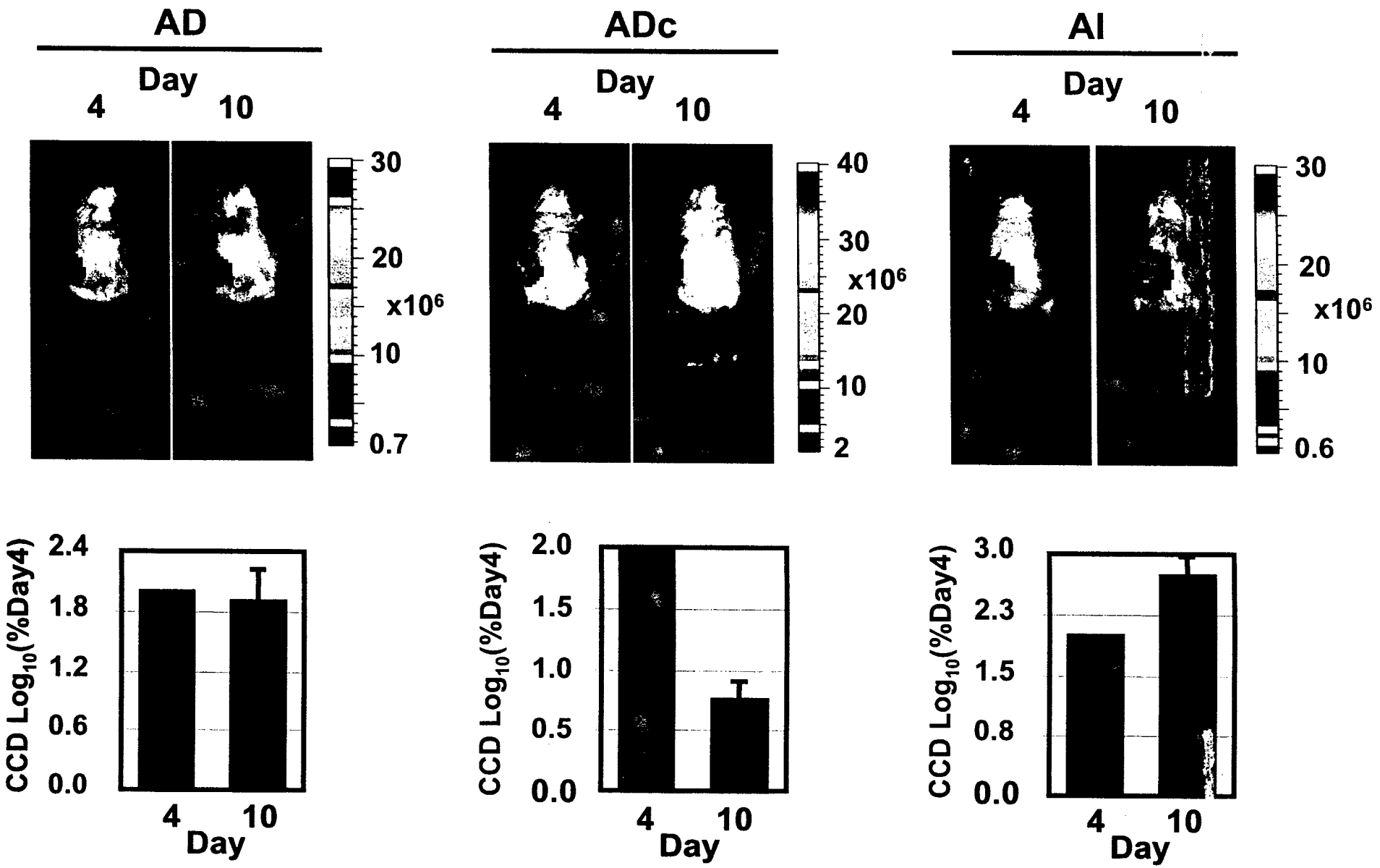
AD
Day
4
10
30
20
x10⁶
10
0.7
ADc
Day
4
10
40
30
x10⁶
20
10
2
AI
Day
4
10
30
20
x10⁶
10
0.6
CCD Log10(%Day4)
2.4
1.8
1.2
0.6
0.0
4
10
Day
CCD Log10(%Day4)
2.0
1.5
1.0
0.5
0.0
4
10
Day
CCD Log10(%Day4)
3.0
2.3
1.5
0.8
0.0
4
10
Day

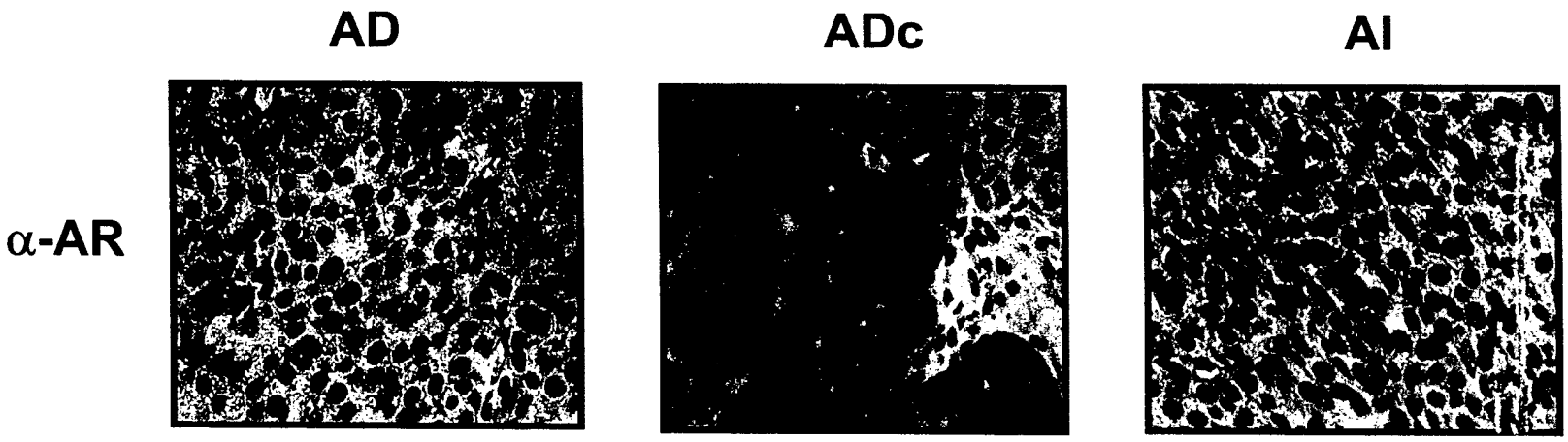
AD
ADc
AI
α-AR

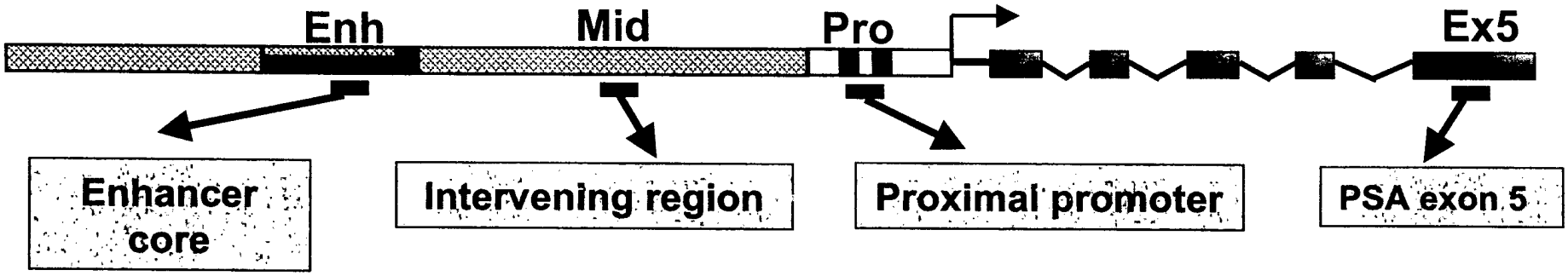
Enh
Mid
Pro
Ex5
Enhancer core
Intervening region
Proximal promoter
PSA exon 5

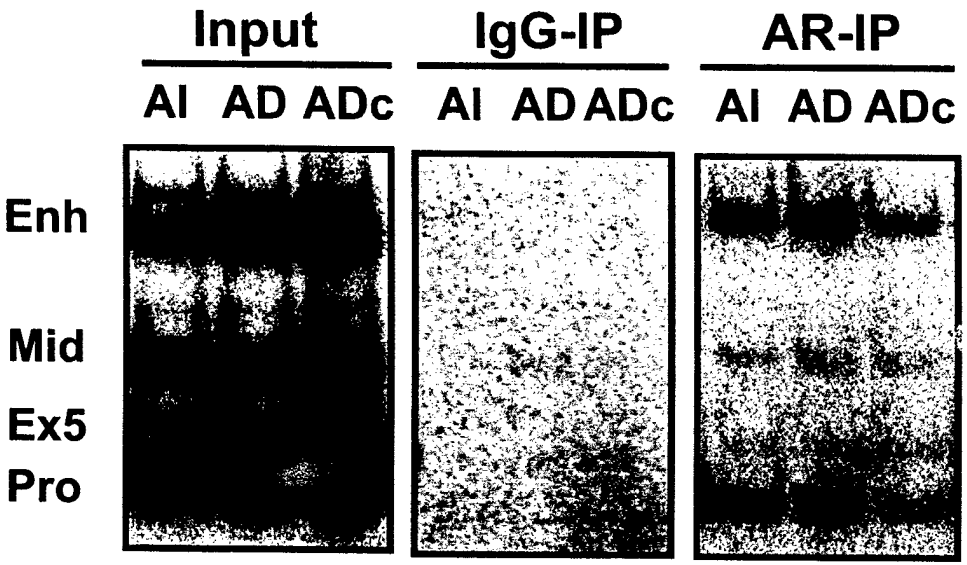
Input
IgG-IP
AR-IP
AI AD ADc
AI AD ADc
AI AD ADc
Enh
Mid
Ex5
Pro

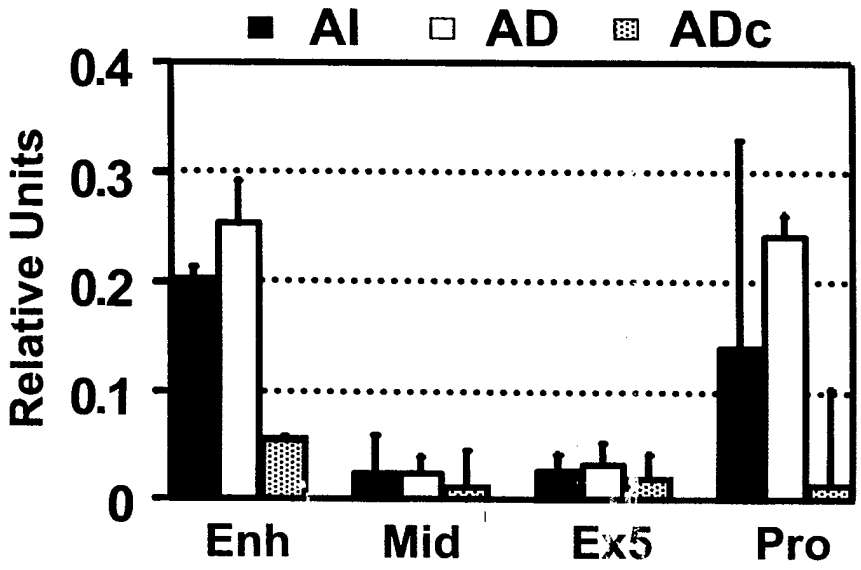
AI
AD
ADc
Relative Units
0.4
0.3
0.2
0.1
0
Enh
Mid
Ex5
Pro

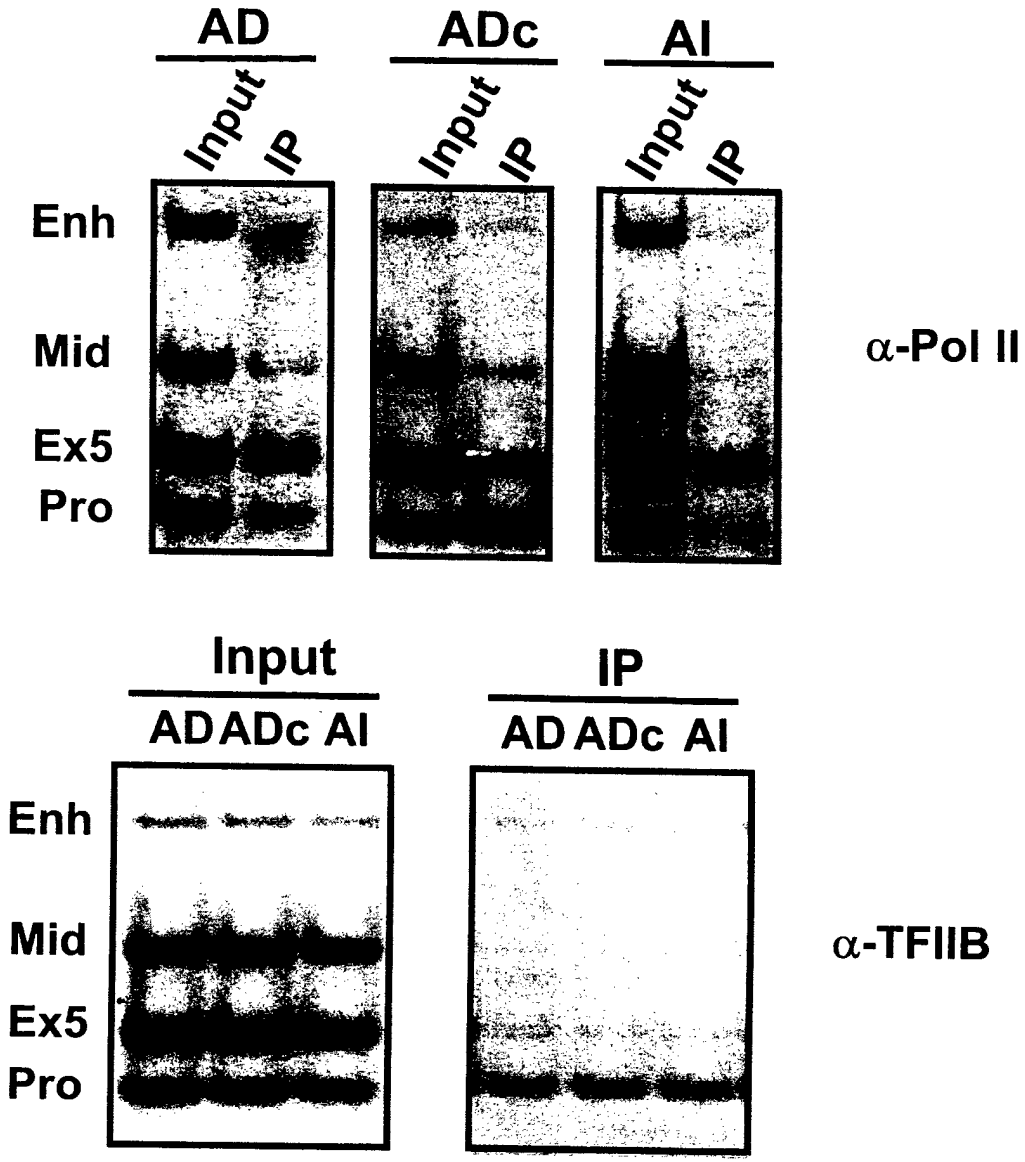
AD
ADc
AI
Input
IP
Input
IP
Input
IP
Enh
Mid
Ex5
Pro
α-Pol II
Input
IP
AD ADc AI
AD ADc AI
Enh
Mid
Ex5
Pro
α-TFIIB

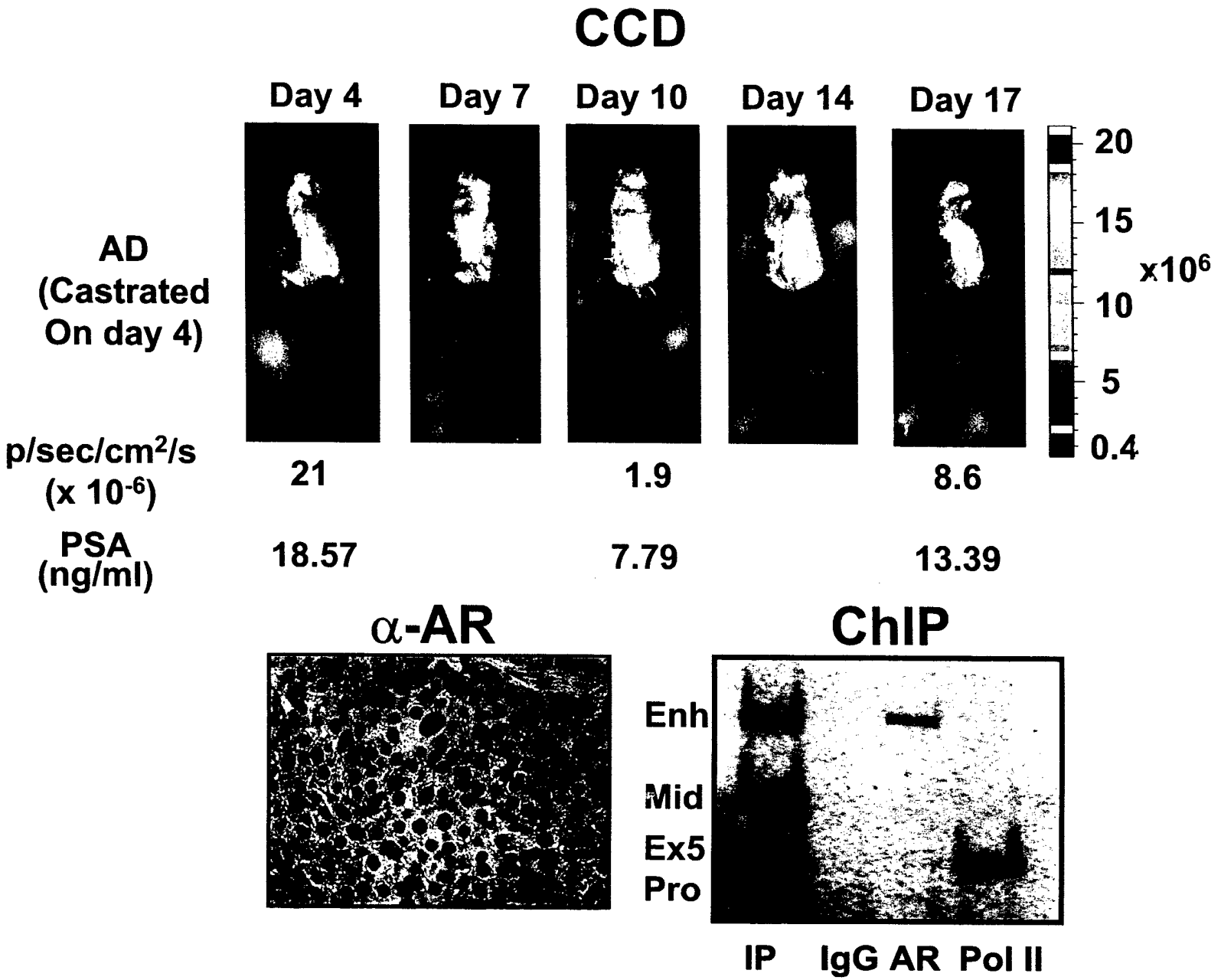
CCD
Day 4
Day 7
Day 10
Day 14
Day 17
20
15
10
5
0.4
x10^6
AD
(Castrated
On day 4)
p/sec/cm²/s
(x 10⁻⁶)
21
1.9
8.6
PSA
(ng/ml)
18.57
7.79
13.39
α-AR
ChIP
Enh
Mid
Ex5
Pro
IP
IgG
AR
Pol II

Supplementary Figure 1 Protein expression in LAPC9 tumors

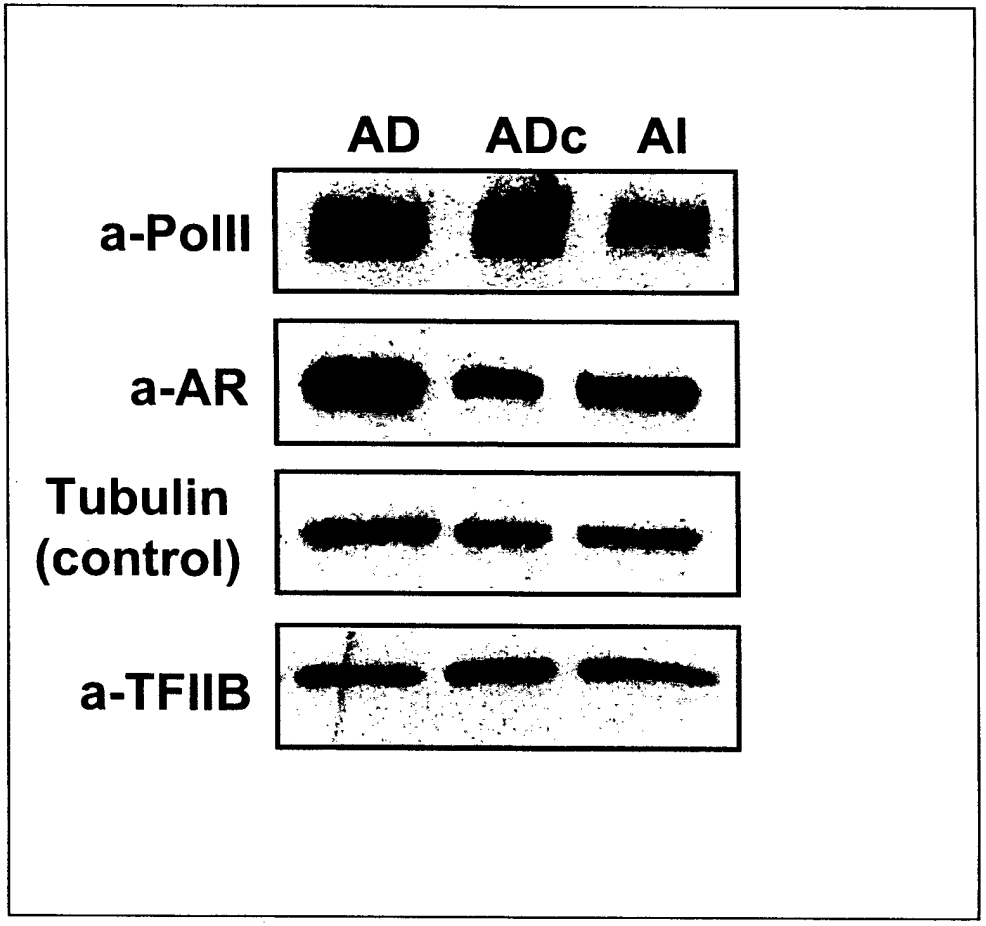

Supplementary Figure 2: AdTSTA specificity in vivo

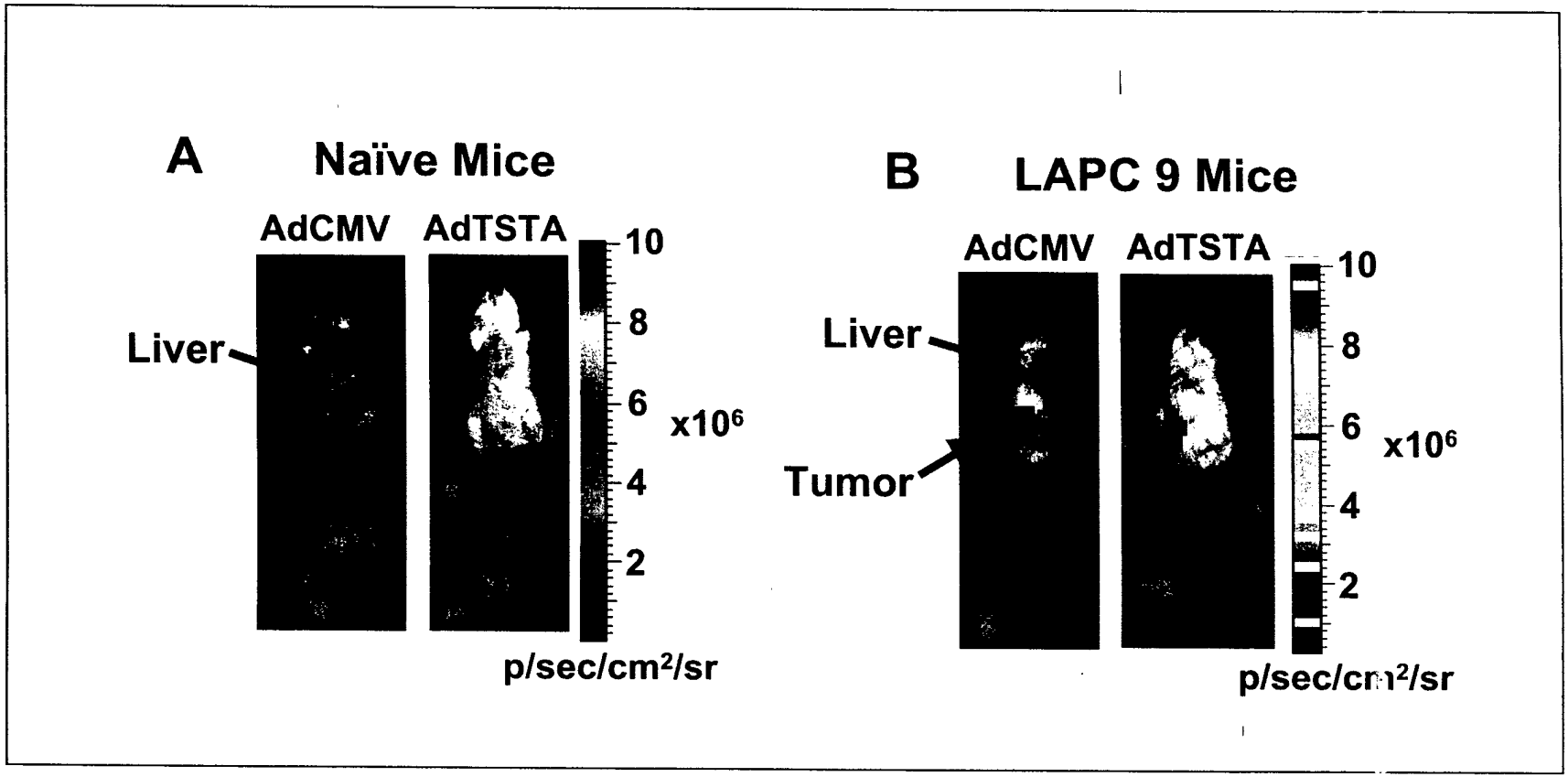

Supplementary Figure 3: Binding preference of PolII

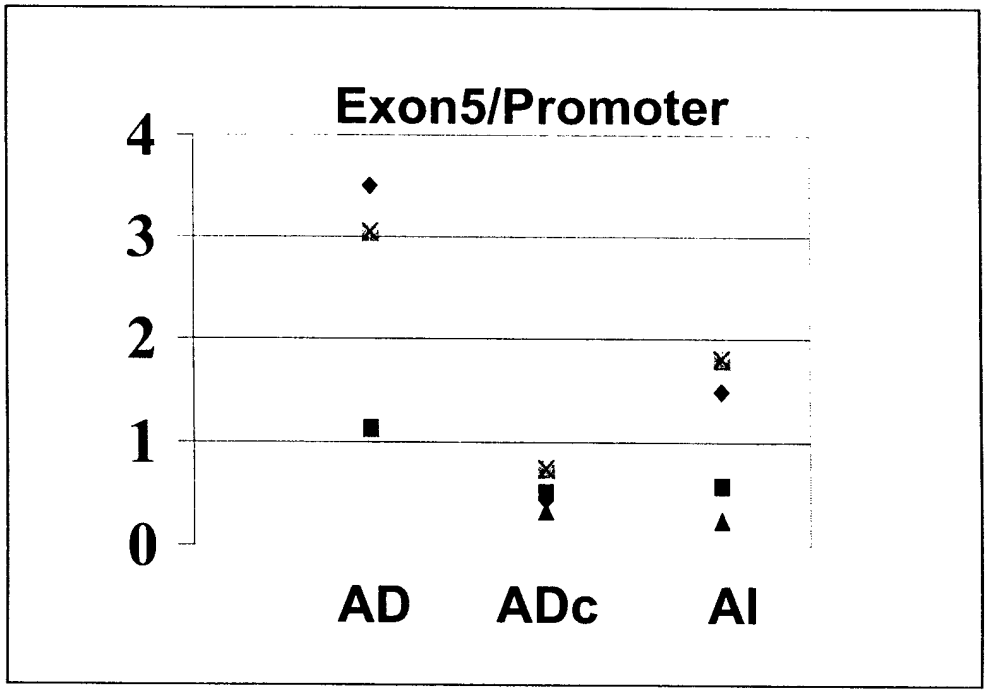

Figure Legend

Supplementary Figure 1 Protein expression in LAPC9 tumors

Androgen dependant (AD), castrated (ADc) or androgen independent/recurrent (AI) LAPC9 xenografts were harvested, homogenized and lysed with RIPA lysis buffer (10mM Tris-HCl, 150mM NaCl, 0.1% SDS, 1% DOC, 1mM EDTA and 1% NP40). The samples were fractionated on 4-15% gradient acrylamide gels (Bio-Rad) and subjected to immunoblot analysis with specific antibodies listed in the figure. Samples are normalized by measuring protein concentration and confirmed by blotting tubulin. Only proteins discussed in the paper are shown.

Supplementary Figure 2: AdTSTA specificity in vivo

Upper panel: 10^7 pfu of AdCMV or AdTSTA virus were injected through the tail vein into 3-month old male SCID mice and imaged by CCD. The pictures show a representative mouse in the supine position injected with AdCMV or AdTSTA on day 14. Lower panel: LAPC9 AD xenografts were grown on the flanks of SCID mice. When tumors reached 0.5 cm diameter tumor size, AdCMV or AdTSTA were injected intratumorally and imaged by CCD. The picture shows representative mice in the prone position on day 14. For all studies, $n \geq 3$ animals were used in each group. For each mouse, a pseudocolor image of the emitted light is superimposed over a gray scale photograph of the mouse. A colored bar, which indicates the intensity of the signals, is shown on the right of the panels, with units of photons (p) acquired per second (sec) per cm^2 per steridian (sr).

Supplementary Figure 3: Binding preference of PolII

Four individual ChIP experiments with PolII antibody were analyzed by ImageQuant (Amersham Bioscience) and ratios of polII binding at exon 5 vs. the proximal promoter are plotted.

BEYOND CARRIER PROTEINS

Nuclear effects: unexpected intracellular actions of insulin-like growth factor binding protein-3

K-W Lee and **P Cohen**

Division of Pediatric Endocrinology, Mattel Children's Hospital at UCLA, David Geffen School of Medicine at UCLA, 10833 Le Conte Avenue, MDCC 22-315, Los Angeles, California 90095-1752, USA

(Requests for offprints should be addressed to P Cohen; Email: hassy@mednet.ucla.edu)

Abstract

Insulin-like growth factor (IGF) binding protein (IGFBP)-3 has been shown to be a growth inhibitory, apoptosis-inducing molecule by virtue of its ability to bind IGFs, in addition to previously demonstrated IGF-independent effects. The recent discovery of the interaction between nuclear IGFBP-3 and 9-*cis* retinoic acid receptor-α (retinoid X receptor α RXRα), a nuclear receptor, and its involvement in the regulation of transcriptional signaling and apoptosis represents an important paradigm shift in the understanding of IGFBP function. RXRα is required for the apoptosis-inducing effects of IGFBP-3. IGFBP-3 and RXR ligands are additive in inducing apoptosis in cancer cells. IGFBP-3 has direct effects on gene transcription, as RXR response element reporter signaling was enhanced and the all-*trans* retinoic acid receptor response element reporter signaling was inhibited. Accumulating evidence further confirms IGF-independent functions of this multifunction binding protein. Other binding proteins, in addition to other members of the IGF axis, have now been described in the nucleus and are postulated to have effects on transcriptional events. Investigation into these new interactions will expose new protein partners in the interface between the nuclear receptor and growth factor pathways and reveal new targets to be exploited in the treatment of cancer and other diseases.

Journal of Endocrinology (2002) **175**, 33–40

Introduction

The growth-promoting and metabolic activities of the insulin-like growth factors (IGFs)-I and -II are modulated by a family of six high-affinity IGF-binding proteins (IGFBPs) and two IGF receptors (IGF-IR and IGF-IIR), most of the biological functions of the IGFs being mediated via the type-I receptor (LeRoith 1996, Wetterau *et al.* 1999). The actions of IGFs may be modulated by the IGFBPs in either a positive or a negative way, depending on tissue type and physiological/pathological status (Rajaram *et al.* 1997).

The majority of IGFs-I and -II in serum are found in a 150 kDa ternary complex formed by an IGF, IGFBP-3/IGFBP-5, and a glycoprotein known as the acid-labile subunit (ALS) (Baxter 1994). This ternary complex increases the half-life of IGF-I or IGFBP-3 an order of magnitude over those of the free forms (Hasegawa *et al.* 1995). Most tissue IGFs are bound to IGFBPs as binary complexes, leaving only small amounts of local free IGF. The liver produces most of the circulating IGFs, although physiologically important autocrine and paracrine production occurs within other tissues (Cohen & Rosenfeld 1995).

The first five IGFBPs demonstrate high affinity for both IGFs-I and -II, share at least 50% homology among themselves, and share 80% homology between different species (Lamson *et al.* 1991, Shimasaki & Ling 1991). Homology is most conserved at the amino (N)- and carboxy (C)-terminal regions, which are involved in IGF binding (Bramani *et al.* 1999, Imai *et al.* 2000, Song *et al.* 2000). IGFBP-6 has 100-fold greater affinity for IGF-II than for IGF-I (Baxter & Saunders 1992). Recent experiments in neuroblastoma (Grellier *et al.* 2002), colon cancer (Kim *et al.* 2002), and rhabdomyosarcoma (Gallicchio *et al.* 2001) cells suggest that growth inhibition may result, at least in part, from IGFBP-6-mediated disruption of the IGF-II autocrine loop in these cancer cells.

IGFBP genes lie in close proximity to homeobox gene clusters HoxA to HoxD, which produce DNA-binding proteins that are widely expressed in multicellular

0022-0795/02/0175-033

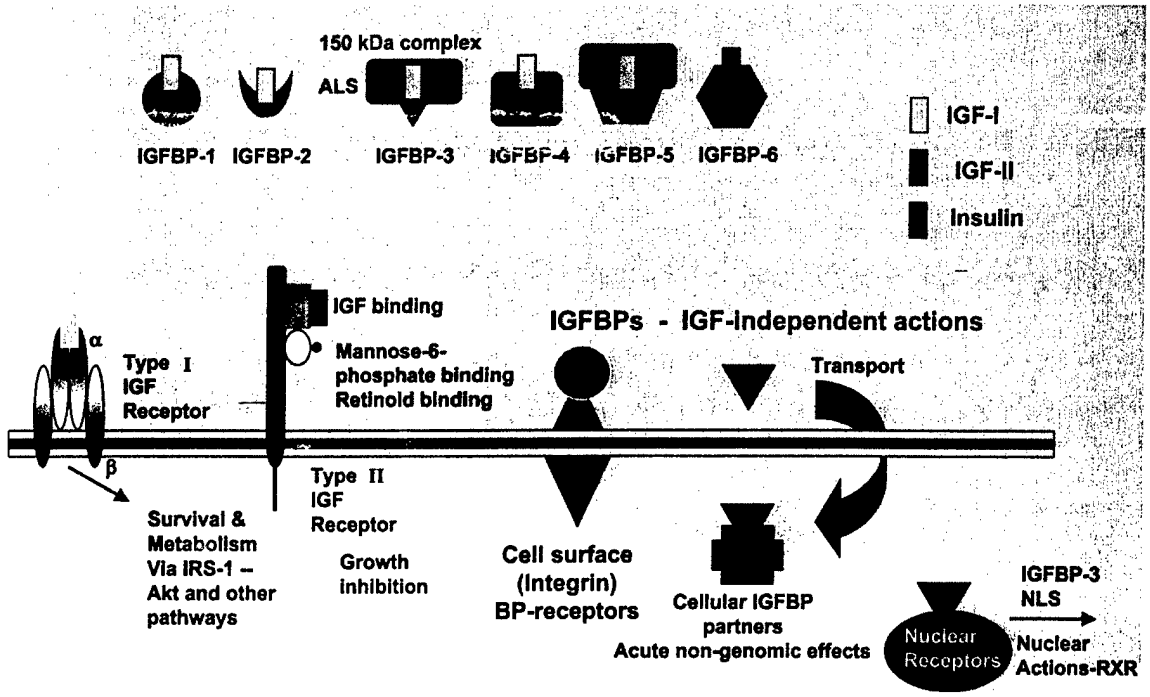

Figure 1 A schematic representation of the IGF–IGFBP axis and its interacting molecules. See text for details.

organisms and encode transcription factors that are crucial for early development. This has been suggested to be a result of linkage before an initial duplication event, implying conservation of their important regulatory processes (Allander *et al.* 1993). The IGF–IGFBP axis is summarized in Fig. 1.

IGFBP-3 – a biological mediator of cancer cell apoptosis

Growth factors in general, and the IGF system in particular, have crucial roles in normal cell proliferation and malignant transformation (Aaronson 1991, Baserga 1995, Werner & LeRoith 1996). Dysregulation at several levels of the axis occur in human cancer (LeRoith *et al.* 1995). This axis has been characterized in many human cancer models, including breast (Sachdev & Yee 2001), hepatocellular (Hanafusa *et al.* 2002), lung (Wegmann *et al.* 1993), colon (Giovannucci 2001), ovary (Krywicki *et al.* 1993), testes (Drescher *et al.* 1997), leukemia (Wex *et al.* 1998), adrenal (Boulle *et al.* 2001), brain (Zumkeller & Westphal 2001) and prostate (Djavan *et al.* 2001).

In vitro, IGFBP-3 both enhances and inhibits IGF-I actions, which was originally believed to be solely through regulation of free IGF bioavailability via high-affinity binding and thereby IGF mitogenic activity (Cohen *et al.* 1991, Giudice *et al.* 1993, Rosenfeld *et al.* 1994, Nickerson *et al.* 1997) depending upon the cell types and culture conditions used (De Mellow & Baxter 1988, Blum *et al.* 1989, Gopinath *et al.* 1989, Conover *et al.* 1990, 2000, Schmid *et al.* 1991, Ramagnolo *et al.* 1994, Martin *et al.* 1995). *In vivo*, *IGFBP-3* transgenic mice exhibit significant reduction in both birth weight and litter size, with a reduction in some organ weights (Modric *et al.* 2001), and non-small-cell lung cancer tumors stably transfected with *IGFBP-3* exhibited a reduction in size compared with controls when transplanted into nude mice (Hochscheid *et al.* 2000).

This critical role of *IGFBP-3* as a gene that may be inactivated on the cellular path to immortalization is supported by the fact that *IGFBP-3* gene expression is uniformly lost in human prostate cancer cell lines and xenografts, and it was detected in DNA microarray analysis of cancerous compared with non-cancerous cells (Schwarze *et al.* 2002). Decreased *IGFBP-3* expression is associated with prostate cancer progression, demonstrating more frequent loss of expression in advanced disease, in both human and mouse models (Hampel *et al.* 1998, Grimberg & Cohen 1999, Kaplan *et al.* 1999). In addition, in a recent experiment that sought to identify genes induced by the inhibitory all-*trans*-retinoic acid in lung epithelial carcinoma cells, *IGFBP-3* was identified as one of 20 upregulated genes in synchronized SCC-25 cells (Le *et al.* 2002). Indeed, *IGFBP-3* is the target of the E7 protein encoded by human papillomavirus type 16, one of the few viral genes that can immortalize primary human cells and thereby override cellular senescence. IGFBP-3-mediated apoptosis is inhibited by E7, which binds to IGFBP-3 and triggers its proteolytic cleavage. Two

transformation-deficient mutants of E7 failed to inactivate IGFBP-3, suggesting that inactivation of IGFBP-3 may contribute to cellular transformation (Mannhardt *et al.* 2000).

New paradigms of IGFBP actions – IGF-independent effects

Transfection of the *IGFBP-3* gene into murine fibroblasts inhibited cell growth by a mechanism that was not reversible by the addition of excess insulin, even though insulin has mitogenic activity in these cells, does not bind IGFBP-3, and would presumably saturate the IGF-IR (Cohen *et al.* 1993). Subsequently, it was shown that a proteolyzed fragment of IGFBP-3, with negligible binding affinity for IGF-I and presumably none for insulin, inhibited insulin- and IGF-I stimulated DNA synthesis in chick embryo fibroblasts (Lalou *et al.* 1996). Additional experiments with this fragment showed inhibition of mitogenesis in murine fibroblasts with a defective IGF-IR that could respond to basic fibroblast growth factor but not IGF, epidermal growth factor, or platelet-derived growth factor (Zadeh & Binoux 1997).

In 1993, our laboratory provided the first direct evidence for IGF-independent apoptotic effects of IGFBP-3 using a mouse fibroblast cell line that lacked IGF-I receptors. The *IGFBP-3* gene was transfected into a cell line derived from an IGF receptor 'knockout' mouse that is not IGF-responsive. Cell growth decreased significantly in this model, showing that IGFBP-3 inhibits cell growth independently of the type-I IGF receptor (Cohen *et al.* 1993). Previously, IGF-independent effects of IGFBP-3 had been suggested in a breast carcinoma line, utilizing IGF analogs with decreased affinity for IGFBP-3 (Oh *et al.* 1993). Since then, several laboratories have confirmed this observation in a variety of cellular systems (Gill *et al.* 1997, Wu *et al.* 2000, Spagnoli *et al.* 2001), culminating recently in the creation of *IGFBP-3* mutants that minimally bind IGFs and still induce apoptosis in prostate cancer cells (Buckway *et al.* 2001, Hong *et al.* 2002).

Further evidence supporting IGF-independent effects of IGFBP-3 includes induction of IGFBP-3 mRNA and protein expression by multiple antiproliferative and pro-apoptotic agents, including transforming growth factor-β (TGF-β) (Martin & Baxter 1991, Oh *et al.* 1995, Gucev *et al.* 1996, Hwa *et al.* 1997, Rajah *et al.* 1997), tumour necrosis factor-α (Rozen *et al.* 1998), retinoids (Adamo *et al.* 1992, Andreatta-Van Leyen *et al.* 1994, Martin *et al.* 1995, Gucev *et al.* 1996, Han *et al.* 1997, Hwa *et al.* 1997), antiestrogens (Huynh *et al.* 1996), p53 (Buckbinder *et al.* 1995) and 1,25 dihydroxyvitamin D_3 (Velez-Yanguas *et al.* 1996, Huynh *et al.* 1998, Boyle *et al.* 2001), and additional data utilizing antisense oligonucleotides and neutralizing antibodies that suggest that IGFBP-3 mediates these effects in part.

The search for IGFBP-3 binding partners

At the cellular level, we and others have described several putative IGFBP-3 binding partners on the cell surface, and in the cytoplasm (Oh *et al.* 1993, Rajah *et al.* 1997, Wu *et al.* 2000, Knudtson *et al.* 2001) and extracellular matrix (Booth *et al.* 1996). The suggestion that the type V TGF-β receptor is the putative IGFBP-3 receptor (Leal *et al.* 1997, 1999) has not been reproduced and probably represents an extracellular matrix protein association. Recently, IGFBP-3 has been shown to modulate the Stat-1 (Spagnoli *et al.* 2002) and Smad (Fanayan *et al.* 2002) signaling cascades, although the precise mechanism by which it interacts with these pathways remains to be established.

Nuclear localization of IGFBP-3

While we were investigating the IGF-independent effects of IGFBP-3 and observing ^{125}I-IGFBP-3 binding in nuclear extracts, a report emerged detailing the presence of IGFBP-3 in the nucleus in opossum kidney cells (Li *et al.* 1997); within the same year, endogenous IGFBP-3 was detected in the nuclei of A549 human lung cancer cells (Jaques *et al.* 1997), and soon thereafter it was found in the nuclei during cell division in human keratinocytes (Wraight *et al.* 1998). Nuclear transport of IGFBP-3 was not unexpected, because both IGFBPs-3 and -5 possess basic C-terminal nuclear localization signals (Radulescu 1994). Recombinant IGFBPs-3 and -5 are actively translocated to the nucleus of human breast cancer cells (Schedlich *et al.* 1998) and this occurs via a nuclear localization signal-dependent pathway, mediated by the importin-β (Schedlich *et al.* 2000) nuclear transport factor. A new mechanism of IGF-independent IGFBP-3 action emerged when we cloned the nuclear retinoid X receptor α (RXRα) as an IGFBP-3 protein partner in a yeast two-hybrid screen (Liu *et al.* 2000).

The nuclear receptor superfamily

Lipophilic hormones exert genetic control of differentiation and homeostasis via a superfamily of highly related transcription factors known as the nuclear receptors (Mangelsdorf *et al.* 1995). Transcriptional regulation depends on specific and ordered interactions with DNA and on subsequent binding of co-repressor or co-activator proteins, or both (Kurokawa *et al.* 1995, Glass *et al.* 1997, Zamir *et al.* 1997). Small lipophilic molecules that serve as ligands tightly control the transcriptional activity of these receptors. Included in this family are many additional factors, known as orphan receptors, which have the characteristics of hormone receptors, but for which the bioactive ligands have not been identified at this time.

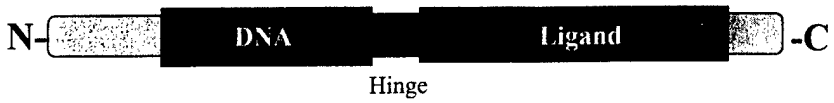

Figure 2 A schematic model of nuclear receptors. See text for details.

The DNA targets of nuclear receptors, known as hormone response elements (HREs), are the sequences through which receptors mediate the control of ligand-responsive genes. Most non-steroid and orphan receptors recognize the consensus sequence 5′-AGGTCA-3′ in DNA that contains one or two copies of this sequence. This group includes nearly all known non-steroid receptors, including the 9-*cis* retinoic acid receptor (the retinoid X receptor, RXR), the all-*trans* retinoic acid receptor (RAR), the thyroid hormone receptor (TR), the vitamin D receptor (VDR), the peroxisome proliferator-activated receptor (PPAR), and nerve growth factor induced-B (NGFI-B). These HREs directly reflect the mode of receptor binding, which can be as heterodimers, homodimers or monomers. In contrast, the steroid hormone receptors bind exclusively as homodimers to palindromes separated by three nucleotides (Mangelsdorf & Evans 1995).

The general architecture of nuclear receptor proteins is shown in Fig. 2. The nuclear receptor DNA-binding domain (DBD) is one of the most prevalent DNA-interacting regions known. It is composed of a highly conserved 66 amino acid core domain located centrally in each nuclear receptor, together with a short, non-conserved extension into the hinge region of the receptor (Fig. 2) (Wilson *et al.* 1992, Rastinejad 1998). Its modular design is composed of two zinc-binding loops and a pair of α-helices (Luisi *et al.* 1991). One of these helices mediates sequence-specific recognition of the AGGTCA sequence via major groove contacts. In some cases, additional sequences in the hinge region contribute to the DNA-binding specificity, nuclear localization or transactivation. The ligand-binding domain (LBD) may also contain sequences important for dimerization, nuclear localization, transactivation, silencing and repression. The major dimerization domain of receptors has been localized in the C-terminal half of the LBD (Fawell *et al.* 1990, Forman & Samuels 1990).

RXR is a combinatorial partner in the nuclear receptor family, able to form heterodimers with a variety of hormone and orphan receptors (Yu *et al.* 1991, Kliewer *et al.* 1992*a*, *b*, Forman *et al.* 1995). The dimerization partners of RXR include itself, RAR, VDR, TR, PPAR and other receptors. The formation of heterodimers between DBDs is induced by specific repertoires of high-affinity response elements containing direct repeats (DRs) with characteristic inter-half-site spacings. These spacings can vary from one to five base pairs (DR1–DR5). The pattern of site selectivity based on the spacing of DRs is known as the 1–5 rule (Umesono *et al.* 1991). In addition, RXR can homodimerize, and signals through the RXR response element (RXRE) (Lehmann *et al.* 1992).

Ligand binding to a nuclear receptor is now recognized to induce a switch in the complex of transcriptional co-factors with which it interacts. In the absence of ligands, receptors such as the RAR–RXR heterodimer are bound to a repression complex that contains histone deacetylases (HDACs), Sin3 and the co-repressors SMRT or NCo-R (Chen & Evans 1995, Horlein *et al.* 1995). Ligand binding triggers release of this complex and promotes interaction with activator complexes containing histone acetylases, including SRC co-activators and CBP/p300, that form a bridge to the basic transcription machinery (Chambon 1996, Perlmann & Evans 1997).

As ligand-activated transcription factors, nuclear receptors make ideal therapeutic targets. The ability to modulate receptor activity with synthetic ligands has led to the development of drugs for a number of diseases, including cancer and diabetes. With the discovery of the co-activator and co-repressor complexes has come the realization that receptor–co-factor interactions may represent another point at which nuclear receptor signaling pathways could be modulated pharmacologically.

An interface between the nuclear receptor and IGF axis – the nuclear association of RXRα and IGFBP-3

A yeast two-hybrid system was used to identify novel IGFBP-3 partners (Liu *et al.* 2000). We isolated a 1200-base pair cDNA fragment encoding the C-terminal portion of the human *RXRα* gene followed by the 3′-untranslated region of the human RXRα cDNA. Yeast mating experiments confirmed the interaction between IGFBP-3 and RXRα. This was further verified via glutathione S-transferase (GST) pull-down experiments using RXRα linked to GST and various forms of natural and recombinant IGFBP-3 proteins. Co-immunoprecipitation and fluorescence immunocytochemistry indicated that RXRα and IGFBP-3 co-localize in both the cytoplasm and nucleus of prostate cancer cells. In addition, after incubation with an RXR-specific ligand, both proteins were more evident in the nucleus, suggesting a ligand-dependent co-transport. This is consistent with previous data that showed that, when nuclear

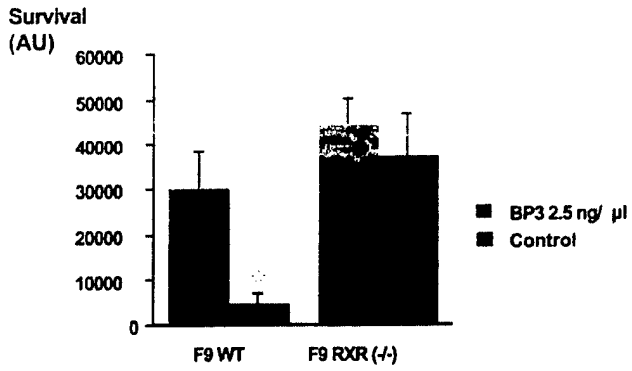

Figure 3 RXR is required for IGFBP-3-induced apoptosis. F9 teratocarcinoma cells were derived to have targeted deletions of RXR (F9 RXR (-/-)). Survival was assessed after IGFBP-3 (BP3) treatment. AU, arbitrary units; WT, wild-type. *$P<0.01$ relative to control.

envelopes were permeabilized, IGFBP-3 is retained within the nucleus (Schedlich *et al.* 2000), suggesting interaction with nuclear components such as RXRα.

Interactions of IGFBP-3 with the DNA-transcription factor complex involving RXRα and the RXRE were confirmed in electromobility shift assays. The addition of an IGFBP-3 antibody supershifts the complex, indicating that IGFBP-3 is bound to the RXRα–RXRE complex. Similarly, labeled RAR response element (RARE) binds RAR in HeLa extracts, but this complex does not nuclear supershift with an IGFBP-3 antibody, suggesting that IGFBP-3 forms a complex only with the RXR–RXR homodimer, not with RXR–RAR heterodimers.

In luciferase-based transcriptional assays, we used the DR1-RXRE and the DR5-RARE reporter systems in COS7 cells. In both cases, luciferase signaling was enhanced by co-treatment with the appropriate ligand. However, IGFBP-3 co-transfections potently and dose-dependently inhibited RA signaling via RARE, but enhanced RXR-specific ligand signaling via the RXRE, indicating that IGFBP-3 enhances RXR–RXR homodimer-mediated signaling via the RXRE, but blocks RAR–RXR heterodimer-mediated signaling via the RARE.

To study further the functional interface of IGFBP-3 and RXRα in the nucleus, we performed viability assays utilizing the F9 embryonic carcinoma cell line and a sister cell line, in which RXRα has been knocked out (Fig. 3). IGFBP-3 treatment dramatically reduced cell viability in the F9 cell line, but IGFBP-3 had no discernible effects in the RXRα knockout line, indicating that RXRα is required for IGFBP-3-induced apoptosis.

Natural and synthetic retinoids have also been used with some success in prostate cancer models (Lewis & Hochadel 1999, Sharp *et al.* 2001). We found that RXRs are expressed at high levels in normal human prostate tissue, in addition to prostate tumor cell lines and primary human tumors (P Cohen unpublished data). Moreover, we have shown that growth of LNCaP, LAPC-4, PC3, and DU-145 prostate cancer cells can be inhibited by the RXR-specific activator, LG 268. These observations illustrate the potential for several nuclear receptor signaling pathways to regulate growth of prostate cells.

In the described cloning and functional studies of RXRα and IGFBP-3, we discovered that IGFBP-3 and the specific rexinoid, LG1069, had additive effects in killing LAPC-4 cells (Liu *et al.* 2000). This is an important observation, as it suggests that IGFBP-3 and RXR ligands co-operate in inducing gene transcription that leads to apoptosis. A recent report described the four and a half LIM domain gene 2, *FHL2*, a transcriptional co-activator, as a specific IGFBP-5 nuclear binding partner cloned from a human osteosarcoma library (Amaar *et al.* 2002). This further establishes the IGFBPs as important modulatory factors involved in DNA transcription and extends the IGF axis beyond the serum and cellular surface. With recent advances in both protein partner discovery and modulation of cellular signaling, we are confident that investigation into the interaction between nuclear receptors, DNA transcription and the IGF axis will reveal several new targets for co-adjuvant treatment in the treatment of malignancy.

References

Aaronson SA 1991 Growth factors and cancer. *Science* **254** 1146–1153.

Adamo ML, Shao ZM, Lanau F, Chen JC, Clemmons DR, Roberts CT Jr, LeRoith D & Fontana JA 1992 Insulin-like growth factor-I (IGF-I) and retinoic acid modulation of IGF-binding proteins (IGFBPs): IGFBP-2, -3, and -4 gene expression and protein secretion in a breast cancer cell line. *Endocrinology* **131** 1858–1866.

Allander SV, Bajalica S, Larsson C, Luthman H, Powell DR, Stern I, Weber G, Zazzi H & Ehrenborg E 1993 Structure and chromosomal localization of human insulin-like growth factor-binding protein genes. *Growth Regulation* **3** 3–5.

Amaar YG, Thompson GR, Linkhart TA, Chen ST, Baylink DJ & Mohan S 2002 Insulin-like growth factor binding protein 5 (IGFBP-5) interacts with a four and a half LIM protein 2 (FHL2). *Journal of Biological Chemistry* **277** 12053–12060.

Andreatta-Van Leyen S, Hembree JR & Eckert RL 1994 Regulation of insulin-like growth factor 1 binding protein 3 levels by epidermal growth factor and retinoic acid in cervical epithelial cells. *Journal of Cell Physiology* **160** 265–274.

Baserga R 1995 The insulin-like growth factor I receptor: a key to tumor growth? *Cancer Research* **55** 249–252.

Baxter RC 1994 Insulin-like growth factor binding proteins in the human circulation: a review. *Hormone Research* **42** 140–144.

Baxter RC & Saunders H 1992 Radioimmunoassay of insulin-like growth factor-binding protein-6 in human serum and other body fluids. *Journal of Endocrinology* **134** 133–139.

Blum WF, Jenne EW, Reppin F, Kietzmann K, Ranke MB & Bierich JR 1989 Insulin-like growth factor I (IGF-I)-binding protein complex is a better mitogen than free IGF-I. *Endocrinology* **125** 766–772.

Booth BA, Boes M, Dake BL, Linhardt RJ, Caldwell EE, Weiler JM & Bar RS 1996 Structure–function relationships in the heparin-binding C-terminal region of insulin-like growth factor binding protein-3. *Growth Regulation* **6** 206–213.

Boulle N, Baudin E, Gicquel C, Logie A, Bertherat J, Penfornis A, Bertagna X, Luton JP, Schlumberger M & Le Bouc Y 2001 Evaluation of plasma insulin-like growth factor binding protein-2 as a marker for adrenocortical tumors. *European Journal of Endocrinology* **144** 29–36.

Boyle BJ, Zhao XY, Cohen P & Feldman D 2001 Insulin-like growth factor binding protein-3 mediates 1 alpha,25-dihydroxyvitamin d(3) growth inhibition in the LNCaP prostate cancer cell line through p21/WAF1. *Journal of Urology* **165** 1319–1324.

Bramani S, Song H, Beattie J, Tonner E, Flint DJ & Allan GJ 1999 Amino acids within the extracellular matrix (ECM) binding region (201–218) of rat insulin-like growth factor binding protein (IGFBP)-5 are important determinants in binding IGF-I. *Journal of Molecular Endocrinology* **23** 117–123.

Buckbinder L, Talbott R, Velasco-Miguel S, Takenaka I, Faha B, Seizinger BR & Kley N 1995 Induction of the growth inhibitor IGF-binding protein 3 by p53. *Nature* **377** 646–649.

Buckway CK, Wilson EM, Ahlsen M, Bang P, Oh Y & Rosenfeld RG 2001 Mutation of three critical amino acids of the N-terminal domain of IGF-binding protein-3 essential for high affinity IGF binding. *Journal of Clinical Endocrinology and Metabolism* **86** 4943–4950.

Chambon P 1996 A decade of molecular biology of retinoic acid receptors. *FASEB Journal* **10** 940–954.

Chen JD & Evans RM 1995 A transcriptional co-repressor that interacts with nuclear hormone receptors. *Nature* **377** 454–457.

Cohen P & Rosenfeld RG (Eds) 1995. *The IGF Axis*. Boca Raton, FL, USA: CRC Press.

Cohen P, Fielder PJ, Hasegawa Y, Frisch H, Giudice LC & Rosenfeld RG 1991 Clinical aspects of insulin-like growth factor binding proteins. *Acta Endocrinologica (Copenhagen)* **124** 74–85.

Cohen P, Lamson G, Okajima T & Rosenfeld RG 1993 Transfection of the human insulin-like growth factor binding protein-3 gene into Balb/c fibroblasts inhibits cellular growth. *Molecular Endocrinology* **7** 380–386.

Conover CA, Ronk M, Lombana F & Powell DR 1990 Structural and biological characterization of bovine insulin-like growth factor binding protein-3. *Endocrinology* **127** 2795–2803.

Conover CA, Bale LK, Durham SK & Powell DR 2000 Insulin-like growth factor (IGF) binding protein-3 potentiation of IGF action is mediated through the phosphatidylinositol-3-kinase pathway and is associated with alteration in protein kinase B/AKT sensitivity. *Endocrinology* **141** 3098–3103.

De Mellow JS & Baxter RC 1988 Growth hormone-dependent insulin-like growth factor (IGF) binding protein both inhibits and potentiates IGF-I-stimulated DNA synthesis in human skin fibroblasts. *Biochemical and Biophysical Research Communications* **156** 199–204.

Djavan B, Waldert M, Seitz C & Marberger M 2001 Insulin-like growth factors and prostate cancer. *World Journal of Urology* **19** 225–233.

Drescher B, Lauke H, Hartmann M, Davidoff MS & Zumkeller W 1997 Immunohistochemical pattern of insulin-like growth factor (IGF) I, IGF II and IGF binding proteins 1 to 6 in carcinoma *in situ* of the testis. *Molecular Pathology* **50** 298–303.

Fanayan S, Firth SM & Baxter RC 2002 Signaling through the Smad pathway by insulin-like growth factor-binding protein-3 in breast cancer cells. Relationship to transforming growth factor-beta 1 signaling. *Journal of Biological Chemistry* **277** 7255–7261.

Fawell SE, Lees JA, White R & Parker MG 1990 Characterization and colocalization of steroid binding and dimerization activities in the mouse estrogen receptor. *Cell* **60** 953–962.

Forman BM & Samuels HH 1990 Interactions among a subfamily of nuclear hormone receptors: the regulatory zipper model. *Molecular Endocrinology* **4** 1293–1301.

Forman BM, Umesono K, Chen J & Evans RM 1995 Unique response pathways are established by allosteric interactions among nuclear hormone receptors. *Cell* **81** 541–550.

Gallicchio MA, Kneen M, Hall C, Scott AM & Bach LA 2001 Overexpression of insulin-like growth factor binding protein-6 inhibits rhabdomyosarcoma growth *in vivo*. *International Journal of Cancer* **94** 645–651.

Gill ZP, Perks CM, Newcomb PV & Holly JM 1997 Insulin-like growth factor-binding protein (IGFBP-3) predisposes breast cancer cells to programmed cell death in a non-IGF-dependent manner. *Journal of Biological Chemistry* **272** 25602–25607.

Giovannucci E 2001 Insulin, insulin-like growth factors and colon cancer: a review of the evidence. *Journal of Nutrition* **131** 3109S–3120S.

Giudice LC, Irwin JC, Dsupin BA, Pannier EM, Jin IH, Vu TH & Hoffman AR 1993 Insulin-like growth factor (IGF), IGF binding protein (IGFBP), and IGF receptor gene expression and IGFBP synthesis in human uterine leiomyomata. *Human Reproduction* **8** 1796–1806.

Glass CK, Rose DW & Rosenfeld MG 1997 Nuclear receptor coactivators. *Current Opinion in Cell Biology* **9** 222–232.

Gopinath R, Walton PE & Etherton TD 1989 An acid-stable insulin-like growth factor (IGF)-binding protein from pig serum inhibits binding of IGF-I and IGF-II to vascular endothelial cells. *Journal of Endocrinology* **120** 231–236.

Grellier P, Berrebi D, Peuchmaur M & Babajko S 2002 The IGF system in neuroblastoma xenografts: focus on IGF-binding protein-6. *Journal of Endocrinology* **172** 467–476.

Grimberg A & Cohen P 1999 Growth hormone and prostate cancer: guilty by association? *Journal of Endocrinological Investigation* **22** 64–73.

Gucev ZS, Oh Y, Kelley KM & Rosenfeld RG 1996 Insulin-like growth factor binding protein 3 mediates retinoic acid- and transforming growth factor beta2-induced growth inhibition in human breast cancer cells. *Cancer Research* **56** 1545–1550.

Hampel OZ, Kattan MW, Yang G, Haidacher SJ, Saleh GY, Thompson TC, Wheeler TM & Marcelli M 1998 Quantitative immunohistochemical analysis of insulin-like growth factor binding protein-3 in human prostatic adenocarcinoma: a prognostic study. *Journal of Urology* **159** 2220–2225.

Han GR, Dohi DF, Lee HY, Rajah R, Walsh GL, Hong WK, Cohen P & Kurie JM 1997 All-trans-retinoic acid increases transforming growth factor-beta2 and insulin-like growth factor binding protein-3 expression through a retinoic acid receptor-alpha-dependent signaling pathway. *Journal of Biological Chemistry* **272** 13711–13716.

Hanafusa T, Yumoto Y, Nouso K, Nakatsukasa H, Onishi T, Fujikawa T, Taniyama M, Nakamura S, Uemura M, Takuma Y, Yumoto E, Higashi T & Tsuji T 2002 Reduced expression of insulin-like growth factor binding protein-3 and its promoter hypermethylation in human hepatocellular carcinoma. *Cancer Letters* **176** 149–158.

Hasegawa T, Cohen P, Hasegawa Y, Fielder PJ & Rosenfeld RG 1995 Characterization of the insulin-like growth factors (IGF) axis in a cultured mouse Leydig cell line (TM-3). *Growth Regulation* **5** 151–159.

Hochscheid R, Jaques G & Wegmann B 2000 Transfection of human insulin-like growth factor-binding protein 3 gene inhibits cell growth and tumorigenicity: a cell culture model for lung cancer. *Journal of Endocrinology* **166** 553–563.

Hong J, Zhang G, Dong F & Rechler MM 2002 Insulin-like growth factor binding protein-3 (IGFBP-3) mutants that do not bind IGF-I or IGF-II stimulate apoptosis in human prostate cancer cells. *Journal of Biological Chemistry* **277** 10489–10497.

Horlein AJ, Naar AM, Heinzel T, Torchia J, Gloss B, Kurokawa R, Ryan A, Kamei Y, Soderstrom M, Glass CK *et al.* 1995 Ligand-independent repression by the thyroid hormone receptor mediated by a nuclear receptor co-repressor. *Nature* **377** 397–404.

Huynh H, Nickerson T, Pollak M & Yang X 1996 Regulation of insulin-like growth factor I receptor expression by the pure antiestrogen ICI 182780. *Clinical Cancer Research* **2** 2037–2042.

Huynh H, Pollak M & Zhang JC 1998 Regulation of insulin-like growth factor (IGF) II and IGF binding protein 3 autocrine loop in human PC-3 prostate cancer cells by vitamin D metabolite 1,25(OH)2D3 and its analog EB1089. *International Journal of Oncology* **13** 137–143.

Hwa V, Oh Y & Rosenfeld RG 1997 Insulin-like growth factor binding protein-3 and -5 are regulated by transforming growth factor-beta and retinoic acid in the human prostate adenocarcinoma cell line PC-3. *Endocrine* **6** 235–242.

Imai Y, Moralez A, Andag U, Clarke JB, Busby WH Jr & Clemmons DR 2000 Substitutions for hydrophobic amino acids in the N-terminal domains of IGFBP-3 and -5 markedly reduce IGF-I binding and alter their biologic actions. *Journal of Biological Chemistry* **275** 18188–18194.

Jaques G, Noll K, Wegmann B, Witten S, Kogan E, Radulescu RT & Havemann K 1997 Nuclear localization of insulin-like growth factor binding protein 3 in a lung cancer cell line. *Endocrinology* **138** 1767–1770.

Kaplan PJ, Mohan S, Cohen P, Foster BA & Greenberg NM 1999 The insulin-like growth factor axis and prostate cancer: lessons from the transgenic adenocarcinoma of mouse prostate (TRAMP) model. *Cancer Research* **59** 2203–2209.

Kim EJ, Kang YH, Schaffer BS, Bach LA, MacDonald RG & Park JH 2002 Inhibition of Caco-2 cell proliferation by all-trans retinoic acid: role of insulin-like growth factor binding protein-6. *Journal of Cell Physiology* **190** 92–100.

Kliewer SA, Umesono K, Mangelsdorf DJ & Evans RM 1992*a* Retinoid X receptor interacts with nuclear receptors in retinoic acid, thyroid hormone and vitamin D3 signalling. *Nature* **355** 446–449.

Kliewer SA, Umesono K, Noonan DJ, Heyman RA & Evans RM 1992*b* Convergence of 9-cis retinoic acid and peroxisome proliferator signalling pathways through heterodimer formation of their receptors. *Nature* **358** 771–774.

Knudtson KL, Boes M, Sandra A, Dake BL, Booth BA & Bar RS 2001 Distribution of chimeric IGF binding protein (IGFBP)-3 and IGFBP-4 in the rat heart: importance of C-terminal basic region. *Endocrinology* **142** 3749–3755.

Krywicki RF, Figueroa JA, Jackson JG, Kozelsky TW, Shimasaki S, Von Hoff DD & Yee D 1993 Regulation of insulin-like growth factor binding proteins in ovarian cancer cells by oestrogen. *European Journal of Cancer* **14** 2015–2019.

Kurokawa R, Soderstrom M, Horlein A, Halachmi S, Brown M, Rosenfeld MG & Glass CK 1995 Polarity-specific activities of retinoic acid receptors determined by a co-repressor. *Nature* **377** 451–454.

Lalou C, Lassarre C & Binoux M 1996 A proteolytic fragment of insulin-like growth factor (IGF) binding protein-3 that fails to bind IGFs inhibits the mitogenic effects of IGF-I and insulin. *Endocrinology* **137** 3206–3212.

Lamson G, Giudice LC & Rosenfeld RG 1991 Insulin-like growth factor binding proteins: structural and molecular relationships. *Growth Factors* **5** 19–28.

Le Q, Soprano DR & Soprano KJ 2002 Profiling of retinoid mediated gene expression in synchronized human SCC cells using Atlas human cDNA expression arrays. *Journal of Cell Physiology* **190** 345–355.

Leal SM, Liu Q, Huang SS & Huang JS 1997 The type V transforming growth factor beta receptor is the putative insulin-like growth factor-binding protein 3 receptor. *Journal of Biological Chemistry* **272** 20572–20576.

Leal SM, Huang SS & Huang JS 1999 Interactions of high affinity insulin-like growth factor-binding proteins with the type V transforming growth factor-beta receptor in mink lung epithelial cells. *Journal of Biological Chemistry* **274** 6711–6717.

Lehmann JM, Jong L, Fanjul A, Cameron JF, Lu XP, Haefner P, Dawson MI & Pfahl M 1992 Retinoids selective for retinoid X receptor response pathways. *Science* **258** 1944–1946.

LeRoith D 1996 Insulin-like growth factor receptors and binding proteins. *Baillière's Clinical Endocrinology and Metabolism* **10** 49–73.

LeRoith D, Baserga R, Helman L & Roberts CT Jr 1995 Insulin-like growth factors and cancer. *Annals of Internal Medicine* **122** 54–59.

Lewis KC & Hochhadel JF 1999 Retinoid metabolism in the prostate: effects of administration of the synthetic retinoid N-(4 hydroxyphenyl)retinamide. *Cancer Research* **59** 5947–5955.

Li W, Fawcett J, Widmer HR, Fielder PJ, Rabkin R & Keller GA 1997 Nuclear transport of insulin-like growth factor-I and insulin-like growth factor binding protein-3 in opossum kidney cells. *Endocrinology* **138** 1763–1766.

Liu B, Lee HY, Weinzimer SA, Powell DR, Clifford JL, Kurie JM & Cohen P 2000 Direct functional interactions between insulin-like growth factor-binding protein-3 and retinoid X receptor-alpha regulate transcriptional signaling and apoptosis. *Journal of Biological Chemistry* **275** 33607–33613.

Luisi BF, Xu WX, Otwinowski Z, Freedman LP, Yamamoto KR & Sigler PB 1991 Crystallographic analysis of the interaction of the glucocorticoid receptor with DNA. *Nature* **352** 497–505.

Mangelsdorf DJ & Evans RM 1995 The RXR heterodimers and orphan receptors. *Cell* **83** 841–850.

Mangelsdorf DJ, Thummel C, Beato M, Herrlich P, Schutz G, Umesono K, Blumberg B, Kastner P, Mark M, Chambon P *et al.* 1995 The nuclear receptor superfamily: the second decade. *Cell* **83** 835–839.

Mannhardt B, Weinzimer SA, Wagner M, Fiedler M, Cohen P, Jansen-Durr P & Zwerschke W 2000 Human papillomavirus type 16 E7 oncoprotein binds and inactivates growth-inhibitory insulin-like growth factor binding protein 3. *Molecular and Cellular Biology* **20** 6483–6495.

Martin JL & Baxter RC 1991 Transforming growth factor-beta stimulates production of insulin-like growth factor-binding protein-3 by human skin fibroblasts. *Endocrinology* **128** 1425–1433.

Martin JL, Coverley JA, Pattison ST & Baxter RC 1995 Insulin-like growth factor-binding protein-3 production by MCF-7 breast cancer cells: stimulation by retinoic acid and cyclic adenosine monophosphate and differential effects of estradiol. *Endocrinology* **136** 1219–1226.

Modric T, Silha JV, Shi Z, Gui Y, Suwanichkul A, Durham SK, Powell DR & Murphy LJ 2001 Phenotypic manifestations of insulin-like growth factor-binding protein-3 overexpression in transgenic mice. *Endocrinology* **142** 1958–1967.

Nickerson T, Huynh H & Pollak M 1997 Insulin-like growth factor binding protein-3 induces apoptosis in MCF7 breast cancer cells. *Biochemical and Biophysical Research Communications* **237** 690–693.

Oh Y, Muller HL, Lamson G & Rosenfeld RG 1993 Insulin-like growth factor (IGF)-independent action of IGF-binding protein-3 in Hs578T human breast cancer cells. Cell surface binding and growth inhibition. *Journal of Biological Chemistry* **268** 14964–14971.

Oh Y, Muller HL, Ng L & Rosenfeld RG 1995 Transforming growth factor-beta-induced cell growth inhibition in human breast cancer cells is mediated through insulin-like growth factor-binding protein-3 action. *Journal of Biological Chemistry* **270** 13589–13592.

Perlmann T & Evans RM 1997 Nuclear receptors in Sicily: all in the famiglia. *Cell* **90** 391–397.

Radulescu RT 1994 Nuclear localization signal in insulin-like growth factor-binding protein type 3. *Trends in Biochemical Sciences* **19** 278.

Rajah R, Valentinis B & Cohen P 1997 Insulin-like growth factor (IGF)-binding protein-3 induces apoptosis and mediates the effects of transforming growth factor-beta1 on programmed cell death through a p53- and IGF-independent mechanism. *Journal of Biological Chemistry* **272** 12181–12188.

Rajaram S, Baylink DJ & Mohan S 1997 Insulin-like growth factor-binding proteins in serum and other biological fluids: regulation and functions. *Endocrine Reviews* **18** 801–831.

Ramagnolo D, Akers RM, Byatt JC, Wong EA & Turner JD 1994 IGF-I-induced IGFBP-3 potentiates the mitogenic actions of IGF-I in mammary epithelial MD-IGF-I cells. *Molecular and Cellular Endocrinology* **102** 131–139.

Rastinejad F 1998 Structure and function of the steroid and nuclear receptor DNA binding domain. In *Molecular Biology of Steroid and Nuclear Hormone Receptors*, pp 105–131. Ed. L Freedman. Boston, MA, USA: Birkhauser.

Rosenfeld RG, Pham H, Cohen P, Fielder P, Gargosky SE, Muller H, Nonoshita L & Oh Y 1994 Insulin-like growth factor binding proteins and their regulation. *Acta Paediatrica Supplementum* **399** 154–158.

Rozen F, Zhang J & Pollak M 1998 Antiproliferative action of tumor necrosis factor-alpha on MCF-7 breast cancer cells is associated with increased insulin-like growth factor binding protein-3 accumulation. *International Journal of Oncology* **13** 865–869.

Sachdev D & Yee D 2001 The IGF system and breast cancer. *Endocrine-Related Cancer* **8** 197–209.

Schedlich LJ, Young TF, Firth SM & Baxter RC 1998 Insulin-like growth factor-binding protein (IGFBP)-3 and IGFBP-5 share a common nuclear transport pathway in T47D human breast carcinoma cells. *Journal of Biological Chemistry* **273** 18347–18352.

Schedlich LJ, Le Page SL, Firth SM, Briggs LJ, Jans DA & Baxter RC 2000 Nuclear import of insulin-like growth factor-binding protein-3 and -5 is mediated by the importin beta subunit. *Journal of Biological Chemistry* **275** 23462–23470.

Schmid C, Rutishauser J, Schlapfer I, Froesch ER & Zapf J 1991 Intact but not truncated insulin-like growth factor binding protein-3 (IGFBP-3) blocks IGF I-induced stimulation of osteoblasts: control of IGF signalling to bone cells by IGFBP-3-specific proteolysis? *Biochemical and Biophysical Research Communications* **179** 579–585.

Schwarze SR, DePrimo SE, Grabert LM, Fu VX, Brooks JD & Jarrard DF 2002 Novel pathways associated with bypassing cellular senescence in human prostate epithelial cells. *Journal of Biological Chemistry* **277** 14877–14883.

Sharp RM, Bello-DeOcampo D, Quader ST & Webber MM 2001 N-(4-hydroxyphenyl)retinamide (4-HPR) decreases neoplastic properties of human prostate cells: an agent for prevention. *Mutations Research* **496** 163–170.

Shimasaki S & Ling N 1991 Identification and molecular characterization of insulin-like growth factor binding proteins (IGFBP-1, -2, -3, -4, -5 and -6). *Progress in Growth Factor Research* **3** 243–266.

Song H, Beattie J, Campbell IW & Allan GJ 2000 Overlap of IGF- and heparin-binding sites in rat IGF-binding protein-5. *Journal of Molecular Endocrinology* **24** 43–51.

Spagnoli A, Hwa V, Horton WA, Lunstrum GP, Roberts CT Jr, Chiarelli F, Torello M & Rosenfeld RG 2001 Antiproliferative effects of insulin-like growth factor-binding protein-3 in mesenchymal chondrogenic cell line RCJ3·1C5·18. Relationship to differentiation stage. *Journal of Biological Chemistry* **276** 5533–5540.

Spagnoli A, Torello M, Nagalla SR, Horton WA, Pattee P, Hwa V, Chiarelli F, Roberts CT, Jr & Rosenfeld RG 2002 Identification of STAT-1 as a molecular target of insulin-like growth factor binding protein-3 (IGFBP-3) in the process of chondrogenesis. *Journal of Biological Chemistry* **277** 18860–18867.

Umesono K, Murakami KK, Thompson CC & Evans RM 1991 Direct repeats as selective response elements for the thyroid hormone, retinoic acid, and vitamin D3 receptors. *Cell* **65** 1255–1266.

Velez-Yanguas MC, Kalebic T, Maggi M, Kappel CC, Letterio J, Uskokovic M & Helman LJ 1996 1-Alpha, 25-dihydroxy-16-ene-23-yne-26,27-hexafluorocholecalciferol (Ro24–5531) modulation of insulin-like growth factor-binding protein-3 and induction of differentiation and growth arrest in a human osteosarcoma cell line. *Journal of Clinical Endocrinology and Metabolism* **81** 93–99.

Wegmann BR, Schoneberger HJ, Kiefer PE, Jaques G, Brandscheid D & Havemann K 1993 Molecular cloning of IGFBP-5 from SCLC cell lines and expression of IGFBP-4, IGFBP-5 and IGFBP-6 in lung cancer cell lines and primary tumours. *European Journal of Cancer* **11** 1578–1584.

Werner H & LeRoith D 1996 The role of the insulin-like growth factor system in human cancer. *Advances in Cancer Research* **68** 183–223.

Wetterau LA, Moore MG, Lee KW, Shim ML & Cohen P 1999 Novel aspects of the insulin-like growth factor binding proteins. *Molecular Genetics and Metabolism* **68** 161–181.

Wex H, Vorwerk P, Mohnike K, Bretschneider D, Kluba U, Aumann V, Blum WF & Mittler U 1998 Elevated serum levels of IGFBP-2 found in children suffering from acute leukaemia is accompanied by the occurrence of IGFBP-2 mRNA in the tumour clone. *British Journal of Cancer* **78** 515–520.

Wilson TE, Paulsen RE, Padgett KA & Milbrandt J 1992 Participation of non-zinc finger residues in DNA binding by two nuclear orphan receptors. *Science* **256** 107–110.

Wraight CJ, Liepe IJ, White PJ, Hibbs AR & Werther GA 1998 Intranuclear localization of insulin-like growth factor binding protein-3 (IGFBP-3) during cell division in human keratinocytes. *Journal of Investigative Dermatology* **111** 239–242.

Wu HB, Kumar A, Tsai WC, Mascarenhas D, Healey J & Rechler MM 2000 Characterization of the inhibition of DNA synthesis in proliferating mink lung epithelial cells by insulin-like growth factor binding protein-3. *Journal of Cell Biochemistry* **77** 288–297.

Yu VC, Delsert C, Andersen B, Holloway JM, Devary OV, Naar AM, Kim SY, Boutin JM, Glass CK & Rosenfeld MG 1991 RXR beta: a coregulator that enhances binding of retinoic acid, thyroid hormone, and vitamin D receptors to their cognate response elements. *Cell* **67** 1251–1266.

Zadeh SM & Binoux M 1997 The 16-kDa proteolytic fragment of insulin-like growth factor (IGF) binding protein-3 inhibits the mitogenic action of fibroblast growth factor on mouse fibroblasts with a targeted disruption of the type 1 IGF receptor gene. *Endocrinology* **138** 3069–3072.

Zamir I, Zhang J & Lazar MA 1997 Stoichiometric and steric principles governing repression by nuclear hormone receptors. *Genes and Development* **11** 835–846.

Zumkeller W & Westphal M 2001 The IGF/IGFBP system in CNS malignancy. *Molecular Pathology* **54** 227–229.

Received 16 April 2002
Accepted 21 May 2002

Int. J. Cancer: **105,** 14–19 (2003)

Publication of the International Union Against Cancer

NOVEL STIMULATORY ROLE FOR INSULIN-LIKE GROWTH FACTOR BINDING PROTEIN-2 IN PROSTATE CANCER CELLS

Michael G. MOORE[1], Lawrence A. WETTERAU[2], Malik J. FRANCIS[1], Donna M. PEEHL[3] and Pinchas COHEN[1]*

[1]*Division of Pediatric Endocrinology, University of California at Los Angeles Medical Center, Los Angeles, CA, USA*
[2]*Department of Pediatrics, Ohio State University College of Medicine, Columbus, OH, USA*
[3]*Department of Urology, Stanford University Medical Center, Stanford, CA, USA*

The insulin-like growth factor (IGF) axis is a complex system composed of 2 mitogenic ligands, IGF-I and -II, 2 receptors, IGF-1R and IGF-2R, and 6 binding proteins, IGFBP-1 to -6. The IGFBPs exert their actions through their regulation of IGF bioavailability for IGF receptors. In addition, some IGFBPs have also been found to have direct cellular actions independent of IGFs. IGFBP-2 is a major IGFBP in the prostate and in seminal fluid. IGFBP-2 levels, which are elevated in many malignancies, are markedly increased in prostate cancer, and show a positive correlation with prostate specific antigen (PSA) and prostate tumor aggressiveness. We investigated the potential role of IGFBP-2 in the pathogenesis of prostate cancer by evaluating its ability to stimulate growth and the expression and activity of the nuclear enzyme, telomerase. We found IGFBP-2 to have a modest suppressive effect on the growth of primary cultures of normal prostate epithelial cells and a potent IGF-antagonistic effect in these cells, similar to previous reports on the inhibitory nature of this molecule. Surprisingly, IGFBP-2 had a potent stimulatory effect on growth of LAPC-4 prostate cancer cells, an effect that was more pronounced in the absence of androgens. IGFBP-2 growth stimulation of LAPC-4 cells was completely blocked by MAP-kinase inhibitors and partially blocked by PI3-kinase inhibitors. IGFBP-2 stimulation of LAPC-4 cell growth seen in serum-free conditions was lost in the presence of 10% FBS. IGFBP-2 also had a growth stimulatory effect on DU 145 prostate cancer cells. IGFBP-2 significantly stimulated telomerase activity in LAPC-4 cells in the absence of androgens. In addition, IGFBP-2 significantly stimulated hTERT expression and telomerase activity in DU 145 cells. Thus, we demonstrated an inhibitory effect of IGFBP-2 on non-malignant prostate cells, but showed it to be stimulatory for prostate cancer cells in a MAP-kinase and androgen-modulated process. In conclusion, IGFBP-2 may play a role in the progression, but not in the initiation of the prostate cancer disease process, suggesting the existence of a molecular switch transitioning IGFBP-2 from a growth inhibitor to a pro-carcinogenic molecule.

Key words: *IGFBP-2; growth; prostate; cancer; telomerase*

The insulin-like growth factors (IGFs) are a family of growth factors with mitogenic effects involved in tissue growth and differentiation. Through their interactions with the Type 1 and 2 IGF receptors (IGFRs), IGF-I and IGF-II have been shown to stimulate cell proliferation and inhibit apoptosis in a variety of tissues,[1,2] and are believed to be involved in the pathogenesis of several malignancies,[3,4] including prostate cancer.[5,6]

The insulin-like growth factor binding proteins (IGFBPs) are a family of binding proteins involved in the regulation of tissue development through their interactions with IGFs. By sequestering free IGFs and reducing their bioavailability for interaction with IGFRs, IGFBPs are able to modulate cellular growth and differentiation on a local level.[7]In addition, some IGFBPs have been found to have direct effects on cellular growth and apoptosis independent of IGFs. It has been demonstrated, for example, that IGFBP-3 exerts pro-apoptotic effects that are IGF-independent through its interaction with the nuclear receptor retinoid X receptor (RXR).[8]IGFBP-3 has also been shown to inhibit cell growth and induce apoptosis in an IGF-IGF-1R-independent fashion.[9,10]

IGFBP-2 is the second most abundant IGFBP in the circulation and can be found in a variety of mammalian fluids and tissues. Its effects have been considered previously as primarily inhibitory in several cell lines, presumably through sequestering free IGFs.[11]This is supported by the fact that IGF analogues with reduced affinity for IGFBP-2 are more potent growth stimulators than IGF-I itself. Serum levels of IGFBP-2 are, however, elevated in individuals with diverse types of cancers including central nervous system (CNS),[12] lung,[13] lymphoid tumors,[14,15] colon,[16] Wilms',[17] adrenal,[18] ovary[19,20] and prostate,[21] and have been found to be positively correlated with the aggressiveness of some tumors,[22] including prostate cancer.[23,24]

In the human prostate, a major IGFBP is IGFBP-2. Its concentration of greater than 10,000 ng/ml in seminal plasma is greater than the concentration of any IGFBP in any other body fluid.[25] When analyzing the sera of patients with prostate cancer, IGFBP-2 has been shown to be elevated 2–3-fold whereas IGF-I, a molecule with known mitogenic effects, is only modestly elevated (by 7–8%).[21] This increase in IGFBP-2 has also been shown to have a significant positive correlation with serum prostate specific antigen (PSA), a tumor marker used to screen for prostate cancer.[26]

Our findings suggest that IGFBP-2 may be involved in the pathogenesis of prostate cancer. To test this hypothesis, we used primary cultures of normal prostate epithelial cells and prostate cancer cell lines to evaluate the effects of IGFBP-2 on cellular proliferation. In addition, we evaluated the effect of IGFBP-2 on prostate cancer expression and activity of telomerase, a nuclear enzyme believed to be involved in cell immortality and cancer pathogenesis.[27]

MATERIAL AND METHODS

Cell culture

Prostate epithelial cell strains from histologically confirmed peripheral zone tissues with no cancer were cultured and characterized as described previously.[28] LAPC-4 prostate cancer cells were generously donated from the lab of C. Sawyer, MD (Division of Hematology, UCLA). DU 145 cells were obtained from the American Type Culture Collection (Rockville, MD). Primary cultures were grown in serum-free Complete MCDB 105. LAPC-4 cells were grown in DMEM + 10% FBS. DU 145 cells were

Grant sponsor: NIH; Grant number: 2R01 DK47591, 1R01AG20954, 1UO1CA 84128; Grant sponsor: American Cancer Society; Grant sponsor: Pharmacia GEM; Grant sponsor: First STAR.

*Correspondence to: UCLA Center for the Health Sciences, 10833 Le Conte Ave, MDCC Rm. 22-315, Los Angeles, CA 90095-1752. Fax: +310-206-5843. E-mail: hassy@mednet.ucla.edu

Received 11 April 2002; Revised 7 October 2002; Accepted 15 November 2002

DOI 10.1002/ijc.11015

grown in IMDM + 10% FBS. LAPC-4 cells were grown in the presence of 10 nM of the androgen R1881.

Proteins and other reagents

Recombinant human IGFBP-2 was obtained from Gropep (Adelaide, Australia). Recombinant human IGF-I was provided by Pharmacia (Piscataway, NJ). PD98059 (MAP-kinase inhibitor) and Wortmannin (PI3-kinase inhibitor) were purchased from Sigma (St. Louis, MO).

Cell proliferation assays

To evaluate growth of the cancer lines we used the Promega Cell Titer 96-cell proliferation assay essentially as described in the product manual. Briefly, cells were inoculated at 200 cells/well into 96-well microtiter dishes and allowed to attach overnight. Media was then removed with gentle suction and replaced with the appropriate treatment condition (see Results section for conditions). LAPC-4 cells were androgen starved for 24 hr before treatment. Normal prostate epithelial cells were tested in similar 96-well growth assays except that they were treated for seven days whereas LAPC-4 and DU 145 cells were treated for 3 days. For the cancer cell line assays, absorbance readings were obtained at 490 nm and 655 nm and 6 samples were counted per control and experiment variable. Growth of the normal prostate cells was quantitated with the sulforhodamine B assay[29] and 4 wells were counted per variable.

Telomerase expression

LAPC-4 and DU 145 cells were prepared at approximately 70% confluence using standard media mentioned previously. Treatment was with serum-free (SF) media or SF media + 1.0 μg/ml rhIGFBP-2. Total cell RNA was first extracted using the RNeasy Mini Kit purchased from QIAGEN, Inc. (Valencia, CA) essentially following the manufacturer's protocol. RNA content and quality were assessed by spectrophotometry at 260 nm and 280 nm. The ratio 260/280 nm was consistently above 1.8. RT-PCR was carried out with 0.5 μg of total RNA using an Ez rTth RNA PCR kit from Perkin Elmer (Branchburg, NJ) according to manufacturer protocol. All primers used were purchased from Sigma Genosys (Pittsburgh, PA). Primer sequences for the control, β-actin, were 5′-CCAAGGCCAACCGCGCGAGAAGA-3′ for the upstream primer and 5′-AGGGTACATGGTGGTGCCGCCAGAC-3′ for the downstream primer.[30] Primer sequences for hTERT mRNA were 5′-CGGAAGAGTGTCTGGAGCAA-3′ for the upstream primer and 5′-GGATGAAGCGGAGTCTGGA-3′ for the downstream primer.[31] RT-PCR products were separated on a 2.0% agarose gel, stained with ethidium bromide. Scanning densitometry using Bio-Rad (Hercules, CA) Quantity One software was employed to quantify relative expression. The relative hTERT mRNA levels were normalized *vs.* the corresponding levels of β-actin.

Telomerase activity

The commercially available Telomerase PCR ELISA kit purchased from Roche Molecular Biochemicals was used to perform the telomerase assays.[32] The preparation of cell lysates and assay procedure was carried out according to the manufacturer's protocol. Absorbance at 450 nm was measured for each sample using a Bio-Rad microplate reader. All precautionary measures against RNAase activity were observed. For each experiment, 2×10^5 cells (LAPC-4 or DU 145) were plated per well, using 6-well plates and grown to 70% confluence. They were subsequently placed in SF media for 12 hr before treatment with 1.0 μg/ml of IGFBP-2. Protein concentrations of cell lysates were determined by Bradford assay and 2 μg of protein was used for each telomerase PCR reaction. Trials of LAPC-4 cells were carried out in the presence and absence of androgens.

Statistical analysis

Experiments are means of sextuplets and each experiment was carried out 3 times. Data are expressed as mean ± SEM. Statistical analyses were carried out using an unpaired, 2-tailed Student's *t*-test. Differences were considered statistically significant when $p < 0.05$. The actual *p*-values for the different experiments are listed in the Results section.

RESULTS

Effect of IGFBP-2 on cell proliferation

We investigated the effect of IGFBP-2 on primary strains of normal prostate epithelial cells placed in SF media by treating with 0.5, 1.0 or 2.0 μg/ml of recombinant human IGFBP-2 (rhIGFBP-2) for 7 days. Trials were carried out in the presence and absence of 10 ng/ml of IGF-I. The effect of IGFBP-2 on normal prostate epithelia growth is shown in Figure 1. IGFBP-2 inhibited cellular proliferation in the absence of IGF-I in a dose-dependent manner, with significant growth inhibition observed only at the highest concentration ($p < 0.01$ for IGFBP-2 of 2.0 μg/ml) as seen in Figure 1*a*. In Figure 1*b*, we show that IGF-I-induced cell growth was also inhibited by IGFBP-2 in a dose-dependent manner.

To study the effect of IGFBP-2 on prostate cancer cells, LAPC-4 cells placed in SF media were treated with 10% FBS, 250 ng/ml IGF-I, or 1.0 μg/ml rhIGFBP-2 for 3 days. These trials were carried out in the absence of androgens. The effect of IGFBP-2 on LAPC-4 cell growth is shown in Figure 2*a*. Compared to IGF-I, IGFBP-2 markedly stimulates cell proliferation of LAPC-4 cells to a level significantly above SF ($p < 0.01$), even to a level similar to that observed in 10% serum. An additional set of experiments was carried out by treating DU 145 cells with SF or SF + 1.0 μg/ml of rhIGFBP-2 for 3 days. The effect of IGFBP-2 on DU 145 cell growth is shown in Figure 2*b*. IGFBP-2 significantly ($p < 0.05$) stimulates DU 145 cell growth compared to SF. A dose response trend for IGFBP-2 growth stimulation of LAPC-4 cells is shown in Figure 2*c*. Significant ($p < 0.01$) growth stimulation was observed with 100 ng/ml of IGFBP-2, with the response increasing at higher concentrations of the protein.

To evaluate the androgen-dependence of IGFBP-2 growth stimulation of LAPC-4 cells, we treated cells with SF or SF + 1.0 μg/ml of rhIGFBP-2 for 3 days after an initial androgen-starvation of 24 hr. Experiments were carried out in the presence and absence of the androgen, R1881 (10 nM). The regulation of androgens on IGFBP-2 growth stimulation of LAPC-4 cells is shown in Figure 3*a*. The growth stimulation of IGFBP-2 over that of SF was statistically significant, both in the presence and absence of androgens ($p < 0.05$ and $p < 0.001$, respectively). The growth stimu-

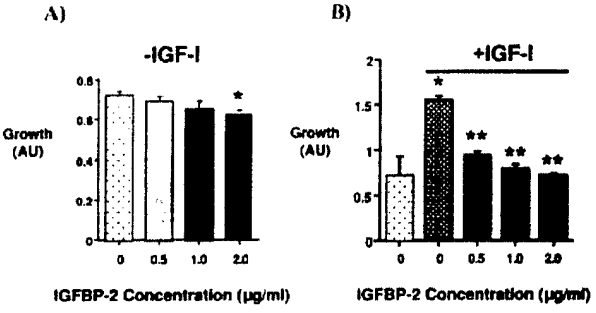

FIGURE 1 – The effects of IGFBP-2 and IGF-I on normal prostate epithelial cell growth. Primary cultures of normal prostate epithelial cells were treated for 7 days with serum-free (SF) media or SF + 0.5, 1.0, or 2.0 μg/ml of rhIGFBP-2. This was carried out in the absence (*a*) or presence (*b*) of IGF-I (10 ng/ml). IGFBP-2 inhibits growth of normal prostate epithelial cells in a dose-dependent manner (*a*). IGF-I (10 ng/ml) significantly stimulates growth in these cells, an effect that is inhibited in a dose-dependent manner by IGFBP-2 (*b*). *Statistically significant difference ($p < 0.05$, Student's *t*-test) compared to SF. **Statistically significant difference ($p < 0.05$, Student's *t*-test) compared to SF + 10 ng/ml IGF-I.

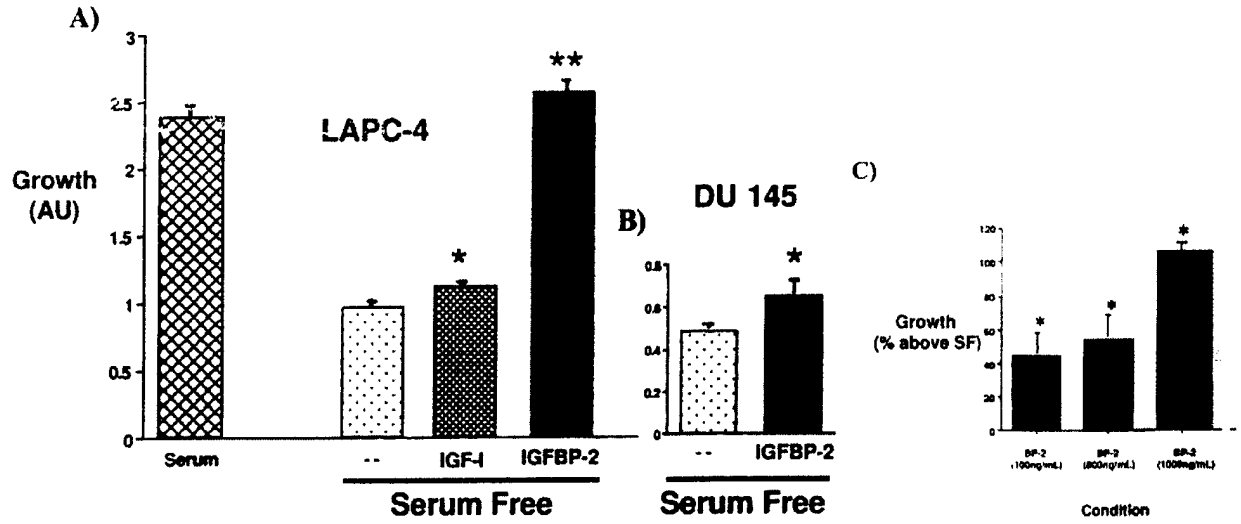

FIGURE 2 – The effects of IGF-I and IGFBP-2 on prostate cancer cell growth. LAPC-4 prostate cancer cells were treated for 3 days with the following: 10 % FBS, SF, or SF with 250 ng/ml of IGF-I or 1,000 ng/ml of rhIGFBP-2. In these cells, IGF-I slightly stimulates growth but IGFBP-2 markedly induces growth similar to serum (*a*). DU 145 cells treated for 3 days with SF or SF + 1,000 ng/ml rhIGFBP-2. IGFBP-2 significantly stimulates cell growth in these cells above serum-free (*b*). Statistically different from SF media. $*p < 0.05$; $**p < 0.001$, Student's *t*-test. (*c*) Dose responsive growth stimulation of LAPC-4 prostate cancer cells with IGFBP-2. LAPC-4 prostate cancer cells were treated for 3 days with the following: SF, SF + 100 ng/ml rhIGFBP-2, SF + 800 ng/ml rhIGFBP-2, or SF + 1,000 ng/ml rhIGFBP-2. Significant growth stimulation occurred in the presence of 100 ng/ml IGFBP-2, with increasing stimulation being observed with higher concentrations of the protein. Statistically different from SF media. $*p < 0.01$, Student's *t*-test.

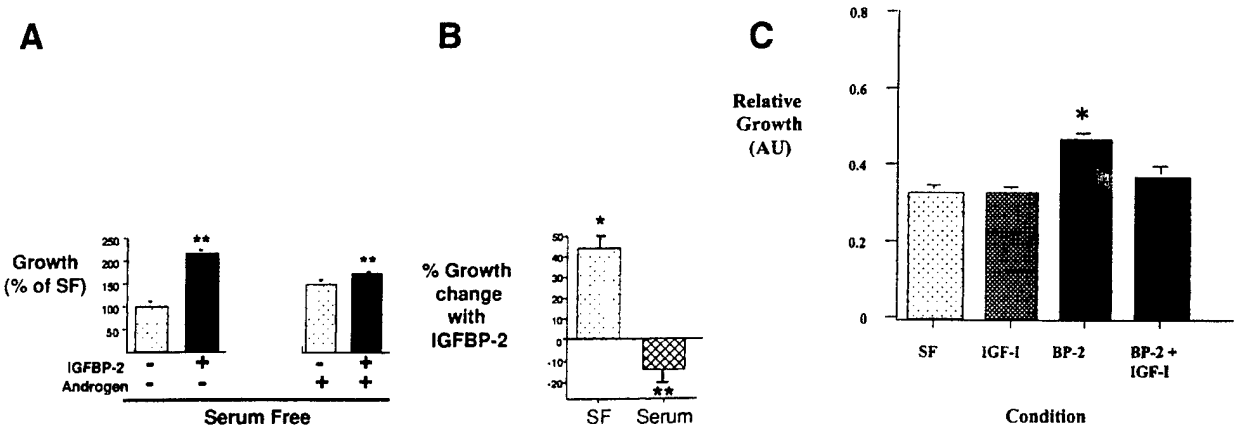

FIGURE 3 – (*a*)Androgen modulation of IGFBP-2 induced growth stimulation of LAPC-4 cells. LAPC-4 prostate cancer cells were treated for 3 days with SF media or SF + 1.0 μg/ml rhIGFBP-2. This graph shows the significant increase in growth with IGFBP-2. The magnitude of the stimulation is much greater in the absence of androgens. Statistically significant difference from SF. $**p < 0.01$, Student's *t*-test. (*b*) IGFBP-2 stimulates LAPC-4 growth in SF and inhibits LAPC-4 growth in 10% FBS. LAPC-4 prostate cancer cells were treated for 3 days with SF media, SF + 1.0 μg/ml rhIGFBP-2, 10% FBS, or 10% FBS + 1.0 μg/ml rhIGFBP-2. When added to serum-free media, IGFBP-2 has a growth stimulatory effect relative to SF. When added in the presence of 10% FBS, IGFBP-2 inhibits cell growth relative to 10% FBS. Statistically significant difference from SF and 10% FBS, respectively. $*p < 0.01$; $**p < 0.05$, Student's *t*-test. (*c*) IGF-1 diminishes IGFBP-2 growth stimulatory effects on LAPC-4 prostate cancer cells. LAPC-4 prostate cancer cells were treated for 3 days with SF media, SF + 250 ng/ml IGF-1, SF + 1.0 μg/ml rhIGFBP-2, or SF + 250 ng/ml IGF-1 + 1.0 μg/ml rhIGFBP-2. IGF-1 did not significantly stimulate growth when compared to SF. As was seen previously, IGFBP-2 had a growth stimulatory effect relative to SF, when added in the absence of IGF-1. When added in the presence of IGF-1, IGFBP-2 did not significantly stimulate growth above growth in SF media. Significant difference from SF. $*p < 0.01$, Student's *t*-test.

lation was much more pronounced, however, in the absence of androgens.

To study the effect of serum on IGFBP-2 growth stimulation of prostate cancer cells, we treated LAPC-4 cells with SF media, SF + 1.0 μg/ml of rhIGFBP-2, 10% FBS, or 10% FBS + 1.0 μg/ml of rhIGFBP-2 for 3 days. The effect of serum on IGFBP growth stimulation of LAPC-4 cells is shown in Figure 3*b*. When added in the absence of serum, as was seen in the above experiments, IGFBP-2 significantly ($p < 0.05$) stimulated LAPC-4 cell growth above SF. When added in the presence of 10% FBS, however, IGFBP-2 significantly ($p < 0.05$) inhibited LAPC-4 cell growth compared to 10% FBS alone.

To study the effect of IGF-1 on IGFBP-2 growth stimulation of prostate cancer cells, we treated LAPC-4 cells with SF media, SF + 250 ng/ml IGF-1, SF + 1.0 μg/ml rhIGFBP-2, or SF + 250 ng/ml IGF-1 + 1.0 μg/ml rhIGFBP-2 for 3 days. The results are reported in

Figure 3*c*. IGF-1 did not significantly stimulate growth when compared to SF. As was seen previously, IGFBP-2 had a growth stimulatory effect relative to SF ($p < 0.01$), when added in the absence of IGF-1. When added in the presence of IGF-1, IGFBP-2 did not significantly stimulate growth above growth in SF media.

To determine whether IGFBP-2 growth stimulatory effect on prostate cancer cells involved the MAP-kinase and PI3-kinase pathways, LAPC-4 cells were treated with SF media, SF + 1.0 μg/ml of rhIGFBP-2, SF + 20 nM of PD98059 (MAP-kinase inhibitor), SF + 1.0 μg/ml of rhIGFBP-2 and 20 nM of PD98059, SF plus 40 nM of Wortmannin (PI3-kinase inhibitor), or SF plus 1.0 μg/ml of rhIGFBP-2 and 40 nM of Wortmannin (PI3-kinase inhibitor) for 3 days. The effect of MAP-kinase and PI3-kinase inhibitors on IGFBP-2 growth stimulation of LAPC-4 cells is shown in Figure 4. Both PD98059 and Wortmannin demonstrated significant growth inhibitory effects, whereas IGFBP-2 significantly stimulated growth above SF. IGFBP-2 growth stimulation was completely and partially blocked by PD98059 and Wortmannin, respectively. Of note, this concentration of Wortmannin fully blocked IGF-I growth stimulation (data not shown).

Telomerase activity

To study the effect of IGFBP-2 on telomerase activity in prostate cancer cells, we treated LAPC-4 and DU 145 cells with SF media or SF + 800 ng/ml of rhIGFBP-2. LAPC-4 cells were treated in the presence and absence of the androgen R1881 (10 nM). The effect of IGFBP-2 on telomerase activity in LAPC-4 (without androgens) and DU 145 cells is shown in Figure 5*a*. IGFBP-2 significantly stimulated telomerase activity in LAPC-4 ($p < 0.05$) and DU-145 cells ($p < 0.05$). The effect of androgens on IGFBP-2 ability to stimulate telomerase activity in LAPC-4 cells is shown in Figure 5*b*. In the absence of androgens, as was demonstrated previously, IGFBP-2 significantly ($p < 0.01$) stimulated telomerase activity in LAPC-4 cells. When added to LAPC-4 cells in the presence of androgens, IGFBP-2 stimulated telomerase activity to a modest but not significant ($p < 0.1$) degree.

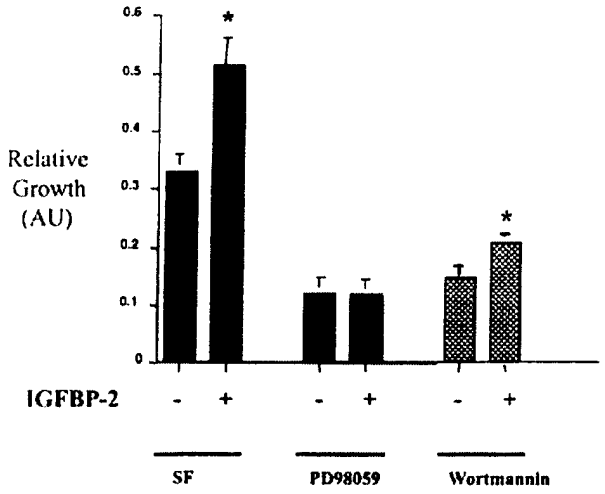

FIGURE 4 – IGFBP-2 growth stimulatory effect is blocked by MAP- and PI3-Kinase inhibitors. LAPC-4 prostate cancer cells were treated for three days with SF media, SF + 1.0 μg/ml rhIGFBP-2, SF + 20 nM PD98059, SF + 1.0 μg/ml rhIGFBP-2 + 20 nM PD98059, SF + 40 nM Wortmannin, or SF + 1.0 μg/ml rhIGFBP-2 + 40 nM Wortmannin. IGFBP-2 stimulates growth of LAPC-4 cells relative to SF (carried out in the absence of androgens). LAPC-4 growth is significantly inhibited by PD98059 (MAP-kinase inhibitor) and Wortmannin (PI3-kinase inhibitor). IGFBP-2 growth stimulatory effect is completely and partially blocked by PD98059 (MAP-kinase inhibitor) and Wortmannin (PI3-kinase inhibitor), respectively. Significant difference compared to growth in the condition in the absence of IGFBP-2. *$p < 0.01$, Student's *t*-test.

Telomerase expression

To evaluate the effect of IGFBP-2 on prostate cancer expression of the telomerase subunit, hTERT, we treated DU 145 cells with SF media or SF + 800 ng/ml of rhIGFBP-2. The effect of IGFBP-2 on hTERT expression in DU 145 cells is shown in Figure 5*c*. IGFBP-2 significantly ($p < 0.05$) stimulated hTERT expression above SF.

DISCUSSION

Our studies showed that IGFBP-2 had a growth inhibitory effect on normal prostatic epithelial cells, while having a potent stimulatory effect on growth of prostate cancer cells. In addition, in the LAPC-4 cell line, we found IGFBP-2 effects to be more pronounced in the absence of androgens and to be completely and partially blocked by MAP-kinase and PI3-kinase inhibitors, respectively. We also demonstrated that IGFBP-2 has a potent stimulatory effect on the expression and activity of telomerase in prostate cancer cells.

IGFBP-2, the second most abundant IGFBP in circulation, has traditionally been thought of primarily as a growth inhibitor. In transgenic mouse models, for example, IGFBP-2 overexpression through the CMV-promoter resulted in significantly reduced weight gain, presumably through IGFBP-2 sequestering of IGFs, reducing the bioavailability of these growth factors for their receptors.[33,34] This phenomenon was further supported by the more pronounced phenotype observed when crossing the IGFBP-2 overexpressing transgenic mouse with a model producing elevated growth hormone and IGF-I levels.[35] Mice with targeted inactivation of the IGFBP-2 gene, however, displayed only a subtle change in phenotype, suggesting functional compensation by other binding proteins.[36,37]

Conversely, serum IGFBP-2 has been found to be increased in patients with any one of a variety of malignancies[12–21,38] and elevated IGFBP-2 has been correlated with increasing malignant status and levels of tumor markers.[20–22,39–41] Tissue expression of IGFBP-2 has also been found to be positively correlated with tumor grade in CNS tumors, leukemia, thyroid cancer, colon tumors, hepatoblastoma, mammary cancer, ovarian cancer, Wilms' tumors, adrenal tumors and prostate cancer. An indication that IGFBP-2 might have cancer-promoting properties came from a study in which IGFBP-2 was overexpressed in the adrenocortical tumor cell line, Y-1. This resulted in increased cell proliferation and cloning efficiency, as well as significant morphological alterations.[42]

We investigated the novel concept that IGFBP-2 may be involved in the development and progression of prostate cancer. Prostate cancer is the most common non-cutaneous cancer and the second leading cause of cancer death in men, with 180,400 new cases diagnosed and 31,900 men dying of prostate cancer in 2000. Current recommendations for screening are a digital rectal exam and a serum PSA level annually between the ages of 50 and 79 (start at age 45 for African Americans and those with a positive family history of prostate cancer). Treatment consists of "watchful waiting" or local therapy (either surgical or localized radiation, external beam or interstitial brachytherapy) for disease confined to the prostate. For advanced disease, however, medical or surgical castration is often advocated. If the tumor progresses to a "hormone-independent" status, however, chemotherapy may be the only remaining option for control.

As mentioned previously, IGFBP-2 is elevated in the serum of patients with prostate cancer. This finding has since been expanded to show a positive correlation between IGFBP-2 levels and tumor Gleason scores,[24] as well as levels of serum PSA,[26] a screening marker for prostate cancer. It does not appear that IGFBP-2 is the cause of prostate cancer, however, because serum IGFBP-2 levels have no correlation with prostate cancer risk.[43] This was supported by our finding that IGFBP-2 actually had a dose-dependent inhibition of growth when added to normal prostate epithelial cells. This action is most likely due to IGFBP-2 sequestering of IGF-I,

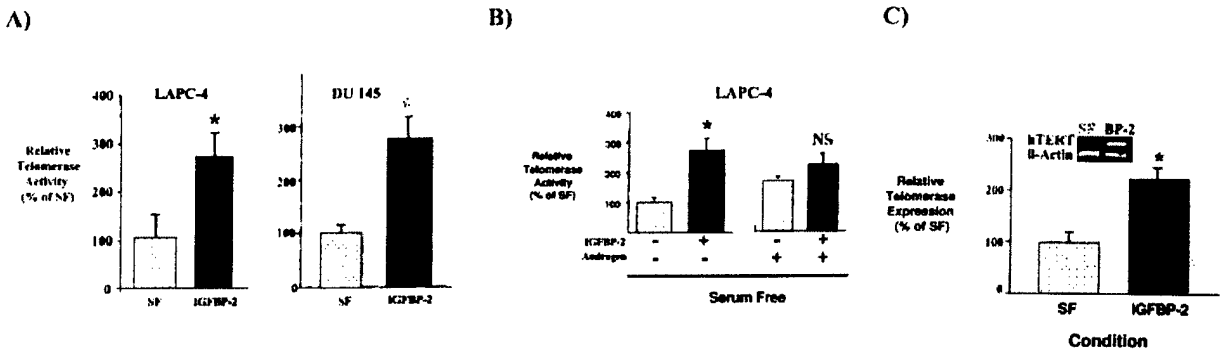

FIGURE 5 – IGFBP-2 stimulates telomerase activity and hTERT expression in prostate cancer cells. (*a*) Telomerase activity was assayed in response to 1.0 μg/ml IGFBP-2 for 48 hr in DU 145 and LAPC-4 prostate cancer cells in androgen-free, serum-free conditions. Treatment with IGFBP-2 stimulated baseline telomerase activity by nearly 3-fold in both cell lines ($p < 0.01$). (*b*) In contrast to observed stimulation of telomerase in LAPC-4 cells in the absence of androgen ($p < 0.01$), IGFBP-2 evoked a more modest and statistically nonsignificant stimulation in the presence of androgen (10 nM R1881). (*c*) DU 145 cells were treated for 48 hr with IGFBP-2 at 1.0 μg/ml and hTERT mRNA expression was determined by quantitative RT-PCR. IGFBP-2 treatment induced a 2-fold increase in baseline hTERT mRNA expression ($p < 0.05$). *Statistically significant difference from SF (see above for *p*-values).

as revealed by the fact that IGFBP-2 addition in the presence of IGF-I only reduced the level of growth equal to serum free media (*i.e.*, IGFBP-2 had a neutralizing action). The growth inhibition of IGFBP-2 observed in the absence of exogenous IGF-I is most likely due to sequestering endogenously produced IGFs.

When added to LAPC-4, an androgen-dependent cell line representing an early metastasis of a relatively well-differentiated prostate cancer, IGFBP-2 enhanced growth over 2 times that of control to a level similar to cell proliferation in serum. Not only this, but IGF-I, a molecule with known mitogenic effects, caused only modest growth stimulation. This finding is of significance because it suggests that some change in cellular physiology occurred during the transition from normal prostate epithelia to malignancy that allowed IGFBP-2 to be a growth stimulator. Just as intriguing is the fact that this stimulation was more pronounced in the absence of androgens. This phenomenon may reflect an interaction of IGFBP-2 with the androgen receptor system. It also may represent a transition to a more aggressive, androgen-independent state of LAPC-4 development; a process that may be in part mediated by IGFBP-2. This possibility is supported by preliminary data in an androgen-independent prostate cancer cell line where IGFBP-2 is 1 of only 2 molecules with markedly increased expression.[44] These findings warrant further investigation because of their theoretical significance in the pathogenesis of prostate cancer and for their possible implications in the medical management of the disease.

When added to LAPC-4 cells in the presence of 10% FBS, IGFBP-2 had a significant growth inhibitory effect. This may be due to its ability to sequester IGF-I and IGF-II, which are present in serum. Furthermore, it is possible that IGFBP-2 growth stimulatory actions are redundant with other molecules is serum. Consequently, addition of the IGFBP-2 protein in this context appears to have no growth stimulatory effect.

To investigate the mechanism of IGFBP-2 growth stimulatory effects, we utilized MAP-kinase (PD98059) and PI3-kinase (Wortmannin) inhibitors. When added to serum-free media in the presence of PD98059, IGFBP-2 induced no significant growth stimulation, whereas with Wortmannin, IGFBP-2 significantly stimulated growth but at a magnitude only half of that without the inhibitor. The MAP-kinase inhibitor completely blocks IGFBP-2 growth stimulation, whereas the PI3-kinase inhibitor only partially blocks IGFBP-2 action. These findings put into question the mechanism by which IGFBP-2 stimulates proliferation. One possibility is that IGFBP-2 acts through a novel cellular receptor in an IGF-independent manner. This receptor may have downstream signals that are similar to or overlap with those of the IGFRs and consequently there is less growth stimulation with the addition of the inhibitors.

In an additional attempt to evaluate the mechanism of IGFBP-2 potential contributions to prostate cancer growth or progression, we evaluated IGFBP-2 ability to stimulate the expression and activity of telomerase, a nuclear enzyme that is elevated in several malignancies and is believed to play a role in cell immortality. We demonstrated in DU 145 cells that IGFBP-2 stimulated the expression of hTERT, the regulatory subunit of telomerase whose expression is directly correlated with telomerase expression. IGFBP-2 also stimulated telomerase activity in these cells as well as in LAPC-4 cells. The stimulation in LAPC-4 cells was greatly diminished in the presence of androgens, again suggesting that IGFBP-2 may interact with the androgen receptor system or that it may allow cells to progress to an androgen-independent state.

In summary, we showed that IGFBP-2 has inhibitory effects on normal prostate epithelial cells, while having a stimulatory effect on prostate cancer cells. The stimulatory effects appear to be androgen-regulated and at least in part mediated through the MAP-kinase and PI3-kinase pathways. These findings suggest that there must be a molecular change during the transition from normal to malignant prostate cells that allows IGFBP-2 to adopt a stimulatory role. One possibility would be the activation or inactivation of a regulatory "switch" molecule that alters cellular physiology in a way that favors IGFBP-2 carcinogenic role. Further investigation in this area could provide valuable information that can used to generate better prostate cancer screening strategies and more effective treatment modalities.

ACKNOWLEDGEMENTS

Supported in part by a Pharmacia GEM grant (P.C.) as well as fellowship awards from the LWPES and from Eli Lilly (L.A.W.) and a First STAR grant (M.G.M.).

REFERENCES

1. Stewart CEH, Rotwein P. Growth, differentiation, survival: multiple physiological functions for insulin-like growth factors. Physiol Rev 1996;76:1005–26.
2. Baserga R, Prisco M, Hongo A. IGFs and cell growth. In: Rosenfeld RG, Roberts CT, eds. The IGF system: molecular biology, physiology, and clinical applications. Totowa, NJ: Humana Press; 1999. 329–53.
3. Ma J, Pollak MN, Giovannucci E, Chan JM, Tao Y, Hennekens CH, Stampfer MJ. Prospective Study of colorectal cancer risk in men and

plasma levels of insulin-like growth factor (IGF)-I and IGF-binding protein-3. J Natl Cancer Inst 1999;91:620–5.
4. Hankinson SE, Willett WC, Colditz GA, Hunter DJ, Michaud DS, Deroo B, Rosner B, Speizer FE, Pollak M. Circulating concentrations of insulin-like growth factor-I and risk of breast cancer. Lancet 1998;351:1393–6.
5. Wolk A, Mantzoros CS, Andersson SO, Bergstrom R, Signorello LB, Lagiou P, Adami HO, Trichopoulos D. Insulin-like growth factor-I and prostate cancer risk: a population-based, case-control study. J Natl Cancer Inst 1998;90:911–5.
6. Chan JM, Stampfer MJ, Giovannucci E, Gann PH, Ma J, Wilkinson P, Hennekens CH, Pollak M. Plasma insulin-like growth factor-I and prostate cancer risk: a prospective study. Science 1998;279:563–6.
7. Wetterau LA, Moore MG, Lee KW, Shim ML, Cohen P. Novel aspects of the insulin-like growth factor binding proteins. molecular genetics and metabolism. 1999;68:161–81.
8. Liu B, Lee HY, Weinzimer SA, Powell DR, Clifford JL, Kurie JM, Cohen P. Direct functional interactions between insulin-like growth factor-binding protein-3 and retinoid X receptor-α regulate transcriptional signaling and apoptosis. J Biol Chem 2000;275:33607–13.
9. Rajah R, Valentinis B, Cohen P. Insulin-like growth factor (IGF)-binding protein-3 induces apoptosis and mediates the effects of transforming growth factor-β1 on programmed cell death through a p53- and IGF-independent mechanism. J Biol Chem 1997;272:12181–8.
10. Valentinis B, Bhala A, DeAngelis T, Baserga R, Cohen P. The human insulin-like growth factor binding protein-3 inhibits the growth of fibroblasts with a targeted disruption of the IGF-I receptor gene. Mol Endocrinol 1995;9:361–7.
11. Hoflich A, Lahm H, Blum W, Kolb H, Wolf E. Insulin-like growth factor-binding protein-2 inhibits proliferation of human embryonic kidney fibroblasts and of IGF-responsive colon carcinoma cell lines. FEBS Lett 1998;434:329–34.
12. Muller HL, Oh Y, Lehrnbecher T, Blum WF, Rosenfeld RG. Insulin-like growth factor-binding protein-2 concentrations in cerebrospinal fluid and serum of children with malignant solid tumors or acute leukemia. J Clin Endocrinol Metab 1994;79:428–34.
13. Lee DY, Kim SJ, Lee YC. Serum insulin-like growth factor (IGF)-I and IGF-binding proteins in lung cancer patients. ' Korean Med Sci 1999;14:401–4.
14. Mohnike KL, Kluba U, Mittler U, Aumann V, Vorwerk P, Blum WF. Serum levels of insulin-like growth factor-I, -II, and insulin-like growth factor binding protein-2 and -3 in children with acute lymphoblastic leukaemia. Eur J Pediatr 1996;155:81–6.
15. Crofton PM, Ahmed SF, Wade JC, Elmlinger MW, Ranke MB, Kelnar CJ, Wallace WH. Effects of a third intensification block of chemotherapy on bone and collagen turnover, insulin-like growth factor I, its binding proteins and short-term growth in children with acute lymphoblastic leukaemia. Eur J Cancer 1999;35:960–7.
16. el Atiq F, Garrouste F, Remacle BM, Sastre B, Pommier G. Alterations in serum levels of insulin-like growth factors and insulin-like growth-factor-binding proteins in patients with colorectal cancer. Int J Cancer 1994;57:491–7.
17. Zumkeller W, Schwander J, Mitchell CD, Morrell DJ, Schofield PN, Preece MA. Insulin-like growth factor (IGF)-I, -II and IGF binding protein-2 (IGFBP-2) in the plasma of children with Wilms' tumour. Eur J Cancer 1993;29A:1973–7.
18. Boulle N, Logie A, Gicquel C, Perin L, Le Bouc Y. Increased levels of insulin-like growth-factor II (IGF-II) and IGF-binding protein-2 are associated with malignancy in sporadic adrenocortical tumors. J Clin Endocrinol Metab 1998;83:1713–20.
19. Karasik A, Menczer J, Pariente C, Kanety H. Insulin-like growth factor-I (IGF-I) and IGF-binding protein-2 are increased in cyst fluid of epithelial ovarian cancer. J Clin Endocrinol Metab 1994;78:271–6.
20. Flyvbjerg A, Mogensen O, Mogensen B, Nielsen OS. Elevated serum insulin-like growth factor-binding protein 2 (IGFBP-2) and decreased IGFBP-3 in epithelial ovarian cancer: correlation with cancer antigen 125 and tumor-associated trypsin inhibitor. J Clin Endocrinol Metab 1997;82:2308–13.
21. Cohen P, Peehl DM, Stamey TA, Wilson KF, Clemmons DR, Rosenfeld RG. Elevated levels of insulin-like growth factor-binding protein-2 in the serum of prostate cancer patients. J Clin Endocrinol Metab 1993;76:1031–5.
22. Fuller GN, Rhee CH, Hess KR, Caskey LS, Wang R, Bruner JM, Yung WK, Zhang W. Reactivation of insulin-like growth factor binding protein 2 expression in glioblastoma multiforme: a revelation by parallel gene expression profiling. Cancer Res 1999;59:4228–32.
23. Bubendorf L, Kolmer M, Kononen J, Koivisto P, Mousses S, Chen Y, Mahlamaki E, Schraml P, Moch H, Willi N, Elkahloun AG, Pretlow TG, et al. Hormone therapy failure in human prostate cancer: analysis by complementary DNA and tissue microarrays. J Natl Cancer Inst 1999;91:1758–64.
24. Figueroa JA, De Raad S, Tadlock L, Speights VO, Rinehart JJ. Differential expression of insulin-like growth factor binding proteins in high versus low Gleason score prostate cancer. J Urol 1998;159: 1379–83.
25. Schwander J, Mary JL. The RIA for IGFBP-2 in man: a meager catch? Growth Regul 1993;3:104–8.
26. Kanety H, Madjar Y, Dagan Y, Levi J, Papa MZ, Pariente C, Goldwasser B, Karasik A. Serum insulin-like growth factor-binding protein-2 (IGFBP-2) is increased and IGFBP-3 is decreased is patients with prostate cancer: correlation with serum prostate-specific antigen. J Clin Endocrinol Metab 1993;77:229–33.
27. Holt SE, Shay JW. Role of telomerase in cellular proliferation and cancer. J Cell Physiol 1999;180:10–8.
28. Peehl DM. Culture of human prostatic epithelial cells. Culture of epithelial cells, Freshney, RI. New York, NY: Wiley-Liss, Inc.; 1992. 159–80.
29. Skehan P, Storeng R, Scudiero D, Monks A, McMahon J, Vistica D, Warren JT, Bokesch H, Kenney S, Boyd MR. New colorimetric cytotoxicity assay for anticancer-drug screening. J Natl Cancer Inst 1990;82:1107–12.
30. Ponte P, Ng SY, Engel J, Gunning P, Kedes L. Evolutionary conservation in the untranslated regions of actin mRNAs: DNA sequence of a human β-actin cDNA. Nucleic Acids Res 1984;12:1687–96.
31. Nakamura TM, Morin GB, Chapman KB, Weinrich SL, Andrews WH, Lingner J, Harley CB, Cech TR. Telomerase catalytic subunit homologs from fission yeast and human. Science 1997;277:955–9.
32. Bosserhoff AK, Glabl A, Stolz W, Buettner R. Detection of telomerase activity in skin, melanocytic nevi, and melanoma by telomerase PCR ELISA. Biochimica 1997;3:16–8.
33. Hoeflich A, Wu M, Mohan S, Foll J, Wanke R, Froehlich T, Arnold GJ, Lahm H, Kolb HJ, Wolf E. Overexpression of insulin-like growth factor-binding protein-2 in transgenic mice reduces postnatal body weight gain. Endocrinology 1999;140:5488–96.
34. Schneider MR, Lahm H, Wu M, Hoeflich A, Wolf E. Transgenic mouse models for studying the functions of insulin-like growth factor-binding proteins. FASEB J 2000;14:529–40.
35. Hoeflich A, Nedbal S, Blum WF, Erhard M, Lahm H, Brem G, Kolb H, Wanke R, Wolf E. Growth inhibition in giant growth hormone transgenic mice by overexpression of insulin-like growth factor-binding protein-2. Endocrinology 2001;142:1889–98.
36. Pintar JE, Schuller A, Cerro JA, Czick M, Grewel A, Green B. Genetic ablation of IGFBP-2 suggests functional redundancy of the IGFBP family. Prog Growth Factor Res 1995;6:437–45.
37. Wood TL, Rogler LE, Czick ME, Schuller AG, Pintar JE. Selective alterations in organ sizes in mice with a targeted disruption of the insulin-like growth factor binding protein-2 gene. Mol Endocrinol 2000;14:1472–82.
38. Elmlinger MW, Deininger MH, Schuett BS, Meyermann R, Duffner F, Grote EH, Ranke MB. In vivo expression of insulin-like growth factor-binding protein-2 in human gliomas increases with the tumor grade. Endocrinology 2001;142:1652–8.
39. Renehan AG, Jones J, Potten CS, Shalet SA, O'Dwyer ST. Elevated serum insulin-like growth factor (IGF)-II and IGF binding protein-2 in patients with colorectal cancer. Br J Cancer 2000;83:1344–50.
40. Kaaks R, Toniolo P, Akhmedkhanov A, Lukanova A, Biessy C, Dechaud H, Rinaldi S, Zeleniuch-Jaquotte A, Shore RE, Riboli E. Serum C-peptide, insulin-like growth factor (IGF)-I, IGF-binding proteins, and colorectal cancer risk in women. J Natl Cancer Inst 2000;92:1592–600.
41. Kanety H, Madjar Y, Dagan Y, Levi J, Papa MZ, Pariente C, Goldwasser B, Karasik A. Serum insulin-like growth factor-binding protein-2 (IGFBP-2) is increased and IGFBP-3 is decreased in patients with prostate cancer: correlation with serum prostate specific antigen. J Clin Endocrinol Metab 1993;77:229–33.
42. Hoeflich A, Fettscher O, Lahm H, Blum WF, Kolb HJ, Engelhardt D, Wolf E, Weber MM. Overexpression of insulin-like growth factor-binding protein-2 results in increased tumorigenic potential in Y-1 adrenocortical tumor cells. Cancer Res 2000;60:834–8.
43. Stattin P, Bylund A, Rinaldi S, Biessy C, Dechaud H, Stenman UH, Egevad L, Riboli E, Hallmans G, Kaaks R. Plasma insulin-like growth factor-I, insulin-like growth-factor binding proteins, and prostate cancer risk: a prospective study. J Natl Cancer Inst 2000;92:1910–7.
44. Bubendorf L, Kolmer M, Kononen J, Koivisto P, Mousses S, Chen Y, Mahlamaki E, Schraml P, Moch H, Willi N, Elkahloun AG, Pretlow TG, et al. Hormone therapy failure in human prostate cancer: analysis by complementary DNA and tissue microarrays. J Natl Cancer Inst 1999;91:1758–64.

0013-7227/02/$15.00/0
Printed in U.S.A.

The Journal of Clinical Endocrinology & Metabolism 87(12):5351–5352

doi: 10.1210/jc.2002-021467

Special Editorial: Growth Hormone Treatment and Neoplasia—Coincidence or Consequence?

The discovery that GH action in primates was species specific and the ability to extract GH from human pituitaries ushered in the era of GH therapy for humans in the 1950s. At the outset, these were investigational programs facilitated by a centralized and usually government-sponsored distribution program that also enabled monitoring of data on beneficial or adverse effects. Recombinant DNA-derived GH became available in 1985, shortly after human-derived GH was discontinued because of the occurrence of Creutzfeldt-Jakob disease in several recipients from different countries. With the introduction of recombinant DNA-derived GH, the indications for GH replacement therapy were broadened to include Turner's syndrome, chronic renal failure, Prader-Willi syndrome, and small-for-gestational-age, in addition to established GH deficiency in children. However, monitoring of potential adverse effects was meticulously continued, facilitated by scrupulously maintained, and continually enlarging, databases involving both government and pharmaceutical companies in concert with pediatric investigators.

The Lawson Wilkins Pediatric Endocrine Society (LWPES) has closely and carefully monitored reports of adverse events via its Drug and Therapeutics Committee, which regularly informed the LWPES membership (1, 2). Early reports of an increase in childhood leukemia following GH therapy proved to be unfounded when the growing international databases were carefully monitored. Existing evidence indicates that GH treatment does NOT increase tumor recurrence in those whose primary lesion has been successfully treated. The LWPES has also endorsed the prudent policy of waiting for 1 yr after the completion of tumor treatment with no further evidence of tumor recurrence or growth before starting GH treatment in these children. Because a person treated for a malignancy is at risk for a second malignancy, ongoing surveillance of such persons is recommended, especially in those with genetic syndromes that are known to confer an increased risk of malignancy (Down's syndrome, Bloom's syndrome, Fanconi's anemia, neurofibromatosis-1). These recommendations also are part of the recent consensus conference by the Growth Hormone Research Society, which the LWPES has endorsed (3). This careful monitoring by LWPES contributes to the remarkable record of safety and efficacy of GH treatment for recommended indications in children and adolescents. Although adverse events are known to occur (raised intracranial pressure, edema, slipped capital femoral epiphyses, hyperglycemia, gynecomastia), an increased risk of cancer has not been an issue in pediatric patients treated with GH (2).

The article by Swerdlow *et al.* (4), in *Lancet*, reports on the risk of cancer in patients treated with human pituitary GH in the United Kingdom from 1959 to 1985. The cohort consisted of 1848 patients in the United Kingdom treated in childhood and early adulthood with human pituitary GH and followed for cancer incidence through December 1995 and for mortality through December 2000. Risks of cancer were compared with that in the general population after controlling for age, sex, and calendar period. Among this cohort, risks of mortality from cancer overall was increased approximately 3-fold and from colorectal cancer and Hodgkin's disease approximately 11-fold. The incidence of colorectal cancer was increased approximately 8-fold, and both incidence and mortality of colorectal cancer as well as that of Hodgkin's disease were increased even after excluding patients whose original diagnosis gave them a higher risk of cancer.

These results are potentially important but clearly preliminary, as the authors themselves point out. Only two deaths each of colorectal cancer and Hodgkin's disease were reported. Although highly more prevalent than expected in the control population, a chance occurrence of one case or of one death each from colon cancer or Hodgkin's disease may have skewed the results. It would also be essential to know whether the incidence of such malignancies is increased in patients with GH deficiency who did not receive GH therapy. Are the incidence rates of patients with GH deficiency who are not treated with GH comparable with the matched general population? The relatively small cohort and small number of cases argue strongly for caution in the rush to judgment or conclusion. Similar concerns with leukemia proved unfounded when larger cohorts were carefully examined; some cases of leukemia actually preceded the institution of GH therapy. Failure to treat GH deficiency is itself associated with premature mortality, especially from cardiovascular causes (4).

Despite these caveats, the authors are to be applauded for bringing this issue to scrutiny. They have carefully analyzed their cohort and cautiously presented their inferences and conclusions. They provide a potential rational basis through the known effects of IGF-I on promoting cell growth and inhibiting apoptosis. They point out reported associations between status of GH excess such as acromegaly and gastrointestinal cancer, although they do not mention several reports to the contrary (5). They infer that former dosing schedules with human-derived GH may have resulted in higher IGF-I levels than are likely with modern regimens, although they cannot substantiate this assertion, nor is it likely based on GH purity, potency, and dosages used in the 1959–1985 era (6–8).

The available data in pediatrics do not support any concern for excess malignancy at this time. In the two largest international databases and surveillance studies, with a total of some 86,000 patients on GH, representing almost 250,000 GH treatment years, there is only one report of a gastrointestinal carcinoma—an adenocarcinoma in a 15-yr-old girl initially treated by radiotherapy and chemotherapy for a

brain tumor (astrocytoma). She developed gastrointestinal bleeding 3.5 yr after the start of GH therapy when the tumor was diagnosed. There is also a report of spontaneous colon cancer in a girl with Turner's syndrome many years after discontinuation of GH therapy (personal communication).

With these considerations in mind, the LWPES believes:

1. Current treatment recommendations with recombinant human GH for children with documented GH deficiency are safe and without proven increased risk of inducing malignancy (2, 9, 10). Treatment for any indication with recombinant GH therapy in children should be accompanied by regular monitoring of IGF-I and IGF-binding protein-3 concentrations to ensure that they are maintained within age appropriate limits.

2. The possible association between increased cancer incidences and/or mortality and GH treatment be further critically investigated in a large cohort, especially in those treated with human-derived GH by protocols similar to those reported by Swerdlow *et al.* (4). Large databases of such patients are available and should be critically reviewed.

3. Surveillance and monitoring of ongoing long-term results of GH therapy should be encouraged and supported.

Lawson Wilkins Pediatric Endocrine Society (LWPES) Writing Committee: Mark A. Sperling (University of Pittsburgh School of Medicine, Pittsburgh, PA), Paul H. Saenger (Albert Einstein College of Medicine, Bronx, NY), Ray Hintz (Stanford University School of Medicine, Stanford, CA), Tom Wilson (State University of New York, Stony Brook, NY), and Susan R. Rose (Cincinnati Children's Hospital Medical Center, Cincinnati, OH) on behalf of the LWPES Executive Committee and the LWPES Drug and Therapeutics Committee

Acknowledgments

Received September 7, 2002. Accepted September 10, 2002.

Address all correspondence and requests for reprints to: Mark A. Sperling, M.D., Department of Pediatrics/Endocrinology, Children's Hospital of Pittsburgh, 3705 Fifth Avenue, Pittsburgh, Pennsylvania 15213-2583. E-mail: masp@pitt.edu.

Other members of the LWPES Drug and Therapeutics Committee are: Philippe Backeljauw, M.D. (Cincinnati Children's Hospital Medical Center, Cincinnati, OH); Rosalind Brown, M.D. (University of Massachusetts Medical School, Boston, MA); Pinchas Cohen, M.D. (David Geffen School of Medicine at UCLA, Los Angeles, CA); Dana S. Hardin, M.D. (University of Texas Southwestern, Dallas, TX); Stephen F. Kemp, Ph.D. (University of Arkansas School of Medicine, Little Rock, AR); Margaret Lawson, M.D. (Children's Hospital of Eastern Ontario, Ottawa, Ontario, Canada); Sally Radovick, M.D. (The University of Chicago, Chicago, IL); Steve M. Rosenthal, M.D. (University of California San Francisco, San Francisco, CA); Lawrence Silverman, M.D. (University of Medicine and Dentistry of New Jersey-New Jersey Medical School, Camden, NJ); Phyllis Speiser, M.D. (New York University School of Medicine, New York, NY).

References

1. 1995 Guidelines for the use of growth hormone in children with short stature. A report by the Drug and Therapeutics Committee of the Lawson Wilkins Pediatric Endocrine Society. J Pediatr 6:857–867
2. 2002 Update of guidelines for the use of growth hormone in children. Drug and Therapeutics Committee of the Lawson Wilkins Pediatric Endocrine Society
3. 2001 Consensus. Critical evaluation of the safety of recombinant human growth hormone administration: statement from the Growth Hormone Research Society. J Clin Endocrinol Metab 86:1868–1870
4. **Swerdlow AJ, Higgins CD, Adlard P, Preece MA** 2002 Risk of cancer in patients treated with human pituitary growth hormone in the UK, 1959–85: a cohort study. Lancet 360:273–277
5. **Melmed S** 2001 Clinical perspective: Acromegaly and cancer: not a problem? J Clin Endocrinol Metab 86:2929–2934
6. **Cohen P, Clemmons DR, Rosenfeld RG** 2000 Does the GH-IGF axis play a role in cancer pathogenesis? Growth Horm IGF Res 10:297–305
7. **Cohen P** 2001 Clinical implications of the IGF-cancer connection. Growth Horm IGF Res 11:336–338
8. **Shim M, Cohen P** 1999 IGFs and human cancer: implications regarding the risk of GH therapy. Horm Res 51(Suppl 3):42–51
9. **Lee K-W, Cohen P** 2001 Individualizing growth hormone dosing in children. Horm Res 56(Suppl 1):29–34
10. **Leung W, Rose SR, Zhou Y, Hancock ML, Burstein S, Schriock EA, Lustig R, Danish RK, Evans WE, Hudson MM, Pui CH** 2002 Outcomes of growth hormone replacement therapy in survivors of childhood acute lymphoblastic leukemia. J Clin Oncol 20:2959–2964